Star and Branch Shaped Polymers for Delivery of Therapeutics

By

Mark Byrne B.Sc.

Supervisor: Dr. Andreas Heise

A thesis submitted to Dublin City University

in partial fulfillment of the requirements

for the degree of

Doctor of Philosophy (PhD)

November 2014

Declaration

I hereby certify that this material, which I now submit for assessment on the programme of study leading to the award of a degree of Doctor of Philosophy is entirely my own work, and that I have exercised reasonable care to ensure that the work is original, and does not to the best of my knowledge breach any law of copyright, and has not been taken from the work of others save and to the extent that such work has been cited and acknowledged within the text of my work.

Signed: _____ (Candidate) ID No.: 56533973

Date: _____

Acknowledgement

After three and a half years, I still can't believe that my PhD is almost finished and I am finally submitting my thesis. It has been a great few years with a lot of ups and downs along the way and a magnificent journey which I will never forget. I have learned so much both on a scientific and personal level and feel this journey has contributed significantly to my development as a person. As I did all of the hard work to achieve this PhD I would like to congratulate myself and acknowledge nobody. All joking aside there are some special people who played an integral role in my personal support, motivation, development and training throughout this journey.

Firstly, I would like to pay enormous appreciation to my supervisor Dr. Andreas Heise with which it has been a great pleasure to work alongside. Your knowledge, ideas and motivation have really strengthened my scientific knowledge and pushed me to high standards in my research. You gave me enormous freedom to conduct my research and provided me with great opportunities to further my personal and career development e.g. collaboration with IBM in California. Aside from being a mentor, your friendship and approachable nature means you were always a pleasure to have a conversation with outside of a working environment even if it involved your complaints about Irish weather! Again thank you for all of your support and I hope you were pleased with my work and conduct throughout.

I would like to thank Dr. Andrew Kellet and Prof. Neil Cameron for being my internal / external examiners and providing feedback with regards to my thesis. I would also like to pay particular thanks the all of the guys at IBM notably Joe Sly, Bob Miller and Joe Sly for all of their support in helping me to settle in and work effectively at IBM, Almaden, San Jose, California. You are all very knowledgeable people yet very interesting fun people to be around. To Sally-Ann Cryan, Danielle Victory and Alan Hibbitts your tremendous help and support was greatly appreciated throughout our collaboration. You all made me feel very welcome at RCSI and contributed greatly to the success of our project together. I would also like to thank IRCSET for funding thius research and giving me the opportunity to undertake a PhD programme.

The DCU chemistry community has been a big part of my life the past few years so I would to show my gratitude to its members. In particular I would like to thank all of the technical staff; Vinny –great ability to have the "crack" with and your help with regards to the pump systems was greatly appreciated, Ambrose – always dependable and patient in providing consumables which keep our labs running, Damien – always provided great lab safety and had a magnificent

ability to have a joke with and not take life too seriously, Veronica – always very helpful and do a great job keeping the department running, John – Mr. NMR spectroscopy and IT who has generously provided IT help to me on numerous occasions, Catherine – always a great help in ordering chemicals and ever so patient when I messed up my order, Brendan – great help with SEM and Mary – very helpful in providing support to our lab when GPC systems were having problems.

Great appreciation must be paid to my fellow group members for all of their help particularly when I initially joined the group. Your knowledge and support really helped me settle in and provided me with a better understanding of different cultures seeing as I was the only Irish member! I would like to pay particular thanks to Dr. Paul Thornton or "Plastic Paddy" as he's more commonly known for his continued friendship and enormous help during my PhD. Your expertise and novel ideas thought me a lot and demonstrated how research should be approached. Your mindset of "working smart" really instilled a new approach to science in me. I'll sadly miss the great football banter we had and our discussions on all things Liverpool. Hopefully someday Rotherham F. C. will make it to the Premier League! To Jin Huang, my favourite Chinese person, your friendship has been greatly appreciated. It was always a pleasure to meet socially even if your taste in food and movies was somewhat questionable. Your vibrant presence in the lab was sadly missed when you left for better things but I'm sure our friendship will continue well into the future. Your scientific knowledge, ideas and hard working mentality really set a great example for me to follow and if I even achieve half of what you have I will be very successful. However, please stop publishing countless high impact papers which makes the rest of us mere mortals look really bad. Fabrice, your enormous knowledge of polymers and GPC thought me a huge amount very quickly and helped to quickly establish a solid chemical platform from which I could advance my knowledge and research efforts. It was always fun to discuss football and the failures of the Bordeaux football team. I would like to say thank you to Jacoo who provided some good friendship and was the only member of PRG who could really drink. Your love of rugby was unfortunate but could be overlooked with your ability to have the "crack". Zeliha it was a great pleasure to work alongside you and even greater pleasure to always beat you at squash. Also, thank you for all of your delicious cakes at our group meetings. Claudia, thanks for being a good friend and organizing all of the birthday card arrangements. Your Italian flair was great to have around the lab but your organic chemistry and column chromatography skills were very much appreciated. Tushar, thank you for all of your polypeptide expertise and it was a pleasure to witness your great optimism with regards to your work i.e. "minimum JACS". Anton, it was a

great pleasure to work alongside you and some of California together. I wish you all the best with your PhD. Marcello, I hope your PhD works out well and you get the job you deserve. To Saltuk and Timo, although we only briefly worked together it was a great honour and you are both really good guys who I have no doubt will do very well in their PhDs and future work.

To Declan Daly my good friend, your great friendship was of great support to me during my PhD. Your knowledge of organic chemistry is tremendous and I am sure you will do very well in the future. Your organic chemistry help and tips contributed to improving my chemistry skills and knowledge. I'll definitely miss our lunch time banter and discussions on everything football related even if your opinions are ridiculous.

Finally, I owe tremendous gratitude to my wonderful girlfriend, Cathy and mother, Serena for tolerating me particularly in the final often stressful year of my PhD. Without you guys I would not be where I am today and owe you everything. Cathy, your positive attitude and motivation to drive me to succeed was very supportive whilst it was comforting to know that even after a bad day I could always depend on you for help and cheering up. Even after spending 6 months out in California, you stuck with it and are very much a part of this success so thank you. To my Mam, I would not be here today without you, your hard work and support has guided me to become the person I am today. Your patient and sincere nature enabled me to give my all to this PhD in spite of my often testing moods. I am sure I would not have been able to finish this PhD with your unwavering support so thank you.

Again, a big thank you to everybody.

List of Publications

- M. Byrne, P. D. Thornton, S. A. Cryan and A. Heise; Star polypeptides by NCA polymerisation from dendritic initiators: synthesis and enzyme controlled payload release, *Polym. Chem*., **2012**, 3, 2825.

- M. Byrne, D. Victory, A. Hibbitts, M. Lanigan, A. Heise, S. –A. Cryan; Molecular weight and architectural dependence of well-defined star-shaped poly(lysine) as a gene delivery vector, *Biomater. Sci*., **2013**, 1, 1223.

Conference Presentations

- Mark Byrne, Andreas Heise; Star polypeptides by NCA polymerisation from dendritic initiators; **ChemCareers Finalist**, London / UK, November 2011.

- Mark Byrne, Andreas Heise; Star polypeptides by NCA polymerisation from dendritic initiators: synthesis and enzyme controlled payload release; **Macro UK Young Researcher Meeting**, Liverpool / UK, April 2011.

- Mark Byrne, Andreas Heise; Molecular weight and architectural dependence of well-defined star-shaped poly(lysine) as a gene delivery vector; **243rd ACS National Meeting**, San Diego / USA, March 2012.

List of Abbreviations

AAM – Activated monomer mechanism

AAN – Average arm number

AFM – Atomic force microscopy

AMPDA – 2-(aminomethyl)-2-methyl-1,3-propanediamine

ATR – Attenuated total reflectance

ATRP – Atom transfer radical polymerization

BLG – Benzyl-L-glutamate

BOC – tert-butyloxycarbonyl

BOP – Bis(oxepanyl-2-one)

CCS – Core cross-linked star polymer

(D) – Dispersity

DIC – Diisopropylcarbodiimde

DIPEA – Diisopropylethyl amine

DLS – Dynamic light scattering

DMAEMA – Dimethylamino ethyl methacrylate

DMF - Dimethylformamide

DMTMM – 4-(4,6-Dimethoxy-1,3,5-triazin-2-yl)-4-methylmorpholinium chloride

DP – Degree of polymerization

DRI – Differential refractive index

DTT – Dithiothreitol

DVB – Divinyl benzene

EG_2-L-Glutamte – diethylene glycol-L-glutamate

FTIR – Fourier transform infrared spectroscopy

GAMA – D-gluconamidoethyl methacrylate

GATBE – L-glutamic acid 5-tert-butyl ester

GPC – Gel permeation chromatography

GTP – Group transfer polymerization

HBPO – poly[3-ethyl-3-(hydroxymethyl)oxetane]

LBL – layer-by-layer

LCST – Lower critical solution temperature

MALS – Multi-angle light scattering

M_n – Normal average molecular weight

MWCO – Molecular weight cut-off

M_w – Weight average molecular weight

NAM – Normal amine monomer mechanism

NCA – N-carboxyanhydride

NMP – Nitroxide mediated polymerization

NMR – Nuclear magnetic resonance

OROP – Organocatalytic ring opening polymerization

PAMAM – poly(amido amine)

PBLG – poly(benzyl-L-glutamate)

PBS – Phosphate buffer saline

PDI – Polydispersity index

PEG – poly(ethylene glycol)

PEI – poly(ethylene imine)

PGA – poly(glutamic acid)

PHis – poly(histidine)

pI – Isoelectric point

PLGA – poly(lactide-co-glycolide)

PLL – poly(lysine)

POSS – polyhedral oligomeric silsesquioxane

PPABLG – poly(γ-4-((2-(piperidin-1-yl)ethyl)aminomethyl)benzyl-L-glutamate)

PPI – poly(propylene imine)

PPO – poly(propylene oxide)

PS – poly(styrene)

PS – OH – poly(styrene) with OH end group

PVL – poly(valerolactone)

PZLL – poly(ε-carbobenzyloxy-L-lysine)

QELS – Quasi elastic light scattering

RAFT – Reversible addition-fragmentation chain transfer

RES – Reticuloendothelial

R_h – hydrodynamic radius

RI – Refractive index

ROP – Ring opening polymerization

ROMP – Ring-opening metathesis polymerization

SDS – Sodium dodecyl sulphate

SEC – Size exclusion chromatography

TBD – 1,5,7-Triazabicyclo[4.4.0]dec-5-ene

TFA – Trifluroacetic acid

THF - Tetrahydrofuran

TMSEM – Trimethyl silyl ethyl methacrylate

UV – Ultroviolet

Vis - Visible

ZLL – ε-carbobenzyloxy-L-lysine

Contents

Abstract

Star and Branch Shaped Polymers for Delivery of Therapeutics

By

Mark Byrne B.Sc.

The area of nanomedicine has witnessed a surge in research interest in recent years owing to the huge potential offered by this domain to significantly impact on the healthcare industry. To progress, the advent of novel materials capable of meeting the stringent demands of conducting medical applications at a molecular level is required. Consequently, polymers are one such nanomaterial attracting considerable interest. In particular, star shaped polymers have emerged as strong candidates for the next generation of nanoparticle platforms considering the unique structural benefits offered by such architectures; ability to combine a high local density of polymeric arms and functionality within a size confined structural space. Furthermore, the inherent introduction of distinctive nano-environments achieved only by star shaped architectures advocates the concept of simultaneous multiple cargo loading, protection, transport and site specific delivery via the confines of a single star shaped polymeric enclosure. To achieve the next generation of star shaped polymers, new synthetic strategies for the design of well-defined star polymers of biocompatible compositions is required. The aim of this PhD was to develop novel synthetic star shaped polymer based biomaterials capable of biomedical applicability towards areas such as drug delivery and biorecogniton. The main synthetic strategies employed were ring opening polymerization (ROP) of amino acid N-carboxyanhydrides (NCA) and efficient amide coupling chemistries. Three different platforms were designed including stimuli responsive star shaped polypeptides, star shaped poly(lysine) as a vector for DNA and siRNA delivery and biologically active star shaped glycopolypeptides. Finally a fourth platform comprising a series of hybrid nanogel star polymers was developed in conjunction with IBM.

Chapter 1

Introduction: NCA Derived Star and Branch Shaped Polypeptides for Delivery of Therapeutics

1.1 Ring Opening Polymerization (ROP) of N-Carboxyanhydrides (NCA)

Originally known as Leuchs's anhydrides owing to their discovery by Hermann Leuchs in 1906, N-carboxyanhydrides (NCA) are simply anhydrides of α-amino acids.[1] Depending on the amino acid selected, NCAs are not typically synthetically challenging and are commonly synthesised through the use of chlorinating agents such as triphosgene or phosphorus pentachloride to cyclize the amino/carboxylic acid functionality on the α-carbon **(Scheme 1.1)**.[2] A prerequisite of NCA formation is that any amino acid side chain possessing nucleophilic or acidic functionality must be protected which otherwise leads to unwanted side reactions or polymerization of the formed NCA. NCAs are reactive compounds owing to activation of the carbonyl functionality at C-5 position of the anhydride, whilst simultaneously providing protection of the amino group. Storage of NCAs remains difficult with water posing a particular problem. Hydrolysis of the NCA even in solid state can readily occur resulting in undefined, uncontrolled oligopeptides.[3-5]

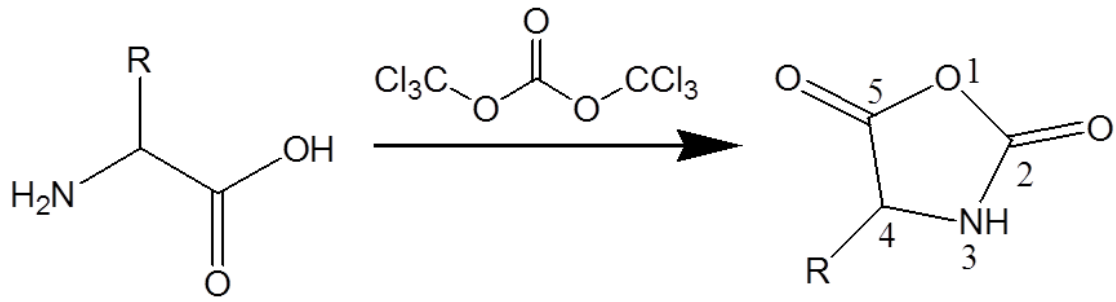

Scheme 1.1: Synthesis of N-carboxyanhydrides from α-amino acids from triphosgene.

Treated as a monomer, the NCA ring can be opened in a process known as ring opening polymerization (ROP) thus permitting the synthesis of poly(amino acids) or the step wise growth of more complex polypeptides.[6,7] ROP of NCAs occurs via two mechanisms: Normal Amine Mechanism (NAM) and Activated Monomer Mechanism (AMM).

1.1.1 Normal Amine Mechanism (NAM)

This mechanism is usually observed with initiating groups such as primary and secondary amines, alcohols and water, groups which are stronger nucleophiles than bases. Initiation of this type occurs for both types of NCA i.e. N-unsubstituted (R_2 = H) and N-substituted ($R_2 \neq$ H) (**Scheme 1.2**). ROP initiation of the NCA occurs via nucleophilic attack on the anhydride carbonyl group at position 5 owing to its strong activation. The resulting unstable, carbamic acid readily decarboxylates to provide a new amino group which is subsequently free to attack

the next molecule of NCA. The use of primary amines as initiators is more profound given they are more nucleophilic than the propagating amines leading to a faster initiation rate than propagation rate and therefore leading to well controlled polymerization and polypeptides of a low polydispersity index (PDI <1.2).[8,9] Moreover, the NAM results in a polypeptide with the amine initiator attached to the polypeptide chain thus opening opportunities for end-group engineering. Unwanted termination and kinetic deviations of polypeptide growth are apparent however and are strongly dependent on reaction conditions such as type of monomer,[10,11] monomer purity [12,13] and solvent.[14] One such unwanted side reaction involves nucleophilic attack of the less reactive carbonyl at position 2 resulting in the formation of an ureido acid side chain.[6,15] However, such a reaction is limited and can be further inhibited by the choice of a more nucleophilic initiator.

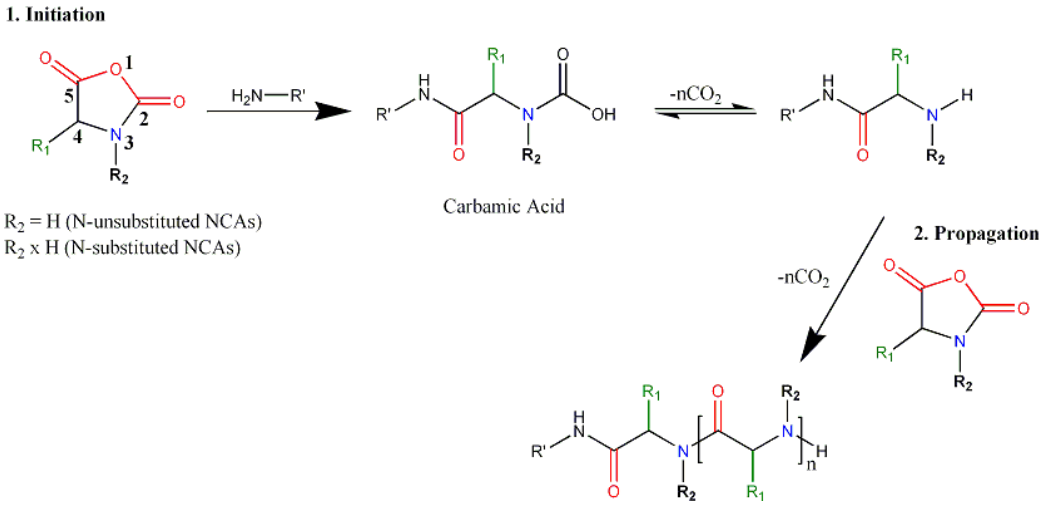

Scheme 1.2: NAM of NCA ring opening polymerization via a primary amine initiator. Initiation: Carbamic acid formation following nulceophilic attack on the anhydride at position 5 by primary amine. Decarboxylation of unstable carbamic acid to generate a new free amino group. Propagation: New free amino group capable of nulceophilic attack on another anhydride molecule and the process continues i.e. polymerization.

1.1.2 Activated Monomer Mechanism (AMM)

In contrast to NAM, initiation arises from the basicity of the initiator and not as a result of its nucleophilicity.[16,17] Common initiators employed here include tertiary amines and the resultant mechanism is only applicable to N-unsubstituted NCAs due to the requirement of removal of a proton from the N-3 position as part of the initiation. As outlined in **Scheme 1.3** the subsequent anion attacks the C-5 carbonyl which further reacts with another NCA anion releasing CO_2. Apart from its mechanism and terminations,[18-21] this mechanism differs from

NAM in that it can potentially lead to higher molecular weight polypeptides of often broad PDIs since propagation rate is faster than initiation rate.[22]

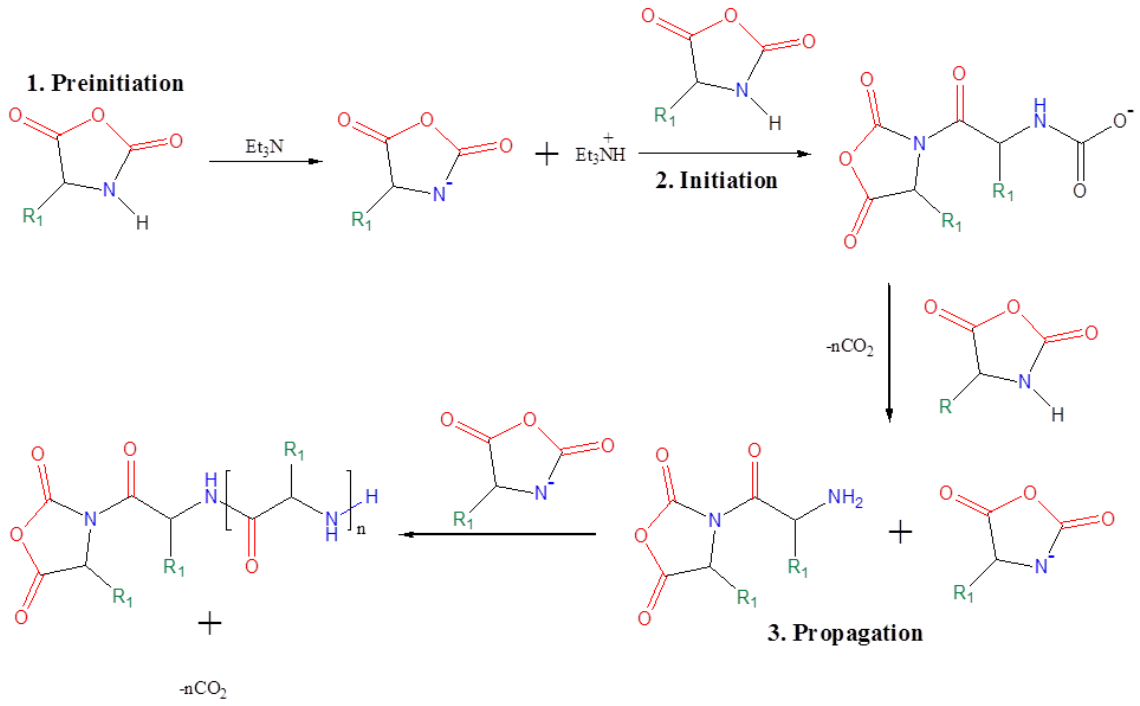

Scheme 1.3: AMM of NCA ring opening polymerization. Preinitiation: Tertiary amine acts as a catalyst (base) and abstracts a proton from the amine in NCA ring resulting in the formation of an anion. Initiation: The resulting anion acts as the initiator and attacks the carbonyl group at position 5 of another NCA molecule to form a dimer. Reaction with a new NCA molecule results in the simultaneous decarboxylation and formation of new NCA anion. Propagation: Reaction with the new NCA anion forms a trimer and the process continues with the formation of a new NCA anion in each step.

Although both mechanisms are synthetically effective in achieving polypeptides, only the NAM can be described as controlled producing low polypeptide PDI, predictable M_n and end group fidelity.[23] Other techniques to initiate ROP of NCAs have reported using initiators such as silazane derivatives,[24] primary amine hydrochlorides[25] and Deming's transitional metal complexes[26-28] but these will not be discussed further here.

1.2 Synthesis of Star and Branch Shaped Polypeptides by NCA ROP

Star shaped or branched polypeptides describe a particular architectural class of polypeptides consisting of a number of linear polypeptide chains or "arms" bound to a central core. Within this architectural class there is great scope for versatility arising from the potential to control the number of arms, molecular weight and type of polypeptidic arm and core employed. Depending on the synthetic approach employed, characterization of these architecturally diverse materials remains quite challenging. Two different synthetic methodologies are generally used to generate these materials: divergent and convergent.

1.2.1 Divergent Approach

The most commonly employed divergent method, generally describes the synthesis of a star or branched polymer using a "core first" approach i.e. the growth of a polymer, in this case polypeptide, from a multifunctional initiator or more simply a multi-amino macromolecule. The presynthesised core containing multiple initiating sites allows for the simultaneous initiation and subsequent growth of linear polypeptide arms from the central core thus creating star or branched polypeptide architectures. Such cores must contain multiple but equally reactive initiation sites with a slower propagation rate than initiation rate in order to permit the synthesis of branched polypeptides with controlled and well defined molecular weights and architectures. Characterization of such materials often proves challenging however, owing to the inability to measure the polypeptide "arm" directly. This drawback may be overcome by utilising a cleavable moiety linking arm to the core but such an approach further complicates the synthetic methodology. The determination of arm number requires end group analysis or investigation of comparative branching parameters against an equivalent linear polypeptide but such methods are often complex and just an approximation of arm number.

1.2.1.1 Dendrimer Initiated ROP of NCAs

In terms of cores and subsequent polypeptide growth, amino terminated dendrimers are one of the most commonly used. This is related to the fact that dendrimers are well defined macromolecules which are structurally versatile and possess unprecedented functionality within a localised area.[29-34] As the dendrimer generation increases, the degree of branching

and subsequent peripheral functionality also increases generating macromolecules with variable size, structural flexibility, surface functionality and molecular weight.[35-37] Poly(amido amine) (PAMAM) and polypropylene imine (PPI) dendrimers are the two most widely employed dendrimers in NCA polymerization partly owing to their commercial availability. Both types possess the inherent structural and functional versatility associated with dendrimers but more importantly possess a multivalent primary amino periphery required for controlled NCA polymerization **(Figure 1.1)**.

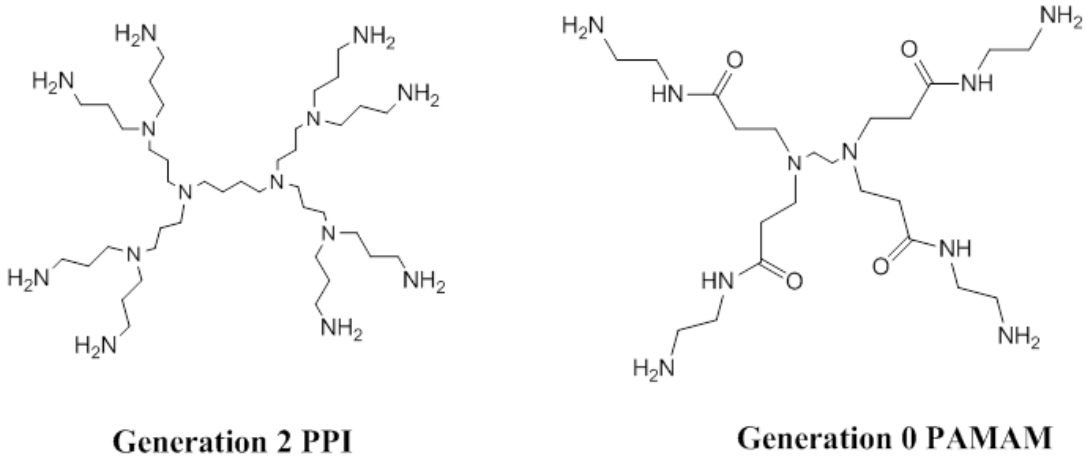

Figure 1.1: Structure of PPI and PAMAM dendrimers (ethylenediamine core).

The first such reported case of polypeptide growth from a dendritic core via NCA polymerization was reported by Okada et al., who constructed a short armed glycosylated star polypeptide from the ROP of glycosylated NCA via generation 3 PAMAM **(Scheme 1.4)**.[38] The polymers, dubbed "sugar balls" were shown to be well defined in terms of molecular weight distribution with NCA ROP proceeding via NAM. ^{13}C NMR spectroscopy suggested initiation by all peripheral primary amino groups.

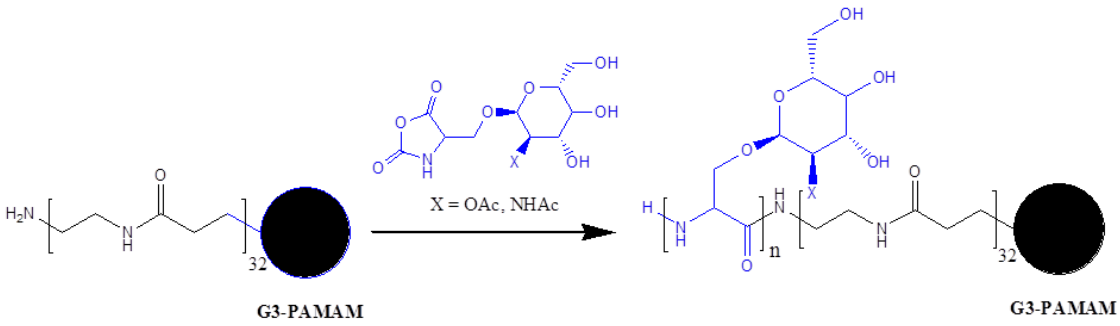

Scheme 1.4: Synthesis of "sugar balls" by ROP of the NCA monomer of a glucopyranosyl-L-serine derivative initiated with a generation 3 PAMAM dendrimer.[38]

In addition to the work performed by Okada et al., subsequently, numerous groups have attempted the dendrimer initiated ROP of a variety of NCA monomers.[39,40] The G0 and G3-PAMAM initiated ROP of γ-benzyl-L-glutamate (BLG) NCA afforded star polypeptides with 4 and 32 poly(γ-benzyl-L-glutamate) (PBLG) arms respectively whereas G5-PPI was employed to generate a series of poly(sarcosine) decorated G5-PPI dendrimers with narrow molecular weight distributions.[41-44] A series of star shaped copolymers of PBLG and poly(DL-valine) were synthesized using G1 and G2-PPI dendrimers.[45] The described polymers showed good agreement with theoretical molecular weights and quantitative reaction of all dendritic primary amino groups.

Aliferis et al. investigated the effect the type of multifunctional initiator had on ROP of ε-butyloxycarbonyl-L-lysine and γ-benzyl-L-glutamate NCAs via G0-PAMAM, G1-PPI and 2-(aminomethyl)-2-methyl-1,3-propanediamine (AMPDA).[46] The tertiary amine deficient AMPDA resulted in star polypeptides exhibiting unimodality and narrow molecular distributions whereas the tertiary amine proficient PAMAM and PPI dendrimers corresponded to polypeptides with bimodality and were less defined as denoted by uncontrolled molecular weights and higher polydispersity indices. Such a feature is explained by the participation of both the NAM and AMM in the ROP of the described NCAs via PAMAM and PPI resulting in predominantly primary amine initiated star polypeptides (NAM) with high molecular weights and low molecular weight tertiary amine derived linear polypeptide chains (AMM). Such an observation has not been reported elsewhere and may potentially be as a consequence of the use of low generation dendrimers thus sterically permitting NCA monomer initiation via tertiary amines. The employment of suitable deprotection chemistry of the aforementioned dendrimer derived star polypeptides afforded amino and carboxylic acid functionalised polypeptides.

Owing to the living nature of NCA derived polypeptides, a key feature of NCA ROP is the potential to modify polypeptide end groups (NH_2) via in situ or post modification. Qui et al. utilised this feature to great effect by functionalising the polypeptide amino end groups of a four armed PAMAM derived PBLG star polypeptide with α-bromoisobutyryl bromide **(Scheme 1.5).**[47] The resultant ATRP proficient star polypeptide permitted controlled radical polymerization of D-gluconamidoethyl methacrylate (GAMA) glycomonomer to form star shaped biohybrid polymers. As expected, the star shaped hybrids exhibited inferior molecular weight distributions towards their linear counterparts, yet the difference was only minimal.

Furthermore the distribution was unimodal implying no unreacted polypeptide star whilst polypeptide and methacrylate block lengths could be readily controlled.

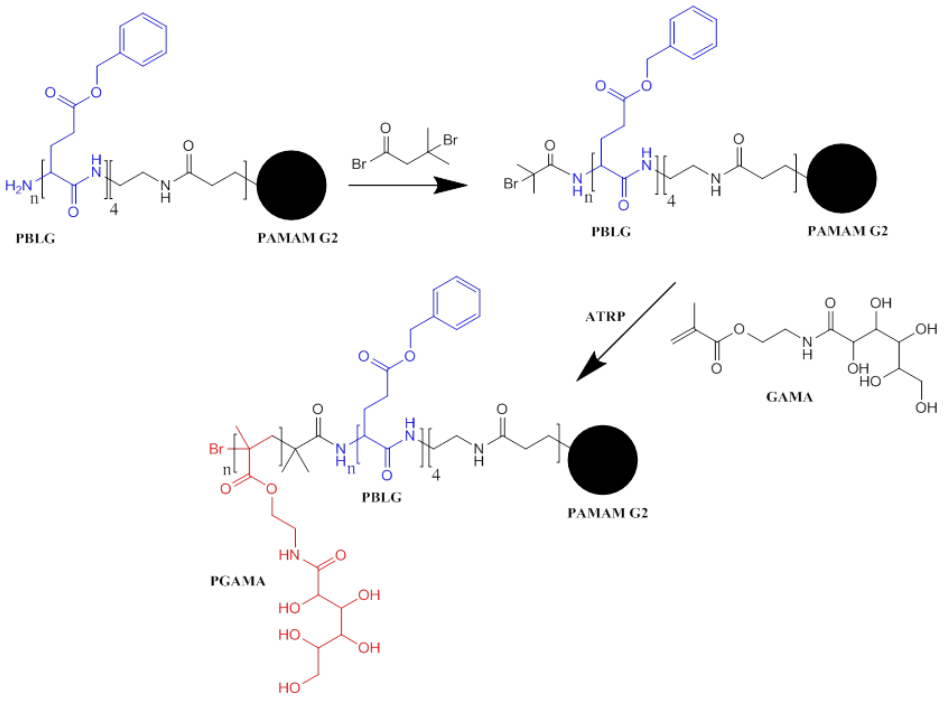

Scheme 1.5: Star Shaped PBLG-b-PGAMA biohybrid by combination of NCA polymerization and ATRP. Initially, generation of star shaped PBLG by ROP of BLG NCA with a generation 2 PAMAM dendrimer and the subsequent modification of its amino end groups with an ATRP initiator. Polymerization of a glycosylated methacrylate monomer from this star polymer by ATRP generated a biohybrid star polymer.[47]

1.2.1.2 NCA Derived Polypeptides from Branched Polymers

Aside from dendrimers, branched versions of poly(ethylene imine) (PEI), poly(ethylene glycol) (PEG) and poly(propylene oxide) (PPO) have demonstrated their ability to successfully serve as multifunctional initiators for the synthesis of star polypeptides. Like PAMAM and PPI, these branched polymers possess peripheral primary amino groups capable of ROP of NCAs. Several examples of PEI initiated ROP of benzyl protected histidine and BLG NCAs have been reported which have recently been exhaustively expanded by the work of Liu et al. to include a series of star polypeptides boasting variation in hyperbranched PEI cores and polypeptide peripheries and densities.[48-55] One such example demonstrated the formation of a series hyperbranched PEI decorated with various ratios of poly(lysine) (PLL).[56] Size exclusion chromatography (SEC) highlighted the absence of tertiary amine initiated ROP, however polydispersity indices were significantly higher than those obtained by dendrimer initiated ROP possibly due to the inferior

structural integrity and monodispersity of branched PEI as compared to a dendrimer. Post modification of the "living" polypeptide amino end groups with a nitrophenyl-carbonate functionalized PEG resulted in star polypeptides with a PEG outer shell. ^{1}H NMR spectroscopy confirmed the highly efficient quantitative PEG conjugation to polypeptide chains. Similarly, 4-armed PEG led to the successful synthesis of star shaped PBLG, PZLL and poly(alanine) (PAla) **(Scheme 1.6)**. Quantification of polypeptide conjugation was obtained via ^{1}H NMR spectroscopy and corresponded well to monomer feed ratios.[57-59] In particular SEC analysis of $(PEG\text{-}b\text{-}PBLG)_4$ by Karatzas et al. confirmed star polymer with a narrow molecular weight distribution and good agreement of molecular weight with the targeted value.[60] In contrast the PEG derivative, PPO (polypropylene oxide) resulted in a more polydisperse range of $(PPO\text{-}b\text{-}PBLG)_3$ star polypeptides possibly arising from the unequal initiation reactivity and subsequent polypeptide distributions amongst the multiple amino sites.[61]

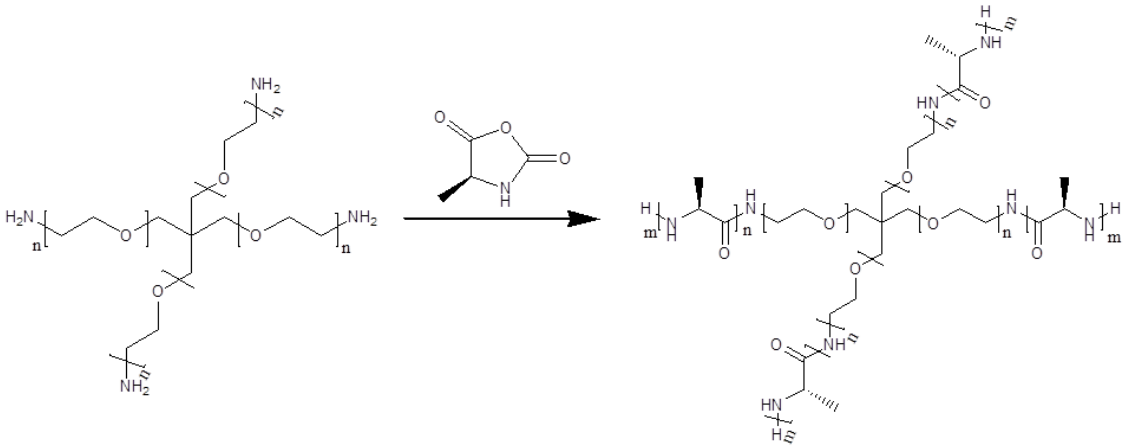

Scheme 1.6: ROP of alanine NCA by a 4-armed amino terminated PEG derivative.[59]

Well defined, tri-armed polystyrene-b-PBLG (PS-b-PBLG) star polymers were reported by Abraham et al. who sequentially modified tri-functional PS to generate amino terminated PS. Subsequent ROP of BLG NCA resulted in star shaped block copolymers boasting controlled molecular weights and molecular weight distributions similar to a linear counterpart.[62]

1.2.1.3 Miktoarm Star Polypeptides from NCA

A new type of star polypeptide, miktoarm star polymers, has led to considerable interest within this area. Miktoarm star polymers are star polymers possessing numerous arms in which the arms are of various compositions i.e. chemically and/or molecular weight emanating from a central core **(Figure 1.2)**.[63] Consequently, such polymers are synthetically challenging. However, the advent of efficient living polymerisation techniques such as ROP and ATRP and

their sequential synthetic employment has helped to overcome these synthetic limitations somewhat leading to a more diverse range of miktoarm star polymers.

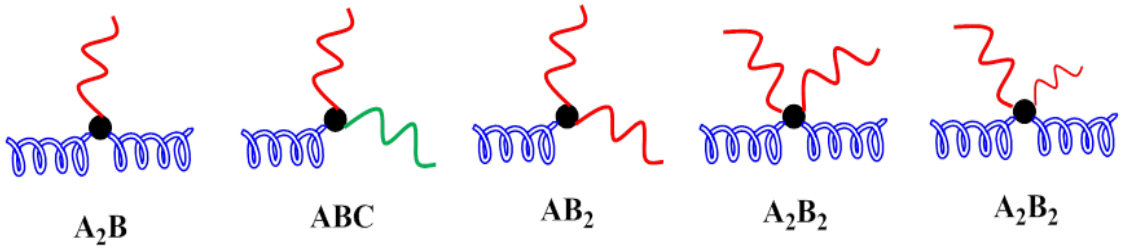

Figure 1.2: Miktoarm star polymers encompassing various arm compositions and molecular weights. Each symbol represents a polymeric arm wherein different arm compositions are denoted by a change in symbol type, colour or size. The helix type symbol represents a polypeptide arm.

Concerning polypeptides, several examples of miktoarm star polypeptides have been divulged.[64,65] A miktoarm star polymer comprising 3 arms, two of which are PBLG and the other PS were synthesised by initially employing ATRP to afford linear PS(Br).[66,67] Subsequent modification of the bromine end group via nucleophilic substitution with 1-aminotriethylenetriamine, followed by crude purification techniques afforded a diamino functionalized PS polymer capable of ROP of BLG NCA. Molecular weights were verified by ^{1}H NMR spectroscopy whilst SEC confirmed the well defined and monomodal nature of the described polymers (PDI <1.3). The removal of PBLG protecting groups ultimately led to carboxylic acid functionalized miktoarm star polypeptides. More recently, Junnila et al. used anionic polymerization and ROP to generate 3 and 4-armed PLL miktoarm star polypeptides. The ability to control molecular weight, number and type of polymeric arms in conjunction with narrow molecular weight distributions demonstrated the versatility and superior control of these materials.[68,69] Asides from PS, the versatile technique of "click" chemistry has also shown promise as an efficient route towards miktoarm star polypeptides.[70] AB_2 type miktoarm star polypeptides were prepared using an tri-functional initiator containing a primary amine and dual alkyne functionality.[71] The described initiator permitted NCA ROP from the primary amine whereas alkyne groups allowed for the "clicking" on of preformed azide terminated linear polypeptide chains **(Figure 1.3)**. The beauty of this system is the wide range of NCA derived polypeptides and combinations that can be potentially attached thus readily creating a vast library of miktoarm star polypeptides. The chemistry employed is not particularly challenging yet leads to very well defined star polymers (PDI <1.2) with tunable molecular weights and functionality depending on the NCA selected.

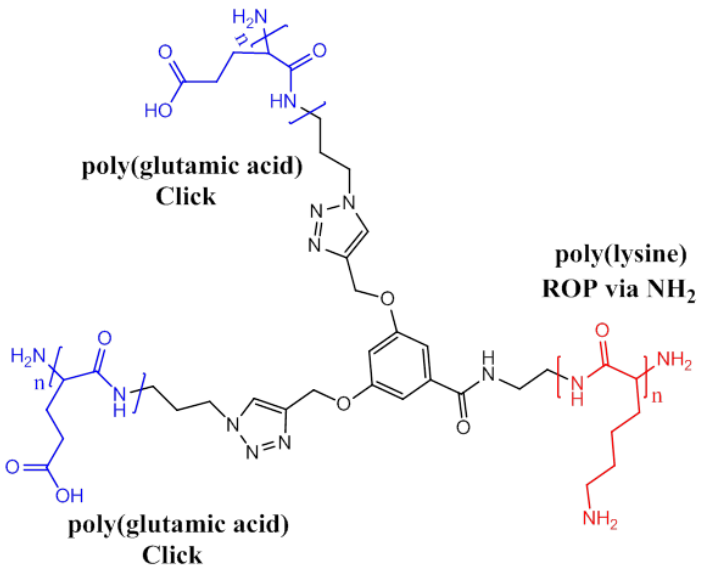

Figure 1.3: AB_2 miktoarm star polymer synthesized via ROP of BLG NCA with a dual functional initiator (primary amine / azide) to form linear PBLG. The subsequent ROP of lysine NCA from a pre-designed tri functional initiator possessing a primary amine and two alkyne functionalities (primary amine / alkyne) permitted the "click" of two azide terminated PBLG chains and formation of the resultant AB_2 type miktoarm polypeptide based system.[71]

1.2.1.4 Polypeptides from Other Multifunctional Molecules

Polypeptide growth from amino functionalised chromophores has led to the facile preparation of fluorescently labelled star polypeptides, a feature with particular relevance in the biomedical field, namely materials for flourescent probes.[72] Perylene derivatives employing four primary amines at the periphery were used to generate chromophoric star polypeptides comprising of four PBLG or PZLL arms **(Figure 1.4)**.[73,74] The resultant polypetides however, particularly PZLL had broad molecular weight distributions, low yields and molecular weights inconsistent with the theoretical values. In particular, long polypeptide chains (number of units > 200) were uncontrolled and could not achieve their desired molecular weights. The authors speculate this was possibly due to unwanted chain-breaking, chain transfer and termination reactions although the rigid atructure of this multifunctional initiator may also hamper efficient polypeptide growth.

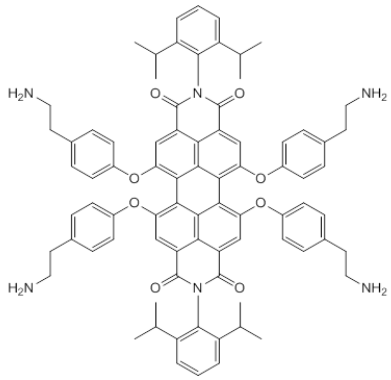

Figure 1.4: Amino terminated perylene derivative for NCA ROP to form star shaped fluorescent polypeptides.[73,74]

Although not as widely investigated as a class of initiator, several other examples of multifunctional amino terminated molecules for NCA ROP have been reported. These initiators are of a wide variety of chemical compositions and capable of generating star polypeptides possessing multiple polypeptide arms **(Figure 1.5)**. The NCAs employed in conjunction with these initiators include BLG, BA (β-benzyl-L-aspartic acid) and EG_2-L-glutamate (diethylene glycol-L-glutamate). In terms of composition, cyclotriphosphazenes have led to the successful polymerization of NCAs to generate star polypeptides.[75,76] Similarly, polypeptide growth from the amino side chain of linear PLL produced densely branched materials comprising 100% polypeptide.[77] Although such materials allowed for versatility in branching density the polymers were limited by their inferior structural control. Concerning cyclotriphosphazenes, although polypeptide growth is readily achieved, these materials lack the structural flexibility and synthetic control associated with a dendrimer derived star polypeptide. More recently, the generation of anionic and cationic star shaped polypeptides derived from the ROP of BLG and ZLL NCAs by polymerization from an amino terminated multifunctional cyclodextrin and porphyrin / polyester moiety respectively were reported.[78,79] The described star polypeptides exhibited broadened PDIs (1.3 – 1.5) whilst initial results demonstrated some control over polypeptide density. Removal of protecting groups afforded star shaped poly(glutamic acid) and poly(lysine) with a cyclodextrin and porphyrin / polyester core respectively.

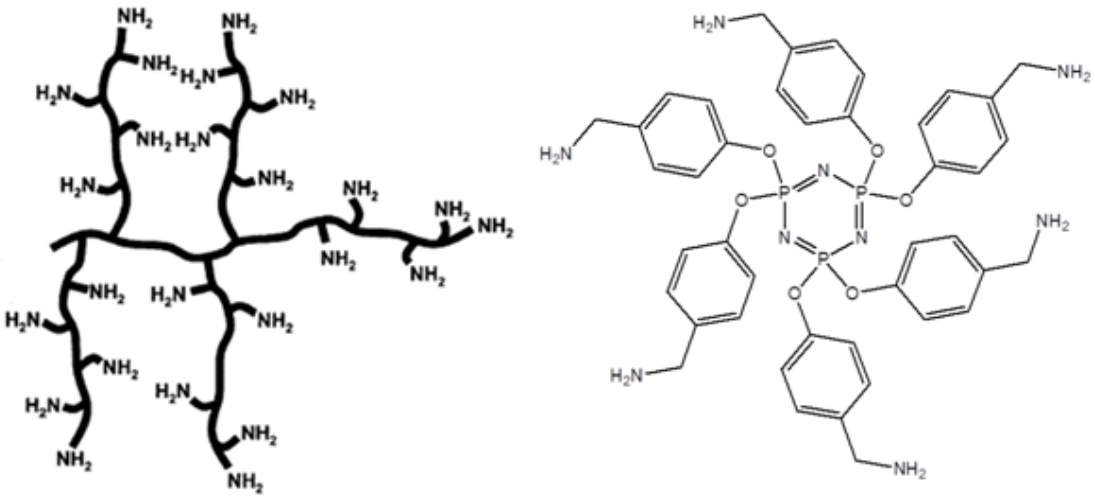

Figure 1.5: Polylysine (left) and cyclotriphosphazene (right) based initiators for the primary amine initiated ROP of NCAs.[75-77]

1.2.2 Convergent Approach

The convergent or "arm first" approach generally describes the generation of star polymers by "stitching" linear polymeric arms to a core via a multifunctional linking agent. This methodology initially employs the synthesis of living linear polymeric arms which permit further reactivity with a suitable linking agent. As a consequence of the independent arm synthesis, conventional characterization of arm and final star product can be carried out. Due to its often quantitative nature, arm length and star polymer functionality can be readily and accurately determined whilst accurate arm number determination remains challenging and imprecise.[80-82] In spite of the synthetic ease and excellent control afforded, the convergent approach does pose several difficulties including extended linking reaction time and the need to remove unreacted linear arms often using the crude purification process of fractionation.

1.2.2.1 Core Cross Linked Star (CCS) Polypeptides from NCA

The convergent approach for star polypeptide synthesis is an area of growing interest in recent times. In particular, the Qiao group has intensively researched this area reporting star polypeptides or CCS polymers based wholly on polypeptides derived from NCAs.[83,84] Their approach involved the HMDS initiated synthesis of linear PZLL or PBLG arms and subsequent crosslinking of these arms with L-cystine NCA **(Scheme 1.7)**. Removal of the polypeptide protecting groups afforded water soluble star polypeptides possessing amino and carboxylic acid functionalised arms. As well as the arms, functionality is also present in the core owing to the presence of unreacted NCA species from the core crosslinking agent. This feature was utilised to introduce further functionality such as alkyne, alkyl and even fluorescent moieties

into the core via an NCA reactive amino group. In terms of structural control, a vast library of described CCS polypeptides were readily prepared boasting arm number (3 – 349), molecular weight (6 – 15 kDa), core size and total star molecular weight control. Star formation was readily monitored in real time by ^{1}H NMR spectroscopy and SEC further highlighting the absolute control offered by this methodology. As expected, CCS molecular weight distributions (PDI: 1.2 – 1.6) did broaden in comparison to linear polypeptide arms (PDI: < 1.1) and contained residual unreacted linear arm, a feature typical of CCS polymer preparation. The use of DTT to cleave disulphide bonds is well known, therefore its use in conjunction with these disulphide cored CCS polymers afforded star polymer degradation and in some cases triggered the formation of macroscopic structures i.e. organogels. The beauty of this methodology is the ample versatility permitted through the choice of NCA/ polypeptide arm and initiator. For example Qiao et al., through their use of a bifunctional initiator, have further expanded on their work to include CCS polymers with peripheral alkene functionality, a feature they have utilized for thiol-ene "click" chemistry of thiol functionalized poly(ethylene glycol) (PEG).[85] Similarly, the employment of an amino functionalised PEG, served as an initiator for the ROP of L-phenylalanine and L-cystine NCAs to generate CCS polymers with hydrophilic (PEG) periphery.[86]

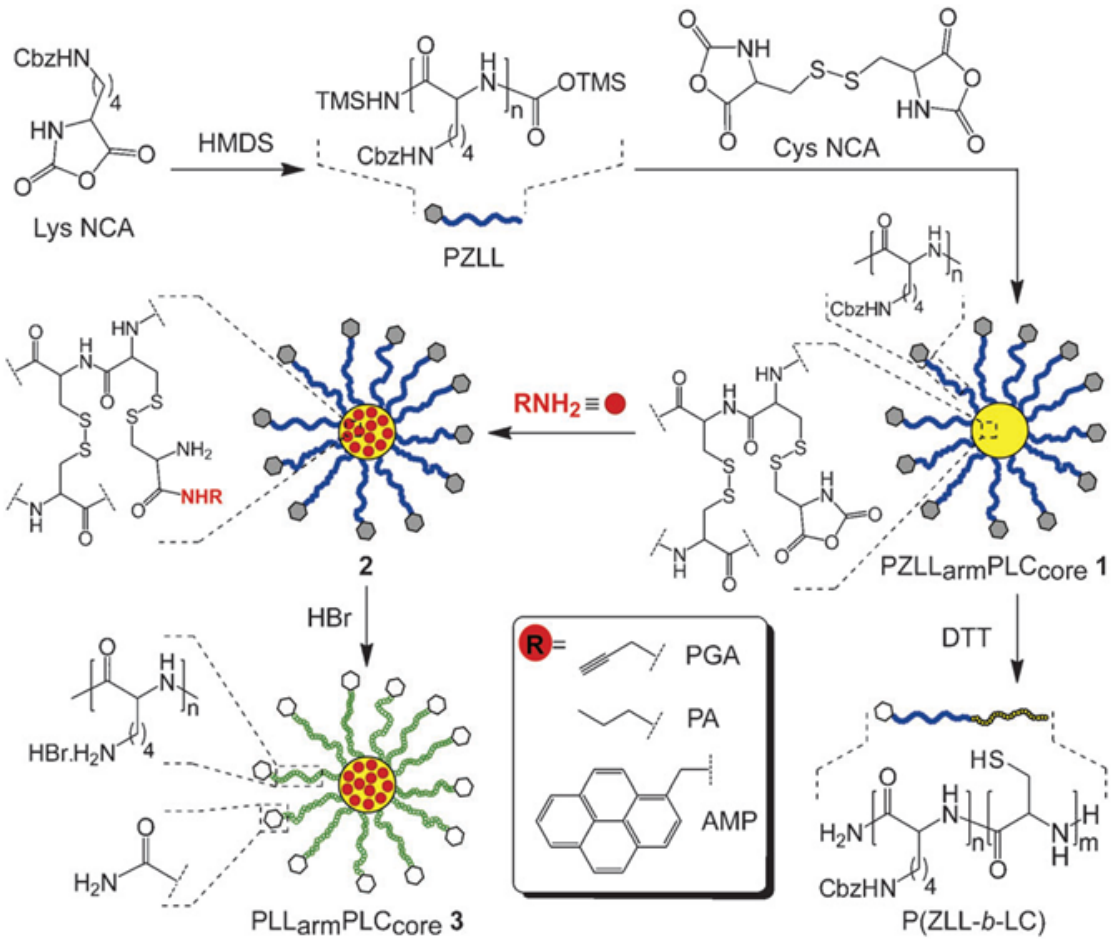

Scheme 1.7: Synthesis of amino acid based CCS polymers. HMDS initiated ROP of lysine NCA afforded linear poly(lysine). The cystine NCA derivative acted as a crosslinker resulting in the formation of CCS polymers with an amino acid core and poly(lysine) arms. Core functionalization was permitted by conjugation of amino functionalized moieties to any unreacted core NCAs.[83]

CCS polymers with polypeptide periphery and styrene cores were synthesized via the cross-linking of styrenic terminated PBLG arms with divinylbenzene.[87] Styrenic terminated PBLG was generated using 4-vinyl benzylamine as initiator for BLG NCA ring opening polymerization and the resultant arms were crosslinked with varying feed ratios of divinylbenzene in a free radical polymerization or RAFT process. Star formation was readily followed using SEC from which a range of high molecular weight (200 kDa – 10000 kDa) CCS polymers were synthesised. The polypeptide arms enabled water soluble and pH responsive CCS polymers.

1.2.2.2 Multifunctional Linking of Linear Polypeptides

Apart from CCS polymers, the "arm first" approach towards star polypeptides, was further investigated using alkyne terminated PBLG and multifunctional azide terminated polyhedral oligomeric silsesquioxane (POSS).[88] Click chemistry efficiency was confirmed by ^{1}H NMR and ^{13}C NMR spectroscopy, generating POSS decorated with multiple polypeptide arms. Furthermore, Hadjichristidis et al. used a trifunctional isocyanate linking agent to couple PBLG-b-PZLL linear arms to this small core **(Scheme 1.8)**.[89] The 3-armed polymers synthesized using this methodology displayed unprecedented homogeneity and excellent stoichiometric molecular weight agreement.

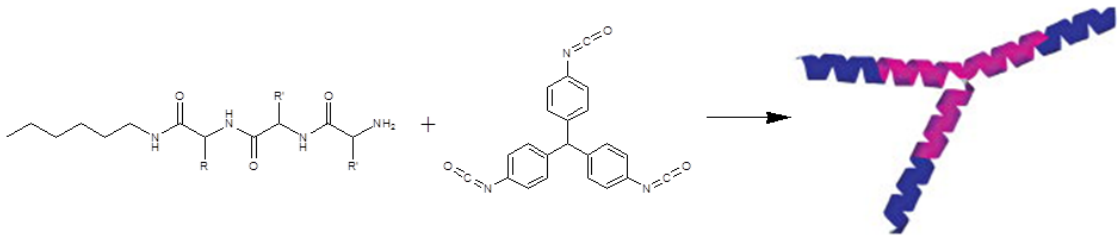

Scheme 1.8: Synthesis of a 3-armed PBLG-b-PZLL star polypeptide by coupling of preformed linear polypeptide arms (via amino end group) to a trifunctional isocyanate moiety.[89]

1.3 NCA Derived Star Polypeptides for Delivery of Therapeutics

The field of nanomedicine and in particular the use of synthetic materials within this biomedical context has promoted materials/polymers to the forefront of nanotechnology research in the quest for the next generation of "smart" materials.[90] Nanomedicine is itself a broad field encompassing the strategic use of nanotechnology within the healthcare sector. Applications include regenerative medicine,[91] drug delivery,[92] imaging [93-95] and diagnostics.[96-98] The idea of targeted drug delivery or Ehrlich's "magic bullet" concept has generated great interest in this area owing to the wealth of potential therapeutic and administrative benefits involved.[99] Targeted drug delivery has the potential to enable delivery of potent drug molecules which otherwise exhibit poor biodistribution properties, improve efficacy of existing drugs, reduce adverse side effects and create new administrative pathways.[91,100] In terms of materials, numerous types of nano based materials, specifically designed for targeted drug delivery applications have been reported. Materials include dendrimers,[101,102] polymers,[103,104] liposomes,[105,106] micelles,[107,108] vesicles/polymersomes [109,110] and inorganic nanoparticles **(Figure 1.6)**.[111,112]

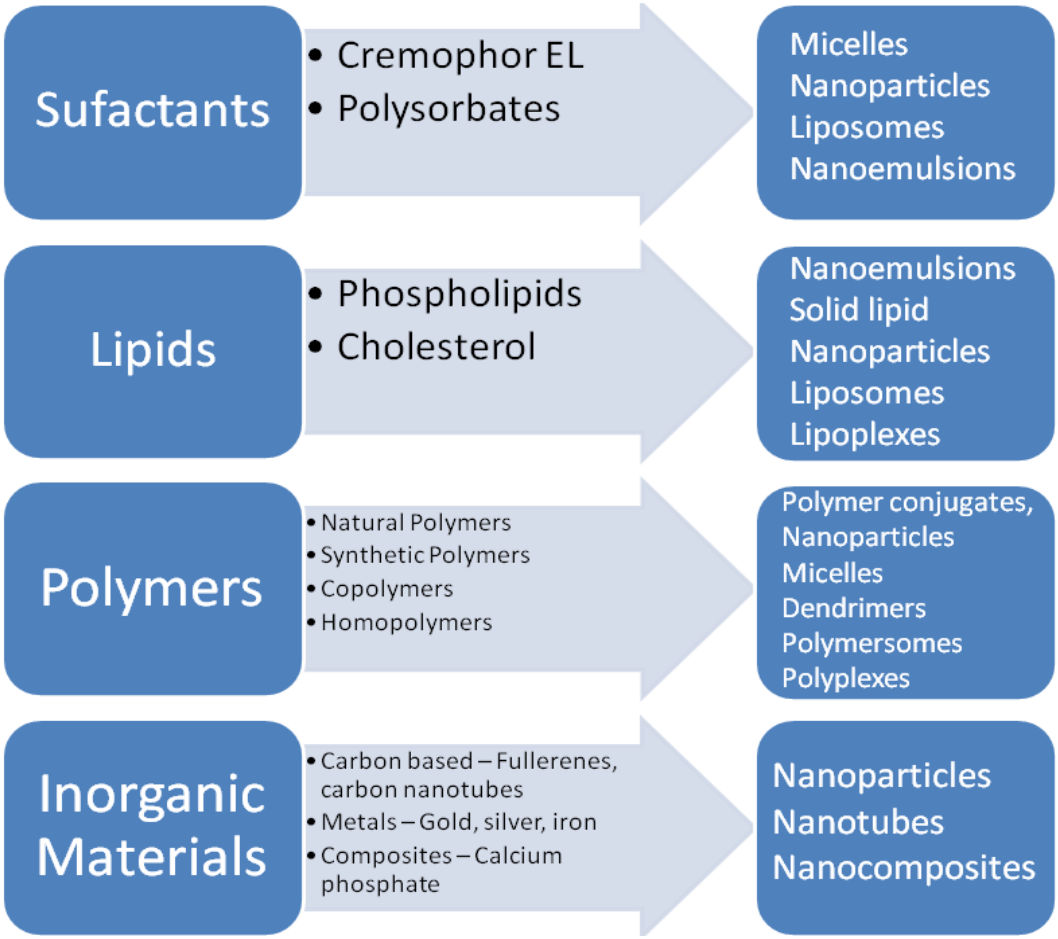

Figure 1.6: Materials used for nano-based drug delivery.[90]

In addition to the conventional drug molecules employed in the treatment of disease, recent times have witnessed the emergence of plasmid DNA (pDNA) and other genetic material as an unconventional but potentially effective therapeutic agent for the treatment and prevention of certain diseases.[113,114] These "drugs" are advantageous over the past small molecule type drugs in that they could potentially treat all diseases whilst being disease specific therefore limiting unwanted side effects observed for example, with common anticancer treatments.[115,116] Furthermore, gene therapy may potentially lead to the prevention of a disease before its presentation whereas conventional drugs can presently only aim to treat a disease after its development and progression.[117] One of the major issues associated with gene therapy is the actual delivery of the genetic therapeutic to the target site. Vectors must be able to protect, deliver, and release their cargo at the target site without triggering an immunological response themselves. Viral vectors although effective carry the safety and potential immunological issues associated with them thus leading to intensive research into the design of effective non-viral gene delivery vectors.[118]

Numerous polymeric based materials have been considered for this role. In particular polypeptide based materials, specifically NCA derived polypeptides have emerged as promising candidates as therapeutic delivery vehicles owing to their inherent biocompatibility and versatility.[119,120] This section, will specifically focus on the applicability of NCA derived star polypeptides towards targeted delivery of therapeutics.

The versatile architectures and compositions of NCA derived star polypeptides renders these materials very useful within a biomedical and in particular a therapeutic delivery context. Their unique architecture and polypeptidic functionality presents unique opportunities for potential cargo encapsulation, cargo binding, cell targeting, stimuli responsive controlled release and enhanced biocompatibility.

1.3.1 Drug Delivery

Star polypeptides from branched amino functionalised PEG have led to the development of a series of materials capable of delivering a wide variety of biologically important cargoes. Complexation of cationic drug molecules such as the anti-cancer drug doxorubicin, with the anionic poly(glutamic acid) (PGA) shell of star shaped PEI-PGA-PEI resulted in the formation of doxorubicin loaded nanoparticles which exhibited controlled release upon a pH trigger (< pH 7.4).[58] Drug loading content could be controlled by configuring the PGA density. Similarly the replacement of PGA with a cationic PLL afforded a star polypeptide capable of complexation with an anionic drug molecule, in this case diclofenac sodium.[59] Elevated pH (> pH 7.4)

provided a trigger for drug release. However a limitation of the two aforementioned delivery vehicles is the fragile stability of the complexes, as observed by leaking of cargos outside of the pH trigger range. In particular a drug delivery vehicle employing a pH trigger of > 7.4 would find very limited applicability, if any, in the human body. More promising however was the complexation, delivery and pH triggered release (< pH 7.4) of a model anionic protein such as insulin using PEI-PLL-PEG star polymer.[57] By using the pH functionality of insulin (isoelectric point (pI) of 5.4), release of the cargo at a potentially applicable pH of <5 was realised in addition to effective cellular uptake. Further development of such materials resulted in star polypeptides capable of the simultaneous loading with both hydrophobic and hydrophilic moieties. [59] Encapsulation of the hydrophobic pyrene was permitted by the incorporation of a poly(phenyl alanine) inner shell whereas PLL and PGA outer shells permitted encapsulation of hydrophilic molecules such as doxorubicin and rose bengal respectively. Again pH, depending on the type of polypeptide outer shell, provided the trigger for controlled release. No hydrophobic cargo release mechanism was provided, however, thus limiting such a multi cargo delivery platform.

PEI-PBLG star polypeptides enabled the formation of micelles capable of encapsulating pH responsive dyes. The efficient encapsulation resulted in the reversible phase transfer of dyes between aqueous and organic solutions. Although encapsulation of just dyes was reported, such materials should in theory be able to replicate these results for drug molecules.[53] Star shaped poly(histidine) (PEI-PHis-PEG) provided a branched material capable of encapsulating insulin with impressive encapsulation efficiency via the cationic/hydrophobic imidazole ring of histidine **(Figure 1.7)**.[51] The described complexes exhibited superior stability towards high salt concentrations and particle sizes capable of loading into poly(lactide-co-glycolide) (PLGA) microspheres. The star shaped poly(histidine) offered improved buffering capacity within the microsphere, therefore prolonging microsphere degradation to afford a long term sustained release of insulin. In mice this material was shown to effectively control blood glucose levels over a one month period highlighting its potential as a long term drug delivery vehicle.

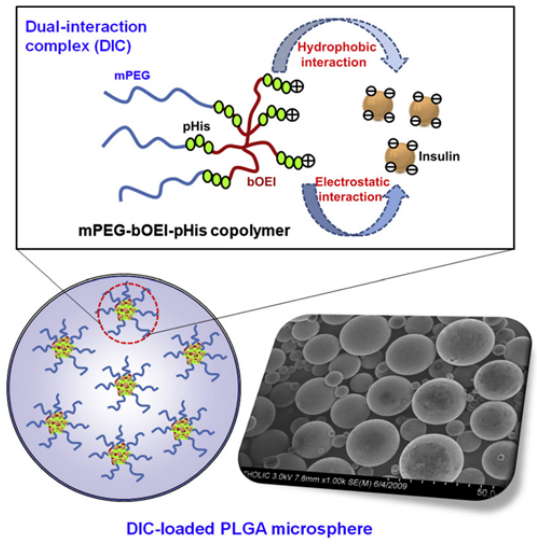

Figure 1.7: Microsphere encapsulation of star shaped poly(histidine)/insulin nanocomplexes. Sustained release of insulin was afforded by prolonged degradation of the poly(lactide-co-glycolide) (PLGA) microspheres resulting in effective control of glucose.[51]

Several examples of the drug delivery potential of star polypeptides comprising a dendrimer core and polypeptide periphery have been reported. Using a four-armed amino terminated, disulphide cored PAMAM dendrimer derivative with a diethylene glycol-L-glutamate outer shell, reduction and thermo sensitive micelles and hydrogels were readily prepared **(Figure 1.8)**.[121] Temperature (LCST at 40°C) and DTT triggered reduction permitted micelle and hydrogel size control. Release of doxorubicin from reduction sensitive micelles was shown to increase the release rate by 50% but the star polypeptide exhibited a more prolonged release profile than a comparative linear analogue. Such an effect highlights the benefit of a star architecture in controlled release applications. In spite of this the trigger specific drug release was questionable due to nonspecific release of doxorubicin without DTT limiting the realistic applicability of this material.

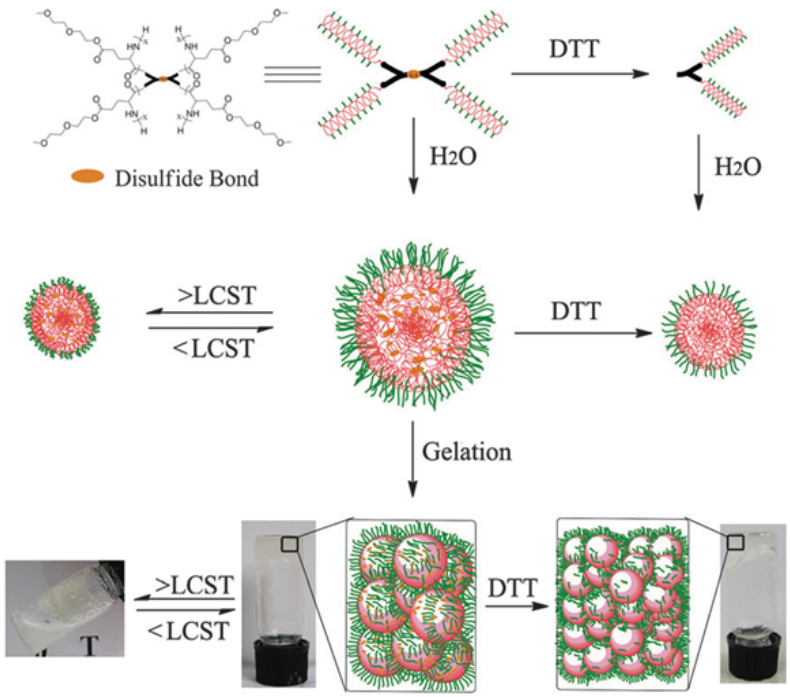

Figure 1.8: Dual responsive micelle and hydrogel behaviour of star shaped diethylene glycol-L-glutamate. The disulphide core of PAMAM dendrimer and diethylene glycol periphery elicits both thermo and reduction responsiveness towards the controlled release of doxorubicin.[121]

The potential of a series of generation 2 and 3 PAMAM dendrimers decorated biodegradable PGA were investigated as drug delivery vehicles.[122] Albeit drug encapsulation, the polymers showed susceptibility to enzymatic degradation, a potential release stimulus, whilst selectively targeting and labelling tumorous cells. The polypeptidic nature of these materials i.e. glutamic acid rendered them enzymatically sensitive and the branched architecture prolonged enzymatic degradation in comparison to linear PGA. Furthermore the star architecture resulted in superior functionality arising from the numerous PGA arms and terminal amines present on these arms. Consequently post modification of these materials was readily achieved via the covalent attachment of folic acid, a targeting moiety for cancer cells typically over expressing folate receptors, and a fluorescent moiety for diagnostic purposes.

The use of sugars as a targeting moiety was employed by Qiu et al. in their use of star polypeptide/methacrylate hybrids as polymers for drug delivery.[50] The glycol moiety favoured specific targeting to the lectin, Concanavalin A. As before the star architecture again emphasized its advantages through superior encapsulation efficiency and prolonged drug release profile as opposed to a linear counterpart. Release rate was triphasic however,

suggesting initial uncontrolled release and then subsequent controlled release of doxorubicin by diffusion.

Star polypeptides of 4-armed PEG-PZLL could self assemble to form vesicles and were shown to exhibit low cytotoxicity (cell viability up to concentration of 0.5 g/L).[61] Vesicles were successfully loaded with doxorubicin and the anti-cancer drug loaded polymeric vesicles were effectively internalized by breast cancer cells. Such a material shows promise as an effective anti-cancer drug delivery vehicle.

Amongst star polypeptides, amino acid based CCS polymers have emerged as leading candidates for the delivery of chemotherapy agents. Their synthetic design of 100% amino acid composition and disulphide functionalised core provides these materials with potentially superior biocompatibility and specific but effective drug release triggers. Qiao et al. have reported a CCS polymer with PLL arms which provided the cationic functionality required to aid cell internalization.[88] Furthermore the lysine amino side chain enabled further CSS polymer modification through pegylation, fluorescent labelling and attachment of folic acid for cell targeting. Pegylation provided the polymers with "stealth" properties further enhancing their biocompatibility and effectiveness as drug delivery vehicles.[123] The polymers were shown to be significantly biocompatible and were shown to be selectively internalized by breast cancer cells owing to the use of a folic acid targeting moiety. In a similar approach, Ding et al. adopted a poly(phenylalanine)-b-PEG armed CCS polymer for the cellular delivery of doxorubicin **(Figure 1.9)**.[89] As a result of the disulphide cross-linked core a suitable reducing agent such as glutathione, an agent suspected of elevated concentration levels in certain cancerous cells, was used to trigger the release of doxorubicin. Release was glutathione concentration dependent but more importantly, release was only observed in cells specifically treated with glutathione highlighting the site specific release profile of such materials. This feature in combination with a suitable targeting agent identifies these materials as truly realistic candidates for the targeted delivery of drug molecules.

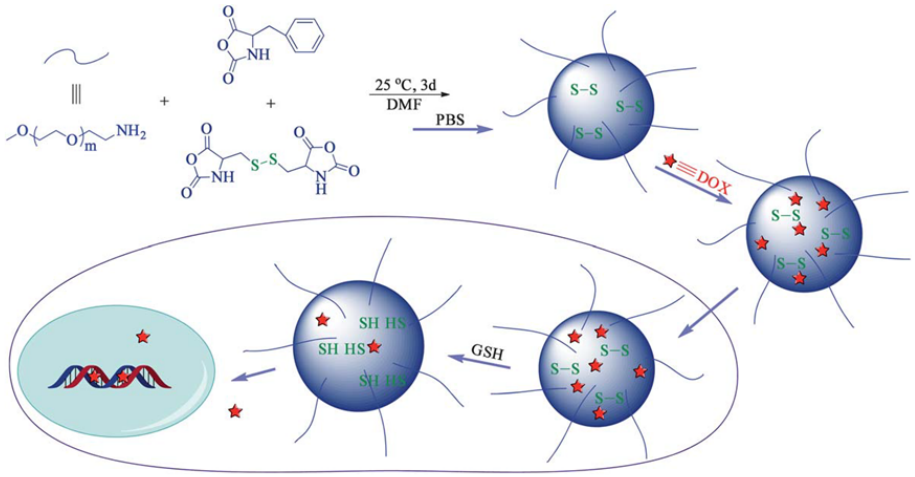

Figure 1.9: Synthesis, loading and triggered release of doxorubicin from CCS polypeptides. The hydrophobic phenylalanine moieties of the CCS polymers permitted loading with doxorubicin. Release was triggered by cleavage of the reduction sensitive CCS polymer cores with glutathione.[89]

1.3.2 Gene Delivery

A minimum prerequisite in the design of non-viral gene delivery vectors is that the material must be able to complex the genetic cargo. The easiest and most common way of doing so takes advantage of the anionic nature of pDNA, siRNA etc. therefore permitting the formation of an electrostatic complex with a cationic vector. Complexation capacities of genetic material by cationic vectors are characterised in terms of N/P ratio i.e. ratio between the molar concentration of amine or cationic charge from the vector and the molar concentration of phosphate or anionic charge from the genetic cargo. Considering NCA derived star polypeptides, several examples of their use as non-viral gene delivery vectors have been reported. Tian et al. utilised a branched PEG-b-PEI-b-PBLG copolymer as proof of principle **(Figure 1.10)**.[52,53] The PEI segment afforded complexation with pDNA whereas PBLG helped to introduce limited biodegradability to the system through use of the enzyme trypsin. Characterization of the complexes was limited however, thus highlighting the potential but limited applicability of this material. Similarly branched PEI-b-PBLG successfully complexed pDNA to form discrete adequately sized nanocomplexes (96 nm).[54] The described polymers were shown to effectively enhance protection of their cargo from enzymatic degradation by DNase whilst also showing improved cytotoxicity over unmodified hyperbranched PEI. Furthermore, these polymers displayed improved transfection efficiencies over PEI possibly arising from their improved cytotoxicity and favourable hydrophobic cellular interactions with PBLG.

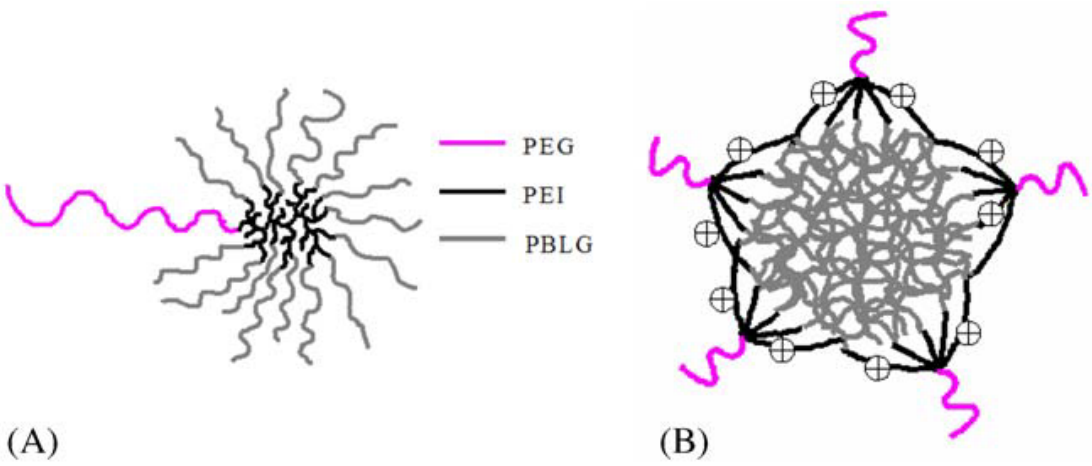

Figure 1.10: (A) PEI-PBLG-PEG star polymer comprising a branched PEI core, PBLG arms and and (B) cationic micelle due to protonation of PEI.[52]

Lysine, a well known cationic amino acid has shown great promise as a gene delivery vector owing to its cationic character and potential degradability and biocompatibility. The polymerization of lysine NCA has readily led to the development of several poly(lysine) decorated dendrimer systems for gene delivery. A series of G3-PAMAM dendrimers with variable poly(lysine) chain lengths (n = 5,10,20,40) were readily complexed with pDNA.[42] Star polypeptides with longer poly(lysine) chain lengths were shown to favourably interact with pDNA to form stronger complexes as determined by gel electrophoresis. Cellular studies were not provided whereas ^{1}H and ^{13}C NMR spectroscopy provided evidence of polypeptide conjugation to dendrimer but no molecular weight distribution or size analysis was conducted. More recently, generation 4 PAMAM dendrimers with short poly(lysine) arm lengths (2 – 6 units) were prepared by ROP of benzyloxycarbonyl lysine NCA.[124] Polypeptide conjugation and the arm average degree of polymerization were confirmed by ^{1}H NMR spectroscopy highlighting molecular weight control by controlling monomer/initiator feed ratio. Removal of lysine protecting groups afforded cationic star polypeptides capable of effectively complexing pDNA at low N/P ratios as confirmed by ζ- potential and agarose gel electrophoresis. DLS and AFM confirmed the formation of desirably spherical and monodisperse nano-complexes with a size range of 100-200nm. The described system was shown to exhibit greatly improved cytotoxicity and transfection efficiency results compared to linear poly(lysine) and an unmodified G4-PAMAM dendrimer emphasising the importance of architecture and poly(lysine) functionality. Furthermore the stability of complexes towards the destabilising

effects of serum was evaluated with star shaped poly(lysine) of arm length 3.8 monomer units, displaying a resistance capability better than several commercially available transfection agents. The potential of these materials as viable transfection agents was investigated through the delivery of a gene responsible for inhibiting the development of restenosis in a rabbit model. Inhibition of this ailment was significantly enhanced through the use of gene therapy via the described transfection agents.

Star shaped PEG with 8 terminal amino groups led to the generation of a cationic star shaped polypeptide through ROP of the NCA of a piperidinyl derivative of BLG (VB-L-Glu NCA) (**Figure 1.11).**[125] The star shaped polypeptide, PEG-poly(γ-4-((2-(piperidin-1-yl)ethyl)aminomethyl)benzyl-L-glutamate)(PEG-PPABLG) in comparison to suitable homopolymer, diblock, triblock and graft architectures demonstrated an enhanced DNA condensation capacity most likely attributable to a higher density of cationic polymeric arms. However, the described polymer exhibited lower cytotoxicity whilst exhibiting overall superior transfection efficiencies highlighted by its 3-134 fold increase in transfection efficiency performance over the commercially available lipofectamine. Such a feature demonstrates the significant role of polymer architecture in the molecular design of new gene transfection agents.

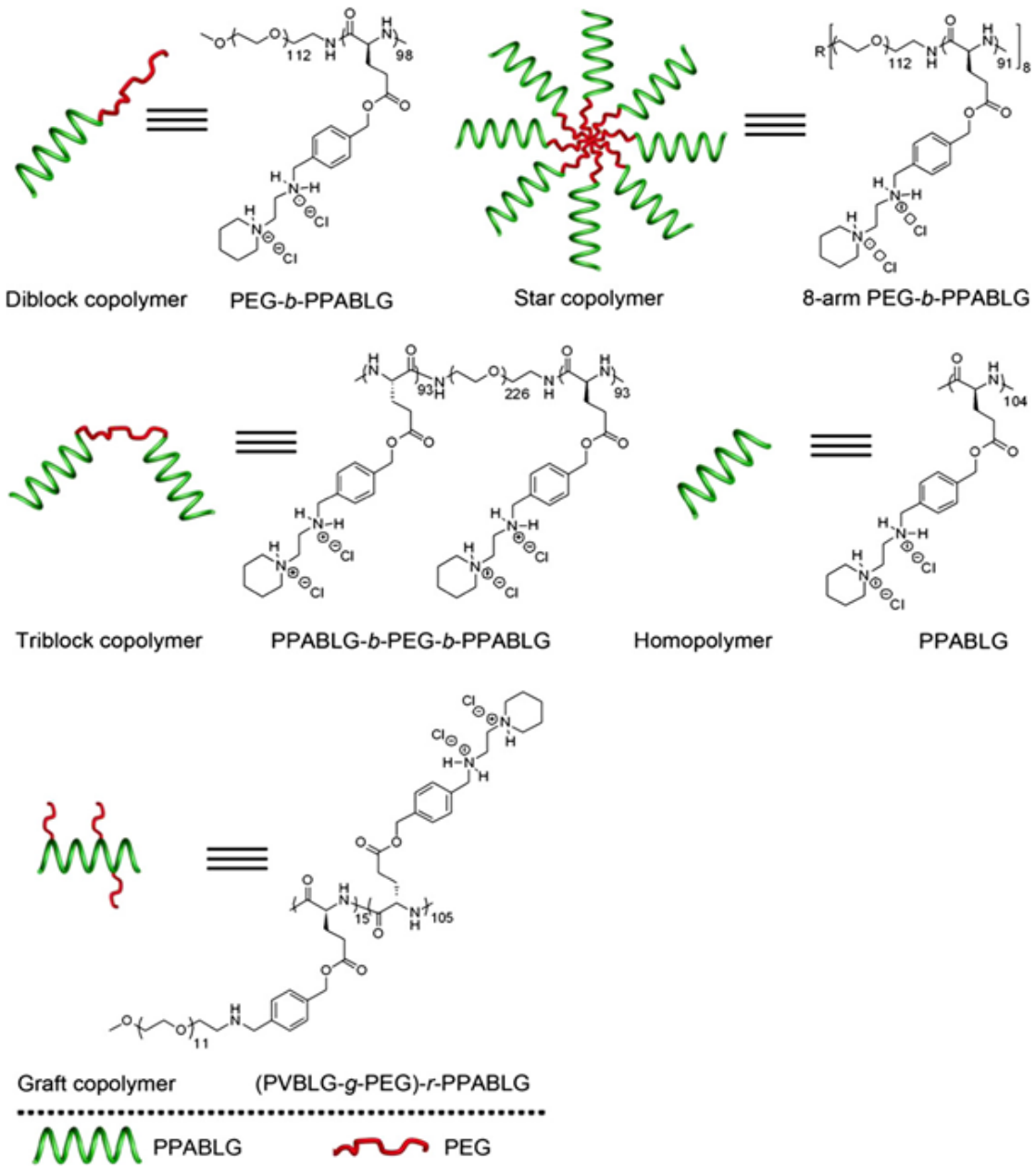

Figure 1.11: Different architectures of PEG-PPABLG conjugates as gene transfection agents. Cationic functionality was introduced via a piperidinyl derivative of BLG NCA and its subsequent polymerization with linear and branched amino terminated PEG derivatives afforded a range of cationic star shaped architectures. [125]

The growth of PBLG from a G2-PAMAM dendrimer and subsequent aminolysis with G1-PAMAM dendrimers resulted in a system comprising a G2-PAMAM dendrimer core, polypeptide inner shell and a G1-PAMAM periphery **(Figure 1.12)**.[126] The described vector, known as ALA, could effectively compact pDNA into monodisperse cationic complexes <200nm in size, something which the individual constituents of ALA could not. ALA displayed negligible cytotoxicity but more importantly however exhibited unprecedented transfection efficiencies

in the presence of serum. Serum was actually shown to improve the transfection efficiencies of ALA, a feature particularly prevalent in the actual real world application of vectors in the human body. Consequently such a feature differentiates this material from the other reported polycationic gene delivery vectors.

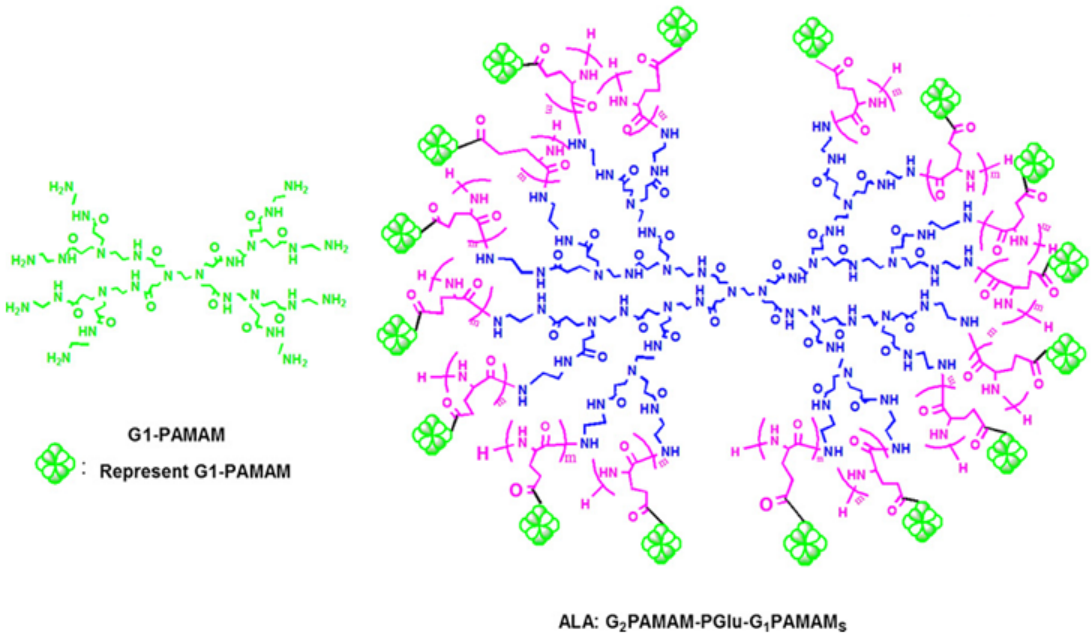

Figure 1.12: ALA as a vector for pDNA transfection. The generation of star shaped PBLG was accomplished using the generation 2 PAMAM initiated ROP of BLG NCA. Aminolysis of the PBLG arms with generation 1 PAMAM dendrimer moieties resulted in a star shaped polypeptide with peripheral dendrimer functionalisation for the electrostatic mediated complexation of pDNA.[126]

To conclude, the generation of star shaped polymers in particular polypeptides can be realized through the use of a number of different strategies to afford a wide range of novel functional materials. The potential applicability of such materials towards the area of therapeutic delivery has already been demonstrated and and will continue to develop with the advent of more advanced novel materials. The aim of this thesis herein, is to develop a range of novel star shaped polymer platforms, boasting versatile functionality, compostion and architecture for the targeted delivery of therapeutics.

1.4 References

1. Leuchs, H., *Ber*., **1906**, 39, 857.

2. G. J. M. Habraken, C. E. Koning, A. Heise, *J. Polym. Sci.: Part A: Polym. Chem*., 2009, 47, 6883.

3. D. Bartlett, H. Jones, *J. Am. Chem. Soc*., **1957**, 79, 2153.

4. D. Bartlett, C. Dittmer, *J. Am. Chem. Soc*., **1957**, 79, 2159.

5. E. Miller, I. Fankuchen, H. Mark, *J. Appl. Phys*., **1949**, 20, 531.

6. H. Leuchs and W. Manasse, *Ber*., **1907** 40, 3235.

7. W. Geiger, H. Leuchs, *Ber*., **1908**, 41, 1721.

8. E. Peggion, H. Leuchs and W. Manasse, *Ber*., **1907**, 40, 3235.

9. M. Goodmann, J. Hutchison, *J. Am. Chem. Soc*., **1966**, 88, 3627.

10. D. Ballard, C. Bamford, *Proc. R. Soc. (London),* **1954**, A223, 495.

11. D. Ballard, C. Bamford, F. Weymouth, *Proc. R. Soc. (London),* **1954/1955**, A227, 155.

12. D. Ballard, C. Bamford, *J. Am. Chem. Soc*., **1957**, 79, 2336.

13. P. Doty, R. Lundberg, *J. Am. Chem. Soc*., **1957**, 79, 2338.

14. D. Thunig, J. Semen, H. Elias, *Makromol. Chem*., **1977**, 178, 603.

15. M. Goodmann, J. Hutchison, *J. Am. Chem. Soc*., **1965**, 87, 3524.

16. C. Bamford, H. Block, *J. Chem. Soc*., **1961**, 83, 4989.

17. M. Szwarc, *Adv. Polym. Sci*., **1965**, 4, 1.

18. W. Diekmann, F. Breest, *Ber*., **1906**, 39, 3052.

19. D. Ballard, C. Bamford, F. Weymouth, *Nature*, **1967**, 174, 173.

20. M. Rothe, D. Muhlausen, *Angew. Chem., Int. Ed.,* **1976**, 15, 307.

21. N. Hadjichristidis, H. Iatrou, M. Pitsikalis, G. Sakellariou, *Chem. Rev*., **2009**, 109, 5528.

22. E. Peggion, E. Cosani, A. Mattuchi, E. Scoffone, *Biopolymers,* **1964**, 2, 69.

23. G. J. M. Habraken, H. R. Karel, M. Wilsens, C. E. Koning, A. Heise, *Polym. Chem*., **2011**, 2, 1322.

24. H. Lu, J. Cheng, *J. Am. Chem. Soc*., **2007**, 129, 14114.

25. I. Dimitrov, H. Schlaad, *Chem. Commun*., **2003**, 2944.

26. T. Deming, *Nature,* **1997**, 390, 386.

27. T. Deming, *J. Am. Chem. Soc*., **1998**, 120, 4240.

28. T. Deming, *Macromolecules*, **1999**, 32, 4500.

29. M. A. Mintzer, M. W. Grinstaff, *Chem. Soc. Rev*., **2011**, 40, 173–190

30. C. C. Lee, J. A. MacKay, J.M. J. Fréchet, F. C. Szoka, *Nat. Biotechnol.*, **2005**, 23, 1517.

31. S. Svenson, D. A. Tomalia, *Adv. Drug Deliv. Rev*., **2005**, 57, 2106.

32. J.M. J. Fréchet, *J. Polym. Sci. Part A: Polym. Chem*., **2003**, 41, 3713.

33. D. A. Tomalia, J.M. J. Fréchet, *J. Polym. Sci. Part A: Polym. Chem*., **2002** 40, 2719.

34. D. A. Tomalia, *Soft Matter*, 2010, 6, 456.

35. D. A. Tomalia, A. M. Naylor, W. A. Goddard, *Angew. Chem., Int. Ed*., **1990**, 29, 138.

36. E. R. Gillies, , J.M. J. Fréchet, *DDT*, **2005**, 10, 35.

37. S. H. Medina, M. E. H. El-Sayed, *Chem. Rev*., **2009**, 109, 3141.

38. K. Aoi, K. Tsutsumiuchi, A. Yamamoto, M. Okada, *Tetrahedron*, **1997**, 53, 15415.

39. N. Higashi, A. Uchino, Y. Mizuguchi, M. Niwa, *I. J. Biol.Macromol.*, **2006**, 38, 120.

40. H. Huang, C. M. Dong, Y. Wei, *Comb. Chem. High Throughput Screening*, **2007**, 10, 368.

41. G. Liang, Q. Wu, S. Bao, F. Zhu, Q. Wu, *Polym. Chem*., **2013**, 4, 5671.

42. N. Higashi, T. Koga, M. Niwa, *Adv. Mater*., **2000**, 12, 1373.

43. N. Higashi, T. Koga, N. Niwa, M. Niwa, *Chem. Commun*., **2000**, 361.

44. K. Aoi, T. Hatanaka, K. Tsutsumiuchi, M. Okada, T. Imae, *Macromol. Rapid Commun*., **1999**, 20, 378.

45. D. Appelhans, H. Komber, R. Kirchner, J.Seidel, C. F. Huang, D. Voigt, D. Kuckling,F. C. Chang, B. Voit, *Macromol. Rapid Commun*. **2005**, 26, 586.

46. T. Aliferis, H. Iatrou, N. Hadjichristidis, J. Messman, J. Mays, *Macromol. Symp*. **2006**, 240, 12.

47. S. Qiu, H. Huang, X. Dai, W. Zhou, C. Dong, *J. Polym. Sci.: Part A: Polym. Chem*, **2009**, 47, 2009.

48. W. Park, D. Kim, H. C. Kang, Y. H. Bae, K. Na, *Biomaterials*, **2012**, 33, 8848.

49. H. Y. Tian, C. Deng, H. Lin, J. Sun, M. Deng, X. Chen, X. Jing, Biomaterials, **2005**, 26 4209.

50. H. Tian, X. Chen, H. Lin, C. Deng, P. Zhang, Y. Wei, X. Jing, Chem. Eur. J., **2006**, 12, 4305.

51. H. Tian, W. Xiong, J. Wei, Y. Wang, X. Chen, X. Jing, Q. Zhu, *Biomaterials*, **2007**, 28 2899.

52. Q. Wang, J. Yu, Y. Yan, S. Xu, F. Wang, Q. Li, J. Wang, X. Zhang, D. Liu, *Polym. Chem*., **2012**, 3, 1284.

53. J. Li, S. Xu, J. Zheng, Y. Pan, J. Wang, L. Zhang, X. He, D. Liu, *Chem. Eur. J*., **2012**, 48, 1696.

54. Y. Yan, D. Wei, J. Li, J. Zheng, G. Shi, W. Luo, Y. Pan, J. Wang, L. Zhang, X. He, D. Liu, *Acta Biomaterialia*, **2012**, 8, 2113.

55. H. Huang, J. Li, L. Liao, J. Li, L. Wu, C. Dong, P. Lai, D. Liu, *Chem. Eur. J*., **2012**, 48, 696.

56. Y. Yan, J. Li, J. Zheng, Y. Pan, J. Wang, X. He, L. Zhang, D. Liu, *Colloids and Surfaces B: Biointerfaces*, **2012**, 95, 137.

57. C. S. Choa, Y. I. Jeong, S. H. Kim, J. W. Nah, M. Kubotae, T. Komoto, *Polymer*, **2000**, 41, 5185.

58. K. Wang, H. Q. Dong, H. Y. Wen, M. Xu, C. Li, Y. Y. Li, H. N. Jones, D. L. Shi, X. Z. Zhang, *Macromol. Biosci*., **2011**, 11, 65.

59. P. D. Thornton, S. M. R. Billah , N. R. Cameron, *Macromol. Rapid Commun*., **2013**, 3, 257.

60. A. Karatzas, P. Bilalis, H. Iatrou, M. Pitsikalis, N. Hadjichristidis, *React. Funct. Polym*., **2009**, 69, 435.

61. A. S. Ferrer, R. Mezzenga, *Macromolecules* **2010**, 43, 1093.

62. S. Abraham, C. S. Ha, I. Kim, *J. Polym. Sci., Part A: Polym. Chem*., **2006**, 44, 2774.

63. K. Khanna, S. Varshney, A. Kakkar, *Polym. Chem*., **2010**, 1, 1171.

64. I. Botiz, N. Grozev, H. Schlaad, G. Reiter, *Soft Matter*, **2008**, 4, 993.

65. J. Sun, X. Chen, J. Guo, Q. Shi, Z. Xie, X. Jing, *Polymer*, **2009**, 50, 455.

66. J. Babin, C. Leroy, S. Lecommandoux, R. Borsali, Y. Gnanou, D. Taton, *Chem. Commun.*, **2005**, 1993.

67. J. Babin, D. Taton, M. Brinkmann, S. Lecommandoux, *Macromolecules,* **2008**, 41, 1384.

68. A. Karatzas, H. Iatrou, N. Hadjichristidis, *Biomacromolecules,* **2008**, 9, 2072.

69. S. Junnila, N. Houbenov, A. Karatzas, N. Hadjichristidis, A. Hirao, H. Iatrou, O. Ikkala, *Macromolecules,* **2012**, 45, 2850.

70. S. S. Naik, J. W. Chan, C. Comer, C. E. Hoyle, D. A. Savin, Polym. *Chem.*, **2011**, 2, 303.

71. J. Rao, Y. Zhang, J. Zhang, S. Liu, *Biomacromolecules,* **2008**, 9, 2586.

72. M. Ormo, A. B. Cubitt, K. Kallio, L. A. Gross, R. Y. Tsien, S. J. Remington, *Science*, **1996**, 273, 1392.

73. H. A. Klok, J. R. Hernandez, S. Becker, K. Mullen, *J. Polym. Sci., Part A: Polym. Chem*., **2001**, 1572.

74. J. R. Hernhdez, J. Qu, E. Reuther, H. A. Klok, K. Mullen, *Polym. Bull*., **2004**, 52, 57.

75. K. Inoue, H. Sakai, S. Ochi, T. Itaya, T. Tanigaki*, J. Am. Chem. Soc*., **1994**, 116, 10783.

76. K. Inoue, S. Horibe, M. Fukae, T. Muraki, E. Ihara, H. Kayama, *Macromol. Biosci*., **2003**, 3, 26.

77. H. A. Klok, J. R. Hernandez, *Macromolecules,* **2002**, 35, 8718.

78. D. Yonga, Y. Luoa, F. Dua, J. Huanga, W. Lua, Z. Daic, J. Yua, S. Liu, *Colloids and Surfaces B: Biointerfaces*, **2013**, 105, 31.

79. M. Jia, T. Ren, A. Wang, W. Yuan, J. Ren, *J. Appl. Polym. Sci*., **2014**, DOI: 10.1002/APP.40097.

80. A. Blencowe, J. F. Tan, To. K. Goh, G. G. Qiao, *Polymer*, **2009**, 50, 5.

81. V. Y. Lee, K. Havenstrite, M. Tjio, M. McNeil, H. M. Blau, R. D. Miller, J. Sly, *Adv. Mater*., **2011**, 39, 4509.

82. E. A. Appel, V. Y. Lee, T. T. Nguyen, M. McNeil, F. Nederberg, J. L. Hedrick, W. C. Swope, J. E. Rice, R. D. Miller, J. Sly, *Chem. Commun*., **2012**, 48, 6163.

83. A. Sulistio, A. Widjaya, A. Blencowe, X. Zhang, G. G. Qiao, *Chem. Commun*., **2011**, 47, 1151.

84. A. Sulistio, A. Blencowe, A. Widjaya, X. Zhang, G. G. Qiao, *Polym. Chem*., **2012**, 3, 224.

85. A. Sulistio, J. Lowenthal, A. Blencowe, M. N. Bongiovanni, L. Ong, S. L. Gras, X.Zhang, G. G. Qiao, *Biomacromolecules,* **2011**, 12, 3469.

86. J. Ding, F. Shi, C. Xiao, L. Lin, L. Chen, C. He, X. Zhuang, X. Chen, *Polym. Chem*., **2011**, 2, 2857.

87. F. Audouin, J. Ruther, I. Knoop, J. Huang, A.Heise, *J. Polym. Sci., Part A: Polym. Chem*., **2010**, 48, 4602.

88. S. W. Kuo, H. T. Tsai, *Polymer*, **2010**, 51, 5695.

89. T. Aliferis, H. Iatrou, N. Hadjichristidis, *J. Polym. Sci., Part A: Polym. Chem*., **2005**, 43, 4670.

90. V. R. Devadasu, V.Bhardwaj, M. N. V. R. Kumar, *Chem. Rev*., **2013**, 113, 1686.

91. A. P. Nowak, V. Breedveld, L. Pakstis, B. Ozbas, D. J. Pine, D. Pochan and T. J. Deming, *Nature*, **2002**, 417, 424.

92. Y. Wang, J. D. Byrne, M. E. Napier, J. M. DeSimone, *Adv. Drug Deliv. Rev*., **2012**, 64, 1021.

93. A. Joseph, L. Villaraza, A. Bumb, M. W. Brechbiel, *Chem. Rev*., **2010**, 110, 2921.

94. N. Lee, T. Hyeon, *Chem. Soc. Rev*., **2012**, 41, 2575.

95. T. Borase, T. Ninjbadgar, A. Kapetanakis, S. Roche, R. O' Connor, C. Kerskens, A. Heise, D. F. Brougham, *Angew. Chem. Int. Ed*., **2013**, 52, 3164.

96. J. H. Ryu, H. Koo, I. C. Sun, S. H. Yuk, K. Choi, K. Kim, I. C. Kwon, *Adv. Drug Deliv. Rev*., **2012**, 64, 1447.

97. M. Perfézou , A. Turner, A. Merkoçi, *Chem. Soc. Rev*., **2012**, 41, 2606.

98. A. Escosura-Muñiz, C. Sánchez-Espinel, B. Díaz-Freitas, A. González-Fernández, M. Maltez da Costa M, A. Merkoçi., *Anal. Chem*., **2009**, 81, 10268.

99. K. Strebhardt, A. Ullrich, *Nature Reviews Cancer*, **2008**, 8, 473.

100. S. Parveen, R. Misra, S. K. Sahoo, *Nanomedicine: Nanotechnology, Biology, and Medicine*, 2012, 8, 147.

101. P. Sharma and S. Garg, Adv. *Drug Delivery Rev*., **2010**, 62, 491.

102. S. Zhu, M. Hong, L. Zhang, G. Tang, Y. Jiang and Y. Pei, *Pharm. Res*., **2010**, 27, 161.

103. P. F. Gou, W. P. Zhu, Z. Q. Shen, *Biomacromolecules*, 2010, 11, 934.

104. G. M. Soliman, A. Sharma, D. Maysinger, A. Kakkar, *Chem. Commun*., **2011**, 47, 9572.

105. F. Maestrelli, M. L. Gonzalez-Rodriguez, A. M. Rabasco, P. Mura*, Int. J. Pharm*., **2006**, 312, 53.

106. J. Adler-Moore, R. T. Proffitt, *J. Antimicrob. Chemother*., **2002**, 49, 21.

107. K. Wang, Y. Liu, C. Li, S. X. Cheng, R. X. Zhuo, X. Z. Zhang, *ACS Macro Letters*, **2013**, 2, 201.

108. H. Wei, R. X. Zhuo, X. Z. Zhang, *Prog. Polym. Sci*., **2013**, 38, 503.

109. H. De Oliveira, J. Thevenot, S. Lecommandoux, Wiley *Interdiscip. Rev. Nanomed. Nanobiotechnol*., 2012, 5, 525.

110. M. Marguet, L. Edembe, S. Lecommandoux, *Angew. Chem. Int. Ed*., **2012**, 5, 1173.

111. D. B. Chithrani, S. Jelveh, F. Jalali, M. van Prooijen, C. Allen, R. G. Bristow, *Radiat. Res*., **2010**, 173, 719.

112. S. P. Foy, V. Labhasetwar, *Biomaterials,* **2011**, 32, 9155.

113. D. Castanotto, J. J. Rossi, *Nature*, **2009**, 457, 426.

114. L. W. Seymour, A. J. Thrasher, *Nat. Biotechnol*., **2012**, 7, 588.

115. O. Humbert, L. Davis, N. Maizels, Crit*. Rev. Biochem. Mol. Biol*., **2012**, 3, 264.

116. C. P. Locher, D. Putnam, R. Langer, S. A. Witt, B.M. Ashlock, J. A. Levy*, Immunol. Lett*., **2003**, 90, 67.

117. A. L. David, S. N. Waddington, *Methods in Molecular Biology (New York, NY, United States)*, **2012**, 891, 9-39.

118. E. Check, *Nature*, **2002**, 6912, 116.

119. T. J. Deming, *Prog. Polym. Sci*., **2007**, 32, 858.

120. J. Huang, C. Bonduelle, J. Thevenot, S. Lecommandoux, A. Heise, *J. Am.Chem. Soc*., **2012**, 1, 119.

121. D. L. Liu, X. Chang, C. M. Dong, *Chem. Commun*., **2013**, 49, 1229.

122. W. Tansey, S. Ke, X. Y. Cao, M. J. Pasuelo, S. Wallace, C. Li, *J. Control. Release*, **2004**, 94, 39.

123. K. Knop, R. Hoogenboom, D. Fischer, U. S. Schubert, *Angew. Chem. Int. Ed*., **2010**, 49, 6288 .

124. S. Pana, C. Wanga, X. Zenga, Y. Wena, H. Wua, M. Feng*, Int. J. Pharm*., **2011**, 420, 206.

125. L. Yin, Z. Song, K. H. Kim, N. Zheng, H. Tang, H. Lu, N. Gabrielson, J. Cheng, *Biomaterials*, **2013**, 34, 2340.

126. H.M. Wu, S.R. Pan, M.W. Chen , Y. Wub, C. Wang, Y.T. Wen, X. Zeng , C.B. Wu, *Biomaterials*, **2011**, 32, 1619.

Chapter 2

Star Polypeptides by NCA Polymerization from Dendritic Initiators: Synthesis and Emzyme Controlled Payload Release

Abstract

Well-defined star polypeptides were successfully synthesised by initiation of γ-benzyl-L-glutamate N-carboxyanhydride (NCA) from polypropylene imine (PPI) dendrimers. The dendrimer generation and the dendrimer to NCA ratio was systematically varied to afford a range of star shaped architectures with a maximum of 8 to 64 poly(γ-benzyl-L-glutamate) (PBLG) arms. High molar masses up to 500 000 g/mol were achieved that were otherwise unobtainable for the analogous linear polypeptides in the absence of the dendrimer core. By deprotection the PBLG star polypeptides were converted into poly(L-glutamic acid) (PGA) star polypeptides. Various concentrations of rhodamine B could be loaded into the polypeptide star architectures dependent on the number of PGA arms and the length of the grafted polypeptide chain produced. Furthermore, the polypeptidic nature of PGA-grafted dendrimers ensures their responsiveness, through controlled degradation, to the target enzyme thermolysin. An enzyme-responsive release mechanism was devised and demonstrated in which rhodamine B payload was released upon incubation with thermolysin but not the control enzyme chymotrypsin. The rate and extend of rhodamine B release was dependent on the composition of the hybrid material, which can be readily tuned to provide highly specific temporal and spatial controlled release.

This work was published in Polymer Chemistry (2012), 3(10), 2825-2831.

2.1 Introduction

N-carboxyanhydride (NCA) ring-opening polymerization (ROP) enables the creation of synthetic polypeptides to a targeted molar mass in a highly controlled manner.[1-3] Such materials have demonstrated their potential biomedical applicability[4] in areas including tissue engineering,[5] drug delivery,[6,7] medical adhesives,[8] antimicrobial agents,[9] and biorecognition applications[10-14] emphasising the significance of NCA polymerisation within a biomedical context. Researchers have recently begun to further increase the macromolecular complexity of synthetic polypeptides in order to stimulate self-assembly into micelles and vesicles (polymersomes) as potential drug delivery vehicles.[15-19] However, the dynamic behaviour of these assemblies puts some limitations on their stability under certain conditions.

Star polypeptides offer an attractive alternative as unimolecular nanoparticles in drug delivery and offer a high local density of polypeptide chains within a single macromolecule. Following synthetic strategies developed initially for controlled polymerisations[20-22] nanogel star polypeptides, i.e. polypeptides emanating from a cross-linked core have been reported recently.[23-25] Alternatively, star shaped polypeptides can be generated by NCA polymerisation from a multifunctional initiator. Of particular interest to our group are amine-terminated dendrimers that have the potential to initiate the ring opening polymerisation of amino acid NCAs to generate high molar mass homopolypeptides grafted to the dendritic core. Polymer grafting from a dendritic core enables the formation of a polymer-dendrimer hybrid, the size, shape, and surface features of which may be readily controlled to modify its payload capacity, biodistribution and pharmacokinetic properties in controlled release applications.

Early reports on the concept of NCA initiation from multifunctional initiators were published by Inoue for the synthesis of a six-arm poly(γ-benzyl-L-aspartate) from cyclotriphosphazene.[26,27] Müllen employed polyphenylene dendrimers with up to 16 amino groups for the polymerisation of lysine NCA.[28] Hyper-branched poly(ethyleneimine)s (PEI) with approximately 15 and 60 amino groups were used to synthesise star-shaped poly(L-lysine) (PLL) and poly(L-glutamic acid) (PLG) by Liu for drug encapsulation and biomineralisation applications.[29,30] Appelhans reported the synthesis of low molar mass polypeptide shells from dendrimers bearing eight amine initiation sites to form star shaped polypeptides for metal ion complexation purposes.[31] Higashi utilised a third generation poly(amidoamine) (PAMAM) dendrimer to produce star shaped poly(γ-benzyl-L-glutamate) (PBLG) and subsequently examined its applicability for amino acid encapsulation.[32] The same author also reported oligo(L-lysine) shelled third generation PAMAM for DNA binding.[33] A fourth generation PAMAM (64 amino groups) was employed by Feng to graft PLL with an average degree of

polymerisation of 6 units per arm from the dendritic core.[34] It was shown that these polymers act as efficient gene vectors for plasmid DNA.

Consequently, we believe that expanding this concept of polypeptide synthesis from a dendritic core may enable the creation of polypeptides possessing systematically variable architecture boasting previously unreported molar masses that may be tuned dependent on the number of initiator sites present on the dendritic core, and the quantity of amino acid NCA within the monomer feed. Furthermore, their larger size may result in an increased 'payload' capacity and an inherent capability to non-covalently withhold a specific quantity of a chosen molecular cargo dependent on the dimensions of the material produced. This hybrid structure may possess the capability to actuate a designed material response such as pH-controlled swelling and enzyme regulated release of a molecular 'cargo', thereby providing bioresponsive carriers.

In this chapter we present a systematic study in which homopolypeptide-dendrimer hybrids can be synthesised with a particularly low dispersity (D) and high molar masses irrespective of the dendrimer generation. We further show enzyme responsiveness to particular, targeted proteolytic enzymes; payload release is only instigated upon polypeptide degradation following its reaction with a target enzyme, and the rate and extent of release is dictated by the degree of polypeptide grafting and the generation of dendrimer.

2.2 Results and Discussion

2.2.1 Star Polypeptide Synthesis

The use of primary amines to initiate the ROP of α-amino acid NCAs to synthesise well-defined synthetic linear polypeptides is well understood.[1,2,35,36] By utilising this methodology it was possible to combine NCA monomers with an amine terminated dendrimer to create polypeptide star polymers containing a dendrimer core and a polypeptide shell **(Figure 2.1).** Benzyl-L-glutamate (BLG) was selected as a suitable amino acid NCA due to the carboxylic acid functionality it presented upon side chain deprotection, and to highlight the versatility that the system offers. PPI dendrimers of generation 2 (G2; 8 terminal amines) up to generation 5 (G5; 64 terminal amines) were employed to generate star shaped polypeptides whose size, shape, arm length and molar mass could be configured by varying the dendrimer generation and the monomer feed ratio **(Figure 2.1)**.

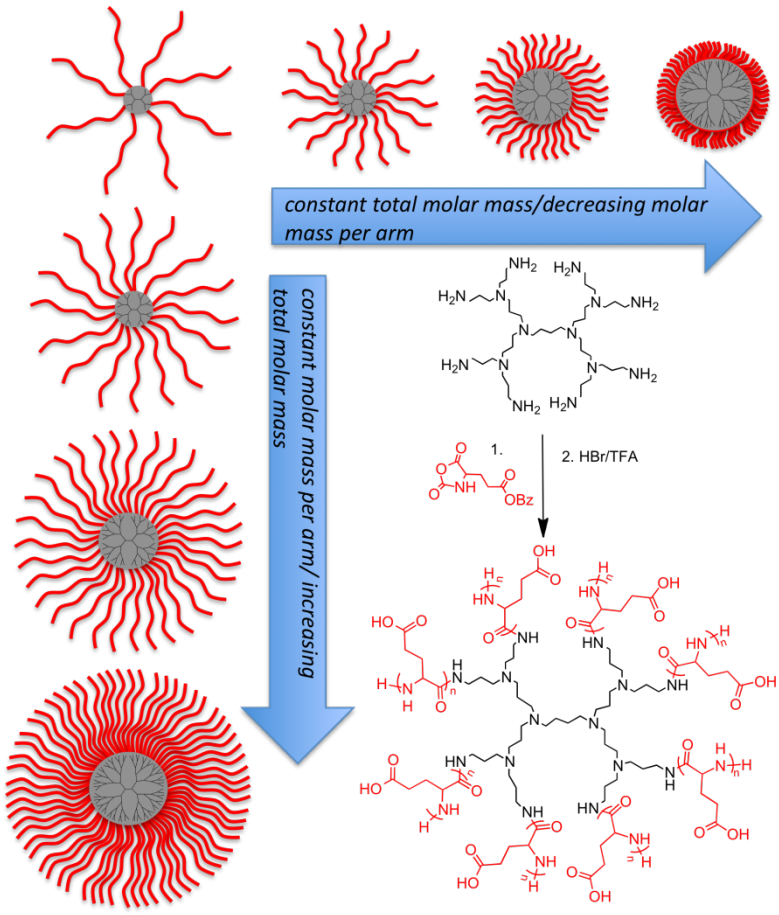

Figure 2.1: Diversity of synthesized star polypeptides and reaction scheme of for the synthesis of poly(L-glutamic acid) star polypeptides using second generation PPI dendrimer as an initiator.

In the initial series of polymerisations the NCA to individual amino group ratio was kept constant at 40, i.e. the ratio of NCA was increased with increasing dendrimer generation **(entries 4-7, Table 2.1)**. The star polymers produced in this series have a constant arm length but with an increasing number of arms, the total molar mass increases systematically with the increasing dendrimer generation. As can be seen from **Figure 2.2**, excellent linear correlation between the polymer molar mass increase and the number of initiating amino groups (dendrimer generation) was found. This linearity indicates that monomer conversion was uniform, which may not have been expected, given that the number of initiating arms differs significantly between dendrimer generations. While the reactions were typically carried out for 24 h it was noted that even after 6 h the maximum molar mass was obtained for the complete range of dendrimer generations.

Table 2.1: Star-shaped PBLG by initiation from PPI dendrimers (L: linear initiator benzylamine; G1-G5: generation of PPI dendrimer; G5(64)-PBLG$_{40}$ = initiator generation 5 dendrimer with maximum 64 arms and theoretical arm length of 40 amino acids) Dispersities of all polymers < 1.2 (SEC MALS detection).

Entry	Polymer	NCA/NH_2	NCA/dendrimer	M_w/g mol$^{-1(a)}$	$M_n^{th\,(b)}$/g mol^{-1}
1	L(1)-PBLG$_{640}$	640	640	47 500	140 000
2	L(1)-PBLG$_{2560}$	2560	2560	55 000	500 000
3	G2(8)-PBLG$_{60}$	60	480	91 700	105 400
4	G2(8)-PBLG$_{40}$	40	320	63 200	70 500
5	G3(16)-PBLG$_{40}$	40	640	110 700	141 000
6	G4(32)-PBLG$_{40}$	40	1280	240 800	282 500
7	G5(64)-PBLG$_{40}$	40	2560	499 800	565 000
8	G5(64)-PBLG$_{20}$	20	1280	227 300	286 200
9	G5(64)-PBLG$_{7.5}$	7.5	480	92 900	111 400
10	G2(8)-PBLG$_{12.5}$	12.5	100	24 900	22 500
11	G3(16)-PBLG$_{6.3}$	6.3	100	24 400	23 500
12	G4(32)-PBLG$_{3.1}$	3.1	100	27 800	25 320
13	G5(64)-PBLG$_{1.6}$	1.6	100	28 900	29 000

(a) determined by SEC (DMF) using MALS detection using the dn/dc of linear PBLG of 0.118. (b) calculated assuming initiation from all amino groups and quantitative conversion: c(monomer)/c(dendrimer) x M(monomer) + M(dendrimer).

These results adhere to the recent work of Habraken et al. who concluded that a linear BLG NCA polymerization reaction at 20 °C and a degree of polymerization (DP) of 40 requires approximately 3 h for complete monomer conversion.[36] Despite the fact that a G2-PPI dendrimer has only 8 points of initiation compared to the 64 of a G5-PPI dendrimer it appears that both have similar monomer conversion times suggesting that the amino groups on the dendrimer act as individual initiators similar to conventional amines. These star shaped polypeptides could be synthesised up to very high molar masses, which were otherwise unobtainable in the absence of the dendritic core. Deming reported the synthesis of linear PBLG with molar masses as high as M_n = 300 000 g/mol using metal based initiators.[37] However, molar masses comparable to the described star shaped polypeptides of almost 500 000 g/mol for the G5 dendrimer cannot be readily synthesised using a linear primary amine initiator and the same NCA to amino group ratio in both $CHCl_3$ and DMF even after a reaction time of 6 days **(entries 1 and 2, Table 2.1)**. The fact that molar masses were typically lower than the theoretical value for PBLG may be attributed to the use of linear PBLG dn/dc values. It is also thought that the PPI core did not contribute significantly to the overall dn/dc values of the polypeptides due to its relatively small composition in the polymers.

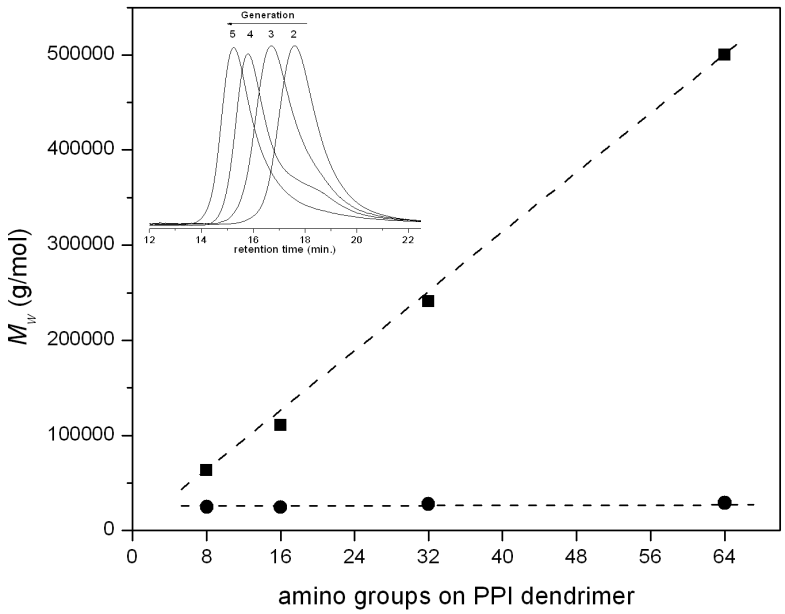

Figure 2.2: Weight average molar mass (M_w) of star-shaped PBLG obtained by initiation of NCA from different generation PPI dendrimers: ■ increasing NCA to dendrimer ratio (Inset shows the corresponding SEC traces; MALS detector; ● constant NCA to dendrimer ratio.

The versatility of the polymerisation was further investigated in a series of reactions in which the total ratio of NCA to PPI dendrimers was kept constant **(entries 10-13, Table 2.1).** This results in a decreasing NCA to amino group ratio with increasing dendrimer generation. As can be seen in **Figure 2.2**, the polymers of this series have a constant total molar mass with more but shorter arms as the dendrimer generation increases. Polymers of low molar mass were observed, particularly for generation 4 PPI dendrimer initiated ROP owing most likely to the presence of a very small amounts of dendrimer molecules with reduced amino end groups. ^{1}H NMR spectroscopy analysis **(Figure 2.3)** confirmed polypeptide conjugation to PPI although the dendrimer peaks were very difficult to observe due to overlapping with the broad polypeptide peaks. Furthermore the relatively small size of the dendrimer core compared to the polypeptide shell rendered the dendrimer signals very weak. Consequently, it was not possible to determine whether all dendritic amino groups initiated polymerisation but the excellent correlation of polymer molar masses with the expected values irrespective of dendrimer generation suggest a high initiation efficiency.

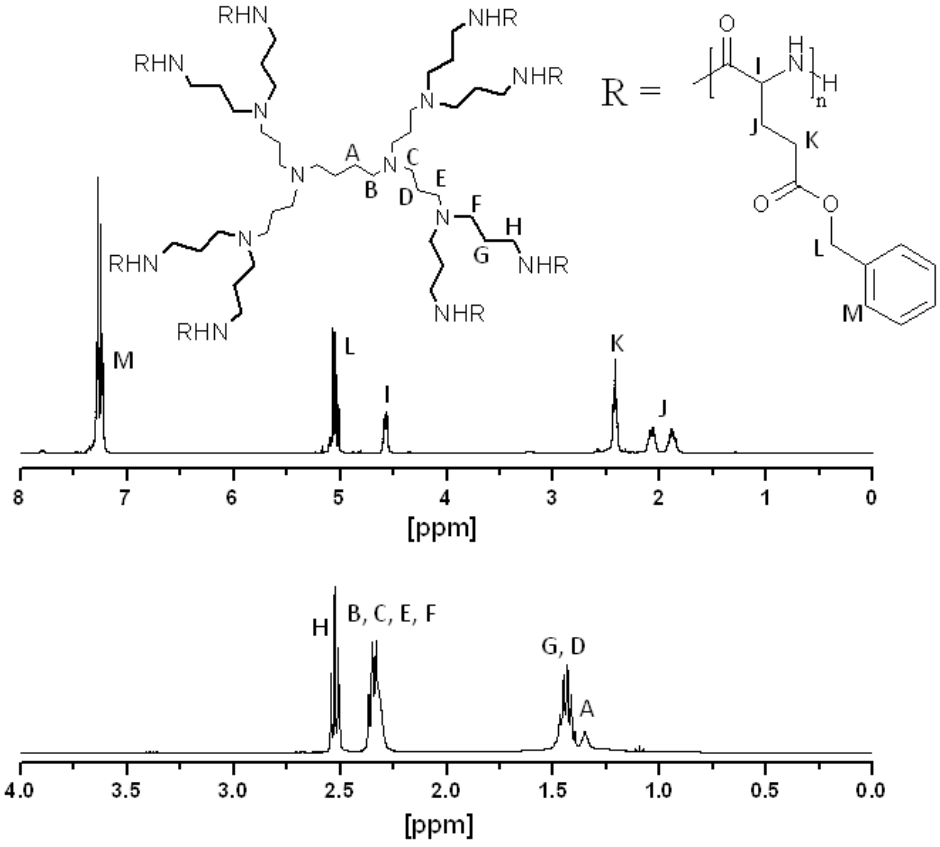

Figure 2.3: ^{1}H NMR spectra of G2(8)-PBLG$_{40}$ (Top) ($CDCl_3$, d-TFA) and G2-PPI dendrimer (Bottom) ($CDCl_3$). R = H for unpolymerized PPI Dendrimer (peaks A - H not visible in top spectrum).

As discussed, primary amines are very efficient initiators for ROP of NCAs. However, tertiary amines are also known to act as initiators albeit via a different mechanism (activated monomer mechanism, AMM) resulting in inferior control over polymerization conditions i.e. polymer M_w and PDI.[1,2] The PPI dendrimers employed here possess numerous tertiary amines in their core the number of which is dependent on dendrimer generation. Therefore it was very important to confirm that the star shaped polypeptides synthesized above were generated via NCA ROP initiated from the primary amine terminated arms and not the core tertiary amines. To achieve this, peripheral primary amines of G2-PPI dendrimer were protected using tert-butoxycarbonyl (BOC) protecting groups **(Figure 2.4)**. Given the dense steric environment of primary amines in these dendrimer structures, BOC was chosen as a suitable protecting group owing to its small size and ability to operate effectively in the presence of ROP of NCAs. ^{1}H NMR spectroscopy confirmed the successful protection of all primary amines and the resultant material was employed as an initiator for ROP of the NCA BLG **(Figure 2.5)**.

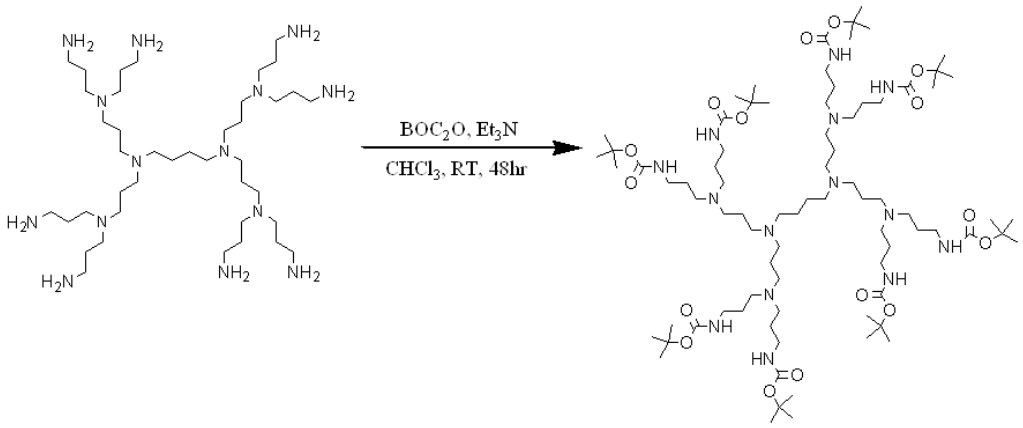

Figure 2.4: Synthesis of BOC protected G2-PPI dendrimer.

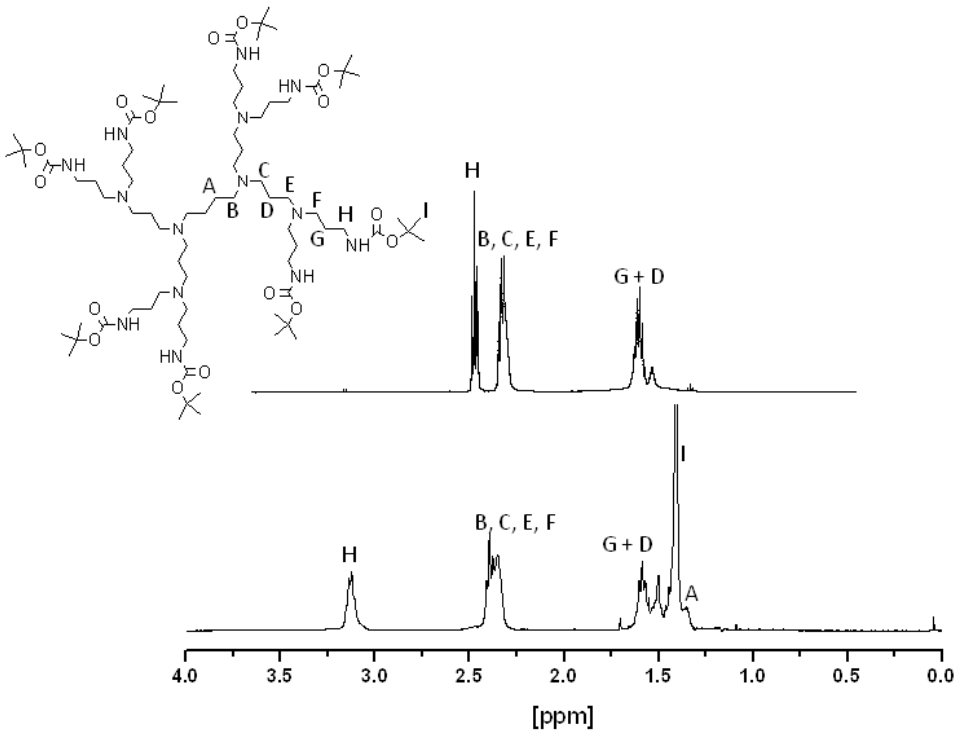

Figure 2.5: ^{1}H NMR spectroscopy analysis of BOC protected G2-PPI (Bottom) ($CDCl_3$) and G2-PPI dendrimer without BOC protection (Top) ($CDCl_3$).

A series of polymerizations were attempted in which the molar ratio of BOC-PPI dendrimer and BLG monomer were varied to ascertain the degree of molecular weight control afforded by tertiary amine initiation. For comparative purposes a linear tertiary amine initiator, diisopropylethylamine (DIPEA) was employed and the results are summarized in **Table 2.2**. The results showed that no precise control over polypeptide M_w was afforded by tertiary amines and the resultant M_w values were dramatically higher than the corresponding theoretical values. Furthermore, variation of the monomer feed ratio had no effect on M_w whilst PDI values were somewhat more elevated than for primary amine derived polypeptides which is in stark contrast to the well-defined polypeptides described in **Table 2.1**. The data in **Table 2.2** is consistent with typical tertiary amine derived polypeptide characteristics and thus confirms the advantage of using primary amines as initiators as well as their overwhelming participation in the PPI generated well-defined star shaped polypeptides discussed above.[1,2,38] Although, the minor coexistence of tertiary and primary amine initiation cannot be completely ruled out it can be concluded that initiation from primary amines is predominant. In addition, it can be hypothesized that as peripheral polypeptide growth proceeds, participation of tertiary amine initiation and subsequent polymerization may be nullified due to steric hindrance from the dense polypeptide periphery.

Table 2.2: PBLG obtained by initiation from BOC protected G2-PPI dendrimers and linear (L) initiator diisopropylethylamine (DIPEA).

Entry	Polymer	NCA/dendrimer	M_w/g mol$^{-1(a)}$	$M_n^{th\,(b)}$/g mol^{-1}	PDI
1	L(1)-PBLG$_{320}$	320	333 000	69 900	1.2
2	G2(8)-PBLG$_{320}$	320	288 000	71 400	1.2
3	G2(8)-PBLG$_{160}$	160	271 600	36 500	1.3
4	G2(8)-PBLG$_{80}$	80	280 100	19 000	1.3

(a) determined by SEC (DMF) using MALS detection using the dn/dc of linear PBLG of 0.118. (b) calculated assuming initiation from all primary amino groups and quantitative conversion: c(monomer)/c(BOC-dendrimer) x M(monomer) + M(BOC-dendrimer).

Finally, FTIR spectroscopy was employed to elucidate the secondary structure of the star polypeptides in the solid state. Linear PBLG and almost all of the PBLG star shaped polypeptides exhibited an α-helical secondary structure with characteristic bands observed at 1650 cm^{-1} and 1545 cm^{-1} **(entries 1-11, Table 2.1)(Figure 2.6, A and B)**. By decreasing the polypeptide chain length to 12 units per arm, the presence of a strong α-helix was still observed **(entry 10, Table 2.1)**. However by further decreasing the average chain length to ~ 2 units per arm for G5(64)-PBLG$_{1.6}$ **(entry 13, Table 2.1)**, the polypeptide lost its α-helicity and assumed some weak β-sheet character (amide I 1642 cm^{-1} amide II 1530 cm^{-1}) **(Figure 2.6, C)**. By varying the PBLG chain length thus it was possible to modify its secondary structure which is consistent with the literature.[30,39,40] A more detailed study on the solution properties as a function of molar mass and architecture is under consideration.

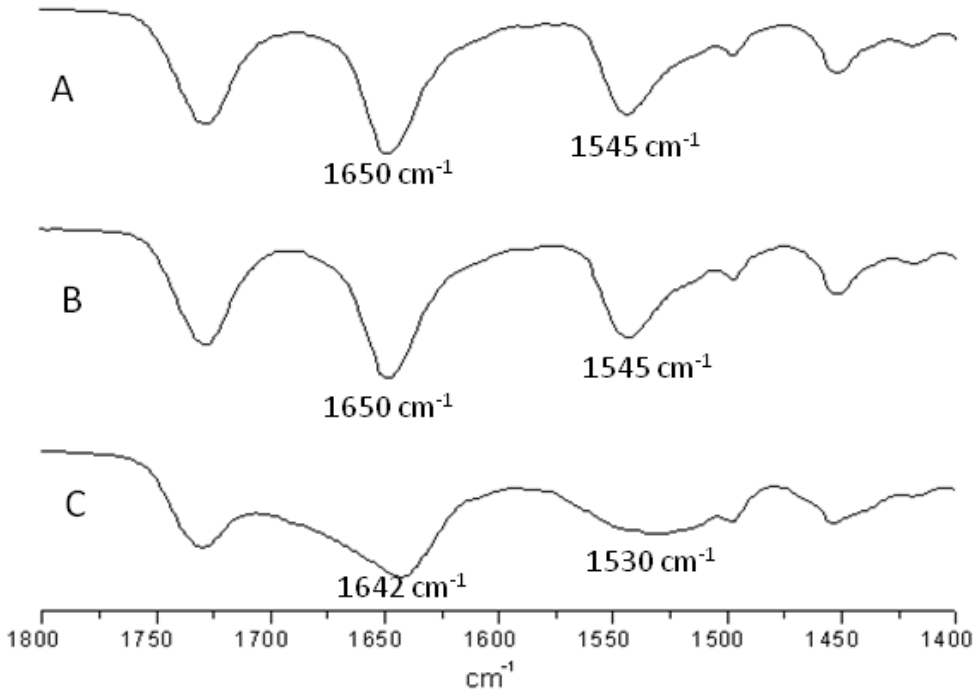

Figure 2.6: FTIR spectra of Linear PBLG (A), G5(64)-PBLG with 40 units per arm (B) and 2 units per arm (C).

Consequently, it was possible to create polypeptide systems in which the length and density of the polypeptide shell could be altered in a highly systematic way. By this method it is possible to synthesise very well defined polypeptides of varying degrees of star shaped architectures and molar mass with low dispersity.

2.2.2 Payload Loading / Enzyme Mediated Release

The high degree of control over the molar mass of the hybrid materials generated ensures their particular relevance for use as carrier vehicles in targeted drug delivery applications. It was hypothesised that the quantity of guest molecules loaded in the polypeptide-dendrimer structures is directly affected by the number and length of the polypeptide chains grafted from the dendritic core. To facilitate loading with a water soluble molecule, selected PBLG star polymers were deprotected to generate poly(L-glutamic acid) (PGA) star polypeptides. Quantitative deprotection was confirmed by ^{1}H NMR spectroscopy spectroscopy by the disappearance of the aromatic and CH_2 peaks of the benzyl protecting group at 7.2 and 5.0 ppm **(Figure 2.7)**.

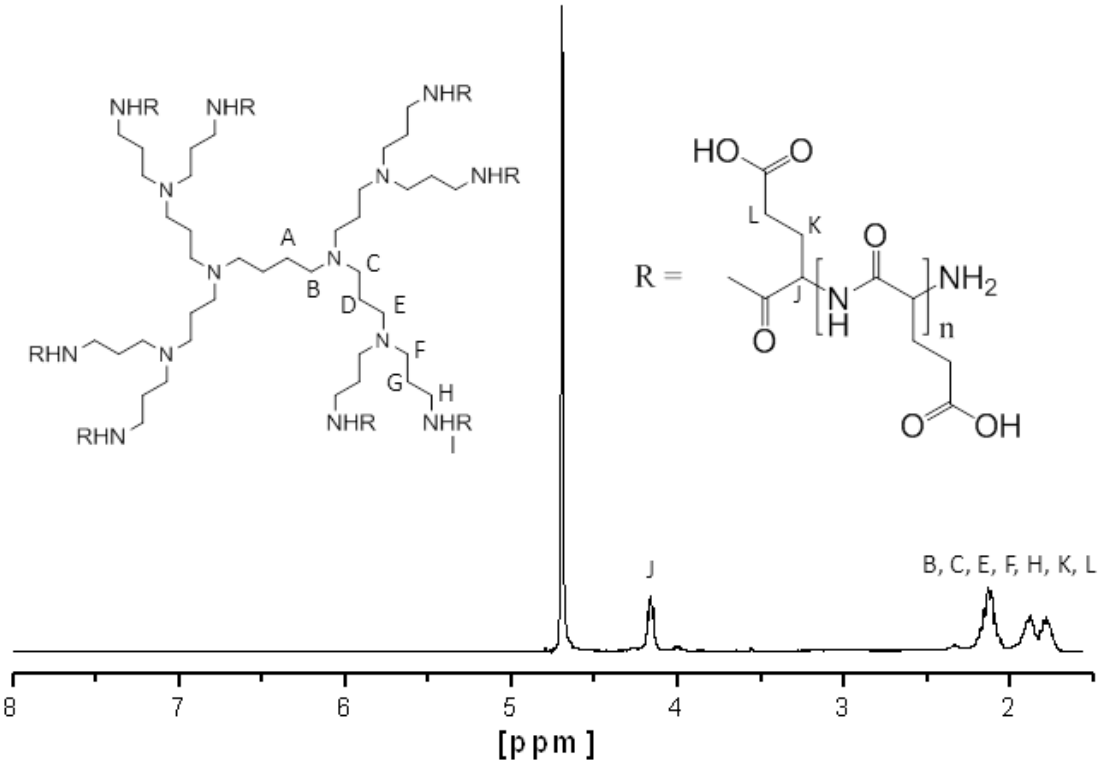

Figure 2.7: ^{1}H NMR spectra of deprotected 8-armed star shaped PGA (D_2O). (Peaks A - I not visible. Labelled as where they should be expected).

A study was conducted whereby a range of PGA-conjugated dendrimers were loaded with fluorescent rhodamine B solution and the quantity encapsulated determined by UV spectroscopy. Dye loading was carried out at pH 11 to facilitate deprotonation of the PGA carboxylic acid groups and solubility in the rhodamine B aqueous solution.[39] The dye was entrapped in the star polypeptide by lowering the pH to 4 resulting in protonation of the PGA and precipitation of dye loaded polymers. Notably, loading only occurred when the solution pH was adjusted from pH 11 to pH 4 and not when the particles were incubated in pH 4 or pH 11 rhodamine solutions. This supports the conclusion that the dye had penetrated the shell as opposed to being adsorbed to the surface. The dye-loaded polymers were stable and no leakage of rhodamine B was observed even over longer periods of time upon storage at room temperature.

Table 2.3: Rhodamine B loading capacity of poly(glutamic acid) (PGA) star polymers with different number of arms and molar masses.

Entry	Polymer	GA per arm[(a)]	Total GA[(a)]	Star PGA:Rhodamine B loading (molar ratio)
1	L(1)-PGA_{252}	252	252	1:0.018
2	G2(8)-PGA_{37}	37	296	1:0.047
3	G5(64)-PGA_{7}	7	448	1:0.024
4	G5(64)-PGA_{16}	16	1024	1:0.111
5	G5(64)-PGA_{36}	36	2304	1:0.333

(a) based on SEC molar mass.

The molar ratio of rhodamine B loaded within linear PGA possessing 252 glutamic acid (GA) units and a molar mass of 55000 g/mol was found to be 1:0.018 (polymer:rhodamine B) **(entry 1, Table 2.3)**. In comparison, the star polypeptide, G2(8)-PGA_{37} with 37 GA units coupled to each of the 8 initiation sites of a 2nd generation dendrimer (total PGA units 296) contained a greater rhodamine B content relative to the moles of the PGA polymer used **(entry 2, Table 2.3)**. This signifies the importance the polymer architecture has over the loading capacity. Similarly, increasing the length of the polypeptide chain and subsequently the molar mass of the star shaped polypeptides had a profound effect on the materials' loading capabilities. The molar ratio for 5th generation PPI initiators bearing a maximum of 64 arms was found to be 1:0.024 when PGA consisting of 7 amino acid units was attached to its periphery. Increasing the length of the polypeptide chain to consist of 16 and 36 PGA units per arm further increased the amount of rhodamine loaded relative to the moles of the star polymer used, highlighting the control over loading offered **(entries 3-5,Table 2.3)**. When comparing the loading capacity of the 8 arm and the 64 arm PGA star polypeptide with comparable polypeptide chain lengths of around 37 GA units **(entries 2 and 5,Table 2.3)** the latter was found to be about seven times higher. This corresponds to the ratio of total molar mass of the two star polymers and suggests that above a certain size and degree of branching the loading capacity is proportional to the total molar mass. This highlights the advantage of using higher generation dendrimers as initiators for these star polypeptides as only they give access to high molar mass unimolecular macromolecular carriers.

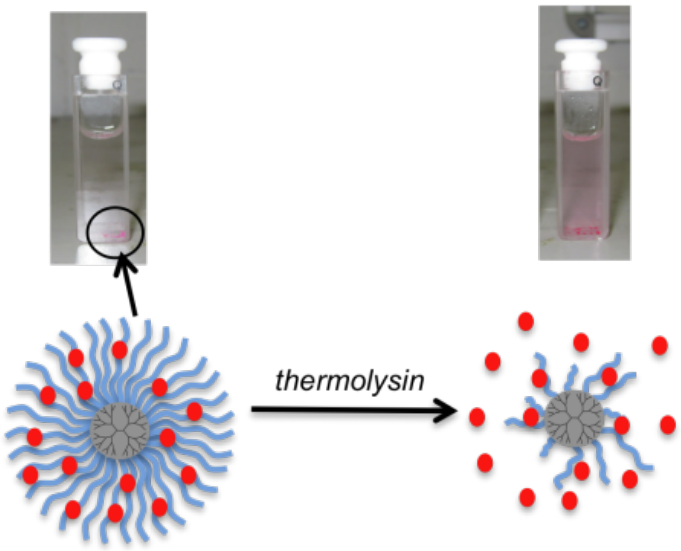

Figure 2.8: Rhodamine B loaded particles and enzyme triggered release.

The same PGA star polypeptides were used in a preliminary study of the release profiles in response to the proteolytic enzymes chymotrypsin and thermolysin **(Figure 2.8)**. Enzyme-responsive materials are a class of responsive material that are expected to play a key role in a number of biomedical applications such as regenerative medicine, medical diagnostics, and drug delivery due to their high selectivity and biocompatibility.[40,41] Enzymes offer key advantages as release triggers; they are not biologically disruptive, function under mild conditions, and possess a high degree of selectivity, e.g. at disease sites including cancer, inflammation and infection.[42] Payload release of the rhodamine B loaded PGA star polymer was anticipated to occur in the presence of an enzyme capable of hydrolytic cleavage of the PGA. Thermolysin has demonstrated the capability to cleave peptide bonds when glutamic acid is present at the P1' site.[43] Indeed significant release monitored by UV spectroscopy following particle incubation occurred in the presence of thermolysin and was dependent upon enzyme concentration **(Figure 2.9)**. By decreasing the enzyme concentration to 0.1 mg/ml the release of rhodamine B from both linear and star shaped PGA was significantly prolonged whereas minimal release was observed for chymotrypsin at both concentrations as expected **(Figure 2.10)**. The low level of rhodamine release observed for linear PGA incubated with chymotrypsin was most likely related to unbound rhodamine B dye molecules, which had not been completely removed during dialysis. The control enzyme chymotrypsin possesses the specificity to cleave amide bonds in which the carboxyl side of the bond (the P1 position) is tyrosine, tryptophan, or phenylalanine and so is non-selective for the homopolypeptide created.[44]

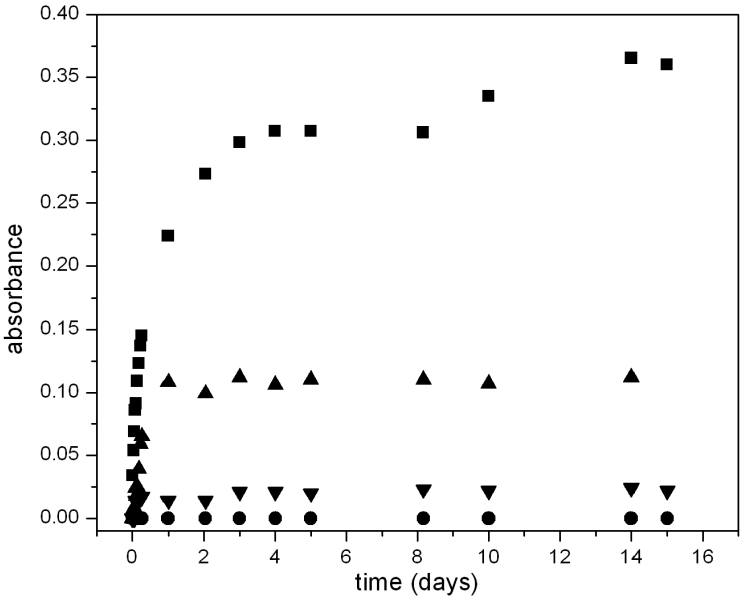

Figure 2.9: Enzymatic release profiles followed by UV spectroscopy at 554nm of rhodamine B loaded L(1)-PGA$_{252}$ (entry 1, Table 3.2) and G2(8)-PGA$_{37}$ (entry 2,Table 3.2) in water (1 mg/mL) of similar molar masses using 1 mg/mL chymotrypsin and thermolysin. ■ : G2(8)-PGA$_{37}$, thermolysin; ● : G2(8)-PGA$_{37}$, chymotrypsin; ▲: L(1)-PGA$_{252}$, thermolysin; ▼: L(1)-PGA$_{252}$, chymotrypsin.

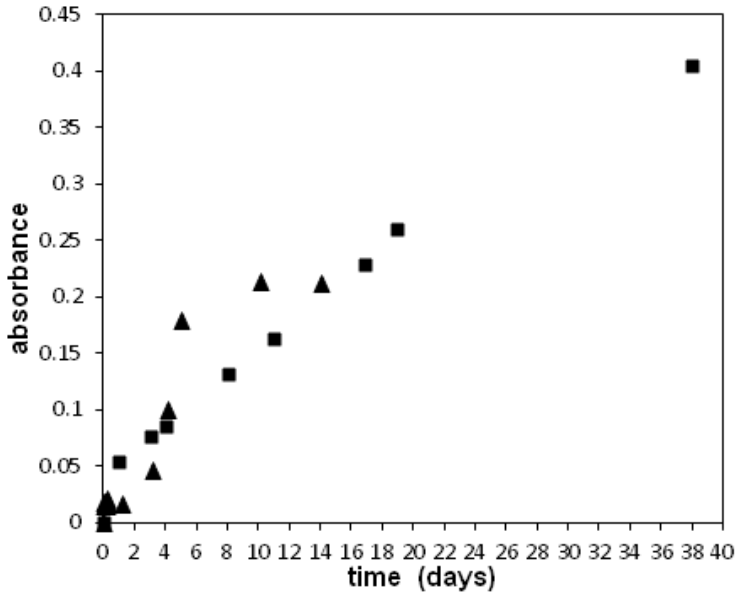

Figure 2.10: Enzymatic release profiles followed by UV spectroscopy at 554nm of rhodamine B loaded L(1)-PGA$_{252}$ (entry 1, Table 3.2) and G2(8)-PGA$_{37}$ (entry 2,Table 3.2) in water (1 mg/mL) of similar molar masses using 0.1 mg/mL of thermolysin. ■ : G2(8)-PGA$_{37}$, thermolysin; ▲: L(1)-PGA$_{252}$, thermolysin.

Figure 2.11 shows the comparison of the release profiles of PGA star polymers with varying number of arms. With the exception of star polymer G5(64)-PGA_7 with short PGA arms **(entry 3, Table 2.3)** the total of rhodamine B loading per polymer mass is quite similar (it only differs in molar loading). As the same mass of rhodamine B loaded polymers was used in these experiments a similar final absorbance is expected after quantitative release from G5-PGA with 16 and 36 monomers per arm **(entry 4 and 5, Table 2.3)**. This is indeed the case but noticeable is a dependence of the polymer architecture on the rate of payload release with the longer PGA arms G5-PGA **(entry 5,Table 2.3)** providing a slower release as evidenced by the release profile **(Figure 2.11)**. Degradation of linear PGA occurred at a greater rate (24 h for complete payload release) compared to release from 2nd generation PPI bearing an average of 37 PGA units coupled to each of its 8 initiation sites using a thermolysin concentration of 1 mg/ml. Similarly by increasing the degree of branching, polypeptide chain length and therefore the polypeptide shell density the release rate can be further prolonged **(Figure 2.11)**. It can be speculated that this difference results from steric hindrance inhibiting enzymatic activity upon the dendrimer-containing material. Azagarsmay et al. have proposed a similar hypothesis.[45] These preliminary results suggest that architecture and molar mass may be useful tools to manipulate the 'cargo' loading and pharmacokinetics of star PGA based drug delivery platforms.

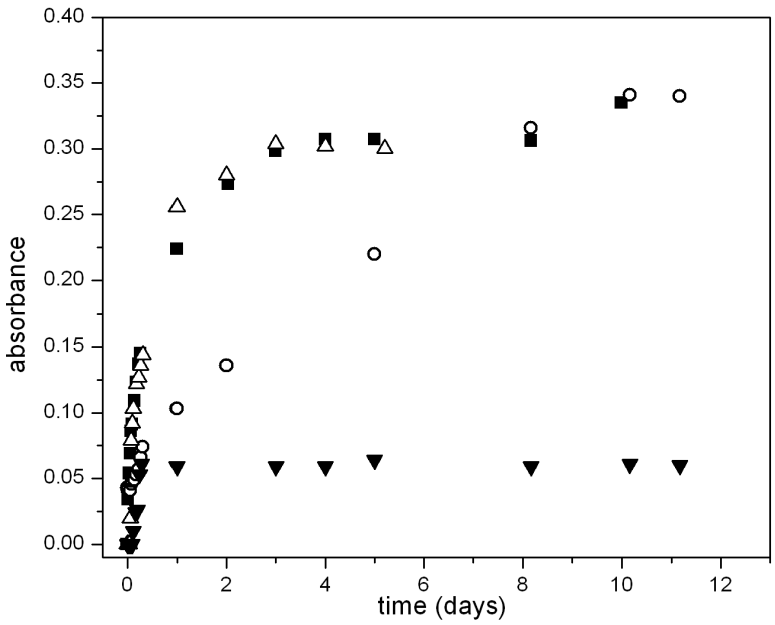

Figure 2.11: Enzymatic release profiles followed by UV spectroscopy at 554nm of rhodamine B loaded PGA star polymers in water (1 mg/mL) using 1 mg/mL thermolysin. ■ : G2(8)-PGA_{37} (296 GA units, entry 2, Table 3.2); ○ : G5(64)-PGA_{36} (2304 GA units, entry 5, Table 3.2); △ : G5(64)-PGA_{16} (1024 GA units, entry 4, Table 3.2); ▼ : G5(64)-PGA_7 (448 GA units, entry 3, Table 3.2).

2.3 Conclusions

Well-defined high molecular polypeptides were successfully synthesised by NCA ROP initiated from PPI dendrimers to afford a range of star shaped architectures. Such high molar masses were unobtainable for the analogous linear polypeptides in the absence of the dendrimer core. The extensive control offered by the method of polymerisation ensures that the products formed have applicability as use as drug delivery vehicles. Various concentrations of rhodamine B could be loaded into the polypeptide star architectures dependent on the generation of dendrimer utilised and the length of the grafted polypeptide chain produced. Furthermore, the polypeptidic nature of PGA-grafted dendrimers ensures their responsiveness, through controlled degradation, to the target enzyme thermolysin. An enzyme-responsive release mechanism was devised and demonstrated in which rhodamine B payload was released upon incubation with thermolysin but not the control enzyme chymotrypsin. The kinetic of rhodamine B release could be controlled carefully dependent on the composition of the hybrid material, which could be readily tuned. The polypeptide-dendrimer hybrid materials produced are created under highly controlled conditions, are tuneable dependent on the dendrimer employed / extent of polypeptide grafted and may have applicability in spatial and temporal controlled release applications.

2.4 Experimental

Star Polypeptide Synthesis

Materials

All air and moisture sensitive compounds were handled under a nitrogen atmosphere using general Schlenk-line techniques. α-pinene (98%) bis(trichloromethyl) carbonate (triphosgene) 99% and benzylamine were purchased from Sigma Aldrich. γ-Benzyl-L-glutamate was supplied by Bachem. PPI (polypropylene imine) dendrimers generations 2-5 were purchased from SyMO-Chem BV (The Netherlands). Chloroform (anhydrous), ethyl acetate (anhydrous), dimethylformamide (anhydrous), tetrahydrofuran (anhydrous), n-heptane, and diethylether were supplied by Sigma Aldrich. All chemicals were used without any purification unless otherwise noted. Chloroform and ethyl acetate were used directly from the bottle and stored under an inert, dry atmosphere. γ-Benzyl-L-glutamate NCA was synthesised following a literature procedure.[46]

Methods

Nuclear magnetic resonance (NMR) spectra were recorded on a Bruker Avance 400 (400MHz) spectrometer at room temperature in $CDCl_3$ and d-TFA as solvents. The following abbreviations for multiplicity are used: s, singlet; m, multiplet; br, broad. Attenuated Total Reflection (ATR) FTIR spectroscopy measurements were performed on a Perkin-Elmer Spectrum 100 in the spectral region of 650-4000 cm^{-1} and were obtained from 4 scans with a resolution of 2 cm^{-1}. A background measurement was taken before the sample was loaded onto the ATR for measurement. Size Exclusion Chromatography (SEC) was performed on an Agilent 1200 system in conjunction with two PSS GRAM analytical (8 x 300 and 8 x 100, 10 µ) columns, a Wyatt Dawn Heleos 8 multi angle light scattering detector (MALS) and Wyatt Optilab rEX differential refractive index detector (DRI) with a 658 nm light source. The eluent was DMF containing 0.1M LiBr at a flow rate of 1 mL min^{-1}. The column temperature was set to 40 ºC with the MALS detector at 35 ºC and the DRI detector at 40 ºC. Molar masses and dispersities were calculated from the MALS signal by the Astra software (Wyatt) using the refractive index increment (dn/dc) of linear poly-benzyl-L-glutamate (PBLG) of 0.118. All samples for GPC analysis were prepared with a concentration of 2 mg/ml and were filtered through a 0.45 µm PTFE filter (13 mm, PP housing, Whatman) prior to injection. UV-Vis spectra were recorded on a Varian Cary 50 using a UV quartz cuvette in the spectral range of 300-700 nm. The concentration of rhodamine B was monitored by recording the absorbance at 554 nm, i.e. the peak of maximum

absorbance for rhodamine B. A baseline correction using deionised water was employed before each measurement.

Synthesis of linear poly(γ-benzyl-L-glutamate) (Representative Procedure)

In a Schlenk tube under a nitrogen atmosphere, a solution of the NCA of γ-benzyl-L-glutamate (BLG) (2.0 g, 7.63 mmol) in $CHCl_3$ (25 ml) was prepared. A solution of benzylamine initiator (0.32 mg, 2.98 x 10-6 mmol) in $CHCl_3$ was also prepared and charged to the reaction solution via syringe. The solution was stirred at room temperature until no further increase in molar mass was achieved. The molar mass was monitored by SEC by precipitating 1 mL of the reaction solution into an excess of cold diethyl ether. Upon no increase in molar mass, the polymer was precipitated into an excess of cold diethyl ether and dried under vacuum (Yield: 51%).

Synthesis of Star Shaped PBLG (Representative Procedure)

As a reference procedure, the NCA of γ-benzyl-L-glutamate (BLG) (2.18 g, 8.3 mmol) was dissolved in 25 mL $CHCl_3$ in a Schlenk tube under a nitrogen atmosphere. A solution of G2 PPI dendrimer (20 mg, 2.59 x 10^{-2} mmol) in 1 mL $CHCl_3$ was quickly charged to the dissolved NCA solution via syringe. The solution was stirred for 24 h at room temperature. Depending on the type of initiator, the used amount of initiator and monomer were adjusted to achieve the desired molar mass of the star shaped polypeptides. The polymer was precipitated into an excess of cold diethyl ether and dried under vacuum (Yield: 90%).

Benzyl Ester Hydrolysis of Poly(γ-benzyl-L-glutamate) (Representative Procedure)

G5-PPI-PBLG (400 mg) was dissolved in 8 mL of trifluoroacetic acid (TFA). A 6-fold excess with respect to γ-benzyl-L-glutamate of a 33% solution of HBr in acetic acid (2.3 mL) was added slowly to the reaction. After 16 h, the solution was precipitated into diethyl ether. The precipitate was redissolved in ethanol and precipitated twice into diethyl ether. The polymer was dissolved in deionised water and dialyzed (molar mass cut-off 8,000 g/mol) for 3 days. The polymer was lyophilized (Yield: 81%). Deprotection was confirmed by ^{1}H NMR spectroscopy due to the absence of signals at 7.2 ppm (benzyl group) and 5.0 ppm and (CH_2-Bz).

Synthesis of BOC protected G2-PPI Dendrimers

G2-PPI dendrimer (0.15g, 0. 19 mmol) was dissolved in 3 ml of anhydrous $CHCl_3$ under a nitrogen atmosphere. Triethylamine (0.37 g, 3.7 mmol, 1.7 eq. per NH_2) was added via syringe and stirred for 20 min. Di-tert-butyl dicarbonate (0.51g, 2.3 mmol, 1.5 eq. per NH_2) was dissolved in 1 ml of anhydrous $CHCl_3$ and added slowly via syringe to the reaction solution. The

reaction was stirred for 48 h and then washed with 5% potassium bisulfate solution (3 times). The aqueous solution was filtered and pH was adjusted to pH 8 with 1M NaOH. The product was extracted with $CHCl_3$ x 3 and the solvent was removed under reduced pressure to afford the target compound as viscous material. (Yield: 71%).^{1}H NMR spectroscopy (400MHz, $CDCl_3$): δ (ppm) 5.40 (br s, NH), 3.13 (br t, 16H), 2.35 (br m, 36H) 1.58 (br t, 24H), 1.41 (br s, 72H), 1.35 (br s, 4H).

Synthesis of Star Shaped PBLG with BOC protected G2-PPI Dendrimers (Representative Procedure)

As a reference procedure, the NCA of γ-benzyl-L-glutamate (BLG) (0.267 g, 1 mmol) was dissolved in 5 mL $CHCl_3$ in a Schlenk tube under a nitrogen atmosphere. A solution of BOC protected G2-PPI dendrimer (5 mg, 3.18 x 10^{-2} mmol) in 1 mL $CHCl_3$ was quickly charged to the dissolved NCA solution via syringe. The solution was stirred for 24 h at room temperature. The used amount of initiator and monomer were adjusted to attempt molecular weight control. The polymer was precipitated into an excess of cold diethyl ether and dried under vacuum (Yield: 88%).

Payload Loading and Enzyme-Mediated Release

Loading of Linear and Star Shaped Poly(glutamic acid) (PGA) with Rhodamine B Dye

A 25 mg/ml solution of polymer (50 mg) in pH 11 buffer was prepared. A 0.1 mg/ml solution of rhodamine B (0.1 mg) was prepared and charged to the polymer solution with stirring for 2 hours. To acidify this solution a few drops of drops of 25% HCl solution and 5ml of pH 4 buffer was added. The suspension was dialyzed (molar mass cut-off 8000 g/mol) against pH 4 buffer until the excess rhodamine B dye was removed.

Enzyme Controlled Release of Rhodamine B Dye from Linear and Star Shaped Polymers

A 1 mg/ml solution of dye encapsulated polymer and a desired concentration of Thermolysin enzyme (50-100 units/mg protein) was prepared in a UV quartz cuvette using deionised water. The UV spectrum of the solution was recorded at selected time intervals and the concentration of rhodamine B was determined using a prepared calibration curve. The solution was incubated in a water bath at 37 ºC between measurements. The enzyme Chymotrypsin (57.24 units/mg solid) was employed as a control as well as a solution without enzyme.

2.5 References

1. H. R. Kricheldorf, *Angew. Chem., Int. Ed*., **2006**, 45, 5752.

2. N. Hadjichristidis, H. Iatrou, M. Pitsikalis, G. Sakellariou, *Chem. Rev*., **2009**, 109, 5528.

3. G. J. M. Habraken, A. Heise, P. D. Thornton, *Macromol. Rapid Commun.* **2012**, 33, 272.

4. T. J. Deming, *Prog. Polym. Sci*., **2007**, 32, 858.

5. A. P. Nowak, V. Breedveld, L. Pakstis, B. Ozbas, D. J. Pine, D. Pochan, T. J. Deming, *Nature*, **2002**, 417, 424.

6. E. P. Holowka, V. Z. Sun, D. T. Kamei, T. J. Deming, *Nat. Mater*., **2007**, 6, 52.

7. A. Constancis, R. Meyrueix, N. Bryson, S. Huille, J. M. Grosselin, T. Gulik-Krzywicki, *J. Colloids Interface Sci.,* **1999**, 217, 357.

8. M. Yu, J. Hwang, T. J. Deming*, J. Am. Chem. Soc*., **1999**, 121, 5825.

9. P. D. Thornton, R. Brannigan, J. Podporska, B. Quilty, A. Heise, *J. Mater. Sci. Mater. Med*. **2012**, 23, 37.

10. C. Xiao, C. Zhao, P. He, Z. Tang, X. Chen, X. Jing, *Macromol. Rapid Commun*., **2010**, 31, 991.

11. J. R.Kramer, T. J. Deming*, J. Am. Chem. Soc*., **2010**,132, 15068.

12. J. Sun, H. Schlaad, *Macromolecules*, **2010**, 43, 4445.

13. H. Tang, D. Zhang, *Biomacromolecules*, **2010**, 11, 1585.

14. J. Huang, G. Habraken, F. Audouin, A. Heise, *Macromolecules*, **2010**, 43, 6050.

15. A. Carlsten, S. Lecommandoux, Curr*. Opin. Colloid Interface Sci*. **2009**, 14, 329.

16. H.-A. Klok, *Macromolecules,* **2009**, 42, 7990.

17. C. Schatz, S. Louguet, J.-F. Le Meins, S. Lecommandoux, *Angew. Chem., Int. Ed.* **2009**, 48, 2572.

18. Y.Y. Choi, J.H. Jang, M.H. Park, B.G. Choi, B. Chi, B. Jeong, *J. Mater. Chem*., **2010**, 20, 3416.

19. Yi Chen, Xiao-Hui Pang, Chang-Ming Dong, *Adv. Funct. Mater*. **2010**, 20, 579.

20. H. Gao, S. Ohno, K. Matyaszewski, *J. Am. Chem. Soc*., **2006**, 128, 15111.

21. A. W. Bosman, R. Vestberg, A. Heumann, J. M. J. Frechet, C. Hawker, *J. Am. Chem. Soc*., **2003**, 125, 715.

22. V.Y. Lee, K. Havenstrite, M. Tijo, M. McNeil, H. M. Blau, R. D. Miller, J. Sly, *Adv. Mater*., **2011**, 23, 4509.

23. R. J. I. Knoop, M. de Geus, G. J. M. Habraken, C. E. Koning, H. Menzel, A.Heise, *Macromolecules,* **2010**, 43, 4126.

24. F. Audouin, R. J. I. Knoop, J. Huang, A. Heise, *J. Polym. Sci. A; Polym. Chem*., **2010**, 48, 6402.

25. A. Sulistio, A. Blecowe, A. Widjaya, X. Zhang, G. Qiao, *Polym. Chem*., **2012**, 3, 224.

26. K. Inoue, H. Sakai, S. Ochi, T. Itaya, T. Tanigaki, J. *Am. Chem. Soc*., **1994**, 116, 13783.

27. K. Inoue, S. Horibe, M. Fukae, T. Muraki, E. Ihara, H. Kayama, *Macromol. Biosci*., **2003**, 3, 26.

28. G. Mihov, D. Grebel-Koehler, A. Lübbert, G. W. M. Vandermeulen, A. Herrmann, H.-A. Klok, K. Müllen, *Bioconjugate Chem*., **2005**, 16, 283.

29. Huihong Huang, Jiayan Li, Lihui Liao, Jinhu Li, Lixin Wu, Chaoke Dong, Peibao Lai, Daojun Liu, *Eur. Polym. J*., **2012**, 48, 696.

30. Qinrong Wang, Jun Yu, Yunsong Yan, Shaoqiang Xu, Fangfang Wang, Qingnan Li, Jinzhi Wang, Xin Zhang, Dajojun Liu*, Polym. Chem*., **2012**, 3, 1284.

31. D. Appelhans, H. Komber, R. Kirchner, J. Seidel, C. F. Huang, D. Voigt, D. Kuckling, F. C. Chang, B. Voit, *Macromol. Rapid Commun*., **2005**, 26, 586.

32. N. Higashi, T. Koga, M. Niwa, *Chem. Biochem*., **2002**, 3, 448.

33. N. Higashi, A. Uchino, Y. Mizuguchi, M. Niwa, *Int. J. Biol. Macromol*. **2006**, 38, 120.

34. S. Pan, C. Wang, X. Zeng, Y. Wen, H. Wu, M. Feng, *Int. J. Pharm*., **2011**, 420, 206.

35. G. J. M. Habraken, H. R. Karel, M. Wilsens, C. E. Koning, A. Heise*, Polym. Chem.*, **2011**, 2, 1322.

36. G.J.M. Habraken, M. Peeters, C. H. J. T. Dietz, C. E. Koning, A. Heise, *Polym. Chem*. **2010**, 1, 514.

37. T. J. Deming, S. A. Curtin, *J. Am. Chem. Soc*. **2000**, 122, 5710.

38. T. Aliferis, H. Iatrou, N. Hadjichristidis, J. Messman, J. Mays, Macromol. Symp. **2006**, 240, 12.

39. T. Borase, M. Iacono, S. I. Ali, P. D. Thornton, A. Heise, *Polym. Chem*. **2012**, 3, 1267.

40. R. V. Ulijn, J*. Mater. Chem*., **2006**, 16, 2217.

41. P. D.Thornton, A. Heise, *J. Am. Chem. Soc*., **2010**, 132, 2024.

42. P. D. Thornton, A. Heise, *Chem. Commun*., **2011**,47, 3108.

43. O. A. Adekoya, I. Sylte, Chem*. Biol. Drug. Des*., **2009**, 73, 7.

44. P. D. Thornton, G. McConnell, R. V. Ulijn, *Chem. Comm*., **2005**, 47, 5913.

45. M. A. Azagarsamy, P. Sokkalingam, S. Thayumanavan, *J. Am. Chem. Soc*., **2009**, 131, 14184.

46. G. J. M. Habraken, C. E. Koning, A. Heise, *J. Polym. Sci. A: Polym. Chem*., **2009**, 47, 6883.

Chapter 3

Molecular Weight and Architectural Dependence of Well-Defined Star Shaped Poly(lysine) as a Gene Delivery Vector

Abstract

A series of well-defined star-shaped polypeptides were successfully synthesised by the ring opening polymerisation (ROP) of the N-carboxyanhydride (NCA) of ε-carbobenzyloxy-L-lysine (ZLL) using a range of generations of polypropylene imine (PPI) dendrimers as multifunctional initiators. The monomer feed ratio and dendrimer generation were varied to afford a series of polypeptide dendrimer hybrids with superior structural versatility and functionality. Subsequent protecting group removal yielded star-shaped poly(lysine) of controlled variation in polypeptide chain length and arm multiplicity. Star-shaped PLL polymers were used to prepare pDNA and siRNA to form "polyplexes" to determine their ability to complex different nucleic acid cargoes and were compared with linear PLL polyplex controls. Significant differences in size and surface charge were seen between star-shaped PLL polyplexes and linear PLL polyplexes for both cargoes. The star-shaped polypeptides were capable of more effective complexation of both nucleic acids at low N/P ratios compared to linear PLL as evidenced by zeta potential and electrophoretic data. This was particularly evident in siRNA polyplexes as linear PLL failed to completely complex siRNA into nanocomplexes of appropriate size for cell transfection i.e. <200 nm in size, while star poly-(lysine) formed siRNA polyplexes <100 nm at certain N/P ratios, albeit strongly dependent on the particular molecular weight and architecture, as analysed by dynamic light scattering (DLS). Atomic force microscopy (AFM) identified discrete spherically shaped polyplexes for all star-shaped polypeptide-based polyplexes while linear PLL formed elongated irregular shaped complexes. This difference in morphology may go some way towards explaining the 300-fold increase in

luciferase expression seen for star-shaped PLL polyplexes G5(64)-PLL40 compared to linear PLL pGLuc polyplexes in epithelial cells. Each of the PPI-PLL polymers appeared to be capable of protecting the nucleic acid cargoes from degradation by the relevant nuclease enzyme as effectively as the positive control polyethyleneimine (PEI) polyplexes. Overall the promising nucleic acid complexation, sizing, morphology and protection capacity of two different genetic "cargoes" highlight the potential of polypeptide dendrimer hybrids as gene delivery vectors.

This work was published in Biomaterials Science (2013), (1), 1223-1234.

3.1 Introduction

Gene delivery is an area which has generated immense interest in recent times.[1,2] The ability to use genetic material such as plasmid DNA, siRNA and microRNA to better understand and potentially treat and prevent diseases that currently lack or have poor therapeutic or prophylactic modalities is very appealing.[3] However, the inability to deliver these nucleic acid-based "drugs" in a safe and efficient manner remains a significant challenge to their commerical and clinical translation. These biomolecules are large, polyanionic structures that can be easily degraded by enzymes and do not readily cross the target cell membrane to reach their intracellular sites of action. The use of viral and non-viral vectors has helped to overcome some of these hurdles but major obstacles remain.[4] Although very efficient, viral delivery vectors possess the inherent immunogenic, safety and production concerns associated with them.[5] Consequently the use of cationic non-viral delivery vectors has been extensively explored with natural and synthetic polymers including poly-L-lysine (PLL),[6] chitosan,[7] dimethylaminoethyl methacrylate (DMAEMA),[8] poly(ethyleneimine) (PEI)[9] and various dendrimers[10,11] being harnessed for nucleic acid delivery.

The concept of dendrimer facilitated gene therapy is of particular interest arising from the unique properties associated with these materials.[12] Dendrimers are monodisperse and at higher generations are globular macromolecules that offer numerous functional groups within a highly defined compact structure. Some of the best-known cationic dendrimers include polypropylene imine (PPI) and poly(amido amine) (PAMAM) which contain peripheral ionisable primary amino groups, the number of which can be varied depending on the generation of dendrimer chosen. This cationic periphery permits the formation of electrostatically derived nanoparticle complexes with nucleic acids such as pDNA, whilst the inner tertiary amines enhance endosomal buffering capacity and therefore transfection.[13] However, some of the major hurdles, which have limited their use in biomedical applications to-date is their inherent cytotoxicity, potential immunogenicity and size limitations.[14]

Star-shaped polymers provide an attractive alternative as unimolecular containers because the molecular weight and the number of polymeric arms can be tightly controlled by choice of the polymerisation method and the multifunctional initiator.[15-17] This facilitates manipulation of the shape and the cargo space available for drug loading. Particularly attractive are polypeptide based star polymers due to their improved biocompatibility, functionality and the ability to introduce stimuli responsiveness when required through inclusion of specific amino acid sequences, whilst maintaining a well-defined globular shape.[18,19] A convenient method of polypeptide introduction is via N-carboxyanhydride (NCA) polymerisation which permits the

versatile and well controlled growth of long chain polypeptides from an (multi) amino terminated initiator.[20-30] NCA derived polypeptides have already demonstrated their potential biomedical applicability in areas such as tissue engineering,[31] drug/gene delivery,[32-35] medical adhesives,[36] antimicrobial agents,[37] and biorecognition applications.[38-45]

Cationic polypeptides such as linear poly(lysine) have also been investigated as a pDNA delivery vector owing to its cationic nature and potential biocompatibility.[46,47] Such complexes, however, exhibited low transfection efficiencies and elevated cytotoxicity thus preventing their clinical application.[48] The incorporation of poly(lysine) into a branched or star shaped architecture may overcome these issues by creating a unimolecular nanoparticle with increased cargo capacity and protection. Pan et. al have reported the growth of short poly(lysine) chains from a fourth generation PAMAM dendrimer and their use as a pDNA transfection agent.[49] These materials showed enhanced transfection efficiencies with reduced cytotoxicity thus highlighting the potential of such polypeptide-dendrimer hybrids. Dendritic poly(lysine) has also shown promise as a pDNA transfection agent but such materials are synthetically challenging and lack the structural versatility of a star shaped polypeptide derived from the NCA / multifunctional initiator approach.[50,51] We have recently reported the versatile synthesis of pH responsive star poly(glutamic acid) using various generations of PPI dendrimers as multifunctional initiators for NCA polymerisation.[30] By this approach the number of arms and the total molecular weight of the star polypeptides was systematically varied. Herein, we report the synthesis and systematic study of a range of well-defined star shaped lysine polymers of controlled molecular weights. We further investigate the potential of these materials as gene delivery vectors using pDNA and siRNA as suitable model cargoes. pDNA and siRNA are polyanionic biomolecules that present several different challenges in terms of their delivery to a cell.[52] Structurally, the much larger pDNA readily collapses into compact nanoparticles with a polycationic vector whereas siRNA carrying much less negative charge, tends to form weaker complexes. As a consequence it was interesting to determine if these star-shaped polypeptides were suitable as vectors for both cargoes in terms of their ability to efficiently package and protect these cargoes. The size, shape and morphology of these nanomaterials were determined by Dynamic Light Scattering (DLS) and Atomic Force Microscopy (AFM) in conjunction with ζ-potential and agarose/ PAGE gel electrophoresis to measure complexation efficiency and stability. The star shaped polypeptides were shown to effectively package and protect both pDNA and siRNA and preliminary transfection studies compared their capacity to transfect pDNA into cells compared to linear PL.

3.2 Results and Discussion

3.2.1 Star Polypeptide Synthesis

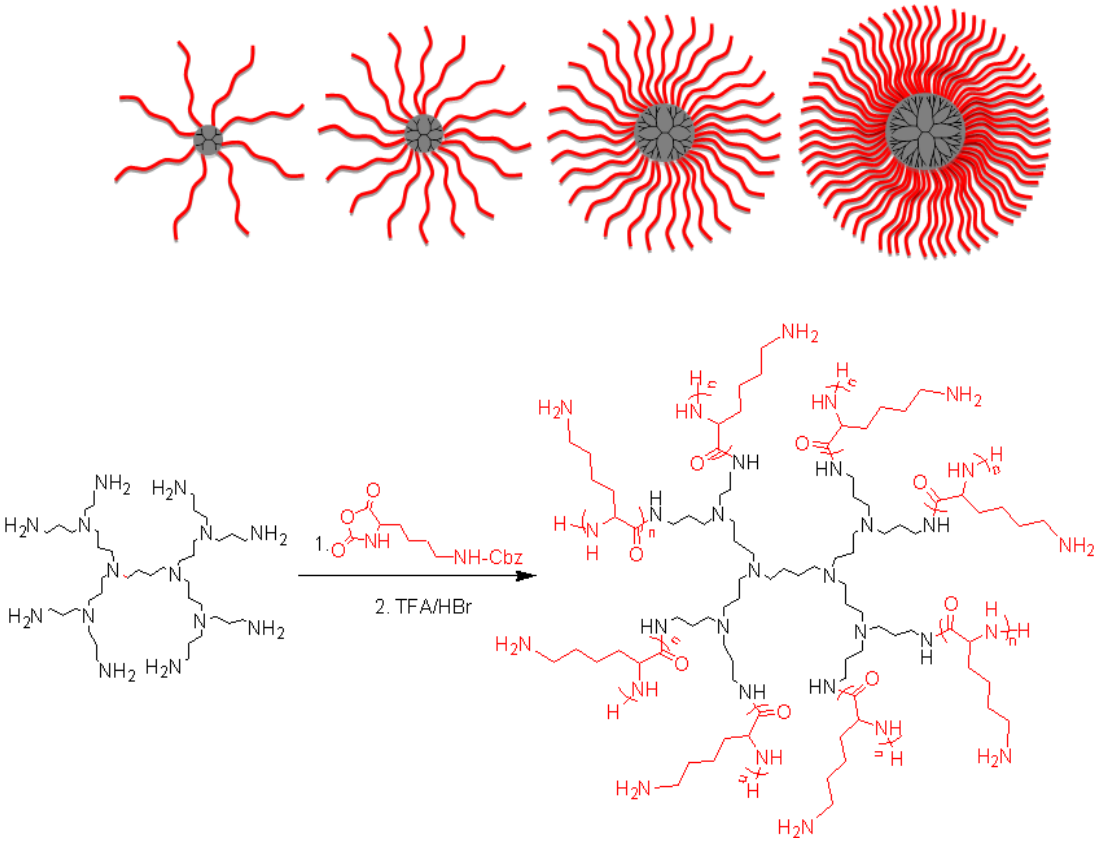

Figure 3.1: Synthesis of poly(L-lysine) star polypeptides by NCA polymerisation using second to fifth generation PPI dendrimers as initiators.

Table 3.1: Star-shaped PZLL by initiation from PPI dendrimers (L: linear initiator benzylamine; G5(64)-PZLL$_{40}$ = initiator generation 5 dendrimer with maximum 64 arms and theoretical arm length of 40 amino acids). Dispersities of all polymers < 1.2 (SEC MALS detection).

Entry	Polymer	NCA/NH_2	NCA/dendrimer	M_w/g mol$^{-1(a)}$	$M_n^{th\,(b)}$/g mol^{-1}
1	L(1)-PZLL$_{320}$	320	320	69 000	83 800
2	G2(8)-PZLL$_{40}$	40	320	96 000	83 800
3	G3(16)-PZLL$_{40}$	40	640	203 000	167 700
4	G4(32)-PZLL$_{40}$	40	1280	420 000	335 400
5	G5(64)-PZLL$_{40}$	40	2560	765 000	670 700
6	G5(64)-PZLL$_5$	5	320	100 000	83 800

(a) determined by SEC (DMF) using MALS detection using the dn/dc of linear PZLL of 0.101. (b) calculated assuming initiation from all amino groups and quantitative conversion: c(monomer)/c(dendrimer) x M(monomer) + M(dendrimer).

The ROP of α-amino acid NCAs via primary amines is a well understood method for the synthesis of well-defined synthetic linear polypeptides.[53-55] Building on previous work conducted in our group, the use of multifunctional amino terminated dendrimers was employed to synthesise well defined star shaped poly(lysine).[30] By employing four different generations of PPI dendrimers and varying the monomer feed ratio of ε-carbobenzyloxy-L-lysine (ZLL) NCA it was possible to create star shaped poly(lysine) whose size, shape, arm length and molecular weight could be readily controlled **(Figure 3.1)**. To develop a systematic library of star polypeptides and demonstrate the versatility of the system, polymers with similar polypeptide arm length (40 monomer units,) but different degrees of branching **(entries 2 - 5, Table 3.1)** were synthesized from the different generation PPI dendrimers (e.g. G5(64)-PZLL$_{40}$). ^{1}H NMR spectroscopy **(Figure 3.2)** confirmed the successful synthesis of PZLL and its conjugation to the dendrimer although PPI dendrimer peaks were difficult to observe for the higher molecular weight polymers due to overlapping with the broad polymer peaks

and its low concentration in comparison to the high density of PZLL. It was thus not possible to confirm NCA initiation from all of the primary amino sites although the agreement with the expected linear increase of molecular weights with increasing dendrimer generation suggests high initiation efficiency **(Figure 3.3)**. This library of materials was further completed by a 64 arm PZLL with only 5 repeating units per arm (entry 6, Table 3.1; G5(64)-$PZLL_5$) thus comparable to G2(8)-$PZLL_{40}$ in total molecular weight yet with more and shorter arms. Finally, a linear PZLL was synthesised **(entry 1, Table 3.1; L(1)-$PZLL_{320}$)**. Deprotection of the described polymers afforded linear and star shaped poly(lysine) possessing amino functionalities. Quantitative deprotection was confirmed by ^{1}H NMR spectroscopy and FTIR spectroscopy **(Figures 3.4 and 3.5).** Polymers 1 – 6 were subsequently investigated as gene delivery vectors.

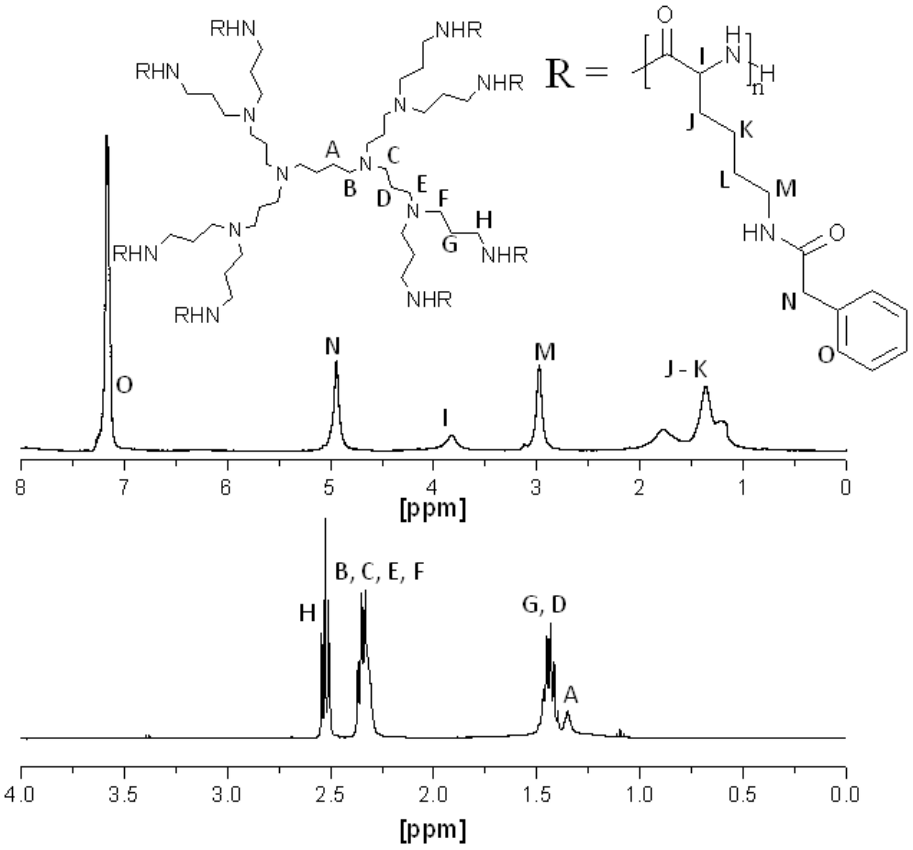

Figure 3.2: ^{1}H NMR spectra of G2(8)-$PZLL_{40}$ (Top) ($CDCl_3$) and G2-PPI Dendrimer (Bottom) ($CDCl_3$). R = H for unpolymerized PPI Dendrimer (peaks A - H not visible in top spectrum).

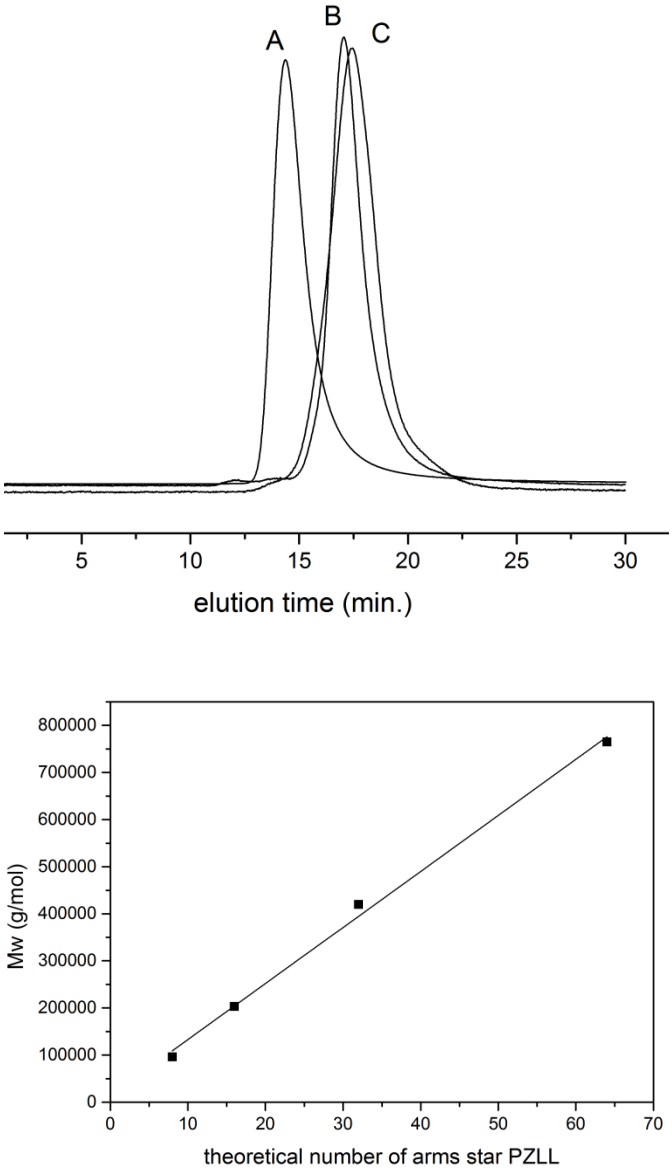

Figure 3.3: SEC traces of selected star shaped and linear poly-ε-carbobenzyloxy-L-lysine (A: G5(64)-PZLL$_{40}$; B: G2(8)-PZLL$_{40}$; C: G5(64)-PZLL$_5$) and weight average molar mass (M_w) of star-shaped PZLL obtained by initiation of NCA from different generation PPI dendrimers. The line represents a linear fit.

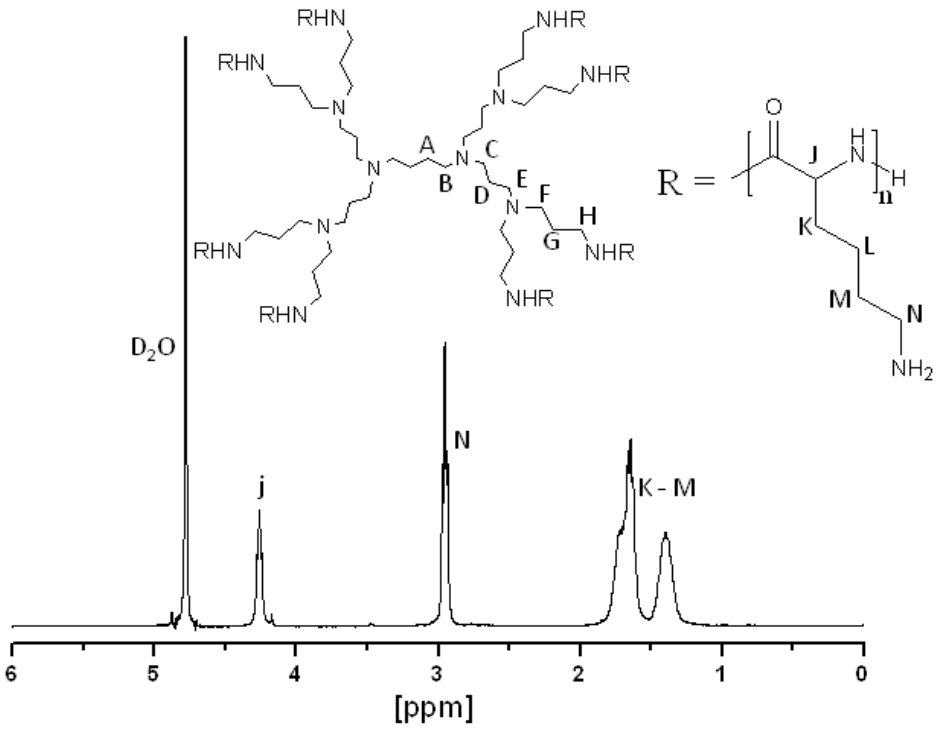

Figure 3.4: ^{1}H NMR spectrum of deprotected G2(8)-PLL$_{40}$ (D_2O). (Peaks A - H not visible)

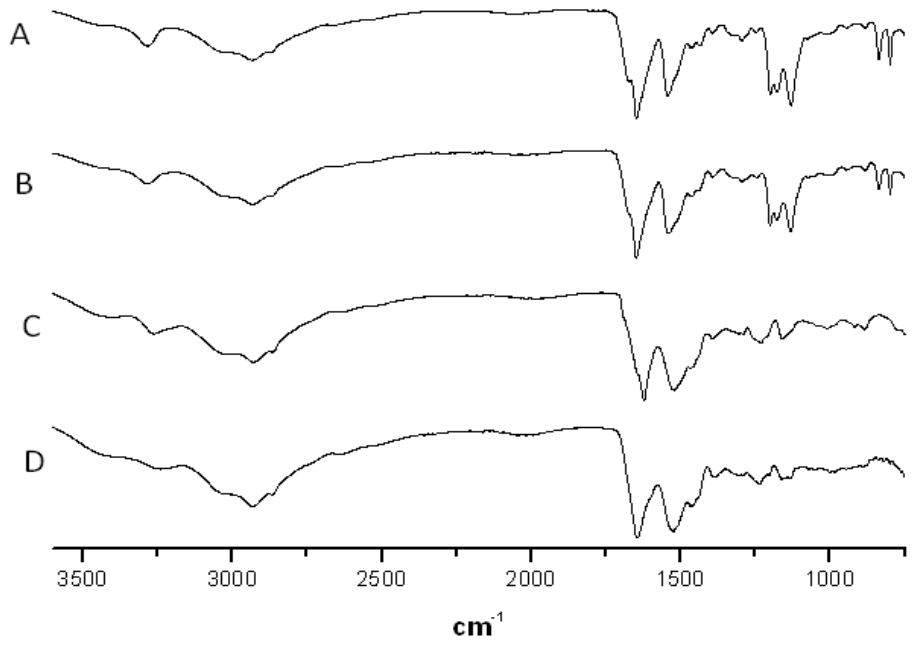

Figure 3.5: FTIR spectra of L(1)-PLL$_{320}$ (A), G2(8)-PLL$_{40}$ (B), G5(64)-PLL$_{40}$ (C) and G5(64)-PLL$_{5}$ (D).

3.2.2 Complexation with Genetic Cargoes

Particle size, surface charge and morphology of pDNA-PLL polyplexes

ζ-potential analysis **(Figures 3.6 and 3.7)** demonstrated that star shaped PLL could successfully form cationic polyplexes with pDNA at N/P 2 - 5 whereas linear PLL required higher ratios of N/P 10 – 20 to neutralise the polyanionic charge of the pDNA. No noticeable effect in pDNA complexation was observed between the different star shaped architectures. For successful pDNA transfection nanoparticles <200nm are required. Nanoparticles with sizes greater than 200 nm will be readily removed from the body by the reticuloendothelial system (RES)[56] and will not be efficiently endocytosed by cell membranes. The particle size **(Figures 3.8 and 3.9)** of cationic pDNA polyplexes formed was investigated over a range of N/P ratios using dynamic light scattering (DLS). Around charge neutrality i.e. complete pDNA neutralisation (as indicated by a ζ-potential around 0 mV in **Figures 3.6 and 3.7**) large sized pDNA polyplexes were observed which would be expected due to a lack of colloidal stability. For pDNA it was observed that at N/P 5 – 100, G2(8)-PLL_{40} and G5(64)-PLL_5 could form nanoparticles <100nm in size with the densely branched, long armed G3(16), G4(32) and G5(64)-PLL_{40} slightly larger nanoparticles over this N/P ratio range. Linear PLL could also compact pDNA into nanoparticles <200nm but only at higher N/P ratios (N/P >10) than star shaped PLL. Atomic force microscopy was used to investigate the morphology of the pDNA polyplexes as the shape of the complexes can impact on gene delivery efficiency.[57] It was observed that star shaped PLL could efficiently complex pDNA into discrete, compact, spherically shaped nanoparticles with sizes in the range 50 – 150nm **(Figures 3.10 and 3.11)**. In comparison linear PLL/pDNA complexes were irregular and elongated in shape. pDNA- L(1)-PLL_{320} polyplexes displayed sizes >200nm, supporting the DLS data. These irregular and large polyplexes would not support efficient gene transfection.

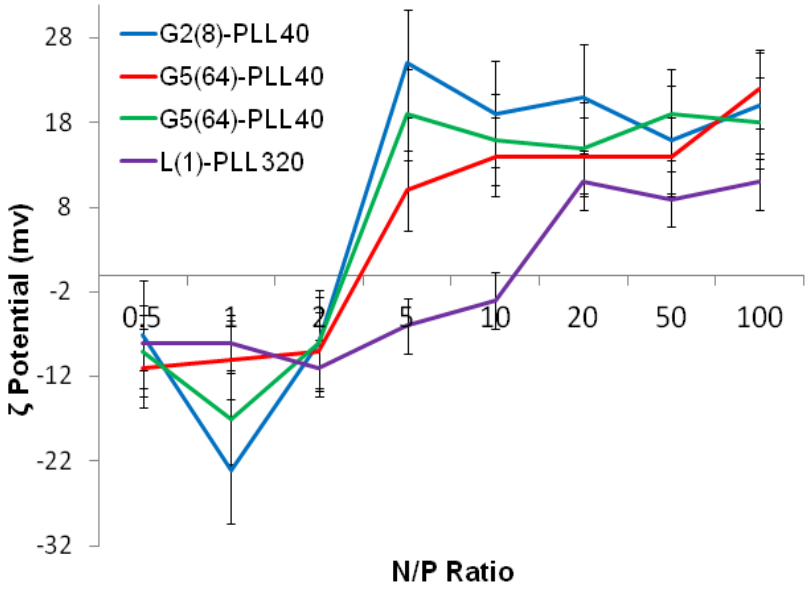

Figure 3.6: ζ-potential of G2(8)-PLL_{40}, G5(64)-PLL_{40}, G5(64)-$PZLL_5$ and L(1)-PLL_{320} polypeptide/pDNA polyplexes at over a range of N/P ratios.

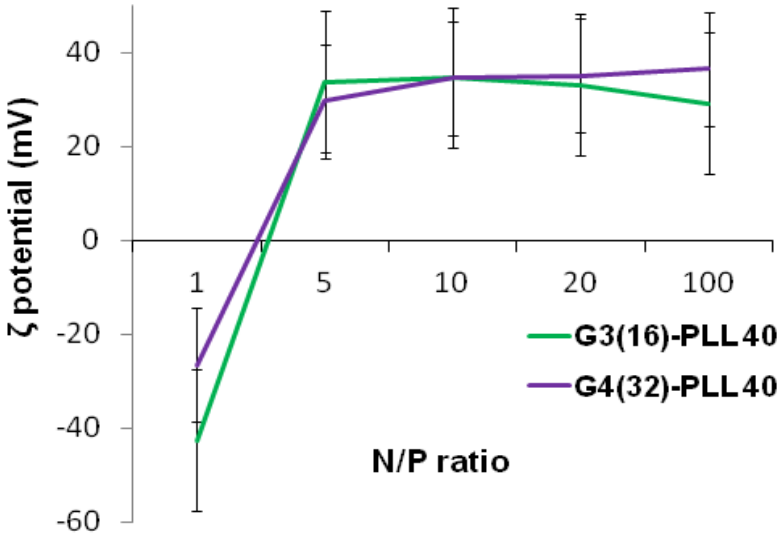

Figure 3.7: ζ-potential of G3(16)-PLL_{40} and G4(32)-PLL_{40} polypeptide/pDNA-PLL polyplexes at various N/P Ratios.

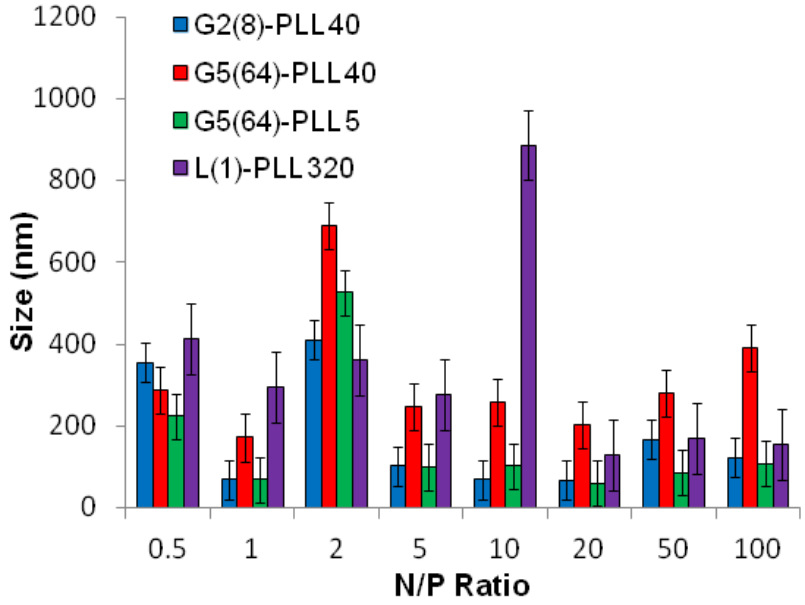

Figure 3.8: Particle size of G2(8)-PLL_{40}, G5(64)-PLL_{40}, G5(64)-$PZLL_5$ and L(1)-PLL_{320} polypeptide/pDNA polyplexes at over a range of N/P ratios.

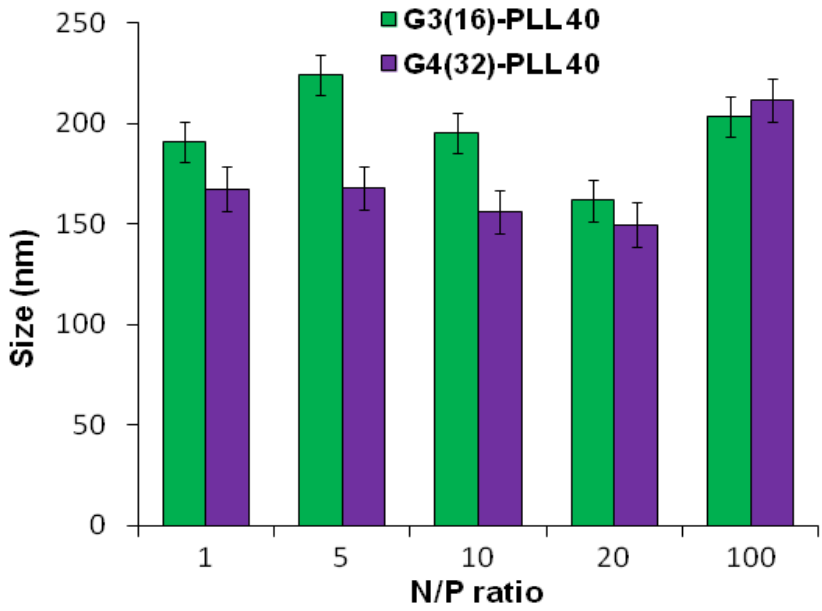

Figure 3.9: Particle size of G3(16)-PLL_{40} and G4(32)-PLL_{40} polypeptide/pDNA-PLL polyplexes at various N/P Ratios.

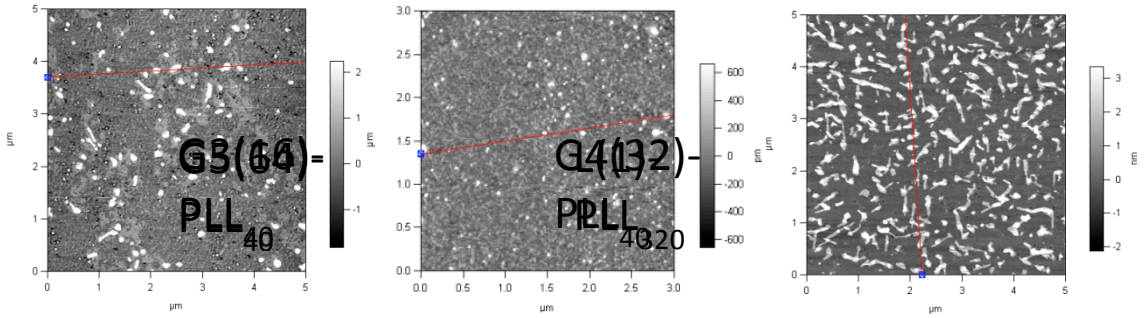

Figure 3.10: Atomic Force Microscopy of G5(64)-PZLL$_5$, G5(64)-PLL$_{40}$, and L(1)-PLL$_{320}$ polypeptide/pDNA polyplexes at N/P 20.

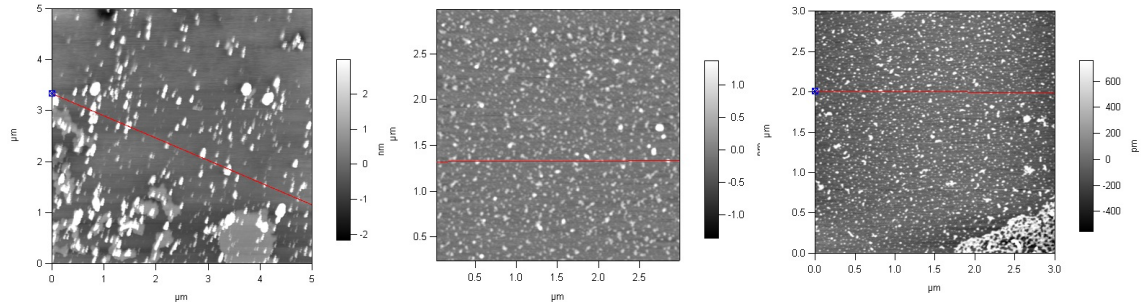

Figure 3.11: Atomic Force Microscopy of G2(8)-PZLL$_{40}$, G3(16)-PLL$_{40}$, and G4(32)-PLL$_{40}$ polypeptide/pDNA polyplexes at N/P 20.

Particle size, surface charge and morphology of siRNA-PLL polyplexes

siRNA are much shorter chain oligonucleotides and therefore interact with and form very different polyplexes to those fabricated with pDNA. L(1)-PLL$_{320}$ failed to effectively complex siRNA even at very high PLL:siRNA N/P ratios up to 300 **(Figure 3.12)**. The inability of linear PLL to neutralise siRNA and form a discrete compact cationic nanostructure clearly relates to its linear architecture as star shaped polypeptides very effectively neutralised the polyanionic siRNA at low N/P ratios <5. The molecular weight and architecture had a significant impact on the overall surface charge of the siRNA polyplexes formed with G2(8)-PLL$_{40}$ and G5(64)-PLL$_5$, with similar molecular weights, both forming cationic siRNA polyplexes at N/P 3 whereas the much larger G3(16), G4(32) and G5(64)-PLL$_{40}$ required a higher polymer:siRNA ratio of N/P 5

(Figures 3.12 and 3.13). For example, G5(64)-PLL_{40} overall possesses more lysine units than G2(8)-PLL_{40} and G5(64)-PLL_5 with a large core and up to 64 long lysine arms. G2(8)-PLL_{40} has a small core with only up to 8 long arms and G5(64)-PLL_5 has a large core with up to 64 short arms, making their overall molecular weight and number of lysine residues smaller. Therefore, it can be determined from this and the L(1)-PLL_{320} data that is not simply the number of cationic lysine residues presented that impacts on siRNA complexation but how they are presented. The large dendrimer core and dense polypeptide shell of G5(64)-PLL_{40} may limit siRNA interaction with PPI-PLL with the siRNA being retained upon the periphery of this star-shaped polypeptide. In contrast the long but relatively few arms of G2(8)-PLL_{40} and the many but short arms of G5(64)-PLL_5 results in a decreased polypeptide density, enabling greater exposure of siRNA to lysine units and potentially the dendrimer core even though these star shaped polypeptides have fewer overall cationic units than G5(64)-PLL_{40}. This difference in ability to complex siRNA between the star shaped PLL was also evident in the particle size analysis **(Figures 3.14 and 3.15)**. siRNA polyplexes composed of G2(8)-PLL_{40} and G5(64)-PLL_5 could form discrete nanoparticles <100nm at N/P 5 – 100 whereas those composed of L(1)-PLL_{320} and G3(16), G4(32) and G5(64)-PLL_{40} could not form polyplexes <200nm at N/P 1 - 100. AFM analysis **(Figures 3.16 and 3.17)** of star shaped PLL siRNA polyplexes showed the efficient complexation and subsequent formation of spherically shaped compact nanoparticles (50 – 150nm) at N/P 20. L(1)-PLL_{320} however, formed large elongated siRNA polyplexes (>200nm) a feature which may inhibit efficient or complete siRNA complexation as observed in ζ-potential analysis of the described polyplex. A small amount of aggregation was observed for siRNA polyplexes of G2(8)-PLL_{40} **(Figure 3.16)** which may be an artefact of sample preparation i.e. as the mica sheet was dried, the gradual loss of solvent may have promoted minor aggregation. In spite of this, the star shaped siRNA-polyplexes were predominantly finely dispersed.

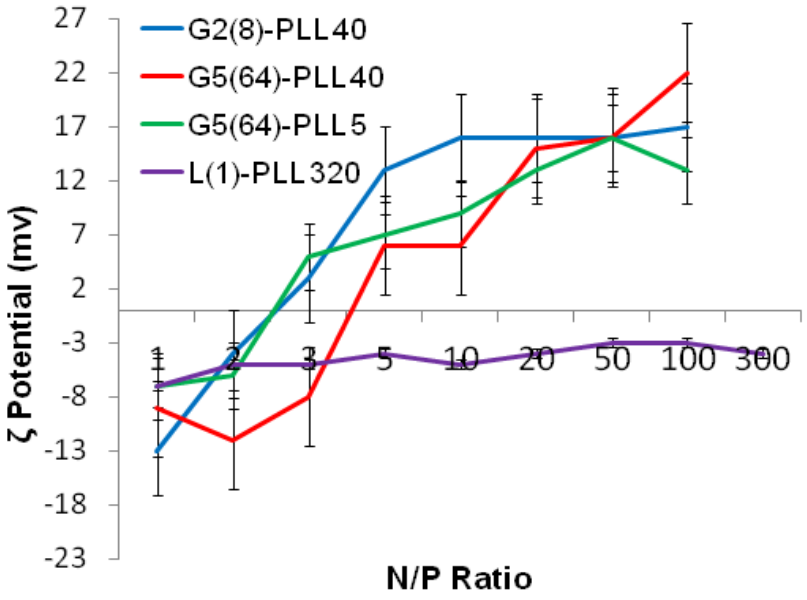

Figure 3.12: ζ-potential of G2(8)-PLL_{40}, G5(64)-PLL_{40}, G5(64)-$PZLL_5$ and L(1)-PLL_{320} polypeptide/siRNA polyplexes at over a range of N/P ratios.

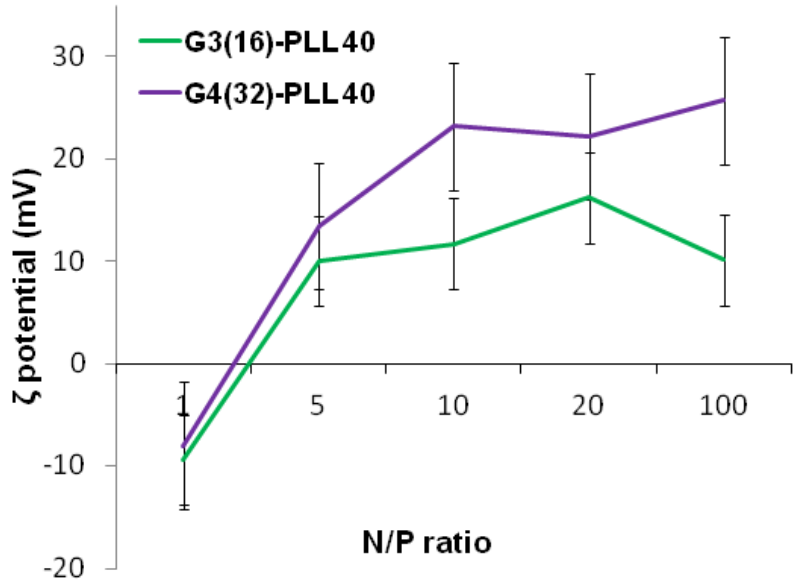

Figure 3.13: ζ-potential of G3(16)-PLL_{40} and G4(32)-PLL_{40} polypeptide/siRNA-PLL.

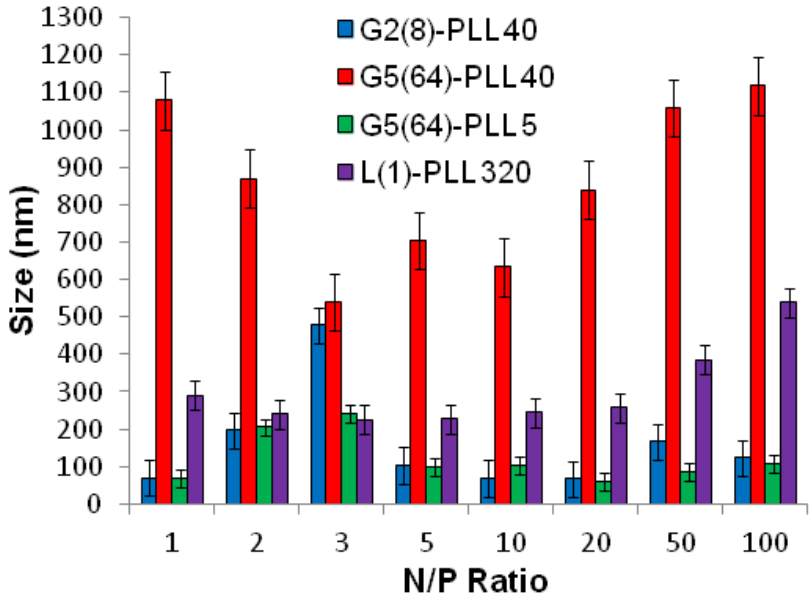

Figure 3.14: Particle size of G2(8)-PLL_{40}, G5(64)-PLL_{40}, G5(64)-$PZLL_5$ and L(1)-PLL_{320} polypeptide/siRNA polyplexes over a range of N/P ratios.

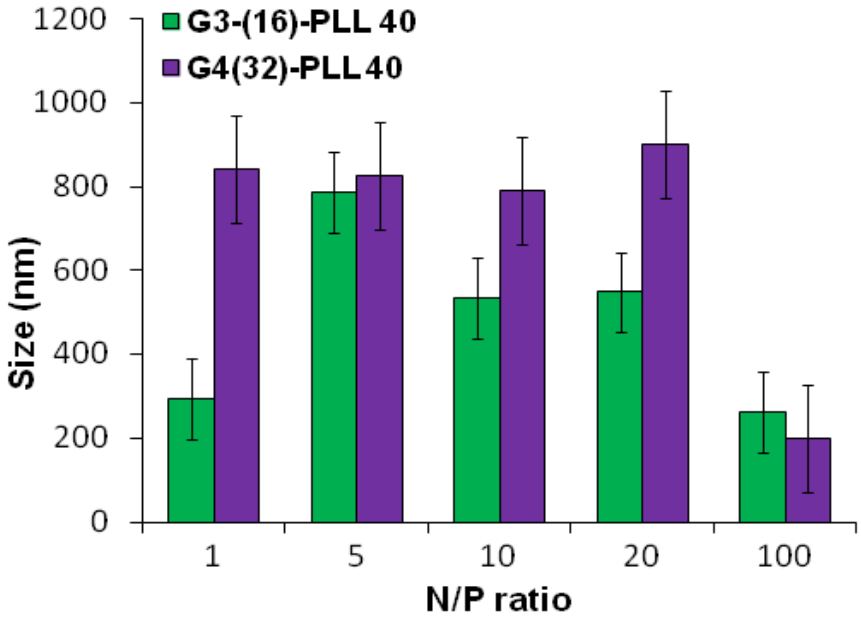

Figure 3.15: Particle size of G3(16)-PLL_{40} and G4(32)-PLL_{40} polypeptide/siRNA-PLL polyplexes at various N/P Ratios.

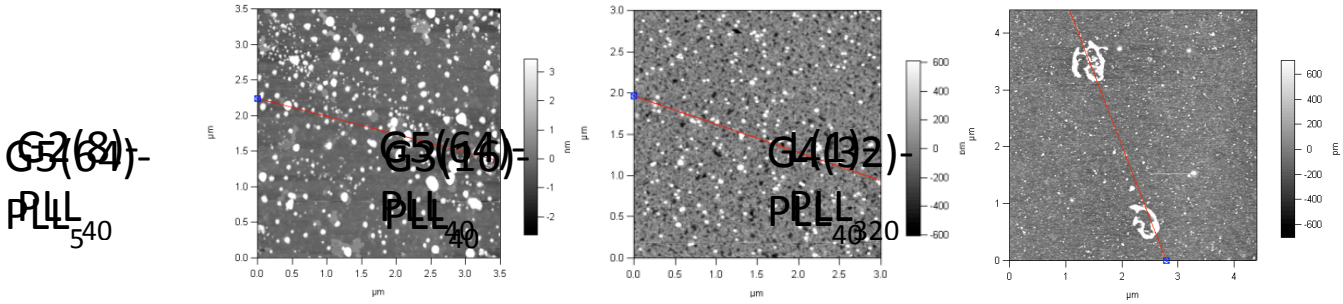

Figure 3.16: Atomic force microscopy of G2(8)-PLL_{40}, G5(64)-PLL_{40} and L(1)-PLL_{320} polypeptide/siRNA polyplexes at N/P 20.

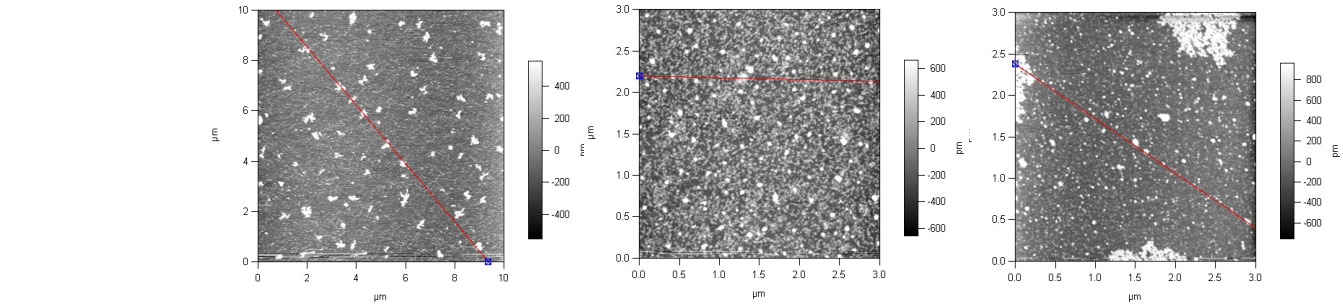

Figure 3.17: Atomic force microscopy of G5(64)-PLL_5, G3(16)-PLL_{40} and G4(32)-PLL_{40} polypeptide/siRNA polyplexes at N/P 20.

Gel retardation assays of siRNA/pDNA polyplexes

The cationic nature of the star shaped polypeptides provides a useful platform for the delivery of nucleic acids into cells. Gel retardation assays were used to evaluate and further confirm **(Figures 3.6 – 3.17)** the ability of both linear and three of the star-shaped polypeptides G2(8)-PLL_{40}, G5(64)-PLL_5 and G5(64)-PLL_{40} to form complexes with the two different nucleic acid cargoes under investigation i.e. plasmid DNA and siRNA. The assays were carried out at different N/P ratios for pDNA (N/P: 0.5, 1, 5, 10, 20) and siRNA (N/P: 1, 2, 3, 5, 10, 20, 50) based on the literature and the previous particle size and zeta potential studies.

From **Figures 3.18** and **3.19** it was noted that all polymers, both linear and star shaped PLL successfully complexed pDNA at N/P 5. This is evidenced by the lack of a pDNA band seen on the gels in Lanes 6, 7 and 8 which represent N/P ratios of 5, 10 and 20 respectively. This observation corroborates the particle size and zeta potential data **(Figures 3.6 and 3.8)**. The effective interaction seen for all the polylysines most likely arises from the large number of nucleic acids presented by pDNA that enables effective electrostatic complexation with all of the described polymers. The nature of the nanoparticle produced by this complexation, however is structure dependent as evidenced in **Figures 3.8**, **3.9**, **3.10** and **3.11**. PEI/pDNA complex and uncomplexed pDNA were used as a reference and control respectively.

Polypeptide architecture had a very significant effect on siRNA complexation **(Figures 3.20 and 3.21)**. L(1)-PLL_{320} was unable to completely complex siRNA even at N/P 50 as evidenced by the presence of siRNA band in lane 9 of gel in **Fig 3.20b**. However, star-shaped PLL could successfully form polyplexes at ratios as low as N/P 1 as evidenced by the lack of siRNA band seen in Lanes 4-9 on the gel in **Figure 3.20a**. Architectural variations within the star shaped polypeptide family also displayed notable differences in siRNA complexation with G5(64)-PLL_5 demonstrating gel retardation i.e. complexation at the lowest N/P ratio of N/P 2 **(Fig 3.20a)** while G5(64)-PLL_{40} and G2(8)-PLL_{40} fully retarded the siRNA at N/P20 and N/P 10 respectively **(Figure 3.21)**. Zeta potential analysis showed a similar trend with G5(64)-PLL_{40} neutralising siRNA at a slightly higher N/P ratio than G5(64)-PLL_5 or G2(8)-PLL_{40} **(Figure 3.6)** and producing the largest polyplexes over a range of N/P ratios **(Figure 3.8)**.

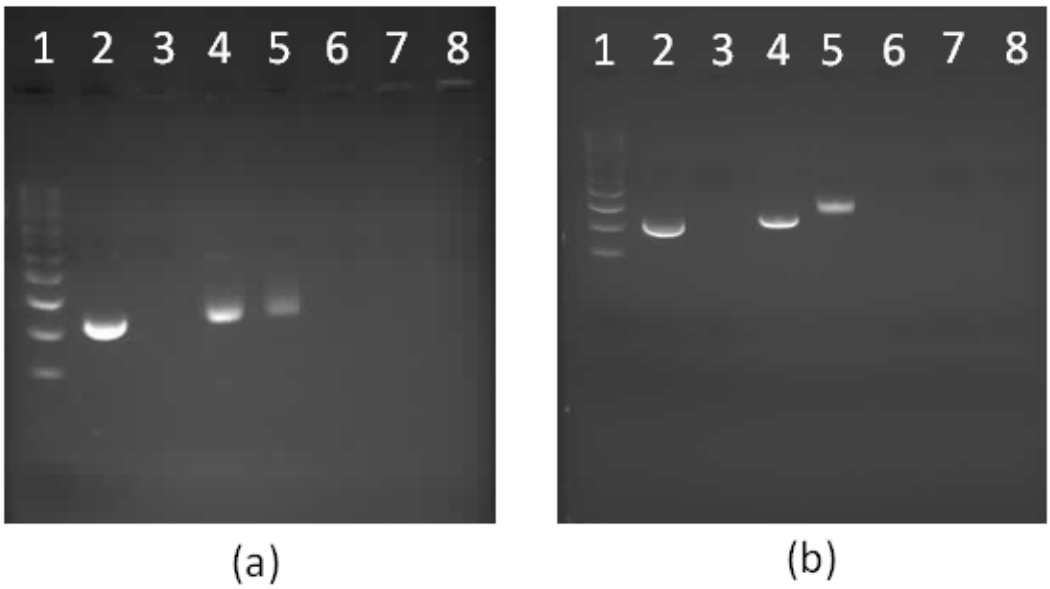

(a) (b)

Figure 3.18: **1% Agarose gel electrophoresis of star shaped PLL and linear PLL complexed with plasmid DNA to form polyplexes as a function of N/P ratio. (a) G5(64)-PLL_5; (b) L(1)-PLL_{320}; Lane 1: pDNA Ladder, Lane 2: pDNA, Lane 3: PEI/pDNA (N/P 10), Lanes 4 – 8: pDNA complexes at the N/P ratios of 0.5, 1, 5, 10, 20.**

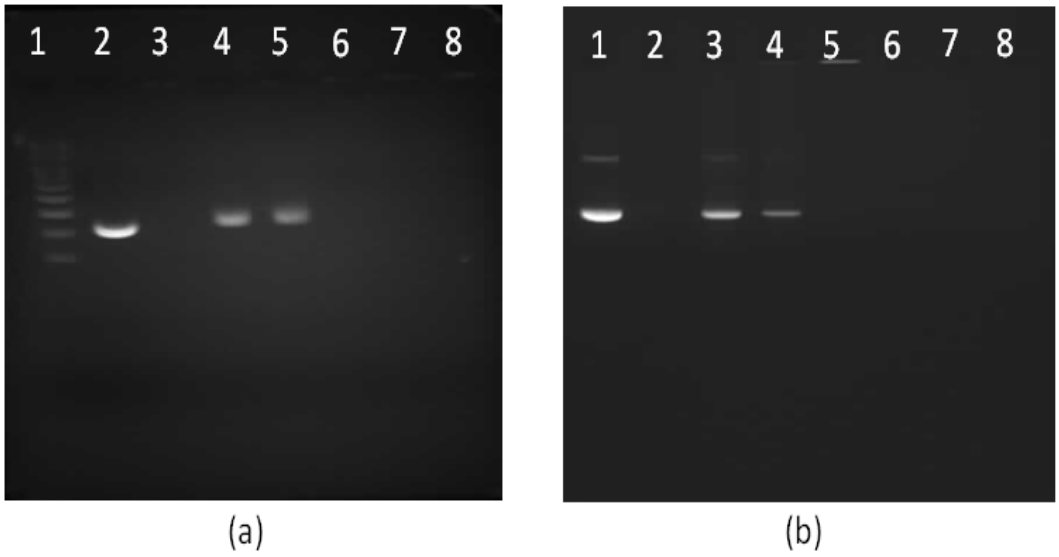

Figure 3.19: 1% Agarose gel electrophoresis of star shaped PLL complexed with plasmid DNA to form polyplexes as a function of N/P ratio. (a) G2(8)-PLL_{40}; (b) G5(64)-PLL_{40}; Lane 1: pDNA Ladder, Lane 2: pDNA, Lane 3: PEI/pDNA (N/P 10), Lanes 4 – 8: pDNA complexes at the N/P ratios of 0.5, 1, 5, 10, 20.

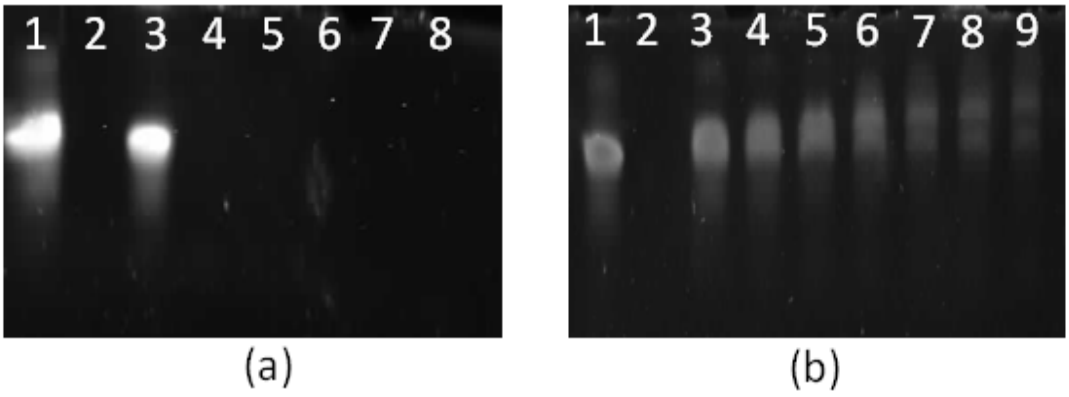

Figure 3.20: **PAGE gel electrophoresis of star shaped PLL and linear PLL complexed with siRNA to form polyplexes as a function of N/P ratio. (a) G5(64)-PLL_5; (b) L(1)-PLL_{320}; Lane 1: siRNA, Lane 2: PEI/siRNA (N/P 10), Lanes 3 – 9: siRNA complexes at the N/P ratios of 1, 2, 3, 5, 10, 20, 50.**

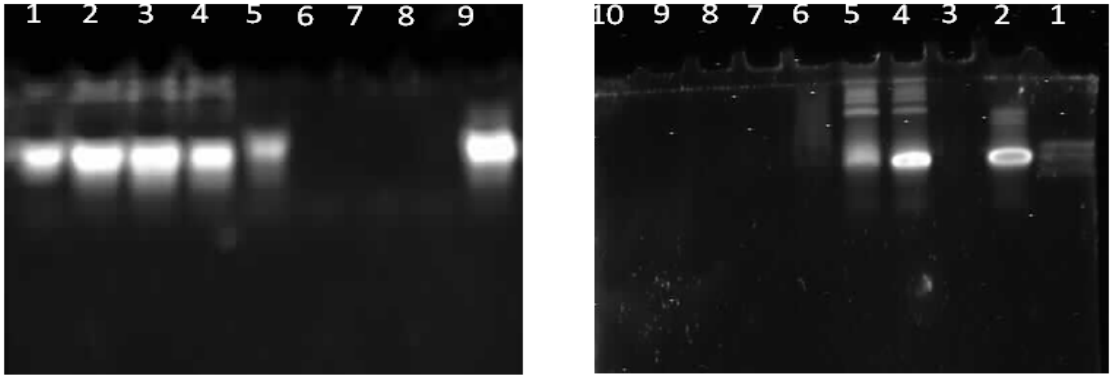

Figure 3.21: PAGE gel electrophoresis of star shaped PLL complexed with siRNA to form polyplexes as a function of N/P ratio. (a) G2(8)-PLL_{40}; Lane 1: siRNA Ladder, Lanes 2 – 7: siRNA complexes at the N/P ratios of 1, 2, 3, 5, 10, 20, Lane 8: PEI/siRNA (N/P 10), Lane 9: siRNA (b) G5(64)-PLL_{40}; Lane 1: siRNA Ladder, Lane 2: siRNA, Lane 3: PEI/siRNA (N/P 10), Lanes 4 – 10: siRNA complexes at the N/P ratios of 1, 2, 3, 5, 10, 20, 50.

Stability of polyplexes: DNase I and RNase I protection assays

Protection of the nucleic acid cargo from nuclease degradation is a vital prerequisite for any potential gene delivery vector. Molecular therapeutics such as pDNA and siRNA in particular are susceptible to hydrolysis and nuclease enzymes *in vivo*. Without sufficient molecular "cargo" protection gene therapy is inefficient or can be rendered completely ineffective. DNase and RNase degrade and nick pDNA and siRNA respectively resulting in extra banding or no bands at all (complete degradation) in gel electrophoresis. The ability of the star shaped polypeptide architectures (G2(8)-PLL_{40}, G5(64)-PLL_5 and G5(64)-PLL_{40}), to protect nucleic acids from this form of enzymatic breakdown was investigated using PEI and linear PLL as controls **(Figures 3.22 and 3.23)**. The polyplexes were exposed to the relevant nuclease and then disrupted to enable the nucleic acids to travel down the gel. The same generations of star shaped poly(lysine) were selected as used in the gel retardation study.

Naked pDNA is completely degraded in the presence of DNase emphasising the requirement and advantage of using a gene delivery vector **(Figure 3.22, Lane 3)**. All of the star shaped poly(lysine) formed tight complexes with pDNA and provided some degree of protection to the pDNA cargo from nuclease degradation similar to that seen for PEI though smearing is seen in the pDNA that did not remain encapsulated **(Figure 3.22, Lanes 6 – 8)**. Their protective ability was similar to that of PEI at an N/P ratio of 10 which is known to offer sufficient protection *in*

vitro and *in vivo*. Interestingly from a stability perspective the star-shaped PLL was more stable to disruption by SDS than PEI as evidenced by the presence of DNA fluorescence in the wells of these samples **(Figure 3.22, Lanes 5-8)** while very little remains in the PEI sample **(Figure 3.22, Lane 4)**.[58] Chain length and degree of branching appeared to have minimal effect on the protective capacity of each family for pDNA with little difference observed amongst star shaped PLL **(Figure 3.22, Lanes 6 – 8)**.

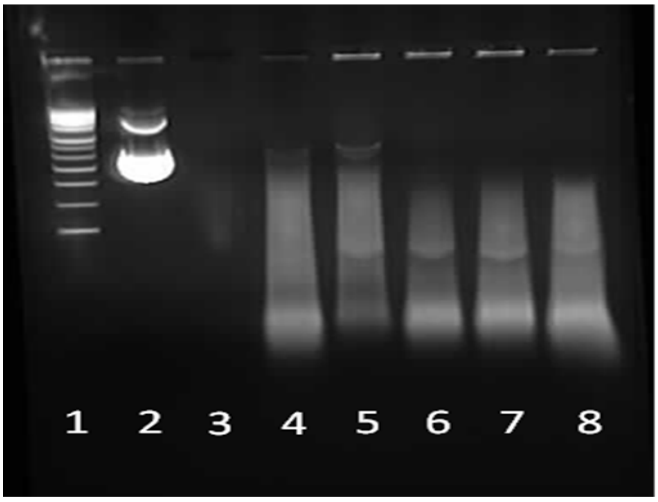

Figure 3.22: **1% Agarose gel electrophoresis of star shaped and linear PLL pDNA polyplexes at N/P 10 and their stability towards the enzyme DNase. Lane 1: pDNA ladder, Lane 2: pDNA, Lane 3: pDNA/DNase, Lane 4: PEI/pDNA/DNase, Lane 5: L(1)-PLL_{320}/pDNA/DNase, Lane 6: G2(8)-PLL_{40}/pDNA/DNase, Lane 7: G5(64)-PLL_{40}/pDNA/DNase and Lane 8: G5(64)-PLL_5/pDNA/DNase.**

RNase stability assays indicated that each of the star shaped polypeptides was capable of protecting siRNA from nuclease degradation via RNase **(Figure 3.23, Lanes 1 – 3)**. Without complexation with a vector, naked siRNA was completely degraded by RNase **(Figure 3.23, Lane 6)**. L(1)-PLL_{320} **(Figure 3.23, Lane 4)** also showed similar protective ability to that of the star shaped polypeptides and PEI **(Figure 3.23, Lane 5)** despite its' inability to completely complex siRNA at N/P 10 **(Figure 3.12)**. From observations of AFM images **(Figure 3.16)** L(1)-PLL_{320}/siRNA complex adopts a very large coiled morphology, which may promote protection of the cargo by sterically hindering degradation by RNase. It was evident that disruption of these polyplexes was readily achieved owing to the sharp bands observed in **Figure 3.23** after siRNA decomplexation from the vectors. Such a feature possibly arises from the inherently small size of siRNA, allowing easier disruption of the polyplexes formed. The much larger pDNA

however, containing more nucleic acids, produced broad smeared bands as a consequence of its ability to form very strong complexes with the described polypeptides resulting in a complex more difficult to disrupt **(Figure 3.22)**.

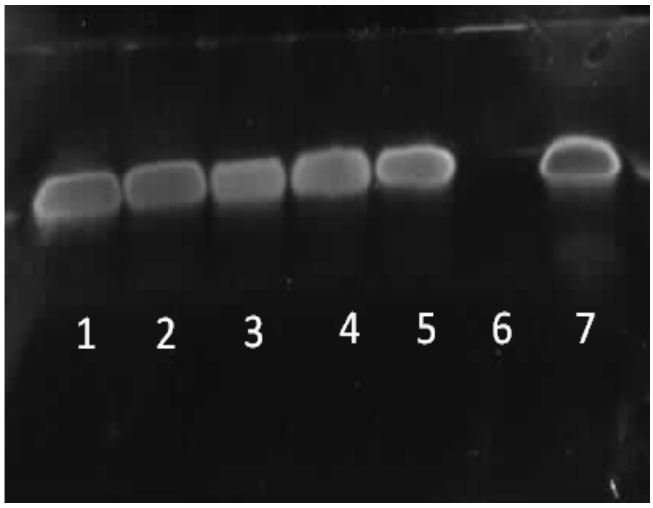

Figure 3.23: **PAGE gel electrophoresis of star shaped and linear PLL siRNA polyplexes at N/P 10 and their stability towards the enzyme RNase. Lane 1: G5(64)-PLL_5/siRNA/RNase, Lane 2: G5(64)-PLL_{40}/siRNA/RNase , Lane 3: G2(8)-PLL_{40}/siRNA/RNase, Lane 4: L(1)-PLL_{320}/siRNA/RNase, Lane 5: PEI/siRNA/RNase, Lane 6: siRNA/RNase and Lane 7: siRNA.**

pDNA transfections of Calu-3 cells using linear and star-shaped G5(64)-PLL_{40} polyplexes

Based on the physicochemical data outlined above one of the star-shaped PLL generations, G5(64)-PLL_{40} was optimised for transfection using a reporter plasmid expressing luciferase, *pGLuc* and compared to linear PLL at its previously determined N/P optimum of 2 for pDNA transfection.[59] **Figure 3.24** illustrates the results of this study with G5(64)-PLL_{40} successfully transfecting Calu-3 cells with the levels of expression dependent on the N/P ratio of the polyplexes used. An optimum N/P ratio of 5 was determined for this star-shaped polymer, similar to that found for other dendrimer-based gene vectors such as Superfect™. From the particle size analysis **(Figure 3.8)** N/P ratios < 5 for G5(64)-PLL_{40} with pDNA formed large nanoparticles >300nm. Optical images taken of cells post treatment **(Figure 3.25)** indicated that at high N/P ratios e.g. N/P50 **(Figure 3.25 - D)** there were signs of significant cellular toxicity, while at the optimum transfection N/P ratio of 5 cells appear healthy and viable **(Figure 3.25 - C)**. The highest levels of expression were seen at day 5 post transfection and these were significantly greater than for linear pLL at each of N/P ratios 5, 10 and 20 ($p<0.05$). These preliminary transfection studies indicate that the star-shaped PLL is capable of

protecting pDNA, enhancing its cellular uptake and ultimately facilitating pDNA expression over prolonged periods, up to 5 days, which could enable applications in both conventional and regenerative medicine.

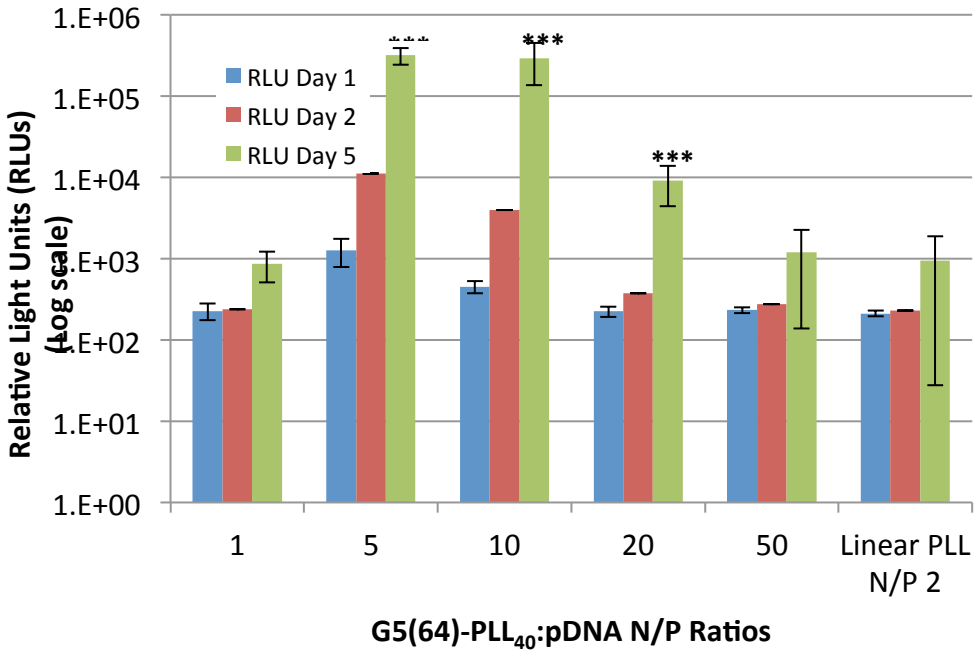

Figure 3.24: **Transfection of Calu-3 cells with p*Luc*/pLL polyplexes composed of linear pLL:pDNA (N/P 2) and star-shaped PLL G5(64)-PLL_{40} over range of N/P ratios (N/P 1-50). Expression of luciferase expressed as RLUs (log scale) was assessed 1, 2 or 5 days post transfection with the polyplexes (n=3 +/- S.D.) Data are represented as mean ± SD and were compared by t-test (non-parametric, one-tailed) against linear PLL at day 5. Differences were considered highly significant at *** p < 0.001.**

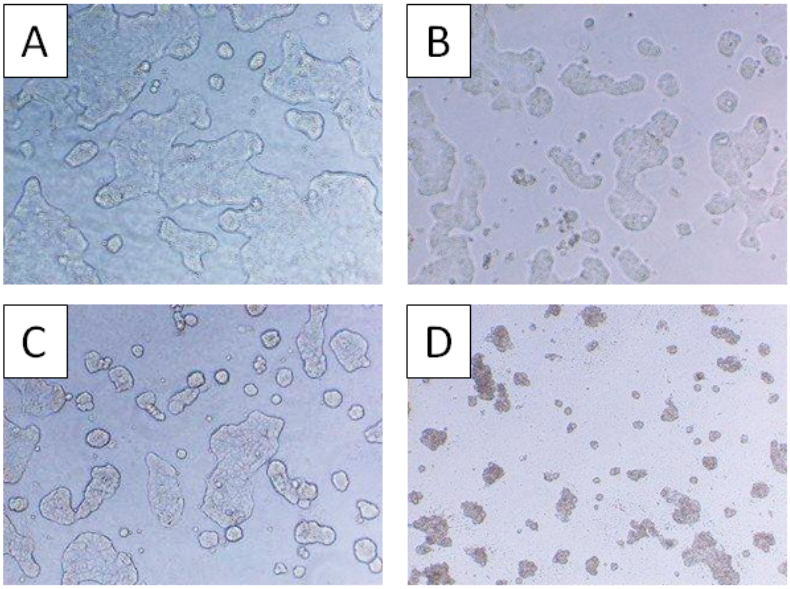

Figure 3.25: Optical images of Calu-3 cells treated with A) untreated cells B) pDNA-Linear PLL N/P 2 C) pDNA-G5(64)-pLL$_{40}$ N/P 5 and D) pDNA-G5(64)-pLL$_{40}$ N/P 50 polyplexes.

3.3 Conclusion

Star-shaped polypeptides are an attractive class of molecules for use as gene delivery vectors owing to their potential improved biocompatibility, structural characteristics and therapeutic "cargo" capacity. In this paper we describe the facile and systematic synthesis of a range of well-defined, monodisperse star shaped poly(lysine) polymers boasting molecular weight, branching and polypeptide chain length versatility. The applicability of the described polypeptides as gene delivery vectors was subsequently investigated. From our study, it was apparent that polypeptide architecture had a significant impact on the nature of the polyplexes formed. In terms of pDNA, all star shaped polypeptides efficiently packaged pDNA into discrete spherically shaped and positively charged nanocomplexes at low N/P ratios with sizes as low as <100nm whereas the equivalent linear polypeptide required a higher complexation ratio. The complexation of siRNA with star-shaped PLL was greatly superior to linear PLL. In particular the small armed, less densely branched star polypeptides were most promising as both pDNA and siRNA delivery vectors owing to their optimum sizing and complexation data. All star polypeptides offered similar protection of pDNA and siRNA from nuclease degradation once complexed. However upon decomplexation it was noted that siRNA complexes were more readily disrupted in comparison to pDNA complexes, highlighting the differences in stability between polyplexes composed of the different nucleic acids. Overall the promising nucleic acid complexation, sizing, morphology and protection capacity of two different genetic "cargos" highlights the potential of polypeptide dendrimer hybrids as gene

delivery vectors (GDVs). Their potential as GDVs was confirmed with preliminary pDNA transfection studies in which one of the G5(64)-PLL_{40} was found to be capable of successfully transfecting epithelial cells with pDNA, and importantly these levels were significantly greater compared to linear PLL with a 300-fold increase in expression seen over the 5 day study. The systematic study reported here may potentially lead to the identification and development of an ideal polypeptide dendrimer hybrid material for use as a versatile platform in gene delivery. Versatility may be readily enhanced through the facile control of polypeptide dimensions such as branching and molecular weight, end group and side chain modification using pegylation, glycosylation and attachment of ligands to further improve biocompatibility, cell targeting and overall efficacy of the delivery platform.

3.4 Experimental

Materials

All air and moisture sensitive compounds were handled under a nitrogen atmosphere using general Schlenk-line techniques. α-pinene (98%) bis(trichloromethyl) carbonate (triphosgene) 99% and benzylamine were purchased from Sigma Aldrich. H-Lys(Z)-OH were supplied by Bachem. PPI (polypropylene imine) dendrimers generations 2-5 were purchased from SyMO-Chem BV (The Netherlands). Chloroform (anhydrous), ethyl acetate (anhydrous), dimethylformamide, tetrahydrofuran, n-heptane, and diethylether were supplied by Sigma Aldrich. All chemicals were used without any purification unless otherwise noted. Chloroform and ethyl acetate were used directly from the bottle and stored under an inert, dry atmosphere. ε-carbobenzyloxy-L-lysine NCA were synthesised following a literature procedure.[60] siGENOME non-targeting siRNA #4 (5' AUGAACGUGAAUUGCUCAA 3') was obtained from Dharmacon and the pGL3-control vector plasmid was sourced from Promega.

Star poly-ε-carbobenzyloxy-L-lysine ((G2-5) PPI-PZLL)

As a reference procedure, the NCA of ε-carbobenzyloxy-L-lysine (ZLL) (2.02 g, 6.6 mmol) was dissolved in 25 ml $CHCl_3$ in a Schlenk tube under a nitrogen atmosphere. A solution of G2 PPI dendrimer (30 mg, 2.07 x 10^{-2} mmol) in 2 ml $CHCl_3$ was quickly charged to the dissolved NCA solution via syringe. The solution was stirred for 24 h at room temperature. Depending on the type of initiator, the used molar amount of initiator and monomer were adjusted to achieve the desired molecular weight of the star shaped polypeptides. The polymer was precipitated into an excess of cold diethyl ether and dried under vacuum (Yield: 95%).

Star poly-L-lysine (PPI-PLL)

G2(8)- $PZLL_{40}$ (1.2 g) was dissolved in 12 ml of trifluoroacetic acid (TFA). A 6-fold excess with respect to ε-carbobenzyloxy-L-lysine of a 33% solution of HBr in acetic acid (5ml) was added slowly to the reaction. After 16 h, the solution was precipitated into diethyl ether. The precipitate was dissolved in ethanol and precipitated thrice into diethyl ether. The polymer was dissolved in deionised water and dialyzed (MWCO 8,000) for 3 days. The polymer was lyophilized. Yield: 68%. Deprotection was confirmed by ^1H NMR spectroscopy due to the absence of signals at 7.2 ppm (benzyl group) and 5.0 ppm and (CH_2).

Linear poly-ε-carbobenzyloxy-l-lysine (L-PLL)

In a Schlenk tube under a nitrogen atmosphere, a solution of the NCA of ε-carbobenzyloxy-L-lysine (ZLL (0.92 g, 3 mmol) in $CHCl_3$ (30 ml) was prepared. A solution of benzylamine initiator (1 mg, 9.33 x 10^{-3} mmol) in 1 ml $CHCl_3$ was also prepared and charged to the reaction solution via syringe. The solution was stirred at room temperature until no further increase in molecular weight was achieved. The molecular weight was monitored by SEC by precipitating 1 ml (63 mg) of the reaction solution into an excess of cold diethyl ether. Upon no increase in molecular weight, the polymer was precipitated into an excess of cold diethyl ether and dried under vacuum (Yield: 70%). For the deprotection the same procedure as for PPI-PZLL was applied. (Yield: 70%).

Methods

Nuclear magnetic resonance (NMR) spectra were recorded on a Bruker Avance 400 (400MHz) spectrometer at room temperature in $CDCl_3$ and d-TFA as solvents. Attenuated Total Reflection (ATR) FTIR spectroscopy measurements were performed on a Perkin-Elmer Spectrum 100 in the spectral region of 650-4000 cm^{-1} and were obtained from 4 scans with a resolution of 2 cm^{-1}. A background measurement was taken before the sample was loaded onto the ATR for measurement. Size Exclusion Chromatography (SEC) was performed on an Agilent 1200 system in conjunction with two PSS GRAM analytical (8 x 300 and 8 x 100, 10 µ) columns, a Wyatt Dawn Heleos 8 multi angle light scattering detector (MALS) and Wyatt Optilab rEX differential refractive index detector (DRI) with a 658 nm light source. The eluent was DMF containing 0.1 M LiBr at a flow rate of 1mL min^{-1}. The column temperature was set to 40 ºC with the MALS detector at 35 ºC and the DRI detector at 40 ºC. Molar masses and dispersities were calculated from the MALS signal by the Astra software (Wyatt) using the refractive index increment (dn/dc) of linear poly-(ε-carbobenzyloxy-L-lysine) (PZLL) of 0.101.[61] All samples for GPC analysis were prepared with a concentration of 2 mg/ml and were filtered through a 0.45 µm PTFE filter (13mm, PP housing, Whatman) prior to injection.

Plasmid preparation

The pGL3-control vector plasmid (Promega) consists of 5256 bp and contains the firefly luciferase gene and an ampicillin resistance gene that are controlled by a SV40 promoter/enhancer. The plasmids were replicated in the high-copy DH5-α Escherichia coli strain grown in selective ampicillin (50 µg/ml) supplemented Luria-Bertani medium, isolated by alkaline lysis followed by anion exchange chromatography using the Giga Qiagen kit (Qiagen)

according to the manufacturer's protocol. Purity of the plasmid and integrity of cDNA insert were determined by agarose gel electrophoresis and UV spectroscopy (E 260/280 nm ratio). After isolation, the pDNA was dissolved to an end concentration of 1.2 μg/ml Tris HCl buffer (pH 8.0). The purity was assayed by 1% agarose gel electrophoresis. This was then used in the preparation of the pDNA polyplexes.

Preparation of siRNA and pDNA polyplexes

siGENOME non-targeting siRNA #4 (5' AUGAACGUGAAUUGCUCAA 3') was obtained from Dharmacon and used in the preparation of the polyplexes. The siRNA/pDNA G2-PLys (40units) and G5-PLys (5 units) polyplexes were freshly prepared prior to use. The ratio of dendrimer to pDNA/siRNA in the polyplexes was calculated according to the molar ratio of amino group in dendrimer to phosphate group in pDNA/siRNA, i.e., the N:P ratio. To prepare the polyplexes, solutions of G2-PPI-PLL or G5-PPI-PLL prepared in buffer (Tris HCl buffer pH 7.4 - 10mM NaCl) were mixed with pDNA/siRNA at various N:P ratios (1, 5, 10, 20 and 100). These mixtures were incubated at room temperature for 30 min for polyplex formation, diluted and analysed.

Particle size and zeta potential analysis

The polyplexes were prepared in triplicate at various N:P ratios as described, and their particle size and surface charge (ζ-potential) measured by a Malvern Zetasizer Nano ZS (Malvern Instruments, Ltd., United Kingdom).

Atomic Force Microscopy (AFM)

Particle size and morphology were also determined using Atomic Force Microscopy (AFM, Asylum MFP-3D-BIO, DIT Focas Institute, Dublin, Ireland). For AFM, the polyplexes were prepared at the N:P ratio of 20 by adding the polypeptide solution to pDNA/siRNA to give a final pDNA/siRNA concentration of 10ng/μL. After incubation at room temperature for 30 min, 2 μL of the complex solution was diluted into 198 μL H2O and deposited onto the surface of freshly cleaved mica sheets (Agar scientific, G250-3, 11 x 11mm mica). After 3 mins, excess solution was removed by careful absorption onto filter paper (Whatman, Fisher Scientific, Ireland) and the mica was further dried at room temperature for 24 hr before analysis by AFM. Samples were imaged using a MFP-3D BIO AFM (Asylum Research). Micromasch silicon NSC18 cantilevers were used. Tips were 225 nm long and had a typical resonant frequency of 75kHz. The AFM operated in AC mode (alternate contact) in order to minimise tip samples interaction. Typical free air amplitudes were ~800 mV and a high amplitude set-point

relative to the set-point was maintained to minimise cell/tip damage. All samples were imaged in air at relative humidity. The images obtained contained 512 pixels per scan line.

Gel retardation assay

The pDNA polyplexes were prepared as outlined above, mixed with a 6X loading dye (Promega G190A-Blue/orange 6x) and analysed by running 1% (w/v) agarose gel electrophoresis at 100 V for 1 hr in TBE buffer (Tris/Borate/EDTA buffer, Gibco, Biosciences, Ireland) with 0.5 μg/ml ethidium bromide. Visualisation was obtained by UV transillumination (G. Box, Syngene, UK). The siRNA polyplexes were also prepared as before, mixed with loading dye (promega G190A-Blue/orange 6x) and analysed by running 20% non - denaturing polyacrylamide gel in TBE buffer at 100V for 1hr. The gel was then stained upon completion using Gelstar nucleic acid gel stain for 30min. Visualisation was then obtained by UV transillumination (G. Box, Syngene, UK).

DNase I protection assay

DNase I protection assay was performed to investigate the ability of dendrimers to protect pDNA from endonuclease degradation. Samples of polyplexes were prepared as before and diluted to 10 μL, 1.5 μL of 10X reaction buffer (as supplied) was then added. Samples were treated with 1 μg of DNase I (1 U/μL, Fermentas) at 37 °C for 30 min. 2 μL of EDTA (50 mM) and 8 μL of sodium dodecyl sulfate (SDS, 1.25% w/v) were then added and the samples were incubated at 37 °C for a further 2 hours to allow complete DNA dissociation from complexes. Prior to running 1% agarose gel electrophoresis as before, 6X loading dye (promega G190A-Blue/orange 6X) was added to these samples and the amount of pDNA released from the complexes was then visualized by UV transillumination (G. Box, Syngene, UK). Naked pDNA with or without DNase I treatment were used as positive and negative controls.

RNase protection assay

RNase protection assay was performed to investigate the ability of dendrimers to protect siRNA from endonuclease degradation. Samples of polyplexes were prepared as before and diluted to 10 μL. Samples were treated with 1 μg of RNase (1 U/μL, Fermentas) and 1μL of EDTA (50mM) at 37 °C for 30 min. 8 μL of sodium dodecyl sulfate (SDS, 1.25% w/v) were then added and the samples were incubated at 37 °C for a further 2 hours to allow complete siRNA dissociation from complexes. The polyplexes were analysed using a 20% non - denaturing polyacrylamide gel in TBE buffer at 100V for 1hr. The gel was then stained upon completion using Gelstar nucleic acid gel stain for 30min. The amount of siRNA released from the

complexes was then visualized by UV transillumination (G. Box, Syngene, UK). Naked siRNA with or without RNase treatment were used as positive and negative controls.

pDNA transfections of Calu-3 cells using linear and star-shaped G5(40) PLL polyplexes

Non differentiated airway epithelial cells (Calu-3 cells) were seeded at a density of $5x10^4$ cells/well in 48-well plates 24hrs prior to transfection. The reporter gene pGaussia luciferase was used for the subsequent transfections and the plasmid was isolated using a Qiagen maxi prep kit as per manufacturer's instructions. Polyplexes of linear PLL at N/P 2 and G5(40) PLL at various N/P ratios were prepared by mixing the star shaped dendrimer G5 (40units) in 100µl Opti-MEM and incubated at room temperature for 30min. The cells were then transfected with these polyplexes for 4 hours. After 4 hours, 150µL of serum-containing media was added to each well and incubated for 24, 120, 168 hours respectively at 37^oC and 5% CO_2. Following this, luciferase activity of each well was analysed as per manufacturer's instructions.

3.5 References

1. E.W. Alton, U. Griesenbach and D.M. Geddes, *Gene Ther*., **1999**, 6, 155.
2. D. N. Nguyen, J. J. Green, J. M. Chan, R. Langer and D. G. Anderson, *Adv. Mater*., **2009**, 21, 847.
3. E. L. Tatum, *Perspect. Biol. Med*., **1966**, 10, 19.
4. S. Y. Wonga, J. M. Pelet and D. Putnam, *Prog. Polym. Sci*., **2007**, 32, 799.
5. E. Marshall, *Science*, **2000**, 288, 951.
6. G. Y. Wu and C. H. Wu, *J. Biol. Chem*., **1987**, 262, 4429.
7. M. Koping-Hoggard, Y. S. Melnikova, K. M. Varum, B. Lindman and P. Artursson, *J. Gene Med*., **2003**, 5, 130.
8. T. K. Georgiou, M. Vamvakaki, L. A. Phylactou and C. S. Patrickios, *Biomacromolecules*, **2005**, 6, 2990.
9. E. G. Tierney, G. P. Duffy, A. J. Hibbitts, S. Cryan and F. J. O'Brien, *J. Controlled Release*, **2012**, 158, 304.
10. O. Taratula, O. B. Garbuzenko, P. Kirkpatrick, I. Pandya, R. Savla, V. P. Pozharov, H. He and T. Minko, *J. Controlled Release*, **2009**, 140, 284.
11. M. L. Patil, M. Zhang, O. Taratula, O. B. Garbuzenko, H. He and T. Minko, *Biomacromolecules*, **2009**, 10, 258.
12. C. Dufes, I. F. Uchegbu and A. G. Schatzlein, *Adv. Drug Delivery Rev*., **2005**, 57, 2177.
13. Y. N. Xue, M. Liu, L. Peng, S. W. Huang and R. X. Zhuo, *Macromol. Biosci*., **2006**, 10, 404.
14. M. Mintzer and M. W. Grinstaff, *Chem. Soc. Rev*., **2011**, 40, 173.
15. H. Gao, S. Ohno and K. Matyaszewski, *J. Am. Chem. Soc*., **2006**, 128, 15111.
16. A. W. Bosman, R. Vestberg, A. Heumann, J. M. J. Frechet and C. Hawker, *J. Am. Chem. Soc*., **2003**, 125, 715.
17. V. Y. Lee, K. Havenstrite, M. Tijo, M. McNeil, H. M. Blau, R. D. Miller and J. Sly, *Adv. Mater*., **2011**, 23, 4509.
18. A. Sulistio, P. A. Gurr, A. Blencowe and G. Qiao, *Aust. J. Chem*., **2012**, 65, 978.
19. J. Huang and A. Heise, *Chem. Soc. Rev.*, **2013**. 42, 7373.

20. Y. Haba, A. Harada, T. Takagishi and K. Kono, *Polymer*, **2005**, 46, 1813.

21. C. Kojima, C.Regino, Y. Umeda, H. Kobayashi and K. Kono, *Int. J. Pharm*., **2010**, 383, 293.

22. C. S. Cho, J. B. Cheon, Y. I. Jeong, I. S. Kim, S. H. Kim and T. Akaike, *Macromol. Rapid Commun.*, **1997**, 18, 361.

23. T. Borase, M. Iacono, S. I. Ali, P. D. Thornton and A. Heise, *Polym. Chem*., **2012**, 3, 1267.

24. T. Borase, T. Ninjbadgar, A. Kapetanakis, S. Roche, R. O'Connor, C. Kerskens, A. Heise, and D. F. Brougham, *Angew. Chem. Int. Ed*., **2013**, 52, 3164.

25. K. Inoue, H. Sakai, S. Ochi, T. Itaya and T. Tanigaki, *J. Am. Chem. Soc.*, **1994**, 116, 10783.

26. G. Mihov, D. Grebel-Koehler, A. Lübbert, G. W. M. Vandermeulen, A. Herrmann, H. A. Klok and K. Müllen, *Bioconjugate Chem.*, **2005**, 16, 283.

27. H. Huang, J. Li, L. Liao, J. Li, L. Wu, C. Dong, P. Lai and D. Liu, *Eur. Polym. J.*, **2012**, 48, 696.

28. Q. Wang, J. Yu, Y. Yan, S. Xu, F. Wang, Q. Li, J. Wang, X. Zhang and D. Liu, *Polym. Chem.,* **2012**, 3, 1284.

29. D. Appelhans, H. Komber, R. Kirchner, J. Seidel, C. F. Huang, D. Voigt, D. Kuckling, F. C. Chang and B. Voit, *Macromol. Rapid Commun.*, **2005**, 26, 586.

30. M. Byrne, P. D. Thornton, S. A. Cryan, A. Heise, *Polym. Chem*., **2012**, 3, 2825.

31. A. P. Nowak, V. Breedveld, L. Pakstis, B. Ozbas, D. J. Pine, D. Pochan and T. J. Deming, *Nature*, **2002**, 417, 424.

32. E. P. Holowka, V. Z. Sun, D. T. Kamei and T. J. Deming, *Nat. Mater*., **2007**, 6, 52.

33. A. Constancis, R. Meyrueix, N. Bryson, S. Huille, J. M. Grosselin and T. Gulik-Krzywicki, *J. Colloids Interface Sci*., **1999**, 217, 357.

34. N. Gabrielson, H. Lu, L. Yin, D. Li, F. Wang and J. Cheng, *Angew. Chem. Int. Ed.,* **2012**, 51, 1143.

35. J. Yen, Y. Zhang, N. P. Gabrielson, L. Yin, L. Guan, I. Chaudhury, H. Lu, F. Wang and J. Cheng, *Biomaterials Sci.,* **2013**, 1, 719.

36. M. Yu, J. Hwang and T. J. Deming, *J. Am. Chem. Soc*., **1999**, 121, 5825.

37. P. D. Thornton, R. Brannigan, J. Podporska, B. Quilty and A. Heise, *J. Mater. Sci. Mater*. *Med*., **2012**, 23, 37.

38. C. Xiao, C. Zhao, P. He, Z. Tang, X. Chen, and X. Jing, *Macromol. Rapid Commun*., **2010**, 31, 991.

39. J. R.Kramer and T. J. Deming, *J. Am. Chem. Soc*., **2010**, 132, 15068.

40. J. Sun and H. Schlaad, *Macromolecules*, **2010**, 43, 4445.

41. H. Tang and D. Zhang, *Biomacromolecules*, **2010**, 11, 1585.

42. J. Huang, G. Habraken, F. Audouin and A. Heise, *Macromolecules*, **2010**, 43, 6050.

43. J. Huang, C. Bonduelle, J. Thévenot, S. Lecommandoux and A. Heise, *J. Am. Chem. Soc.,* **2012**, 134, 119.

44. D. Pati, N. Kalva, S. Das, G. Kumaraswamy, S. S. Gupta and A.V. Ambade, *J. Am. Chem. Soc.,* **2012**, 134, 7796.

45. J. R. Kramer, A. R. Rodriguez, U. J. Choe, D. T. Kamei and T. J. Deming, *Soft Matter,* **2013**, 9, 3389.

46. C. M. Ward, M. Pechar, D. Oupicky, K. Ulbrich and L.W. Seymour, *J. Gene Med*., **2002**, 4, 536.

47. M. Mannisto, S. Vanderkerken, V. Toncheva, M. Elomaa, M. Ruponen, E. Schacht and A. Urtti, *J. Control. Release*, **2002**, 83, 169.

48. H. Lv, S. Zhang, B. Wang, S. Cui and J. Yan, *J. Controlled Release*, **2006**, 114,100.

49. S. Pan, C. Wang, X. Zeng, Y. Wen, H. Wu and M. Feng, *Int. J. Pharm*., **2011**, 420, 206.

50. M. Yamagata, T. Kawano, K.Shiba, T. Mori, Y. Katayama and T. Niidome, *Bioorg. Med. Chem*., **2007**, 15, 526.

51. K. Luo, C. Li, G. Wang, Y. Nie, B. He, Y. Wu and Z.Gu, *J. Controlled Release*, **2011**, 155, 77.

52. C. Scholz and E. Wagner, *J. Controlled Release*, **2012**, 161, 554.

53. H. R. Kricheldorf, *Angew. Chem., Int. Ed*., 2006, **45**, 5752.

54. N. Hadjichristidis, H. Iatrou, M. Pitsikalis and G. Sakellariou, *Chem. Rev*., **2009**, 109, 5528.

55. G. J. M. Habraken, A. Heise and P. D. Thornton, *Macromol. Rapid Commun*., **2012**, 33, 272.

56. G. M. Soliman, A. Sharma, D. Maysinger and A. Kakkar, *Chem. Commun*., **2011**, 47, 9572.

57. H. L. Fu, S. X. Cheng, X. Z. Zhang and R. X. Zhuo, *J. Control. Release*, **2007**, 124**,** 181.

58. J. L. Lee, C. W. Lo, S. M. Ka, A. Chen and W. S. Chen, *J. Control. Release*, **2012**, 160, 64.

59. S.A. Cryan and C.M. O'Driscoll, *Pharm. Res.*, **2003**, 20, 569.

60. G. J. M. Habraken, C. E. Koning and A. Heise, *J. Polym. Sci., Part A: Polym. Chem*., **2009**, 47, 6883.

61. A. Sulistio, A. Blencowe, A. Widjaya, X. Zhang and G. Qiao, *Polym. Chem*., **2012**, 3, 224.

Chapter 4

Glycosylation of Advanced Polypeptide Architectures

Abstract

Well-defined advanced polypeptide architectures including block, sequenced and star shaped arrangements were synthesised via NCA ROP with hexylamine and various generations of PPI dendrimers respectively. Molecular weight, arm length and arm density were readily controlled to afford a series of star shaped poly(glutamic acid) derivatives with accessible high molecular weights (500, 000 g/mol) and structural complexity. Analogous linear derivatives were generated through employment of the NCA of glutamic acid bearing two different amino acid side chain protecting groups to generate a block copolymer and the first reported case of a sequenced polypeptide arrangement. The sequential deprotection and presentation of carboxylic acid moieties for conjugation of glucosamine residues through amide coupling chemistry resulted in the ability to strategically position sugars within a polypeptide scaffold. Similarly, glycosylation of star shaped poly(glutamic acid) resulted in the formation of a diverse range of glycopolypeptide architectures with tuneable sugar substitution and the potential to achieve high conjugation efficiencies. The bioactivity of the described glycopolypeptides towards the lectin ConA was investigated and was shown to be architecturally dependent. The applicability of these materials towards targeted drug delivery, biorecognition applications and the study of new more complex carbohydrate – protein interactions may be attempted in future work.

4.1 Introduction

Glycosylated polymers or glycopolymers, are an emerging polymer technology offering immense potential towards biomedical applications and the study of more complex biological processes. The importance of "glycosylation" and its related cellular interactions has been overwhelmingly demonstrated by the vast array of biological processes dependent upon it in nature.[1-5] Nature sees the prevalent use of glycosylated cell components to perform many vital biological functions such as cellular recognition, signalling, fertilization, inflammation and many more. In particular, much attention has been drawn to specific carbohydrate-protein interactions between sugars and lectins to help better understand these complex biological systems. Specificity has been made possible by the enormous range of possible constructs that carbohydrates can form and it is this diversity and complexity which has led to coining of the phrase "glycocode" thus highlighting the sheer wealth of information possessed by carbohydrates.[6,7] However, the investigation of carbohydrate-protein interactions requires the synthesis of often complicated glycoprotein structures thus somewhat limiting research in this area.[8,9] The synthesis of artificial glycoconjugates, in particular, glycopolymers may help to overcome this somewhat and is this biomimicry which potentially affords materials for an array of biomedical applications such as therapeutics and medical diagnostics.[10-16] In terms of polymer scaffolds, synthetic polypeptides have emerged as a strong candidate owing to their inherent biocompatibility and close mimicry to natural peptides. Particularly, polypeptides derived from the ring opening polymerization (ROP) of amino acid N-carboxyanhydrides (NCAs) are of increasing interest owing to the versatile yet high degree of control offered by such a technique.[17-20] Furthermore their unique ability to form secondary structures and potential to utilise amino acid side chain functionalities affords "smart" polypeptide materials capable of self-assembly and stimuli responsive properties e.g. pH, light and enzymatic.[21]

Preparation of glycopeptides from NCA derived polypeptides can be performed via two methods: polymerization of glycosylated NCA monomers and post modification of amino acid side chains. Polymerization of glycosylated NCA monomers permits 100% glycosylation of the polypeptide but monomer synthesis can prove difficult whilst incorporation of a different sugar into the polypeptide requires the complete synthesis of a new monomer. Rude et al reported the first such synthesis of a glycosylated NCA through combination of acetobromoglucose and N-carboxybenzyl-L-serine benzyl ester via a Koenigs-Knorr reaction.[22] However, the resultant polypeptides were poorly defined. More recently, the Deming group has extensively researched this synthetic pathway to develop, amongst others, several lysine based glycosylated NCA monomers boasting excellent reactivity and ultimately the generation

of a series of well-defined glycopolymers.[23-25] Related progress in this area is discussed in several review articles and this chapter will focus predominantly on the technique of post modification.[26,27]

Post modification of polypeptide amino acid side chains presents greater versatility due to the diverse range of amino acids available i.e. different functionalities and therefore many efficient coupling chemistry options in addition to greater variability in sugar choice. The advent of "click" chemistry has offered a very useful synthetic tool for post modification of polypeptides with sugar moieties owing to the highly efficient and selective nature of such chemistry.[28] "Click" type reactions include thiol-ene and azide-alkyne which means sugars may be readily adapted to include alkyne,[29] azide,[30,31] thiol[32] and alkene functionalities to permit coupling to the corresponding "click" compatible polypeptide side chains. Focusing on azide-alkyne type chemistry, Chunsheng et al. employed an azide functionalised mannose derivative to form a water soluble glycosylated homopolypeptide using the alkyne functionalised NCA, γ-propargyl-L-glutamate developed by Hammond.[33,34] Glycosylation proceeded in high efficiency with close agreement observed between target and measured degrees of glycosylation. Similarly, Donghui Zhang successfully clicked alkyne functionalised sugars to the pendant azide moieties of an azide functionalised derivative of glutamic acid.[35] The described polypeptides although synthetically and structurally appealing do suffer from the presence of an ester bond in linking sugar to polypeptide backbone, thus introducing a hydrolytically susceptible moiety. To overcome this, Huang et al utilised a non-natural amino acid with pendant alkyne functionality i.e. DL-propargylglycine to first synthesise the novel NCA and subsequently generate the polypeptide to elicit modification with azide terminated sugars.[28] However, homopolypeptide molecular weight was limited owing to the ability of this polymer to form strong β–sheet secondary structures. Copolymerization with another NCA monomer, such as γ-benzyl-L-glutamate, alleviated this somewhat and led to generation of a series of biologically relevant polymersomes and nano-assemblies.[36,37]

Asides from the fashionable "click" chemistry, traditional amine to carboxylic acid coupling chemistry is another option which has demonstrated its practicality in conjugating sugars to the side chain of polypeptides. Synthetically, glycopolypeptides obtained via this method negate the requirement of new specialised amino acid derivatives observed in "click" reactions whilst sugars are predominantly introduced via a hydrolytically stable amide linkage. Furthermore, azide-alkyne type "click" chemistry sees the formation of an unnatural triazole ring linkage between polypeptide and sugar in which its effect on sugar behaviour have yet to

be fully explored. The obvious amino acid candidates are lysine, glutamic acid and aspartic acid as amine and carboxylic acid functionalities are found naturally in their side chain groups, respectively. With regards to lysine, numerous attempts have been made to conjugate amine reactive sugars to lysine side chains.[38-42] The sugar gluconolactone was successfully employed by Feng and co-workers to attach ring opened sugars to an amphiphilic lysine based triblock copolymer under basic conditions.[43,44] Sugar density was modified by adjusting the sugar feed ratio but was limited to a maximum of 75%, most likely as a result of steric hindrance. The attachment of isothiocyanate functionalised mannose sugars to poly(L-lysine) via a thio-urea linkage was recently reported.[45] Glycosylation densities of 16% to 23 % were achieved to afford a series of glycopolypeptides with pH and surfactant triggered stimuli responsive self assembly properties. Concerning carboxylic acid functionalised polypeptides, their ability to permit derivatization with amines by amide coupling chemistry has been clearly demonstrated.[46-50] Consequently, glycosylation of NCA derived polypeptides with amino sugars should be possible. Recently, Menzel et al. devised a very effective strategy to achieve this by employing the coupling reagent, 4-(4,6-Dimethoxy-1,3,5-triazin-2-yl)-4-methylmorpholinium chloride (DMTMM) to functionalize a series of linear poly(glutamic acid) precursors with glucosamine.[51] The DMTMM used is known to be a very mild and efficient coupling reagent applicable to both organic and aqueous solvents, thus enabling glycosylation of polypeptides to be achieved in a very "green" and simple way.[52,53] Sugar densities were readily controlled by varying the sugar to carboxylic acid loading ratio with impressive sugar densities of up to 80% achievable by this method. Complete glycosylation was most probably inhibited by steric hindrance of neighbouring sugars. The beauty of this system is in its simplicity throughout the protocol. Synthetically, the polypeptide can be derived from well understood basic NCAs such as BLG (NCA of γ-benzyl-L-glutamate) in which molecular weight can be readily controlled and is not inhibited by the formation of strong secondary structures as in the case of DL-propargylglycine. Coupling of amino sugars is performed in water requiring minimal technical skill whilst sugar densities can be easily controlled.

To expand on this methodology, its application towards more complex architectures such as star shaped polypeptides may be very interesting. Star shaped polypeptides in particular offer a stable yet structurally variable complex nanoparticle platform containing a high local density of functionality.[54-56] Consequently, a high local density of sugars within a size confined structural space may be achievable using very simple post modification chemistry techniques. The resultant structurally diverse glycopolypeptides may be more suitable to investigating highly complex carbohydrate protein interactions such as the interaction of dendritic cells with

viruses.[57-60] Furthermore, star shaped polypeptides have become increasingly prevalent as potential drug delivery vehicles meaning sugar conjugation and its inherent site specific interactions may provide star polypeptides with an attractive targeting function.[61-66] In addition to the employment of star shaped glycopolypeptides, selective positioning of sugars introduces further architectural variation and complexity to these synthetic glycoprotein mimics. Such a feature helps to further probe advanced carbohydrate protein interactions and the effects of sugar positioning and architecture. Haddleton and coworkers recently reported the selective positioning of sugars along an acrylate based polymer through the sequence controlled polymerization of pre-synthesized glycosylated acrylate monomers.[67] Advanced binding studies of these well defined polymers with the biologically important lectin DC-SIGN were undertaken and highlight the significant role of sugar positioning in carbohydrate – protein interactions. Similarly, the effects of architecture and scaffold were shown to exhibit an effect on the binding behavior of DC-SIGN with a series of glycopolypeptides functionalized with mixed ratios of mannose and galactose sugars synthesized via "click" chemistry.[68] Consequently, architectures such as stars and selective sugar positioning will help to significantly advance research in this field.

This chapter will investigate the application of Menzel's methodology towards a series of poly(glutamic acid) architectures, in particular star shaped poly(glutamic acid). Originally developed by Byrne et al., a range of well defined star shaped poly(glutamic acid) derivatives with controllable molecular weights and architectures such as arm density and length will be employed.[52] The subsequent glycosylation of these star shaped polymers will be attempted to explore the feasibility of Menzel's methodology towards these complex architectures in addition to briefly investigating their resultant lectin binding properties. Furthermore, the synthesis of linear glycopolypeptides with selective sugar positioning will be attempted through the block copolymerization of glutamic acid NCAs bearing benzyl and tert-butyl carboxylic acid protecting groups. The sequential removal of these protecting groups in tandem with selective glycosylation will be attempted to afford a simple route towards well defined glycopolypeptides bearing site specific multivalent presentation of sugars.

4.2 Results and Discussion

4.2.1 Advanced Star Shaped Polypeptides

4.2.1.1 Star Polypeptide Synthesis

The technological advancement of NCA ROP has enabled the controlled synthesis of structurally diverse yet well-defined polypeptide scaffolds.[69-72] Through the use of primary amino initiators, the generation of well-defined polypeptides is readily accessible.[18-20] The employment of more complex amino initiators such as multifunctional dendrimers introduces a new avenue of structural complexity to NCA derived polypeptides.[73-76] As previously described, a series of star shaped polypeptide architectures were prepared via ROP of the NCA, BLG using different generations of multifunctional poly(propylene imine) (PPI) dendrimers.[52] The resultant materials consisted of a dendrimer core and a polypeptide shell capable of offering multiple carboxylic moieties upon deprotection of the amino acid side chain protecting groups **(Figure 4.1)**.

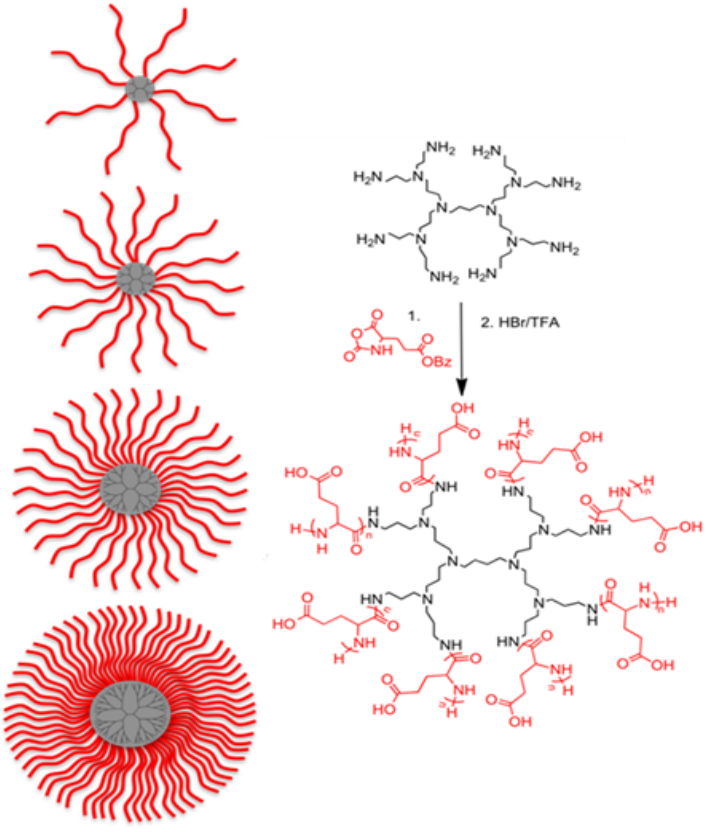

Figure 4.1: Diversity of synthesized star polypeptides and reaction scheme for the synthesis of poly(L-glutamic acid) star polypeptides using second generation PPI dendrimer as an initiator.

As observed in **Table 4.1**, a series of star shaped PBLG architectures and the equivalent M_w linear derivatives were synthesised which boasted controllable molecular weights and degrees of branching. **Entry 1** and **entries 4 – 7 of Table 4.1**, describe PBLG polymers with a constant arm length but different degrees of branching due to the choice of initiator used. Similarly, total molecular weight was maintained to afford a series of polymers with different arm lengths and branching densities **(Entries 2 – 3 and Entry 8, Table 4.1)**.

Table 4.1: Star-shaped PBLG by initiation from PPI dendrimers (L: linear initiator hexylamine; G1-G5: generation of PPI dendrimer; G5(64)-PBLG$_{40}$ = initiator generation 5 dendrimer with maximum 64 arms and theoretical arm length of 40 amino acids). Dispersities of all polymers < 1.2 (SEC MALS detection).

Entry	Polymer	NCA/NH_2	NCA/dendrimer	M_w/g mol^{-1}[(a)]	M_n^{th}[(b)]/g mol^{-1}
1	L(1)-PBLG$_{40}$	40	40	10 000 (8 900)[(c)]	8 700
2	L(1)-PBLG$_{200}$	200	200	41 500 (44 400)[(c)]	43 600
3	G2(8)-PBLG$_{27}$	27	216	40 100	47 100
4	G2(8)-PBLG$_{40}$	40	320	63 200	70 500
5	G3(16)-PBLG$_{40}$	40	640	110 700	141 000
6	G4(32)-PBLG$_{40}$	40	1280	240 800	282 500
7	G5(64)-PBLG$_{40}$	40	2560	499 800	565 000
8	G5(64)-PBLG$_3$	3.5	224	42 300	48 800

(a) determined by SEC (DMF) using MALS detection using the dn/dc of linear PBLG of 0.118 (b) calculated assuming initiation from all amino groups and quantitative conversion: c(monomer)/c(dendrimer) x M(monomer) + M(dendrimer) (c) M_n determined by ^{1}H NMR spectroscopy using the integral ratio of hexylamine and PBLG.

^{1}H NMR spectroscopy was used to elucidate molecular weight (M_n) for linear PBLG whereas star shaped PBLG prevented accurate molecular weight determination via this method due to the lack of visible PPI dendrimer peaks, peak overlap with PBLG, low composition and core location **(Figure 4.2 and Figure 2.3 Chapter 2)**.

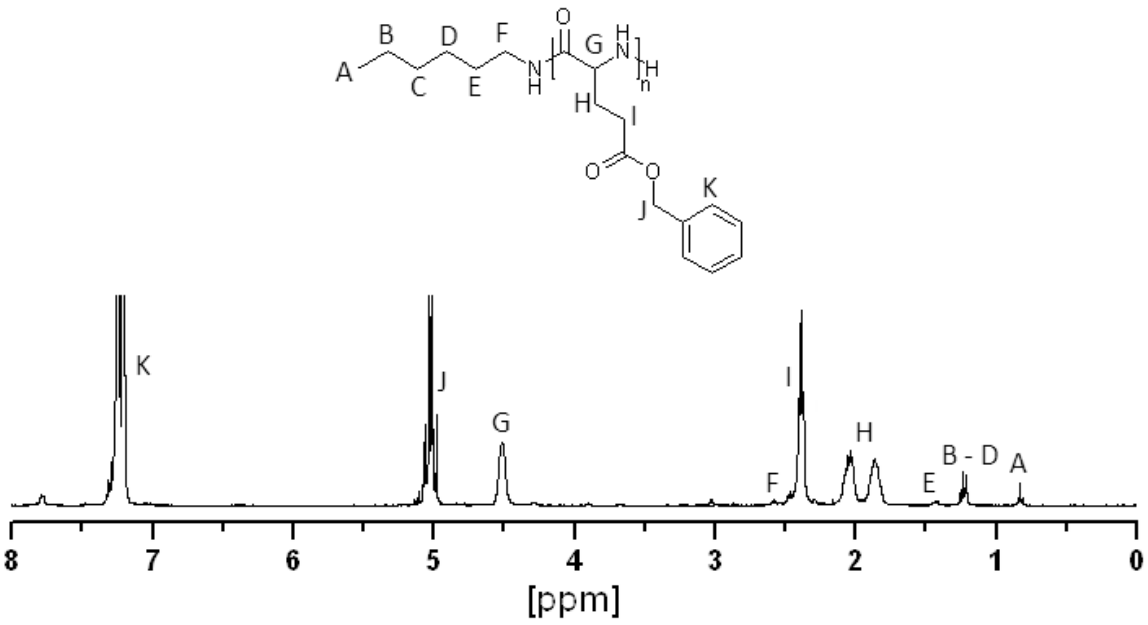

Figure 4.2: ^{1}H NMR spectrum of L(1)-PBLG$_{200}$ ($CDCl_3$, d-TFA).

The described polypeptides were analysed by SEC (size exclusion chromatography) in DMF and the results are summarized in **Table 4.1**. SEC traces of polypeptides with similar M_w **(Entries 2 – 3 and Entry 8, Table 4.1)** and increasing molecular weight **(Entry 1 and entries 4 – 7 of Table 4.1)** can be observed in **Figure 4.3** and **Figure 2.2, Chapter 2** respectively.

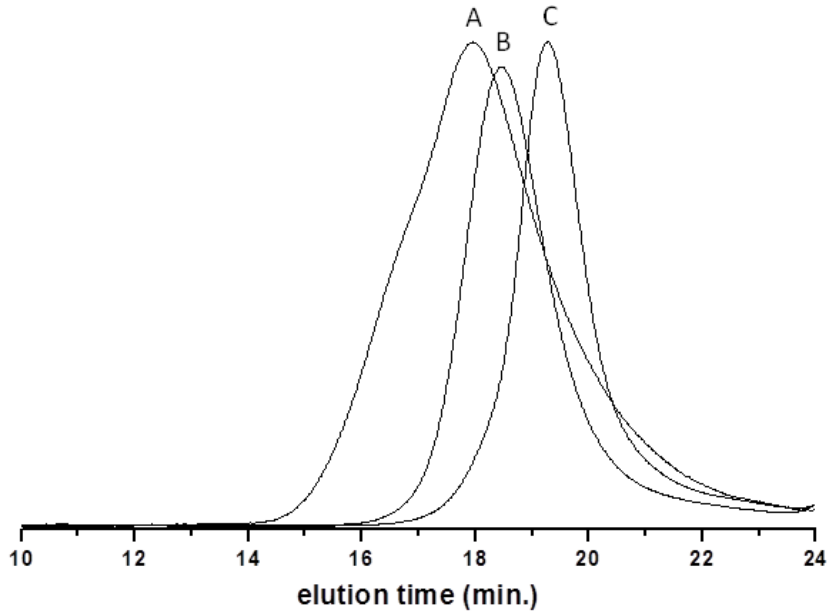

Figure 4.3: SEC traces L(1)-PBLG$_{200}$ (A), G2(8)-PBLG$_{27}$ (B) and G5(64)-PBLG$_3$ (C).

To afford water soluble carboxylic acid functionalised linear and star shaped polypeptides for eventual amide coupling of sugars, the benzyl protecting groups were removed using standard TFA / HBr methods of acidic hydrolysis. Quantitative deprotection was confirmed by ^{1}H NMR spectroscopy **(Figure 4.4 and Figure 2.7, Chapter 2)** due to the disappearance of the benzyl peaks at 7.3 ppm.

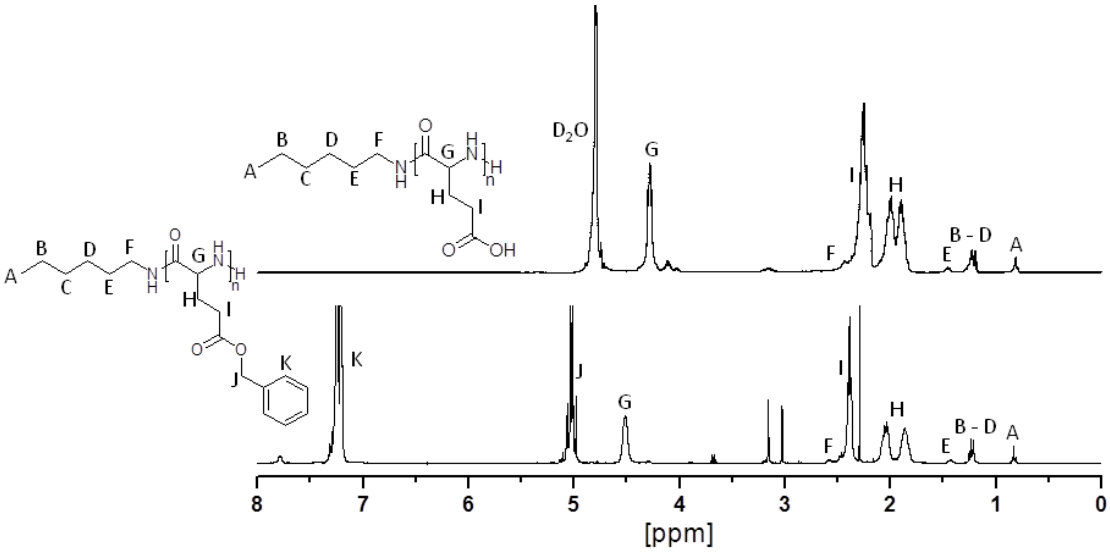

Figure 4.4: ^{1}H NMR spectra of L(1)-PBLG$_{200}$ (bottom) ($CDCl_3$, d-TFA) and L(1)-PGA$_{200}$ (top) (D_2O).

4.2.1.2 Synthesis of Glycosylated Star Shaped Polypeptides

Functionalization of polypeptides with glucosamine was accomplished using DMT-MM medicated amide coupling chemistry **(Figure 4.5)**. Initially polypeptides were converted to their Na salt form to facilitate the formation of an ammonium carboxylate salt with glucosamine hydrochloride. The hydrochloride form of glucosamine was employed as its free form is unstable in water. The formation of this ammonium carboxylate salt promotes higher coupling efficiencies as DMTMM is known to preferentially react with carboxylate anions.[50] The results of glycosylation are summarized in **Table 4.2**.

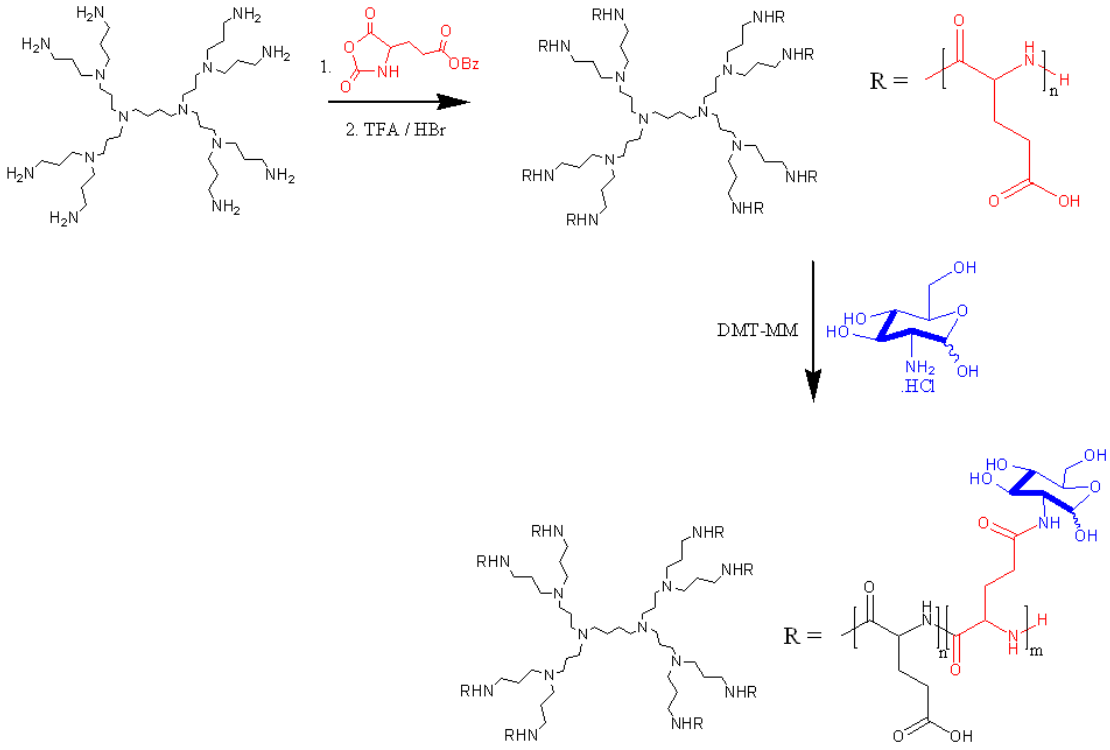

Figure: 4.5: Synthesis of star shaped glycopolypeptides via DMT-MM mediated amide coupling chemistry.

Table 4.2: Results of amide coupling of glucosamine to star shaped poly(glutamic acid).

Entry	Polymer	$M_n^{th\,(a)}$/g mol^{-1}	GA:Amine:DMT-MM[(c)]	Target DS (%)[(d)]	Measured DS (%)[(e)]
1	L(1)-PGA_{40}	5 200[(b)]	1 : 1 : 0.7	50	58
2	L(1)-PGA_{200}	26 100[(b)]	1 : 0.7 : 0.35	25	27
3	L(1)-PGA_{200}	26 100[(b)]	1 : 1 : 0.7	50	53
4	L(1)-PGA_{200}	26 100[(b)]	1 : 2 : 2	100	92
5	G2(8)- PGA_{27}	27 600	1 : 0.7 : 0.35	25	30
6	G2(8)- PGA_{27}	27 600	1 : 1 : 0.7	50	54
7	G2(8)- PGA_{27}	27 600	1 : 2 : 2	100	96
8	G2(8)- PGA_{40}	41 000	1 : 0.7 : 0.35	25	30
9	G2(8)- PGA_{40}	41 000	1 : 1 : 0.7	50	51
10	G2(8)- PGA_{40}	41 000	1 : 2 : 2	100	85
11	G3(16)-PGA_{40}	81 900	1 : 1 : 0.7	50	43
12	G4(32)- PGA_{40}	163 800	1 : 1 : 0.7	50	48
13	G5(64)- PGA_{40}	327 700	1 : 1 : 0.7	50	43
14	G5(64)- PGA_{40}	327 700	1 : 2 : 2	100	73
15	G5(64)- PGA_{3}	24 600	1 : 0.7 : 0.35	25	20
16	G5(64)- PGA_{3}	24 600	1 : 2 : 2	100	48

(a) calculated assuming initiation from all amino groups and quantitative conversion: c(monomer)/c(dendrimer) x M(monomer) + M(dendrimer) (b) actual M_n as determined by ^{1}H NMR spectroscopy using the integral ratio of hexylamine and PGA (c) molar ratio of COOH from PGA : NH_2 of glucosamine : DMT-MM coupling reagent (d) target number of glutamic acid units to be functionalised as calculated by molar ratio coupling reagents to glutamic acid units (e) determined by ^{1}H NMR spectroscopy using the integral ratio of glucosamine and PGA.

Glycosylation of linear derivatives **(Entries 1 – 4, Table 4.3)** was expected to be straightforward owing to its accessible architecture. The degree of substitution (DS) could be easily targeted by carefully controlling the COOH : NH_2 : DMT-MM ratio to afford a series of linear PGA derivatives where actual DS was in close agreement with targeted DS. As determined by ^{1}H NMR spectroscopy a DS of 92% was achieved highlighting the excellent efficiency of this methodology **(Figure 4.6)**.

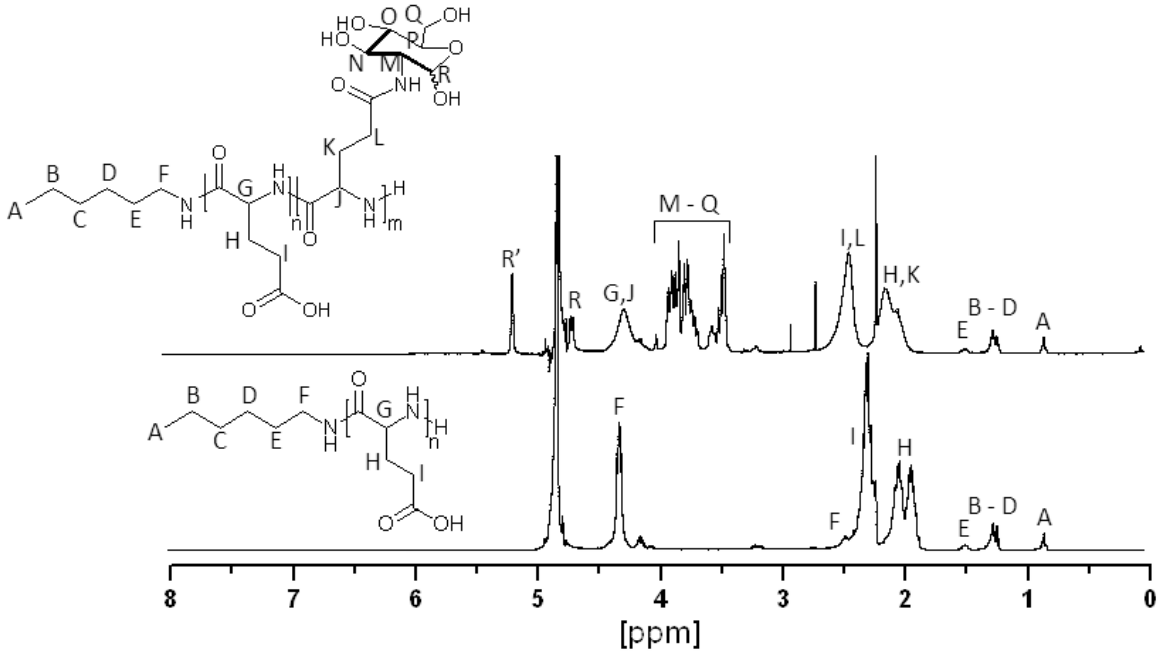

Figure 4.6: ^{1}H NMR spectra of L(1)-PGA_{200} (Bottom) (D_2O) and L(1)-PGA_{200}-(G) 53% (Top) (D_2O).

The subsequent application of this methodology towards the architecturally more complex star polypeptides was performed. Glycosylation proved successful for all star shaped polypeptides **(Figure 4.7)** particularly for the less densely branched derivatives **(Table 4.2)**. Concerning star shaped polypeptides of similar M_w **(Entries 5 – 7 and 15 – 16, Table 4.2)** and therefore similar numbers of PGA units, notable differences in coupling efficacy were observed. The less densely branched G2(8)-PGA_{27} star polymer reported an actual DS of 96% which is in close agreement with the targeted DS of 100% and comparable to the architecturally much simpler linear PGA derivative. However, the densely branched G5(64)-PGA_3 resulted in lower DS numbers (DS = 20% and 48%) particularly for the targeting of 100% glycosylation. This observation most likely arises because of the inaccessibility of the inner carboxylic acid moieties of the densely branched G5(64)-PGA_3, and therefore inhibits their coupling to amino sugars. Such an observation seems reasonable given the steric

considerations of coupling sugars to functional groups within an already densely branched complex network of polymer chains.

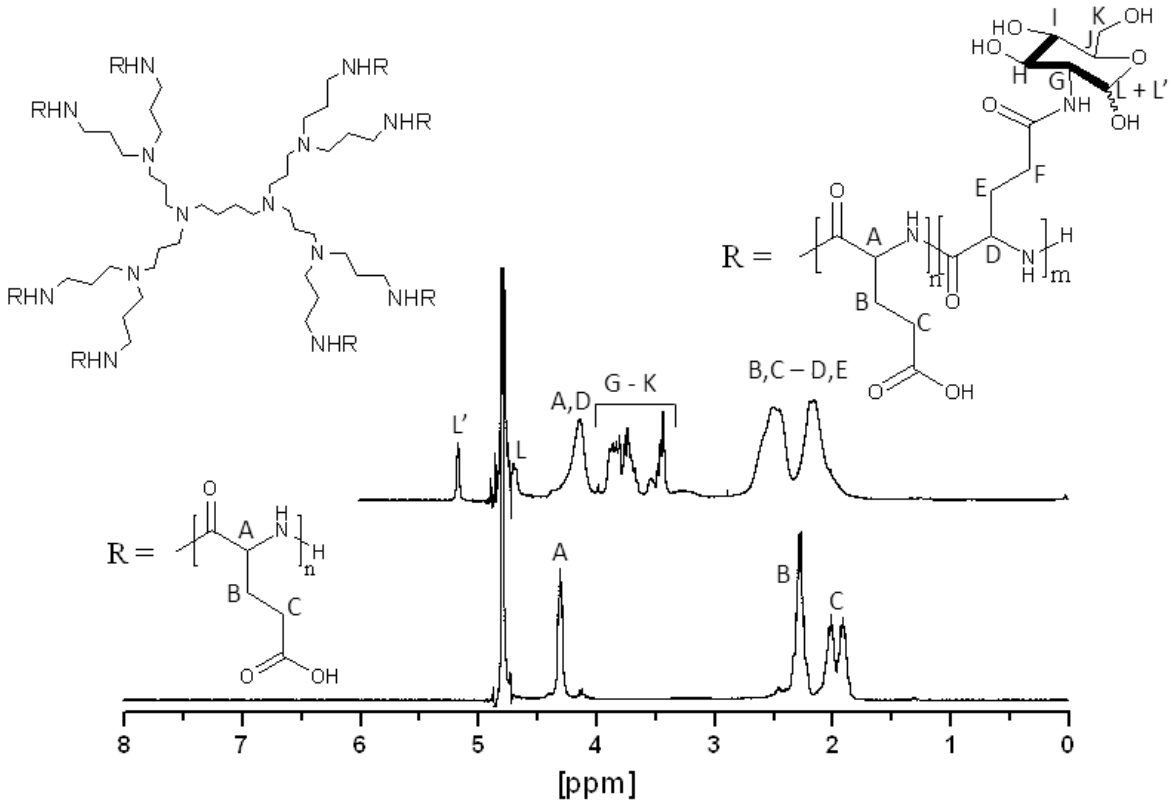

Figure 4.7: ^{1}H NMR spectra of G2(8)-PGA$_{27}$ (Bottom) (D$_2$O) and G2(8)-PGA$_{27}$-(G) 54% (Top) (D$_2$O). Dendrimer peaks not visible.

This hypothesis was further tested when considering the targeted glycosylation of star shaped polypeptides of similar arm lengths but different degrees of branching and total number of PGA units **(Entry 1 and entries 8 – 14, Table 4.2)**. Controlled sugar conjugation was observed for each of these star polymers with targeted DS of 25% and 50% proceeding quite efficiently although incomplete glycosylation became more apparent as branching density increased **(Entries 9 and 11 – 13, Table 4.2)**. As with G2(8)-PGA$_{27}$ and G5(64)-PGA$_3$, this feature was emphasised when 100% glycosylation was targeted resulting in a DS of 85% for G2(8)-PGA$_{40}$ whereas a DS of 73% was observed for the more densely branched G5(64)-PGA$_{40}$. As discussed above, steric factors seem the most plausible explanation for these observations. In spite of this, glycosylation of these complex architectures can be facilely achieved using this straightforward methodology negating the synthetic challenges of designing challenging NCA monomers and their subsequent application to more complex chemistries. Furthermore, sugar density can readily controlled in which high coupling efficiencies of up to 96% can be achieved

for star shaped PGA which is comparable to the linear PGA analogue. Although branching density does impact on sugar conjugation, its effect only becomes notable when a high DS is targeted. Despite this, respectable DS values of up to 48% and 73% were observed for the most densely branched of polypeptide architectures.

FTIR spectroscopic analysis of the described glycopolypeptides helped to elucidate their secondary structures (solid state). All of the glycopolypeptides exhibited α-helical secondary structures irrespective of architecture and sugar density. α-helical character was denoted by the presence of strong Amide I and II bands at approximately 1650 cm^{-1} and 1544 cm^{-1} which are indicative of an α-helix **(Figure 4.8)**.[77] Furthermore the presence of sugar can be observed at 1036 cm^{-1} providing further evidence of successful sugar conjugation. Circular dichromism (CD) provides more detailed analysis of polypeptide secondary structure as sugar conjugation and density are known to have an impact on secondary structure.[49] However, this investigation was not undertaken and is something which will be looked at in future.

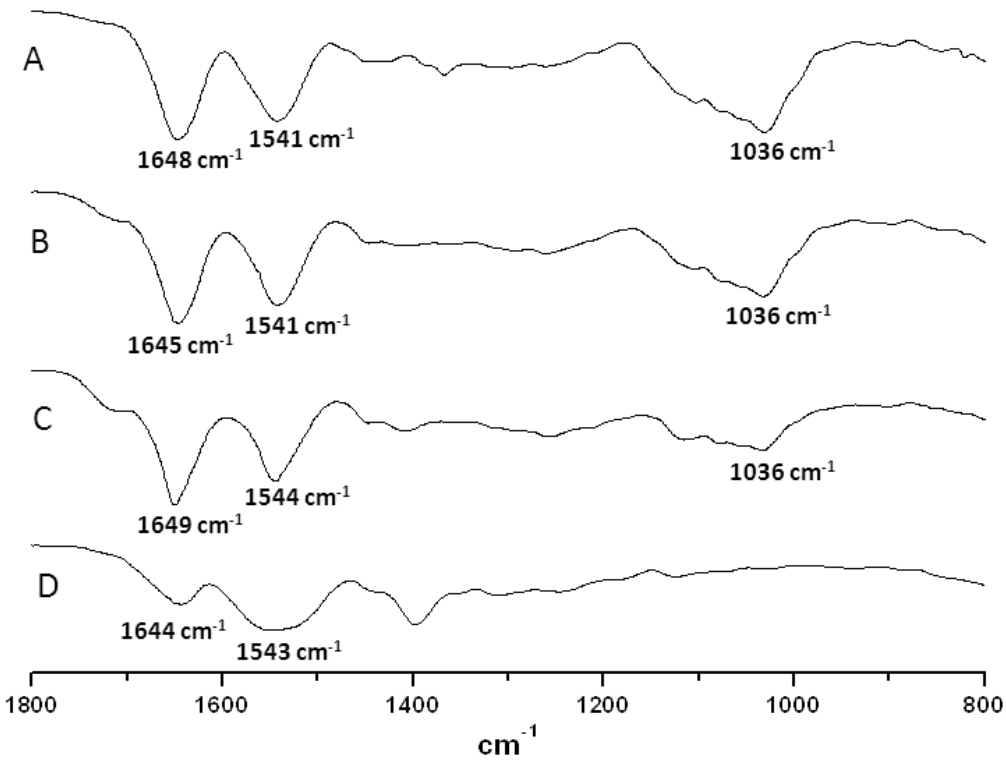

Figure 4.8: FTIR spectra of G2(8)-PGA_{27}-(G) 96% (A), G2(8)-PGA_{27}-(G) 54% (B), G2(8)-PGA_{27}-(G) 31% (C) and G2(8)-PGA_{27} (D).

4.2.1.3 Lectin Binding Studies of Star Shaped Glycopolypeptides

The binding of glycoconjugates, such as glycopolypeptides to lectins is a very effective tool in helping to ascertain the bioactivity of such materials. Lectin specific binding interactions demonstrate the targeting potential of glycosylated materials for targeted drug delivery whilst also highlighting their potential use in the study of advanced carbohydrate-protein interactions. The choice of lectin is very important due to the highly specific nature of these carbohydrate-protein interactions. Preliminary lectin binding studies were performed using turbidimetric assays. Upon mixing a solution of glycopolypeptide with a solution of sugar specific lectin, UV analysis was performed at selected time intervals. Successful sugar-lectin binding was denoted by an increase in turbidity. The lectin chosen was ConA, a lectin known to bind with glucosamine.[78] For this, PBS (pH 7.2) was employed as at this pH ConA is known to exist as a homotetramer with four binding sites for potential sugar interactions.[79] The systematic investigation of the effects of architecture on lectin binding was carried out at 420 nm using a polymer concentration of 2 mg/ml. No immediate precipitation was observed upon mixing of glycopolypeptide and lectin. However, the gradual increase in solution turbidity was observed over time and was shown to be architecturally dependent. Concerning linear and star shaped glycopolypeptides of similar M_w **(Entries 3 – 7 and 15 – 16, Table 4.2)**, lectin binding was observed for each **(Figure 4.9)**. The effects of sugar density can be clearly observed, as expectedly, a higher DS results in a quicker reduction in solution transparency. For example, the G2(8)-PGA_{27} family of star shaped glycopolypeptides with DS 54% and 96% sees the rapid aggregation and thus precipitation of lectin (approx. 10 min). However a DS of 30% resulted in the dramatic decrease in the rate of precipitation and the overall maximum absorbance observed after 1 h. Not notable further absorbance increase was observed even after 24 h. Menzel and co-workers noted that at below a DS of 50% for linear PGA no precipitation occurred due to unsuccessful binding or limited binding in which the aggregates are solubilised by the free carboxylic acid moieties.[51] Although limited binding is evident here, the low sugar density of this particular glycopolypeptide somewhat slows the rate of interaction and the ability to form insoluble aggregates. A similar observation was apparent for L(1)-PGA_{200} and G5(64)-PGA_3 of varying sugar densities. The effect of architecture was notable with the general trend being that increased branching density had a greater effect on lectin binding and aggregate precipitation. Considering glycopolypeptides with an approximate DS of 25%, L(1)-PGA-$(G)_{200}$ 27% and G2(8)-PGA_{27}-(G) 30% sluggishly form lectin aggregates which do not become significantly insoluble over time. In contrast, the densely branched but short armed G5(64)-PGA_3-(G) 20% with approximately the same number of total PGA units and sugar

moieties forms a more turbid solution in a shorter time frame. At this DS it is suggested that a very densely branched polymer network interacts more favourably with lectin. The multivalent binding of lectins to this short armed highly branched polypeptide structure is possibly promoted by a higher local density of sugars within this size confined structural space resulting in superior binding efficiency, steric shielding of free carboxylic acid moieties and consequently more pronounced precipitation of lectin aggregates. Furthermore, the exact positioning of sugars in these star shaped architectures is unknown but it can be speculated that the densely branched star polymers e.g. G5(64)-PGA_3-(G) 20% display their sugars at the periphery due to inefficient sugar coupling at the inner carboxylic acid moieties whereas the less densely branched star polymers e.g. G2(8)-PGA_{27}-(G) 30% sees a more even distribution of sugars throughout its polymeric network. Consequently, these sugars are more accessible to lectins in the case of G5(64)-PGA_3-(G) 20%, therefore promoting superior lectin binding interactions. Glycopolypeptides with a DS of 50% also demonstrated the effect of architecture on lectin interactions particularly in relation to linear architectures. Although no significant difference was observed amongst the two star shaped architectures i.e. G2(8)-PGA_{27}-(G) 54% and G5(64)-PGA_3-(G) 48% a clear impact on the comparable L(1)-PGA_{200}-(G) 53% was noted. Precipitation of lectin aggregates was slower and less pronounced for this architecture. Similarly, G2(8)-PGA_{27}-(G) 96% and L(1)-PGA_{200}-(G) 92% afforded such a variation highlighting the major implications of structural architecture for carbohydrate-protein interactions.

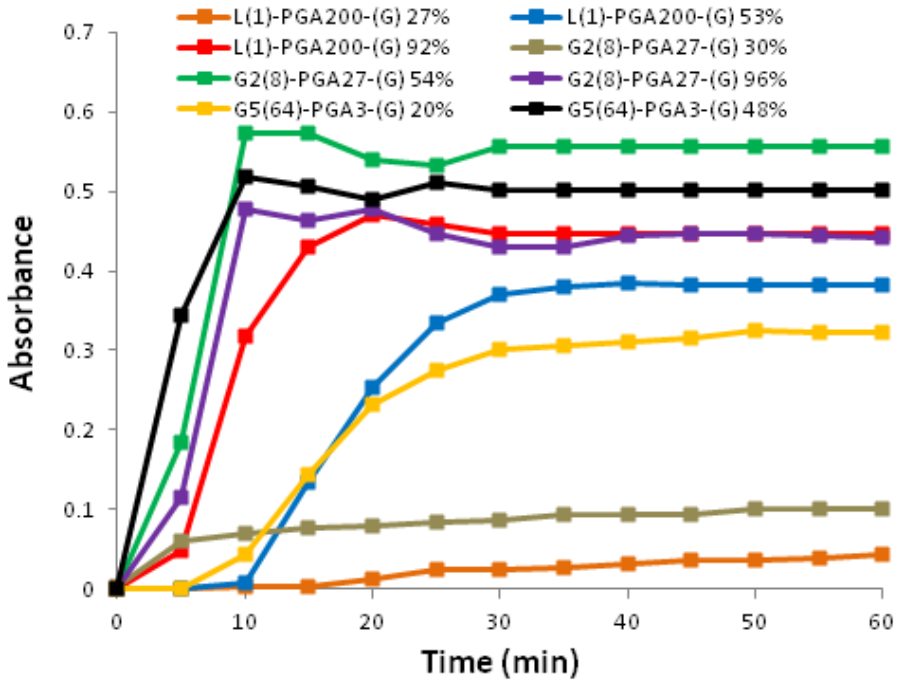

Figure 4.9: Absorbance at 420nm of lectin / glycopolypeptide (comparable M_w) solutions and the effects of architecture and sugar density on binding.

Related glycopolypeptide architectures of constant arm length i.e. 40 but varying branching densities and molecular weights (number of PGA units) were investigated with regards to their potential effects on lectin binding. Again lectin binding was observed throughout whilst architecture was shown to affect lectin binding interactions **(Figure 4.10)**. Comparable to the above results **(Figure 4.9)**, a higher DS resulted in a marked lectin binding interaction difference such that solution turbidity increased more quickly and achieved a greater absorbance maximum **(G2(8)-PGA$_{40}$-(G) 30%, 51%, 85% and G5(64)-PGA$_{40}$-(G) 43%, 73%, Figure 4.10)**. At a DS of approximately 50%, no significant effect of architecture on lectin binding was observed amongst the star shaped conformations **(G2(8)-PGA$_{40}$-(G) 51%, G3(16)-PGA$_{40}$-(G) 43% and G5(64)-PGA$_{40}$-(G) 43%, Figure 4.10),** although G3(16)-PGA$_{40}$-(G) 43% did result in a higher overall absorbance maximum. Notable however, was the rapid increase in turbidity experienced by G5(64)-PGA$_{40}$-(G) 73% in comparison to G2(8)-PGA$_{40}$-(G) 85% of an equivalently targeted DS. Although G5(64)-PGA$_{40}$-(G) 73% has more sugar units overall, its degree of substitution or ratio of sugar : COOH is less which in theory should reduce the speed and formation of insoluble lectin aggregates. However, the opposite was observed in which the densely branched G5(64)-PGA$_{40}$-(G) 73% reached its maximum absorbance after 10 min whereas G2(8)-PGA$_{40}$-(G) 85% obtained the same absorbance max. after 30 min. As discussed above, albeit at a DS of 25% the densely branched G5(64)-PGA glycopolypeptide architectures seem to have a more profound effect on lectin binding interactions at the extremes of DS i.e. 30% > x > 70% due to their favoured presentation of sugars at the accessible surface.

Comparing the effects of arm length using **figures 4.9 and 4.10**, it is shown that a shorter arm length permits a faster lectin binding interaction. For instance, G2(8)-PGA$_{40}$-(G) 51% and 85% achieve their absorbance max. at 30 min whereas G2(8)-PGA$_{27}$-(G) 54% and 96% achieves theirs at 10 min. A similar observation is made for G5(64)-PGA$_{40}$-(G) 43% and G5(64)-PGA$_{3}$-(G) 48%. Although all of their DS are relatively similar, it seems that polypeptide arm length also has a major effect on sugar - lectin interactions. As observed for branching density, it is hypothesised that the positioning of sugars i.e. positioning at accessible periphery is a key factor for lectin binding interactions and it appears that this feature is favoured for star polymers of short polypeptide arm lengths. Consequently, it can be concluded that sugar density at the accessible surface which itself is speculated to be dependent on polypeptide arm length and branching density, is the major contributor towards the modulation of lectin binding interactions.

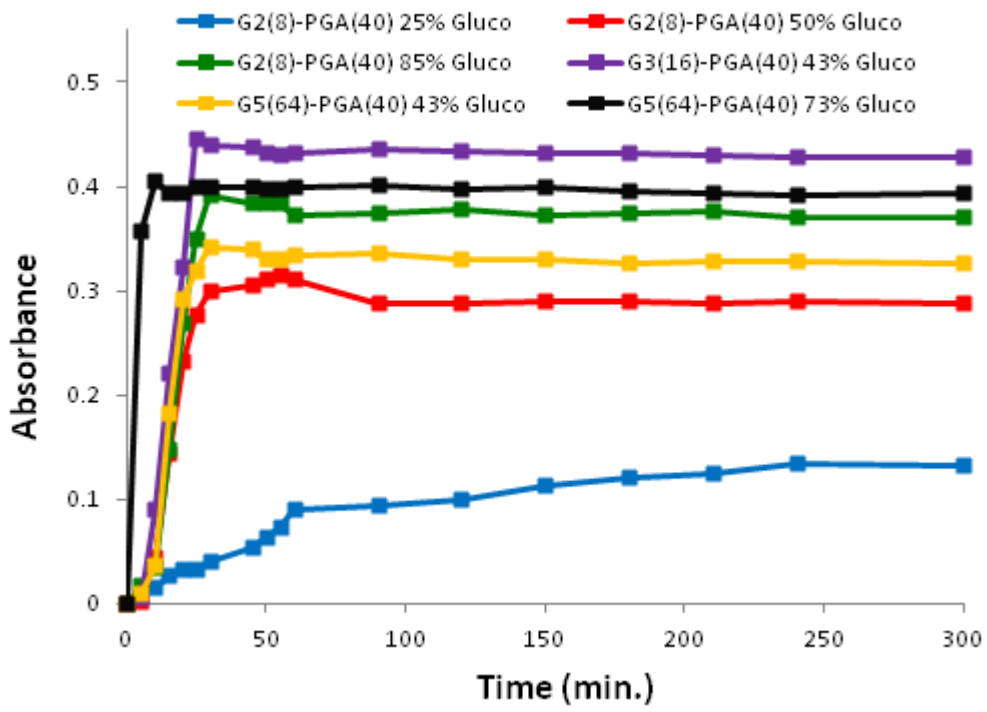

Figure 4.10: Absorbance at 420nm of lectin / star shaped glycopolypeptide (comparable arm length) solutions and the effects of architecture and sugar density on binding.

4.2.2 Advanced Linear Polypeptide Architectures

4.2.2.1 Linear Polypeptide Synthesis

Aside from star shaped polypeptides, the synthesis of more complex linear polypeptide architectures was attempted. Considering the eventual goal of polypeptide glycosylation through aqueous mediated amide coupling chemistry, the targeting of linear polypeptides with selectively positioned carboxylic acid moieties was envisaged. Therefore, to achieve water soluble polypeptides with selectively positioned sugars a methodology involving the use of two NCA monomers both with carboxylic acid side chain functionality but capped with different protecting groups was employed. The use of two different protecting groups should permit the selective removal and subsequent presentation of carboxylic moieties at defined positions thus providing a reactive handle for glycosylation with amino functionalised sugars. Finally, deprotection of the remaining robust protecting groups should afford a universally water soluble polypeptide possessing sugars at well- defined positions.

Concerning NCA monomers with carboxylic acid functionality, γ-benzyl-L-glutamate was chosen due its facile synthesis, well understood NCA ROP behaviour and robust protecting group.[18,19,80] Similarly, the second NCA monomer chosen was based on glutamic acid but possessed a tert-butyl protecting group which permits side chain deprotection under mild acidic conditions whilst in theory preserving the benzyl protecting groups.[76] Therefore, the NCA monomer, L-glutamic acid 5-tert-butyl ester (GATBE) bearing tert-butyl protection of the carboxylic acid side chain functionality was synthesised using typical triphosgene mediated protocols.[81] ^{1}H NMR spectroscopy confirmed its successful synthesis **(Figure 4.11)**.

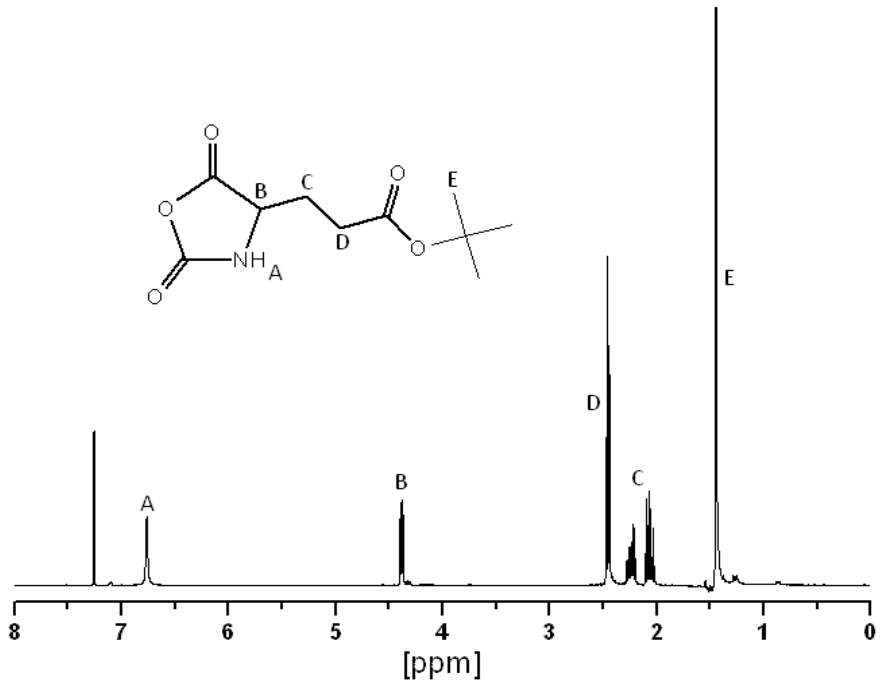

Figure 4.11: ^{1}H NMR spectrum of L-glutamic acid 5-tert-butyl ester (GATBE) NCA monomer ($CDCl_3$).

Initially, a linear block copolymer arrangement was attempted through polymerization of BLG NCA at 0^{o}C and subsequent chain extension by GATBE NCA. The use of 0^{o}C inhibits unwanted side reactions such as termination of the terminal polypeptide primary amine thus allowing for the well controlled chain extension of PBLG chains with other NCAs.[82] Chain extension with GATBE was not attempted until FTIR spectroscopy confirmed the complete consumption of BLG monomer. The observed shift in retention time of homopolymer to block copolymer by SEC confirmed the successful generation of a block copolymer arrangement **(Figure 4.12)**. The presence of terminated homopolymer chains was detected however at an elution time of 23 minutes which prevented chain extension by a second monomer. The M_w of the block copolymer differed significantly from the theoretical M_w due to the unknown dn/dc value of this block copolymer **(Table 4.3, entries 1 and 2)**. However, the distinguishable presence of both PBLG and PGATBE moieties in ^{1}H NMR spectroscopy analysis which helped to accurately elucidate the real M_n and was shown to be in close agreement with the targeted M_n **(Figure 4.13)**.

Table 4.3: Synthesis of block copolymers by initiation from hexylamine (L: linear initiator hexylamine; L(1)-$PBLG_{20}$ = initiator with theoretical arm length of 20 amino acids).

Entry	Polymer	NCA/NH_2	M_w/g $mol^{-1(a)}$	$M_n^{th\,(b)}$/g mol^{-1}	PDI
		L(1)-$PBLG_{20}$-b-$PGATBE_{20}$			
1	L(1)-$PBLG_{20}$	20	5 500 (3 500)$^{(c)}$	4 400	1.1
2	L(1)-$PBLG_{20}$-b-$PGATBE_{20}$	20	17 700 (6 700)$^{(c)}$	8 100	1.4
		L(1)-$PBLG_5$(B)-s-$PGATBE_5$(T)			
3	Block 1 (PBLG) - B	5	2 800	1 200	1.1
4	Block 2 (PGATBE) - BT	5	4 100	2 100	1.2
5	Block 3 (PBLG) - BTB	5	7 400	3 200	1.2
6	Block 4 (PGATBE) - BTBT	5	8 700	4 100	1.2
7	Block 5 (PBLG) - BTBTB	5	14 500	5 200	1.3
8	Block 6 (PGATBE) - BTBTBT	5	15 400	6 100	1.2
9	Block 7 (PBLG) - BTBTBTB	5	18 800	7 200	1.2
10	Block 8 (PGATBE) - BTBTBTBT	5	19 900 (9100)$^{(c)}$	8 100	1.2

(a) determined by SEC (DMF) using MALS detection using the dn/dc of linear PBLG of 0.118 (b) calculated assuming initiation from all amino groups and quantitative conversion: c(monomer)/c(hexylamine) x M(monomer) + M(initiator) (c) determined by ^{1}H NMR spectroscopy using the integral ratio of hexylamine, PBLG and PGATBE.

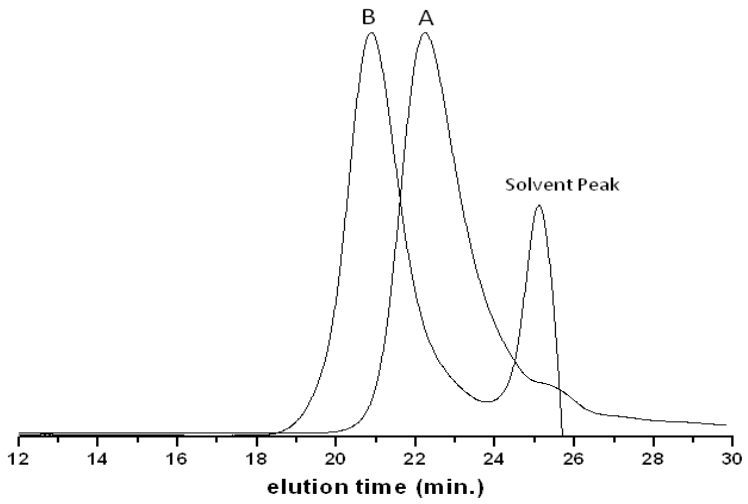

Figure 4.12: SEC traces L(1)-$PBLG_{20}$ (A) and L(1)-$PBLG_{20}$-b-$PGATBE_{20}$ (B).

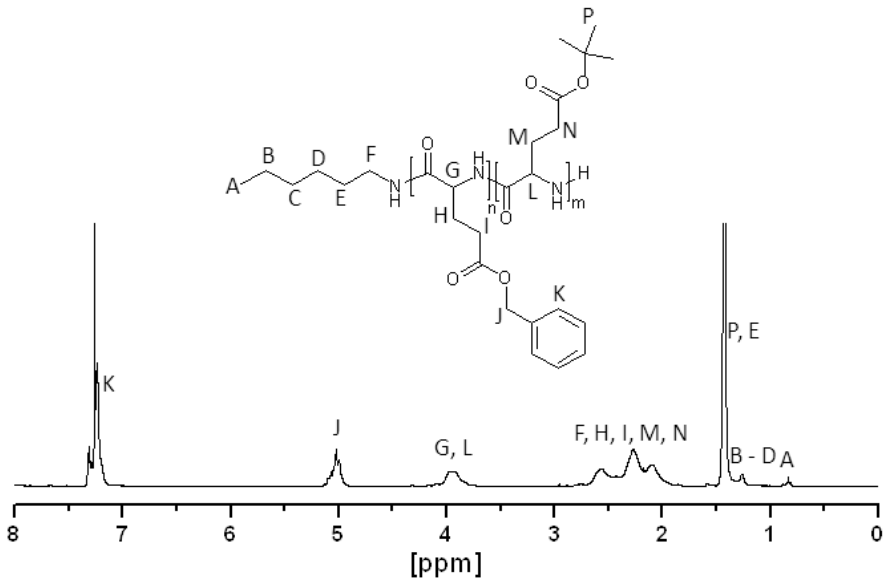

Figure 4.13: ^{1}H NMR spectrum of L(1)-PBLG$_{20}$-b-PGATBE$_{20}$ ($CDCl_3$).

To induce further complexity to this system the creation of an advanced block copolypeptide was envisaged. The field of NCA ROP has developed immensely in recent years but the next major hurdle for NCA ROP is the ability to sequence control amino acids within a polypeptide chain.[17,21,24] Although not strictly sequenced to the individual amino acid, the selective positioning or sequencing of PGATBE segments within a polypeptide chain was attempted **(Figure 4.14)**. The creation of a polypeptide containing multiple short polypeptide blocks positioned selectively is a step towards the "holy grail" of sequence controlled polypeptide synthesis by NCA ROP. This is the first such reported case of amino acid "sequencing" within an NCA derived polypeptide. The subsequent glycosylation of this polypeptide will also be the first reported case of sugar sequencing on an NCA derived polypeptide platform.

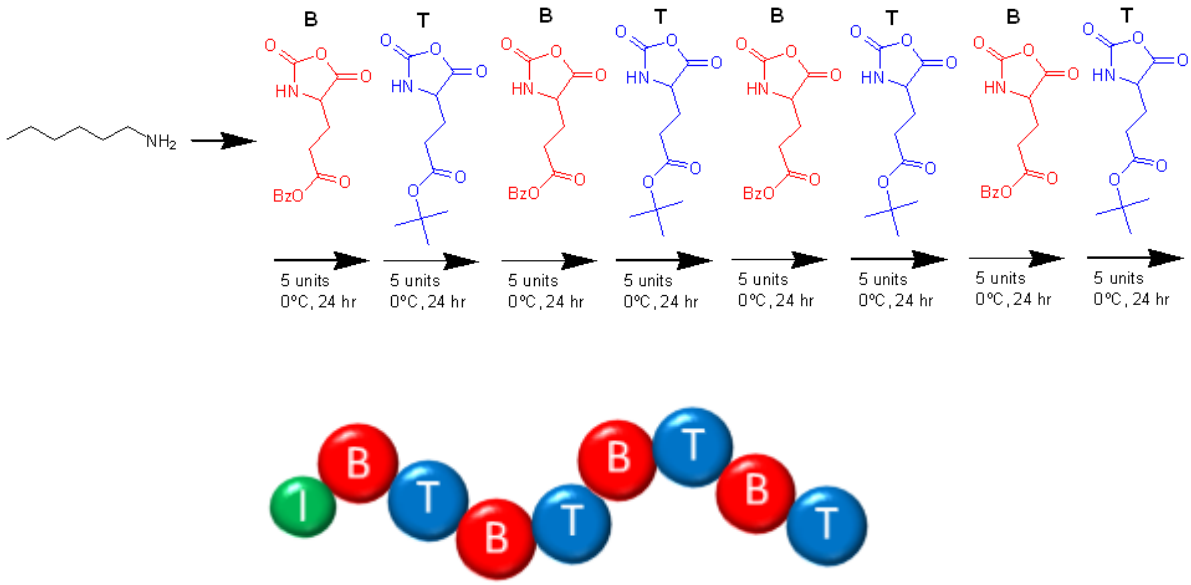

Figure 4.14: Sequence controlled synthesis of linear polypeptides.

The use of BLG and GATBE NCA monomers should prove feasible owing to their above demonstrated ability to generate a simple block copolymer whilst polymerization of individual monomers does not induce the formation of strong secondary structures which has been known to limit polypeptide growth in the case of certain NCAs.[28] NCA ROP was carried out by employing hexylamine to target short polypeptide blocks of 5 amino acid units. The reaction was performed at 0°C and monitored by FTIR spectroscopy to ensure complete monomer consumption. The targeting of 5 amino acid units for each block enabled the use of the available SEC instrumentation to monitor block formation and molecular weight characteristics of the resultant polypeptide chains. The clear shift in retention time after chain extension can be observed in **Figure 4.15** highlighting the ability to closely monitor this sequenced system.

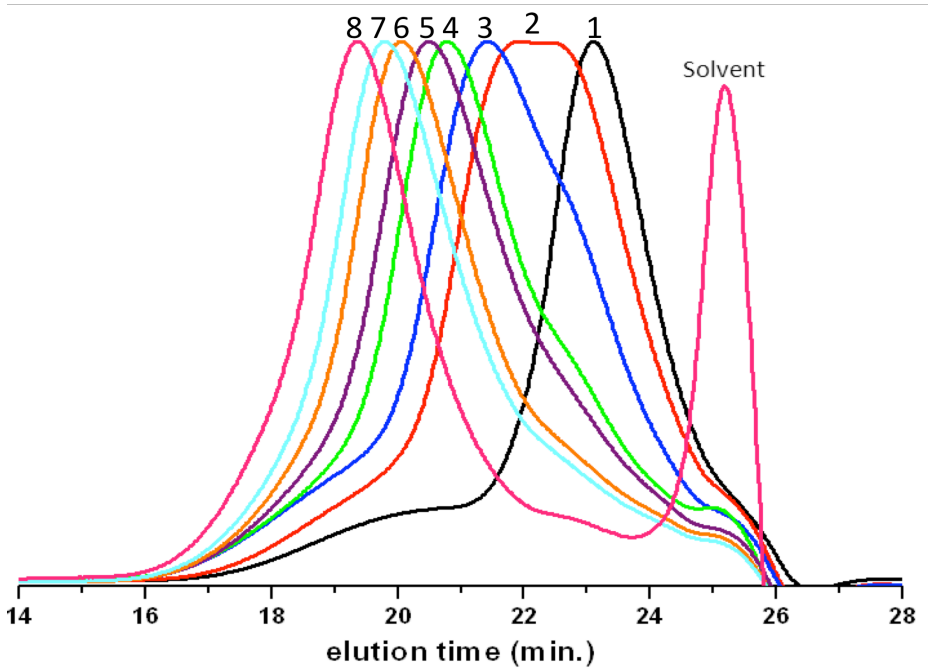

Figure 4.15: SEC traces (RI detector) of L(1)-PBLG$_5$ (B) (Black) (1), L(1)-PBLG$_5$-b-PGATBE$_5$ (BT) (Red) (2), L(1)-BTB (Blue) (3), L(1)-BTBT (Green) (4), L(1)-BTBTB (Purple) (5), L(1)-BTBTBT (Orange) (6), L(1)-BTBTBTB (Light Blue) (7) and L(1)-BTBTBTBT (Pink) (8).

The molecular weight characteristics of the polypeptide after each chain extension are summarized in **Table 4.3**. The actual M_w values are not accurate due to the unknown dn/dc value of this polymer but the retention time shifts in SEC do show that M_w is increasing after each chain extension. Although narrow PDIs were obtained demonstrating the excellent control observed, the SEC traces did exhibit some asymmetry due to peak tailing as a result of the presence of a small amount of terminated polypeptide chains preventing further chain extension. A broad SEC trace was observed for L(1)PBLG$_5$-b-PGATBE$_5$ after initial chain extension. It is postulated that this arose due to the low solubility issues associated with PGATBE in DMF. However, with continued chain extension this feature became less apparent. As shown in **figure 4.16**, ^{1}H NMR spectroscopy analysis permitted accurate M_n determination of the final linear polypeptide and was in close agreement with the overall targeted M_n. Such excellent correlation epitomises the highly controlled nature of this system.

To afford carboxylic moieties for selective glycosylation of the described block and multi-block linear polypeptides, the tert-butyl protecting groups of PGATBE were facilely removed using TFA. ^{1}H NMR spectroscopy confirmed their quantitative removal (no tert-butyl signal at 1.3 ppm) in addition to confirming the preservation of the benzyl protecting groups of PBLG (7.3 ppm) **(Figure 4.16)**.

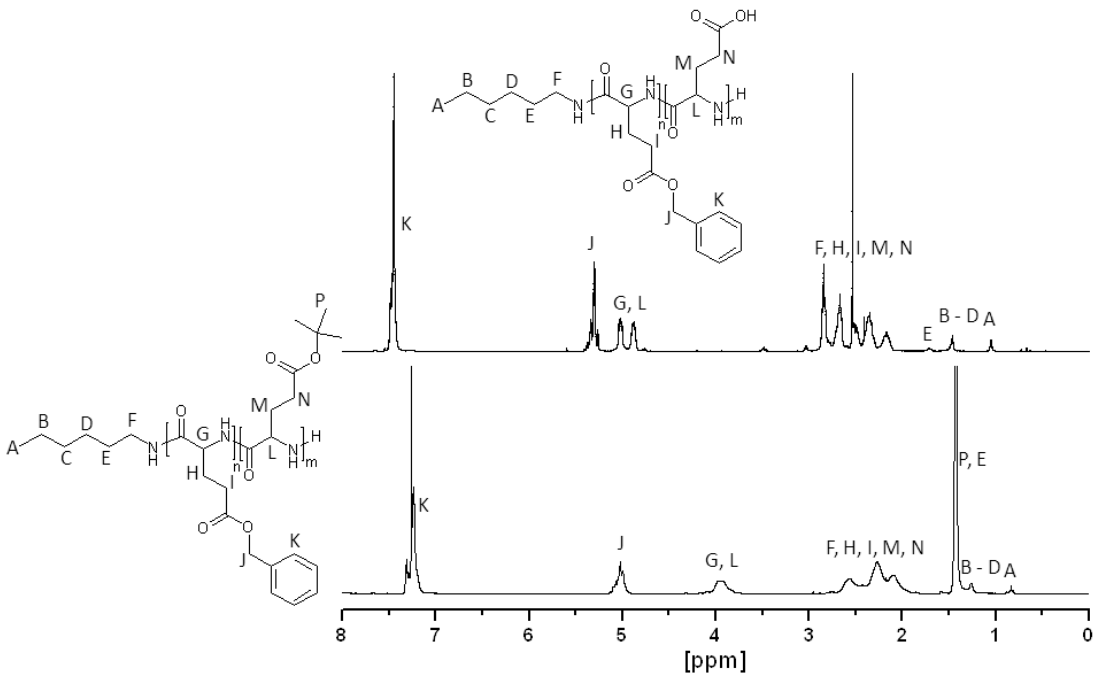

Figure 4.16: ^{1}H NMR spectrum of L(1)-PBLG$_{20}$-b-PGATBE$_{20}$ ($CDCl_3$) (Bottom) and L(1)-PBLG$_{20}$-b-PGA$_{20}$ (d-TFA) (Top).

4.2.2.2 Glycosylation of Advanced Linear Polypeptide Architectures

Glycosylation of linear polypeptide derivatives at selected positions was attempted using the same methodology as described for the star shaped derivatives **(Figure 4.17)**. However, glycosylation was complicated given the inherent water solubility issues associated with such amphiphilic systems. Despite this, glycosylation was attempted in water as only solubility of the targeted functional groups i.e. carboxylic acid of polypeptide and amine of glucosamine is required for effective sugar conjugation. An excess of sugar and coupling reagents were used to attempt 100% glycosylation of the available carboxylic acid groups. The results are summarized in **Table 4.4**.

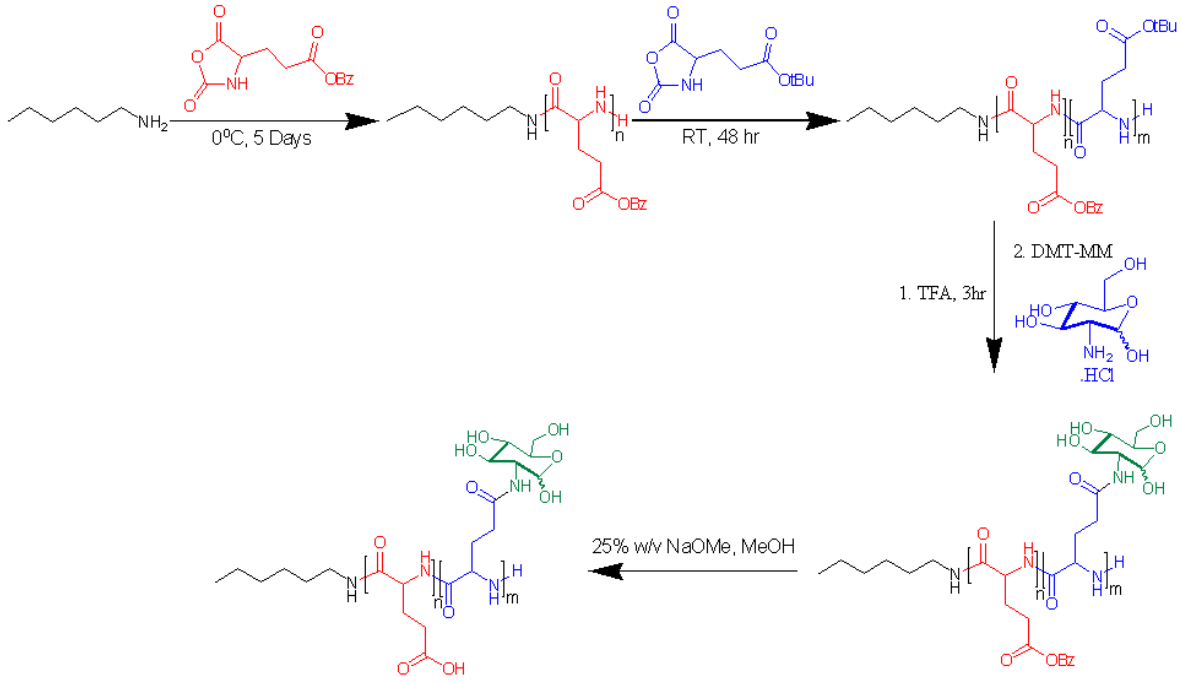

Figure 4.17: Synthesis of advanced linear glycopolypeptide architectures via strategic glycosylation of linear block copolypeptides.

Table 4.4: Results of amide coupling of glucosamine to linear poly(glutamic acid).

Entry	Polymer	$M_n^{th\,(a)}$/g mol^{-1}	GA:Amine:DMT-MM[(c)]	Target DS (%)[(d)]	Measured DS (%)[(e)]
1	L(1)-PBLG$_{20}$-b-PGA$_{20}$	6 100 (5700)[(b)]	1 : 2 : 2	100	100
2	L(1)-PGA$_{20}$-b-PGA$_{20}$-(G)	9 300 (8400)[(b)]	N/a	100	92 [(f)]
3	L(1)-PBLG$_{20}$-s-PGA$_{20}$	6 100 (7700)[(b)]	1 : 2 : 2	100	70
4	L(1)-PGA$_{20}$-s-PGA$_{20}$-(G)	9 900 (10400)[(b)]	N/a	100	94 [(f)]

(a) calculated assuming initiation from all amino groups and quantitative conversion: c(monomer)/c(dendrimer) x M(monomer) + M(dendrimer) (b) actual M_w as determined by ^{1}H NMR spectroscopy using the integral ratio of hexylamine, PGA and Sugar. (c) molar ratio of COOH from PGA : NH_2 of glucosamine : DMT-MM coupling reagent (d) target number of glutamic acid units to be functionalised as calculated by molar ratio coupling reagents to glutamic acid units (e) determined by ^{1}H NMR spectroscopy using the integral ratio of glucosamine and PGA (f) DS result for targeted PGA block / blocks and not DS for whole polymer i.e. entry 2 has a total DS of 46% but 92% for glycosylation of targeted PGA block.

Glycosylation of the block copolymer, L(1)-PBLG$_{20}$-b-PGA$_{20}$, was perceived the most straightforward owing to its relatively simple architecture. As confirmed by ^{1}H NMR spectroscopy a DS of 100% was achieved for this polypeptide which is impressive given the amphiphilic nature of this material which may have somewhat inhibited the attainability of high DS **(Figure 4.16) (Entry 1, Table 4.4)**. However, solubility of this material for ^{1}H NMR spectroscopy analysis proved difficult even in d-TFA meaning that accurate peak identification and thus integral ratios were challenging to obtain. Furthermore, due to its amphiphilic nature potential shielding of sugar moieties by the hydrophobic PBLG may be present. Consequently, the real DS value may be more accurately obtained following deprotection of the remaining benzyl groups to afford a material with superior solubility properties. FTIR spectroscopy also confirmed conjugation due to the presence of a peak at 1030 cm^{-1} corresponding to the C-O functionality of sugar **(Figure 4.17, B)**. Glycosylation of the architecturally more complex, L(1)-

$PBLG_{20}$-s-PGA_{20}, was similarly attempted and afforded a notable DS of 70%. **(Entry 3, Table 4.4)**. Given the amphiphilic nature of this material and elaborate positioning of carboxylic moieties amongst the hydrophobic PBLG segments, the achievement of a high DS here was somewhat surprising. However, as with L(1)-$PBLG_{20}$-b-PGA_{20}, ^{1}H NMR spectroscopy may not yet yield the true DS value until complete deprotection is achieved. FTIR spectroscopy analysis of this material was similar to the aforementioned analysis of L(1)-$PBLG_{20}$-b-PGA_{20}. Finally, to obtain fully water soluble glycopolypeptides the benzyl protecting groups of PBLG were removed using basic conditions as the typical acidic TFA / HBr conditions used to remove this protecting group would react unfavorably with sugars to cleave their ether bonds and/or brominate the α/β hydroxyl group. Sodium methoxide in methanol was employed to achieve deprotection in 1 – 2 h with no undesirable effects on polypeptide backbone or sugars observed as determined by ^{1}H NMR spectroscopy and FTIR spectroscopy **(Figures 4.16 and 4.17, A)**. Post deprotection, the DS values obtained were 92% and 94% (DS of targeted block) or 46% and 47% (DS for whole polypeptide) for L(1)-PGA_{20}-b-PGA_{20}-(G) and L(1)-PGA_{20}-s-PGA_{20}-(G) respectively **(Entries 2 and 4, Table 4.4)**. The DS value for L(1)-$PBLG_{20}$-b-PGA_{20} was in close agreement to its DS pre-benzyl deprotection. However, the post benzyl deprotection DS of 94% obtained for L(1)-PGA_{20}-s-PGA_{20}-(G) was very impressive and differed significantly from L(1)-$PBLG_{20}$-s-PGA_{20} due to its improved solubility and nullification of the potential shielding effects of PBLG. Such a result highlights the very effective nature of this methodology to create a diverse range of glycosylated platforms. Both block and sequenced polypeptide derivatives displayed α-helical character (Amide I and II: 1648 cm^{-1} and 1547 cm^{-1}) in their solid state form with the presence of sugar moieties denoted by the presence of an ether bond at 1030 cm^{-1} **(Figure 4.17, A and B)**.

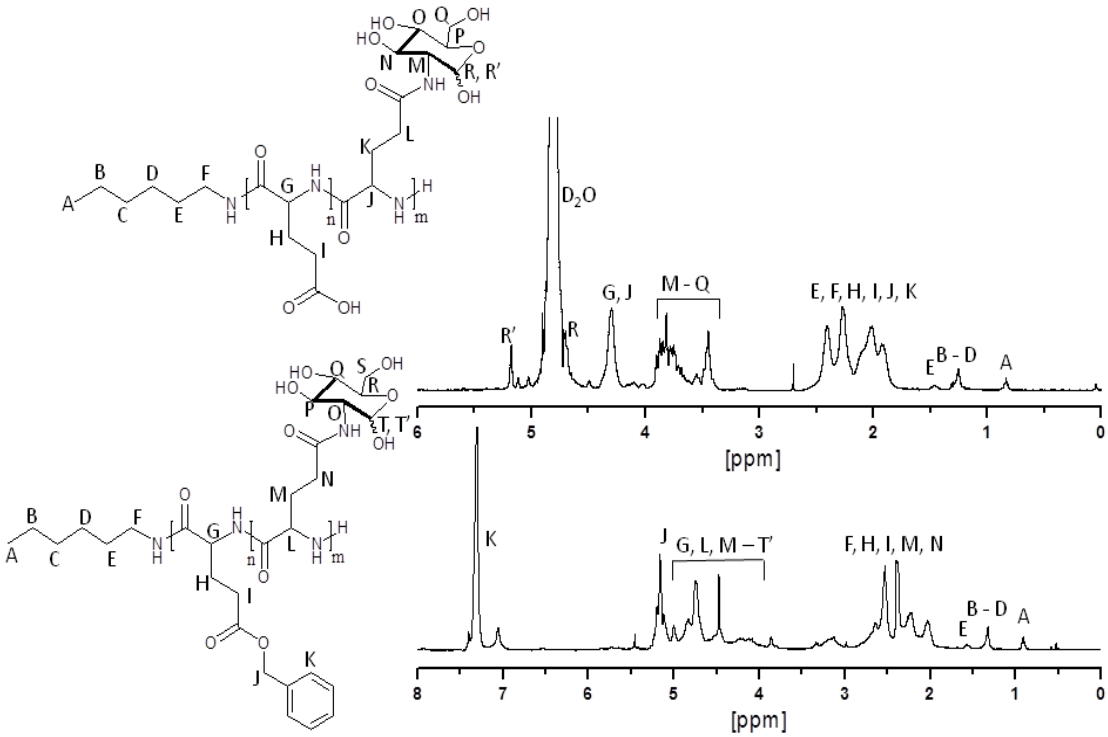

Figure 4.16: ^{1}H NMR spectra of L(1)-PBLG$_{20}$-b-PGA$_{20}$-(G) (Bottom) (d-TFA) and L(1)-PGA$_{20}$-b-PGA$_{20}$-(G) (Top) (D$_2$O).

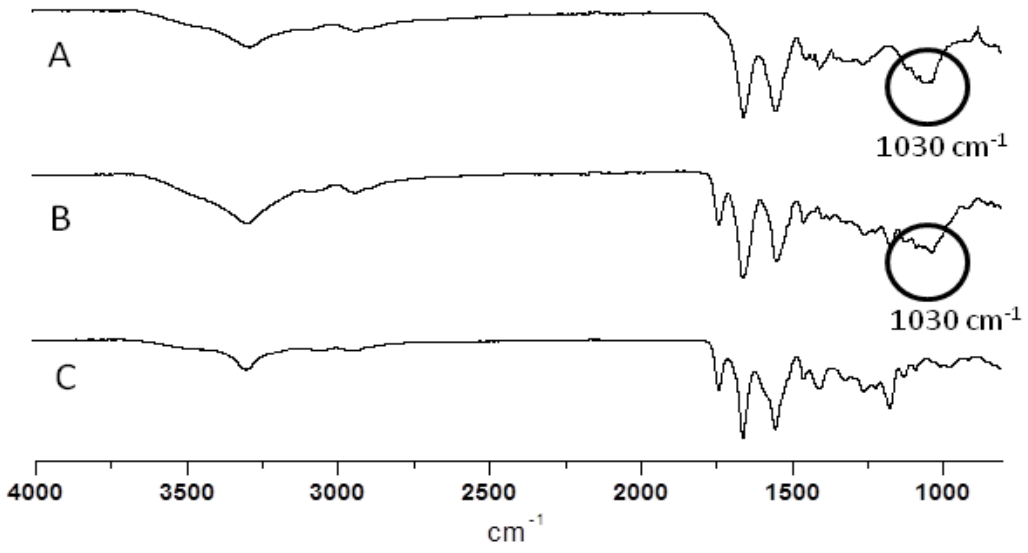

Figure 4.17: FTIR spectra of L(1)-PGA$_{20}$-b-PGA$_{20}$-(G) (A), L(1)-PBLG$_{20}$-b-PGA$_{20}$-(G) (B) and L(1)-PBLG$_{20}$-b-PGA$_{20}$ (C).

4.2.2.3 Lectin Binding Studies of Advanced Linear Glycopolypeptide Architectures

The relationship between sugar positioning and its effects on lectin binding was investigated using various linear glycopolypeptide architectures. The number of amino acid units was constant i.e. 40 whereas sugars were strategically positioned along the polypeptide chain i.e. random, block and sequenced arrangement of sugars. The targeting of linear polypeptides with 40 glutamic acid residues was chosen as it reflects the length of one arm of the equivalent star shaped polypeptides described in **Figure 4.10**. As expected, the lectin binding interaction for these linear derivatives **(Figure 4.18)** was far slower than for the equivalents stars i.e. DS > 50% **(Figure 4.10)** due to their inferior sugar density. With regards to positioning of sugars, it was shown that a random arrangement of sugars had the greatest effect on lectin binding in that the formation of insoluble lectin aggregates was quickest for L(1)-PGA_{40}-(G) 58%. The reason for this may be due to favourable steric conditions for carbohydrate / lectin interactions and screening of the soluble carboxylic acid moieties thus promoting the speedy formation of insoluble lectin aggregates. Lectin interactions with the sequenced sugar arrangement, L(1)-PGA_{20}-s-PGA_{20}-(G) 47% was less pronounced and required a longer time to achieve its maximum absorbance but was in fact, stronger than the block arrangement of sugars, L(1)-PGA_{20}-b-PGA_{20}-(G) 47%. These arrangements are structurally orientated in that they have small but numerous (L(1)-PGA_{20}-s-PGA_{20}-(G)) or large but few (L(1)-PGA_{20}-b-PGA_{20}-(G)) segments of sugars and carboxylic acid moieties which although elicit lectin binding, their formation of insoluble lectin aggregates is somewhat quenched by the presence of readily accessible segments of water soluble carboxylic moieties. In spite of this, these new possibilities of arranging sugars within structurally diverse biocompatible polypeptide scaffolds presents many new opportunities to study new and more complex lectin – carbohydrate interactions. In addition, this methodology may be employed to deliver new polypeptide scaffolds capable of sequencing more than one type of sugar.

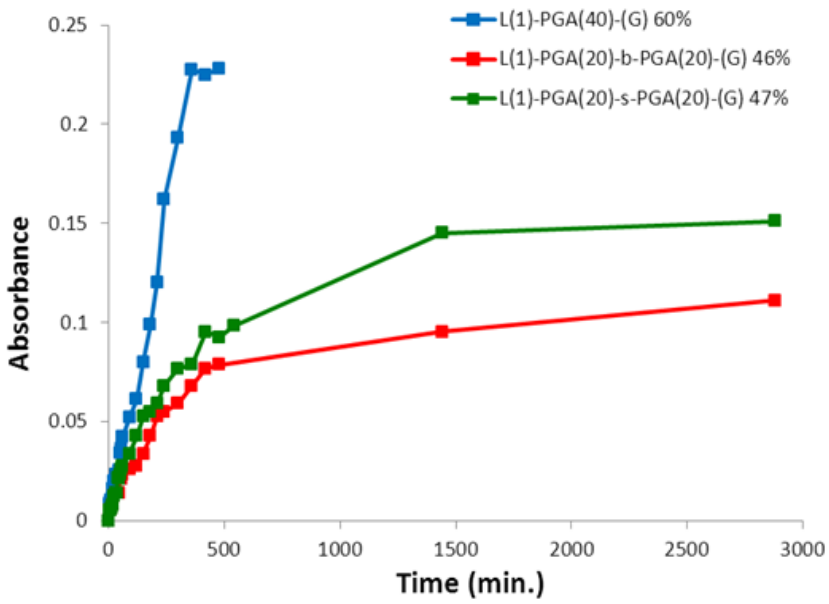

Figure 4.18: Absorbance at 420nm of lectin / linear glycopolypeptide (comparable arm length) solutions and the effects of architecture.

4.3 Conclusion

A series of well-defined block, sequenced and star shaped polypeptides were prepared via NCA ROP initiated by hexylamine and various generations of PPI dendrimers respectively. Star shaped polypeptides were generated in which their molecular weight, arm length and arm density were readily controlled. The employment of the NCA of glutamic acid bearing two different amino acid side chain protecting groups afforded a block copolymer arrangement capable of sequential deprotection and presentation of carboxylic acid moieties. Similarly, a sequenced arrangement of these amino acids was prepared for the first time boasting excellent synthetic control and monitoring throughout. The subsequent glycosylation of these materials with glucosamine via amide coupling chemistry presented a new class of star shaped glycopolypeptide architectures with tuneable sugar densities and potential to achieve high degrees of sugar conjugation. Similarly, linear block and sequenced polypeptide derivatives permitted the strategic positioning of sugar moieties along a polypeptide chain. The bioactivity of the described glycopolypeptide scaffolds towards the lectin ConA was investigated using a turbidimetry assay. The carbohydrate – lectin interactions were shown to be architecturally dependent and consequently these advanced glycopolypeptide architectures may find applicability towards biorecognition applications and the study of more complex carbohydrate – protein interactions.

4.4 Experimental

Materials

All air and moisture sensitive compounds were handled under a nitrogen atmosphere using general Schlenk-line techniques. All chemicals unless otherwise stated were purchased from Sigma Aldrich. γ-Benzyl-L-glutamate and L-Glutamic Acid 5-tert-Butyl Ester were supplied by Bachem. PPI (polypropylene imine) dendrimers generations 2-5 were purchased from SyMO-Chem BV (The Netherlands). Chloroform (anhydrous), ethyl acetate (anhydrous), dimethylformamide (anhydrous), tetrahydrofuran (anhydrous), n-heptane and diethylether were supplied by Sigma Aldrich. All chemicals were used without any purification unless otherwise noted. Chloroform and ethyl acetate were used directly from the bottle and stored under an inert, dry atmosphere. γ-Benzyl-L-glutamate NCA was synthesized following a literature procedure.[82]

Methods

Nuclear magnetic resonance (NMR) spectra were recorded on a Bruker Avance 400 (400MHz) spectrometer at room temperature in $CDCl_3$ and d-TFA as solvents. Attenuated Total Reflection (ATR) FTIR spectroscopy measurements were performed on a Perkin-Elmer Spectrum 100 in the spectral region of 650-4000 cm^{-1} and were obtained from 4 scans with a resolution of 2 cm^{-1}. A background measurement was taken before the sample was loaded onto the ATR for measurement. Size Exclusion Chromatography (SEC) was performed on an Agilent 1200 system in conjunction with two PSS GRAM analytical (8 x 300 and 8 x 100, 10 μ) columns, a Wyatt Dawn Heleos 8 multi angle light scattering detector (MALS) and Wyatt Optilab rEX differential refractive index detector (DRI) with a 658 nm light source. The eluent was DMF containing 0.1M LiBr at a flow rate of 1 mL min^{-1}. The column temperature was set to 40°C with the MALS detector at 35°C and the DRI detector at 40°C. Molar masses and dispersities were calculated from the MALS signal by the Astra software (Wyatt) using the refractive index increment (dn/dc) of linear poly-benzyl-L-glutamate (PBLG) of 0.118. All samples for GPC analysis were prepared with a concentration of 2 mg/ml and were filtered through a 0.45 μm PTFE filter (13 mm, PP housing, Whatman) prior to injection. UV-Vis spectra were recorded on a Varian Cary 50 using a UV quartz cuvette at 420 nm.

Synthesis of NCA of L-Glutamic Acid 5-tert-Butyl Ester

L-Glutamic Acid 5-tert-Butyl Ester (4.5 g, 0.022 mol) and α-pinene (6 g, 0.044 mol) were dissolved in 55 ml of anhydrous ethyl acetate in a three-neck round bottom flask. The reaction was heated to 80^{o}C under nitrogen and then triphosgene (3.8 g, 0.013 mol) in 25 ml of anhydrous ethyl acetate was added drop wise over 1 h. The solution was stirred for a further 5 h until the mixture became clear. The solution was allowed to cool and the 2/3 of the solvent was removed under reduced pressure. The NCA was precipitated by the addition of heptane. The crude product was filtered and recrystallized from ethyl acetate / heptane to afford the target compound as a white powder. (Yield: 2 g, 50%) ^{1}H NMR spectroscopy (400 MHz, $CDCl_3$, δ, ppm): 1.45 (s, 9H,$(CH_3)_3$), 2.07 (m, 1H, CH-CH_2), 2.24 (m, 1H, CH-CH_2), 2.46 (t, J= 6.8 Hz, 2H, CH_2-C=O), 4.39 (dd, J= 5.7 Hz, 1H, CH-C=O) 6.77 (s, 1H, NH), ^{13}C NMR spectroscopy (400 MHz, $CDCl_3$, δ,ppm): 27.00 (-CH(CH_2)CH_2), 28.01 (-C(CH_3)$_3$), 30.97 (-CH_2(CH_2)CO), 57.28 (-NH(CH)), 79.98 (-O(C)CH_3) 152.71 (-O(CO)NH-), 170.62 (-O(CO)CH), 207.24 (-O(CO)CH_2).

Synthesis of Linear poly(γ-benzyl-L-glutamate)-b- poly(L-glutamic acid 5-tert-butyl ester)

In a Schlenk tube under a nitrogen atmosphere, a solution of the NCA of γ-benzyl-L-glutamate (BLG) (0.57 g, 2.22 mmol) in anhydrous DMF (5 ml) was prepared. A solution of hexylamine initiator (11 mg, 0.11 mmol) in DMF was also prepared and charged to the reaction solution via syringe. The solution was stirred at 0^{o}C until no further NCA monomer remained as determined by ATR. The molar mass was monitored by SEC by taking a sample (via syringe – 0.5ml) directly for analysis. The NCA of L-Glutamic Acid 5-tert-Butyl Ester (0.498 g, 2.22 mmol) in 6 ml of DMF was charged to the reaction solution and stirred at room temperature for 48 h. ATR confirmed complete monomer consumption and the polymer was precipitated into an excess of cold diethyl ether and dried under vacuum (Yield: 93%).

Synthesis of Linear poly(γ-benzyl-L-glutamate)-s- poly(L-glutamic acid 5-tert-butyl ester)

In a Schlenk tube under a nitrogen atmosphere, a solution of the NCA of γ-benzyl-L-glutamate (BLG) (71.2 mg, 0.27 mmol) in anhydrous DMF (0.7 ml) was prepared. A solution of hexylamine initiator (5.5 mg, 0.054 mmol) in DMF was also prepared and charged to the reaction solution via syringe. The solution was stirred at 0^{o}C until no further NCA monomer remained as determined by ATR. The molar mass was monitored by SEC by taking a sample (via syringe – 100µL) directly for analysis. The NCA of L-Glutamic Acid 5-tert-Butyl Ester (62.2 mg, 0.27 mmol) in 0.6 ml of DMF was charged to the reaction solution and stirred at 0^{o}C until no further NCA monomer remained as determined by ATR. The molar mass was monitored by SEC by taking a sample (via syringe – 100µL) directly for analysis. This process was repeated to achieve the

target polymer sequence. Finally, the polymer was precipitated into an excess of cold diethyl ether and dried under vacuum (Yield: 85%).

Deprotection of tert-butyl Protecting Groups from Linear poly(γ-benzyl-L-glutamate)-s-poly(L-glutamic acid 5-tert-butyl ester) (Representative Procedure)

L(1)-$PBLG_{20}$-b-$PGATBE_{20}$ (0.3 g, 0.045 mmol) was dissolved in 4 ml of trifluoroacetic acid and stirred at $0^{o}C$ for 1 h and a further 1 h at room temperature. The polymer was precipitated into diethyl ether twice and washed with an aqueous solution of saturated $NaHCO_3$ to form the Na salt of the glutamic acid block. The solution was dialyzed (molar mass cut-off 1,000 g/mol) for 3 days. The polymer was lyophilized (Yield: 85%). Deprotection was confirmed by ^{1}H NMR spectroscopy due to the absence of signal at 1.4 ppm (tert-butyl group).

Synthesis of Glucosamine Functionalized Linear poly(γ-benzyl-L-glutamate)-b- poly(L-glutamic acid) (Representative Procedure)

Targeting a degree of substitution of 100%, L(1)-$PBLG_{20}$-b-$PGATBE_{20}$ (150 mg, 0.44 mmol PGA) and glucosamine hydrochloride (67.3 mg, 1.1 mol, 2eq. per PGA) were dissolved in 4 ml of deionized water and 1 ml of DMSO and stirred under a nitrogen atmosphere for 30 min. 4-(4,6-Dimethoxy-1,3,5-triazin-2-yl)-4-methylmorpholinium chloride (302 mg, 1.09 mmol, 2eq. per PGA) in 3 ml of deionized water was added quickly via syringe and stirred at room temperature for 24 h. 3 ml of 0.1M aqueous $NaHCO_3$ solution was added and stirred for 30 min. The solution was dialyzed for 3 days (molar mass cut-off 1,000 g/mol) against deionized water and later lyophilized to afford the target compound as a white fluffy solid. Yield 190 mg, DS = 92%.

Benzyl Ester Hydrolysis of Linear Poly(γ-benzyl-L-glutamate) -b- poly(L-glutamic acid-glucosamine) (Representative Procedure)

L(1)-$PBLG_{20}$-b-PGA_{20}-Gluco (100 mg, 0.0011 mmol) was added to 1 mL of methanol. 300µL of a 25% w/v solution of NaOMe in methanol was added to the reaction solution and stirred for 1 h. Deionized water was added gradually over a period of 1 h with stirring. The resultant clear solution was for 3 days (molar mass cut-off 1,000 g/mol) against deionized water and later lyophilized to afford the target compound as a white fluffy solid. Yield 60 mg, DS = 92%. Deprotection was confirmed by ^{1}H NMR spectroscopy due to the absence of signals at 7.2 ppm (benzyl group) and 5.0 ppm and (CH_2-Bz).

Synthesis of Linear poly(γ-benzyl-L-glutamate) (Representative Procedure)

In a Schlenk tube under a nitrogen atmosphere, a solution of the NCA of γ-benzyl-L-glutamate (BLG) (2.0 g, 7.63 mmol) in $CHCl_3$ (25 ml) was prepared. A solution of hexylamine initiator (0.32 mg, 2.98 x 10^{-6} mmol) in $CHCl_3$ was also prepared and charged to the reaction solution via syringe. The solution was stirred at room temperature until no further NCA monomer remained as determined by ATR. The polymer was precipitated into an excess of cold diethyl ether and dried under vacuum (Yield: 89%).

Synthesis of Star Shaped PBLG (Representative Procedure)

As a reference procedure, the NCA of γ-benzyl-L-glutamate (BLG) (2.18 g, 8.3 mmol) was dissolved in 25 mL $CHCl_3$ in a Schlenk tube under a nitrogen atmosphere. A solution of G2-PPI dendrimer (20 mg, 2.59 x 10^{-2} mmol) in 1 mL $CHCl_3$ was quickly charged to the dissolved NCA solution via syringe. The solution was stirred for 24 h at room temperature. Depending on the type of initiator, the used amount of initiator and monomer were adjusted to achieve the desired molar mass of the star shaped polypeptides. The polymer was precipitated into an excess of cold diethyl ether and dried under vacuum (Yield: 90%).

Benzyl Ester Hydrolysis of Poly(γ-benzyl-L-glutamate) (Representative Procedure)

G5(64)-$PBLG_{40}$ (400 mg) was dissolved in 8 mL of trifluoroacetic acid (TFA). A 6-fold excess with respect to γ-benzyl-L-glutamate of a 33% solution of HBr in acetic acid (2.3 mL) was added slowly to the reaction. After 16 h, the solution was precipitated into diethyl ether. The precipitate was redissolved in ethanol and precipitated twice into diethyl ether. The polymer was dissolved in excess saturated aqueous $NaHCO_3$ solution and stirred for 30min to form the Na salt. The solution was dialyzed (molar mass cut-off 8,000 g/mol) for 3 days. The polymer was lyophilized (Yield: 81%). Deprotection was confirmed by ^1H NMR spectroscopy due to the absence of signals at 7.2 ppm (benzyl group) and 5.0 ppm and (CH_2-Bz).

Synthesis of Glucosamine Functionalized Star Shaped poly(glutamic acid) (S-PGA)

(Representative Procedure)

Targeting a degree of substitution of 50%, G2(8)-PGA_{40} (40 mg, 3.1 mmol PGA) and glucosamine hydrochloride (67.3 mg, 3.1 mol, 1eq. per PGA) were dissolved in 2 ml of deionized water and stirred under a nitrogen atmosphere for 20 min. 4-(4,6-Dimethoxy-1,3,5-triazin-2-yl)-4-methylmorpholinium chloride (60.5 mg, 2.19 mmol, 0.7eq. per PGA) in 3 ml of deionized water was added quickly via syringe and stirred at room temperature for 24 h. 2 ml of 0.1M aqueous $NaHCO_3$ solution was added and stirred for 30 min. The solution was dialyzed

for 3 days against deionized water and later lyophilized to afford the target compound as a white fluffy solid. Yield 50 mg, DS = 50%.

Carbohydrate-Lectin Binding Tests

The lectin binding assay was performed by analysing the room temperature change in solution turbidity at 420 nm. A 2 mg/ml solution of Concanavalin A (Type IV) from Canavalia ensiformis (Jack bean) was prepared in 0.01M phosphate buffered saline (PBS). 900 µL of this solution was transferred separately to a quartz sample and reference cuvette. Similarly a 2 mg/ml solution of polymer was prepared in PBS solution. 90µL of this solution was transferred to the sample cuvette whereas 90 µL of PBS was added to the reference cuvette. The solutions were briefly mixed using a pipette and the absorbance was set to zero. The change in absorbance at 420 nm was monitored at predetermined time intervals.

4.5 References

1. C. R. Bertozzi, L. L. Kiessling, Science, **2001**, 291, 2357.

2. R. A. Dwek, *Chem. Rev*., **1996**, 96, 683.

3. P. M. Rudd, T. Elliot, P. Cresswell, I. A. Wilson, R. A. Dwek, *Science*, **2001**, 291, 2370.

4. P. Talbot, B. D. Shur, D. G. Myles, *Biol. Reprod*., **2003**, 68, 1

5. A. Varki, *Glycobiology*, **1993**, 3, 97.

6. B. G. Davis, *Chem. Rev*., **2002**, 102, 579.

7. H. J. Gabius, H. C. Siebert, S. Andre, J. Jimenez-Barbero, H. Rudiger, *Chem. BioChem*., **2004**, 5, 740.

8. T. W. Rademacher, R. B. Parekh, R. A. Dwek, *Annu. Rev. Biochem*., **1988**, 57, 785.

9. D. P. Gamblin, E. M. Scanlan, B. G. Davis, *Chem. Rev*., **2009**, 1, 131.

10. S. G. Spain, N. R. Cameron, *Polym. Chem*., **2011**, 2, 60.

11. Y. H. Yun, D. J. Goetz, P. Yellen, W. Chen, *Biomaterials*, **2004**, 25, 147.

12. F. Suriano, R. Pratt, J. P. K. Tan, N. Wiradharma, A. Nelson, Y.-Y. Yang, P. Dubois, J. L. Hedrick, *Biomaterials*, **2010**, 31, 2637.

13. A. E. Smith, A. Sizovs, G. Grandinetti, L. Xue, T. M. Reineke, *Biomacromolecules*, **2011**, 12, 3015.

14. M. Ahmed, R. Narain, *Biomaterials*, **2013**, 34, 4368.

15. T. Borase, T. Ninjbadgar, A. Kapetanakis, S. Roche, R. O'Connor, C. Kerskens, A. Heise, D. F. Brougham, *Angew. Chem., Int. Ed*., **2013**, 52, 3164.

16. C. Deng, F. Li, J. M. Hackett, S. H. Chaudhry, F. N. Toll, B. Toye, W. Hodge, M. Griffith, *Acta Biomater*., **2010**, 6, 187.

17. H. A. Klok, *Macromolecules*, **2009**, 42, 7990.

18. H. R. Kricheldorf, *Angew. Chem., Int. Ed*., **2006**, 45, 572.

19. N. Hadjichristidis, H. Iatrou, M. Pitskalis, G. Sakellariou, *Chem.Rev*., **2009**, 109, 5528.

20. T. J. Deming, *Adv. Polym. Sci*., **2006**, 202,1.

21. J. Huang, A. Heise, *Chem. Soc. Rev*., **2013**, 42, 7373.

22. E. Rude, O. Westphal, E. Hurwitz, M. Sela, *Immunochemistry*, **1966**, 3, 137.

23. J. R. Kramer, T. J. Deming, *J. Am. Chem. Soc*., **2010**, 132, 15068.

24. J. R. Kramer, T. J. Deming, *J. Am. Chem. Soc*., **2012**, 134, 4112.

25. J. R. Kramer, A. R. Rodriguez, U.-J. Choe, D. T. Kamei, T. J. Deming, *Soft Matter*, **2013**, 9, 3389.

26. J. R. Kramer, T. J. Deming, *Polym. Chem*., **2014**, 5, 671.

27. C. Bonduelle, S. Lecommandoux, *Biomacromolecules*, **2013**, 14, 2973.

28. H. C. Kolb, M. G. Finn, K. B. Sharpless, *Angew. Chem*., **2004**, 40, 2001.

29. H. Tang, D. Zhang, *Biomacromolecules*, **2010**, 11, 1585.

30. J. Huang, G. Habraken, F. Audouin, A. Heise, *Macromolecules*, **2010**, 43, 6050.

31. C. Xiao, C. Zhao, P. He, Z. Tang, X. Chen, X. Jing, *Macromol. Rapid Commun*., **2010**, 31, 991.

32. J. Sun, H. Schlaad, *Macromolecules*, **2010**, 43, 4445–4448.

33. C. Xiao, C. Zhao, P. He, Z. Tang, X. Chen, X. Jing, *Macromol. Rapid Commun*., **2010**, 31, 991.

34. A. C. Engler, L. Hyung-il, P. T. Hammond, *Angew. Chem., Int. Ed*., **2009**, 48, 9334.

35. H.Tang, D. Zhang, *Biomacromolecules*, **2010**, 11, 1585.

36. J. Huang, C. Bonduelle, J. Thévenot, S. Lecommandoux, A. Heise, *J. Am. Chem.Soc*., **2012**, 134, 119.

37. C. Bonduelle, J. Huang, E. Ibarboure, A. Heise, S. Lecommandoux, *Chem. Commun*., **2012**, 48, 8353.

38. P. Midoux, C. Mendes, A. Legrand, J. Raimond, R. Mayer, M. Monsigny, A. C. Roche, *Nucleic Acids Res*., **1993**, 21, 871.

39. G. Di Stefano, C. Busi, A. Mattioli, L. Fiume, *Biochem. Pharmacol*., **1995**, 49, 1769.

40. R. I. Mahato, S. Takemura, K. Akumatsu, M. Nishikuwa,Y. Takakura, M. Hashida, *Biochem. Pharmacol*., **1997**, 53, 887.

41. M. Nishikawa, S. Takemura, Y. Takakura and M. Hashida, *J. Pharmacol. Exp. Ther*., **1998**, 287, 408.

42. G. Thoma, J. T. Patton, J. L. Magnani, B. Ernst, R. Ohrlein, R.O.Duthaler, *J. Am. Chem. Soc*., **1999**, 121, 5919.

43. Z. Tian, M. Wang, A. Zhang, Z. Feng, Front. *Mater. Sci. China*, **2007**, 1, 162.

44. Z. Tian, M. Wang, A. Zhang and Z. Feng, *Polymer*, **2008**, 49, 446..

45. R. Wang, N.Xu, F. S. Du, Z. C. Li, *Chem. Commun*., **2010**, 46, 3902.

46. R. Roy, M. G. Baek, Rev. *Mol. Biotechnol*., **2002**, 90, 291.

47. C. Fleming, A. Maldjian, D. D. Costa, A. K. Rullay, D. M. Haddleton, J. St. John, P. Penny, R. C. Noble, N. R. Cameron, B. G. Davis, Nat. Chem. Biol., **2005**, 1, 270.

48. M. Ambrosi, N. R. Cameron, B. G. Davis, S. Stolnik, Org. Biomol. Chem., **2005**, 3, 1476.

49. M. Tranter, Y. Liu, S. He, J. Gulick, X. Ren, J. Robbins,W. K. Jones, T. M. Reineke, *Mol. Ther*., **2012**, 20, 601.

50. K. Godula, C. R. Bertozzi, *J. Am. Chem. Soc*., **2010**, 132, 9963.

51. R. Mildner, H. Menzel, *J. Polym. Sci.: Part A: Polym. Chem*., **2013**, 51, 3925.

52. M. Kunishima, C. Kawachi, J. Monta, K. Terao, F. Iwasaki, S.Tani, *Tetrahedron*, **1999**, 55, 13159.

53. M. Kunishima, C. Kawachi, K. Hioki, K. Terao, S. Tani, *Tetrahedron*, **2001**, 57, 1551.

54. M. Byrne, P. D. Thornton, S. A. Cryan, A. Heise, *Polym. Chem*., **2012**, 3, 2825.

55. A. Blencowe, J. F. Tan, T. K. Goh, G. G. Qiao, *Polymer*, **2009**, 50, 5.

56. J. T. Wiltshire, G. Qiao, *Macromolecules*, **2008**, 41, 623.

57. C. R. Becer , M. I. Gibson, J. Geng , R. Ilyas , R. Wallis , D. A. Mitchell , D. M. Haddleton, *J. Am. Chem. Soc*., **2010**, 132, 15130 .

58. V. Percec, P. Leowanawat, H. J. Sun , O. Kulikov, C. D. Nusbaum, T. M. Tran, A. Bertin, D. A. Wilson, M. Peterca, S. Zhang, N. P. Kamat, K. Vargo, D. Moock, E. D. Johnston, D. A. Hammer, D. J. Pochan, Y. Chen, Y. M. Chabre, T. C. Shiao, M. Bergeron-Brlek, S. Andre, R. Roy, H.-J. Gabius, P. A. Heiney, *J. Am. Chem. Soc.,* **2013**, 135, 9055.

59. N. Baradel, S. Fort, S. Halila, N. Badi, J. F. Lutz, Angew. Chem Int. Ed., **2013**, 52, 2335.

60. C. R. Becer , *Macromol. Rapid Commun*., **2012**, 33, 742.

61. S. Qiu, H. Huang, X. Dai, W. Zhou, C. Dong, *J. Polym. Sci. Part A: Polym. Chem*., **2009**, 47, 2009.

62. A. Sulistio, J. Lowenthal, A. Blencowe, M. N. Bongiovanni, L. Ong, S. L. Gras, X. Zhang, G. G. Qiao, *Biomacromolecules*, **2011**, 12, 3469.

63. W. Tansey, S. Ke, X. Y. Cao, M. J. Pasuelo, S. Wallace, C. Li, *J. Control. Release*, **2004**, 94, 39.

64. K. Knop, R. Hoogenboom, D. Fischer, U. S. Schubert, *Angew. Chem. Int. Ed*., **2010**, 49, 6288 .

65. A. Sulistio, P. A. Gurr, A. Blencowe, G. G. Qiao, *Aust. J. Chem*., **2012**, 65, 978.

66. Y. Nakayama, *Accounts Chem. Res*., **2012**, 45, 994.

67. Q. Zhang, J.Collins, A. Anastasaki, R. Wallis, D. A. Mitchell, C. Remzi Becer, D. M. Haddleton, *Angew. Chem. Int. Ed*., **2013**, 52, 4435.

68. J. Huang, Q. Zhang, G. Z. Li, D. M. Haddleton, R. Wallis, D. Mitchell, A. Heise, C. Remzi Becer, *Macromol. Rapid Commun*., **2013**, 34, 1542.

69. K. Aoi, K. Tsutsumiuchi, A. Yamamoto, M. Okada, *Tetrahedron*, **1997**, 53, 15425.

70. Y. Yan, J. Li, J. Zheng, Y. Pan, J. Wang, X. He, L. Zhang, D. Liu, *Colloids and Surfaces B*., **2012**, 95, 137.

71. I. Botiz, N. Grozev, H. Schlaad, G. Reiter, *Soft Matter*, **2008**, 4, 993.

72. H. A. Klok, J. R. Hernandez, S. Becker, K. Mullen, *J. Polym. Sci., Part A: Polym. Chem*., **2001**, 1572.

73. G. Liang, Q. Wu, S. Bao, F. Zhu, Q. Wu, *Polym. Chem*., **2013**, 4, 5671.

74. N. Higashi, T. Koga, N. Niwa, M. Niwa, *Chem. Commun*., **2000**, 361.

75. D. Appelhans, H. Komber, R. Kirchner, J.Seidel, C. F. Huang, D. Voigt, D. Kuckling, F. C. Chang, B. Voit, *Macromol. Rapid Commun*., **2005**, 26, 586.

76. T. Aliferis, H. Iatrou, N. Hadjichristidis, J. Messman, J. Mays, *Macromol. Symp*., **2006**, 240, 12.

77. B. Henkel, E. Bayer, *J. Peptide Sci*., **1998**, 4, 461.

78. I. J. Goldstein, C. E. Hollerman, E. E. Smith, *Biochemistry*, **1965**, 4, 876.

79. C. W. Cairo, J. E. Gestwicki, M. Kanai, L. L. Kiessling, *J. Am.Chem. Soc*., **2002**, 124, 1615.

80. Green, T. W. **(2006)**. Greene's Protective Groups in Organic Synthesis. Online: Wiley. 1082.

81. G. J. M. Habraken, C. E. Koning, A. Heise, *J. Polym. Sci. A: Polym. Chem*., **2009**, 47, 6883.

82. G. J. M. Habraken, K. H. R. M. Wilsens, C. E. Koning, A. Heise, *Polym. Chem*. **2011**, 2, 1322.

Chapter 5

Synthesis of Hybrid Nanogel Star Polymers

Abstract

A series of hybrid nanogel star polymers was synthesised using a combination of polymerization techniques to afford polymers of mixed compositions. These well-defined polymers were synthesised in a highly controlled manner in which their compositions and functionalities were readily adapted. The first group of hybrids were synthesised using anionic polymerization to generate well-defined poly(styrene) non-degradable nanogel star polymers. Post modification of these stars to introduce primary functionality permitted their use as initiators (core first approach) for NCA ROP resulting in polypeptide conjugation to their periphery. Peripheral functionality was readily adapted through choice of NCA. Secondly, cationic and anionic peripheral functionalised degradable nanogel star polymers were generated via the arm first approach. Linear polymeric arms were generated via RAFT polymerization of functional methacrylate monomers which were subsequently utilised in the organocatalytic ROP of cyclic esters to form the ester core. The size of these hybrid stars was readily controlled by varying the arm to crosslinker ratio. The employment of hydroxyl functionalised linear poly(ethylene glycol) of various molecular weights as initiators for organocatalytic ROP of cyclic esters produced a series of well-defined nanogel star structures boasting thermo responsive behaviour. Star size, molecular weight, hydrophobic content and arm length were readily controlled which enabled the modulation of poly(ethylene glycol) LCST behaviour to a temperature more suitable to potential applications such as drug delivery. The consolidation of several different synthetic approaches within the one organic nanoparticle lead to an array of new materials boasting a well-defined, multifunctional and structurally versatile nature. This synthetic and structural versatility presents many new opportunities for the development of a new generation of “smart” hybrid nanomaterials which can be easily

tailored to meet the demands of specific biomedical applications such as drug delivery (anionic / cationic star polymers for layer-by-layer technology), theranostics (core / shell type star polymers) and antimicrobials (cationic star polymers). This work was carried out under an SFI (Science foundation Ireland) STTF (Short Term Travel Fellowship) funded project at IBM, Almaden, California in collaboration with Dr. Robert D. Miller and Dr. Joseph Sly.

5.1 Introduction

The site specific delivery of functional cargoes such as therapeutics and imaging agents in both a single and dual mode is a major challenge facing the biomedical field.[1-6] If achieved, the potential implications could revolutionise the biomedical industry affording superior diagnosis and treatment of disease.[7-9] An insight into the great potential offered by such a concept was demonstrated through the use of metal-organic frameworks (MOFs) and functional nanotubes for combined therapeutics and imaging delivery.[10,11] Aside from nanomedicine, organic nanoparticle platforms have also shown their potential applicability in areas such as catalysis and photonics highlighting the array of applications open to organic nanoparticles.[12-14] In terms of materials, dendrimers,[15] micelles,[16,17] and liposomes[18,19] are just some of the materials to have achieved considerable research efforts in the pursuit of organic nanoparticles. However such materials all have their specific drawbacks in terms of synthetic design, size limitations and stability. To overcome this, the use of polymers has emerged as a very powerful tool in designing the next generation of nanoparticle delivery systems. The excellent synthetic control and versatility offered by advances in polymer chemistry presents many new exciting opportunities for designing modern nanoparticle systems.[20,21] Specifically star polymers are a particular class of polymers under consideration owing to the structural benefits offered i.e. high local density of polymeric arms and functionality within a stable and size tunable structural space.[22] Star polymers are typically derived using either the "core-first" or "arm-first" approach but nanogel star polymers ("arm-first") have emerged as a strong nanoparticle platform candidate owing to the unique structural and synthetic features offered by such materials.[23-25] The crosslinked nature of these materials affords the ability to generate large, highly functional stars with discrete unique microenvironments whilst maintaining arm length and core size, thus promoting nanogel star polymers to the forefront of organic nanoparticle research. Nanogel star polymers consist of polymeric arms emanating from a cross-linked polymeric core and therefore present the concept of a core / shell type system.[26-28] As a consequence localisation within the one polymeric star polymer may be possible i.e. core and interstitial regions within shell periphery. Such a feature may be utilised for cargo loading or loading of more than one cargo in separate locations within the one unimolecular star polymer.[29] The demands of therapeutic / imaging delivery i.e. cargo uptake, protection and delivery should therefore be well addressed by nanogel star polymers owing to the nature of their confined polymeric architecture. Furthermore the inherent control over nanogel star size (10 – 100nm) promotes a tunable and greater cargo loading capacity than the typically small

dendrimer (<10nm) counterparts highlighting a key restriction of dendrimers as a nanoparticle platform.

The challenge is the synthesis of nanogel star polymers to enable the reproducible control of structural features such as arm number and particles size.[30-32] Zilliox et al. reported the first such synthesis of nanogel star polymers employing anionic polymerization in the controlled polymerization of polystyrene with the crosslinker divinylbenzene (DVB).[26] Since this early breakthrough and with the advent of many new controlled polymerization techniques,[33-37] the development of more complicated and chemically diverse nanogel star polymers has been made possible. Nanogel star polymers have been derived from RAFT (Reversible Addition-Fragmentation Chain Transfer Polymerization),[38-42] ATRP (Atom Transfer Radical Polymerization),[43-46] NMP (Nitroxide Mediated Polymerization), GTP (Group Transfer Polymerization),[52,53] ROMP (Ring Opening Metathesis Polymerization),[54] ROP (Ring Opening Polymerization) of NCAs (N-carboxyanhydrides)[55,56] and cyclic esters,[57-60] cationic polymerization,[61,62] anionic polymerization[26] and metal catalyzed living radical polymerization.[63] Subsequently the range of employable monomers and therefore the range of potential nanogel star polymer compositions is limitless rendering the tailoring of nanogel star polymers for specific applications readily accessible. Further expansion of this idea means it may be possible to combine different polymerization techniques and compositions within the one nanogel star polymer platform.

Depending on the targeted application, properties such as degradability and biocompatibility may become prevalent particularly for drug delivery applications. As a consequence the need for nanogel star polymers of biocompatible compositions has emerged.[56,64-67]In addition, it may be desirable to include one or more than one compositional type i.e. hybrid nanogel star polymers within the one star structure to control and induce properties such as degradation profiles, functionality and stimuli responsiveness, features which may be unobtainable by a single polymer type.

In this chapter, the synthesis of a range of hybrid nanogel star polymer systems boasting a high degree of synthetic control and structural versatility is presented. All polymers comprise mixed compositions achieved through the step-wise combination of several polymerization techniques. Detailed analysis of each synthetic step is presented emphasising the excellent control observed throughout.

5.2 Results and Discussion

5.2.1 Polystyrene Core (Nondegradable) / Polypeptide Periphery (Degradable) Nanogel Star Polymers

The design of well defined, size controlled nanogel star polymers of hydrophobic composition have been reported by Sly et al.[29] Such materials are formed by the "arm first" approach which can subsequently be utilised in a "core first" approach to afford core/shell type nanogel star polymer architectures boasting a hydrophobic core and a hydrophilic periphery if so desired. The presence of peripheral functionality i.e. hydroxyl functionalised end groups of polystyrene arms provides a reactive handle from which further polymerization can be performed depending on the type of modification employed at this position e.g. modification with an ATRP type initiator. Consequently extension of the nanogel star polymer scaffold is achieved to obtain more complex structures in terms of composition, functionality and overall material properties.

The development of these materials towards potential applications is the natural progression for such research. The identification of suitable applications may require modification of the current nanoparticle platform to meet the demands of particular applications. For example an application such as drug delivery requires a non-toxic biocompatible delivery vehicle capable of delivering sufficient cargo to a targeted site and then releasing its cargo in a controlled manner.[68] Consequently, the incorporation of biocompatible/degradable polymer compositions is imperative and provides for an attractive class of new hybrid nanogel star polymer architectures.

Polypeptides, in particular polypeptides derived through ROP of NCAs are becoming increasingly prevalent in the biomaterials field owing to their composition of natural building blocks, the synthetic control afforded, scalability and their ability to form secondary structures and elucidate a stimuli response.[69] These materials have already demonstrated their potential applicability towards biomedical applications such as drug and gene delivery.[70-72] Synthetically, the ROP of NCAs can be achieved through the use of a primary amine as an initiator to obtain well defined polypeptides.[73,74] Consequently, post modification of the hydroxyl terminated polystyrene nanogel star polymers (S-PS-OH) towards primary amine terminated star polymers (S-PS-NH_2) provides a multifunctional initiator or "core first" approach for the ROP of NCAs.

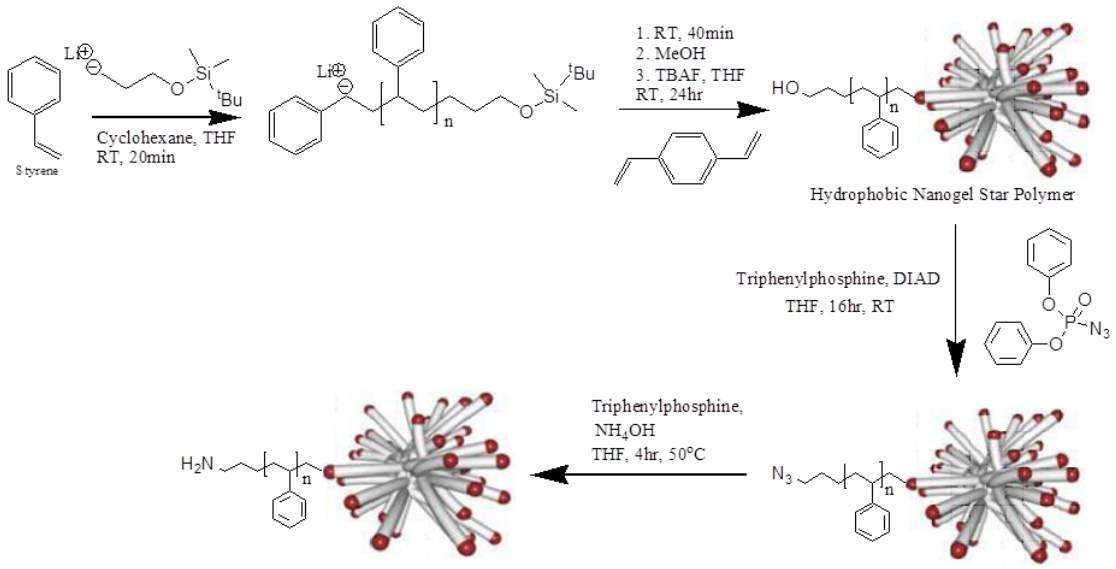

Figure 5.1: Synthesis of poly(styrene) nanogel star polymers using "arm-first" approach.

Using the expertise developed by Sly et al. a hydroxyl terminated polystyrene nanogel star polymer was synthesized by anionic polymerization **(Figure 5.1)**. A nanogel star polymer comprising an average of 36 arms each of 3 kDa molecular weight with total star polymer molecular weight of 110 kDa and R_h of 6.4 nm was developed **(Table 1, S-PS-OH) (Figure 5.2)**. The amination of the nanogel star polymers was performed using Mitsonobu type chemistry.[75] The methodology employed involved converting the hydroxyl terminated nanogel star polymer to the corresponding azide using a Mitsonobu reaction and then reducing the azide to the corresponding primary amine. Diphenylphosphoryl azide was successfully employed under typical Mitsonobu reaction type conditions to afford azide terminated nanogel star polymers. ^{1}H NMR spectroscopy confirmed the quantitative conversion of all hydroxyl groups to the corresponding azide denoted by the absence of peak **A** at 3.5 ppm (**CH_2**-OH) and its complete shift upfield to 3.1 ppm as a result of azide formation (**CH_2**-N_3) **(Figure 5.3)**. Size exclusion chromatography (SEC) showed no significant change in M_w, PDI and R_h after azide formation **(Table 5.1, S-PS-N_3)**. Subsequent reduction of the azide to the corresponding primary amine using triphenylphosphine and ammonium hydroxide resulted in the complete conversion of all azides to the primary amine functionality. Quantitative conversion was ascertained by ^{1}H NMR spectroscopy highlighting the absence of peak **A** at 3.1 ppm and its complete shift upfield to 2.5 ppm **(Figure 5.3, S-PS-NH_2)**. Due to solubility issues in THF a comparison of SEC results with the aforementioned hydroxyl and azide terminated nanogel star polymers could not be obtained. However with SEC in DMF, the amine terminated star polymer displayed an

apparent molecular weight of 44.2 kDa (dn/dc = 0.187) and PDI of 1.5 with dynamic light scattering (DLS) showing an R_h of 4.7 nm **(Table 5.1, S-PS-NH_2)**.

Table 5.1: poly(styrene) derived nanogel star polymers (L: linear, S: Star).

Polymer	M_w (kDa)[(a)]	PDI	M_w (kDa)[(b)]	*PDI*	*No. Of Arms*[(c)]	Size R_h (nm)[(e)]
L-PS	3	1.1	N/a	N/a	1	N/a
S-PS-OH	44	1.2	110	1.02	36	6.4
S-PS-N_3	46.3	1.3	109	1.02	36	6.5
S-PS-NH_2[(d)]	44.2	1.5	N/a	N/a	N/a	4.7[(f)]

(a) determined by SEC (THF) using RI detector and calibrated against linear poly(styrene) standards (b) determined by SEC (THF) using MALS detection (dn/dc 0.187). (c) calculated using linear arm M_w and absolute star M_w from MALS detection (d) determined by SEC (DMF) using RI detector (e) determined by DLS in THF (f) determined by DLS in DMF.

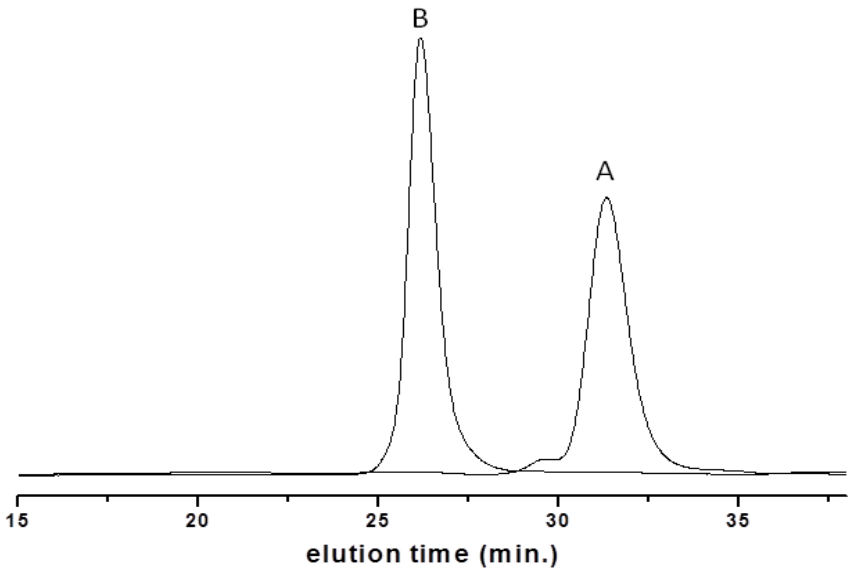

Figure 5.2: SEC traces of linear poly(styrene) arm, M_w = 3 kDa (A) and star poly(styrene)-OH, M_w = 44 kDa (B).

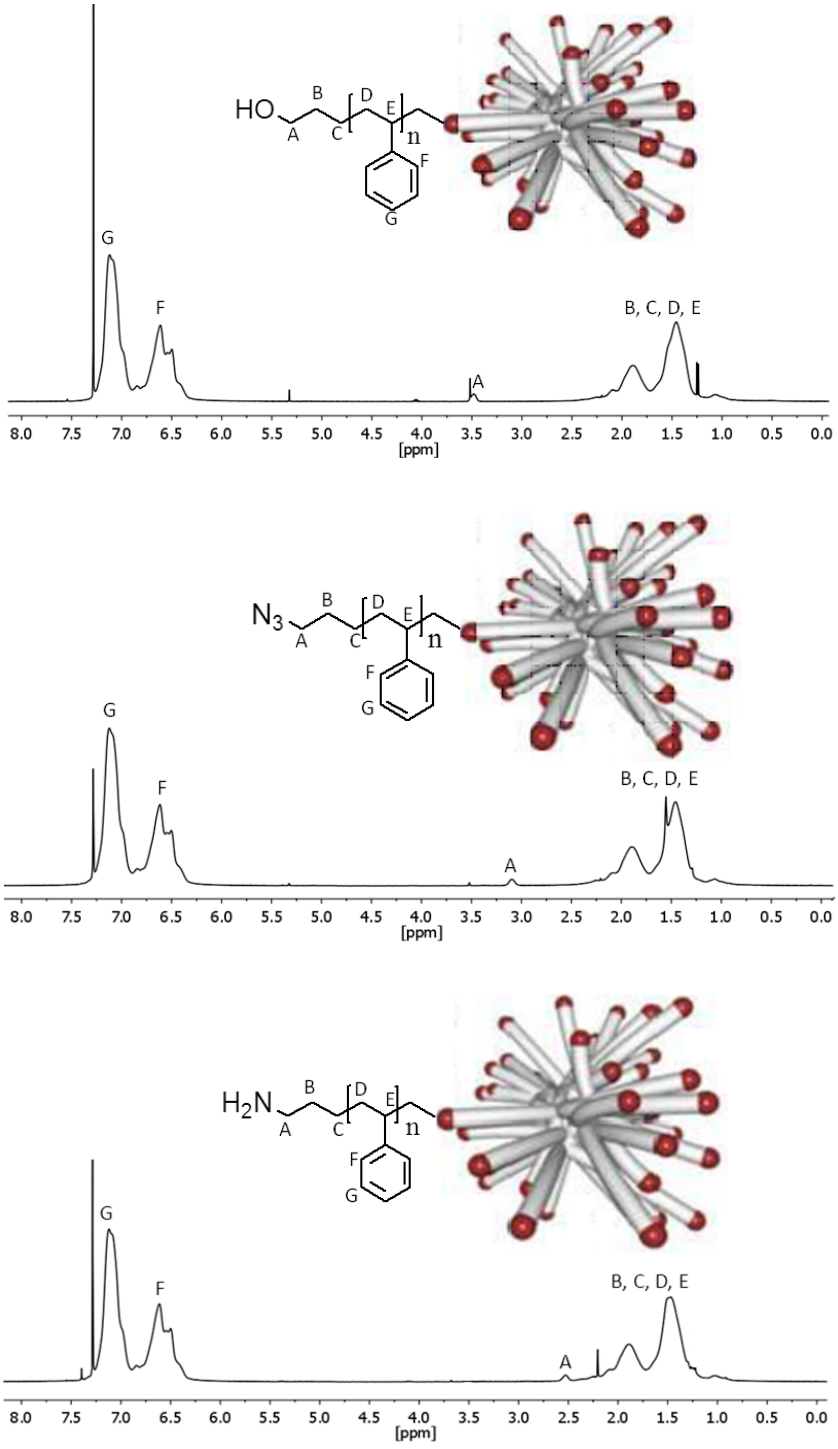

Figure 5.3: ^{1}H NMR spectrum spectrum of star PS-OH (top), PS-N_3 (middle) and PS-NH_2 (bottom) ($CDCl_3$).

Polypeptide conjugation to the polystyrene nanogel star polymers was performed using a "core first" approach i.e. ROP of NCAs initiated by terminal primary amino groups on the arms of the nanogel star polymers **(Figure 5.4)**. Two different NCAs were employed; benzyl-L-glutamate (BLG) and carbobenzyloxy-L-lysine (ZLL) i.e. protected versions of glutamic acid and

lysine respectively to afford nanogel star polymers of a core shell type architecture boasting a polystyrene core and a polypeptide periphery **(Table 5.2)**. Removal of the amino acid side chain protecting groups presents nanogel star polymers with carboxylic acid and primary amine functionalities and therefore anionic and cationic type star polymers. Polypeptide conjugation involved the targeting of 30 units of amino acid per arm or per amino group on the nanogel star polymers resulting in targeting approximately 1080 units overall. The successful growth of polypeptide chains from the star polymers was confirmed by ^{1}H NMR, SEC and FTIR sprectroscopy . Conjugation of both BLG and ZLL was determined by ^{1}H NMR spectroscopy to be approximately half of the targeted number of units (BLG = 57% and ZLL = 45%) irrespective of the reaction time **(Table 5.2)**. One explanation for this could be due to the high density of growing polymeric arms within a size confined space. As the polypeptide arms become longer the complex and dense nature of the polypeptide shell inhibits accessibility of the polypeptide amino end group towards unreacted NCA monomer, therefore preventing further growth. Consequently, a drawback of these multifunctional nanogel star polymers for NCA ROP may be their limited accessibility for polypeptide conjugation. Although difficult to confirm for S-PS-b-PBLG due to overlapping peaks **(Figure 5.5)**, ^{1}H NMR spectroscopy of S-PS-b-PZLL **(Figure 5.6)** confirmed initiation of NCA ROP by all amino terminated polystyrene arms (peak at 2.5 ppm corresponding to **CH_2**-NH_2) resulting in 36 polypeptide arms albeit no knowledge on the extent of growth or length of each arm.

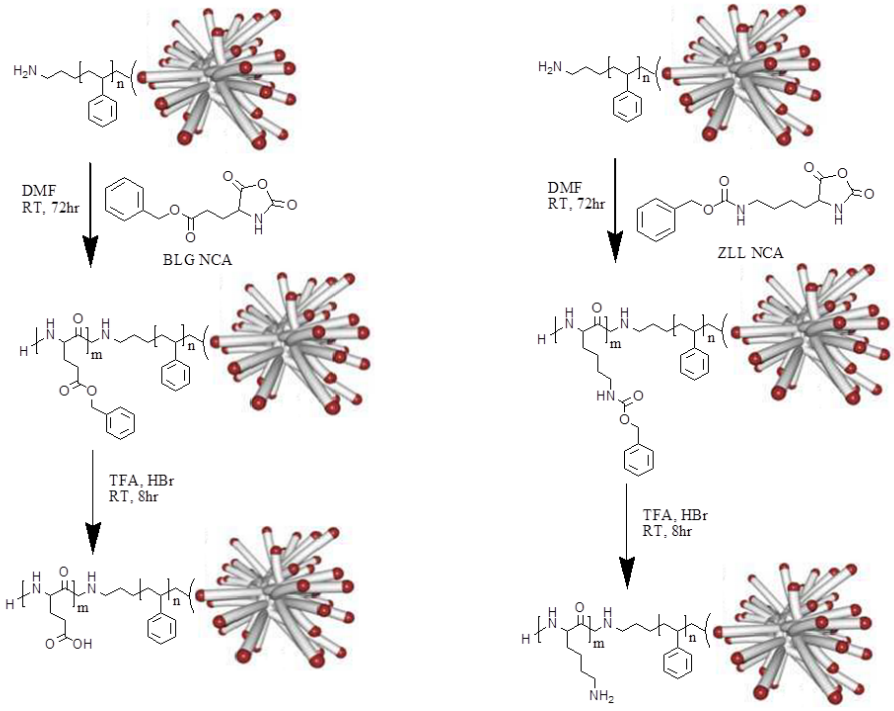

Figure 5.4: The "core-first" use of poly(styrene) nanogel star polymers for the synthesis of PGA and PLL grafted nanogel stars.

Table 5.2: Polypeptide functionalized poly(styrene) nanogel star polymers (S: Star).

Polymer[(a)]	M_n (kDa)[(b)]	PDI	M_n PBLG/PZLL (kDa)[(c)]	Theoretical M_n[(d)] (kDa)	Size R_h (nm)[(e)]
	SEC		**NMR**		
S-PS-NH_2	44.0	1.5	N/a	N/a	4.7
S-PS-b-$PBLG_{30}$	147.6	1.5	134	235	8.3
S-PS-b-$PZLL_{30}$	193.7	1.5	128	283	9.5
S-PS-b-PGA_{30}	N/a	N/a	78.7	138	6.5[(f)]

(a) The subscript number denotes the targeted number of polypeptide units per –NH_2 of star poly(styrene) (assuming number of –NH_2 groups is 36) (b) determined by SEC (DMF) using RI detector and calibrated against linear poly(styrene) standards (c) determined by ^{1}H NMR spectroscopy using integral ratio of CH of polypeptide and CH_2 peaks of PS (d) calculated assuming initiation from all amino groups and quantitative conversion: c(monomer)/c(star poly(styrene)) x M(monomer) (e) determined by DLS in DMF (f) determined by DLS in H_2O.

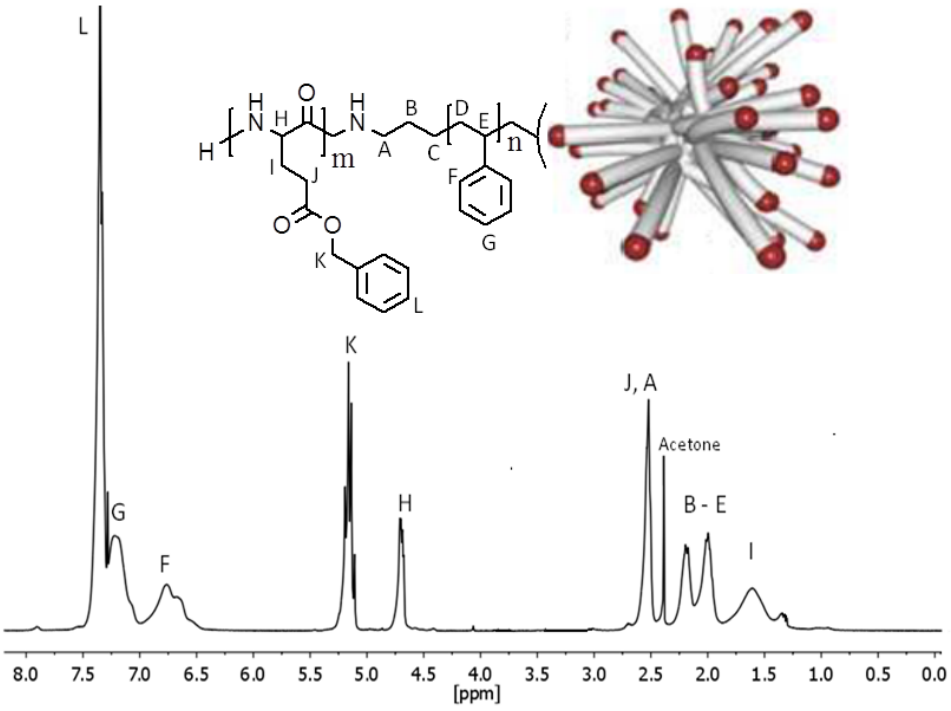

Figure 5.5: ^{1}H NMR spectrum of star PS-b-$PBLG_{30}$ ($CDCl_3$).

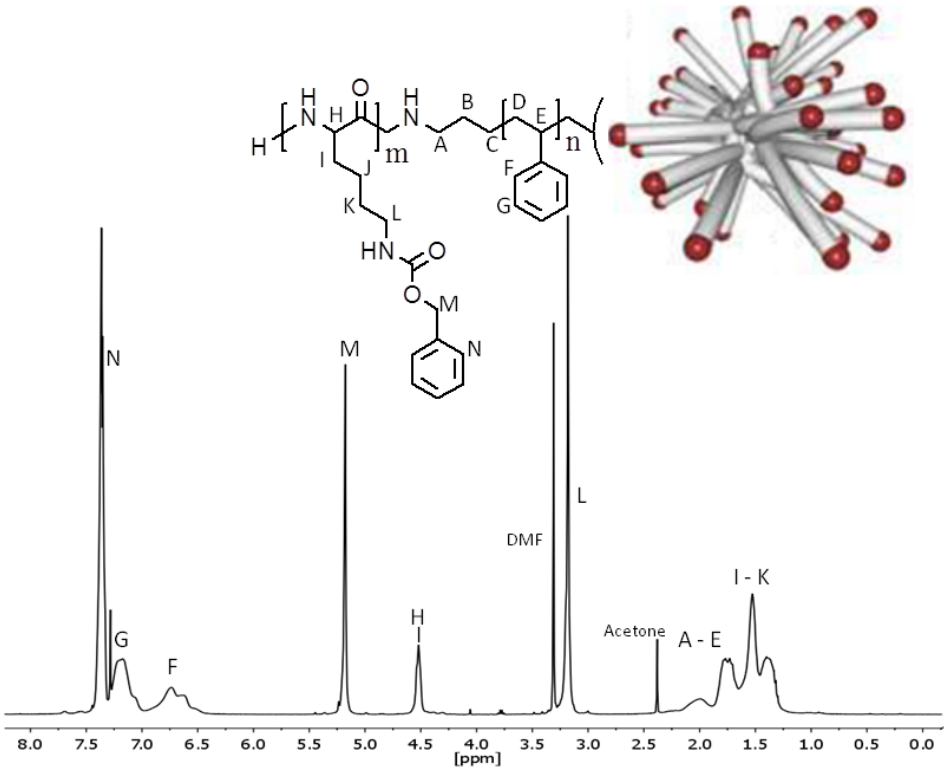

Figure 5.6: ^{1}H NMR spectrum of star PS-b-PZLL$_{30}$ ($CDCl_3$).

SEC further confirmed polypeptide conjugation owing to the clear shift in retention time of the polypeptide functionalized nanogel star polymers to a higher molecular weight **(Figure 5.7)**. As determined by DLS, the size, R_h of the star polymers increased after polypeptide conjugation. In DMF, S-PS-b-PBLG and S-PS-b-PZLL displayed an R_h of 8.3nm and 9.5nm respectively compared to 4.7 nm of the S-PS-NH_2 starting material. FTIR sprectroscopy identified the presence of polypeptide and the adoption of a α-helical conformation denoted by the strong amide I and II peaks at approx. 1650 cm^{-1} and 1530 cm^{-1} which are typical of an α-helical conformation **(Figure 5.8 and 5.9)**.[76]

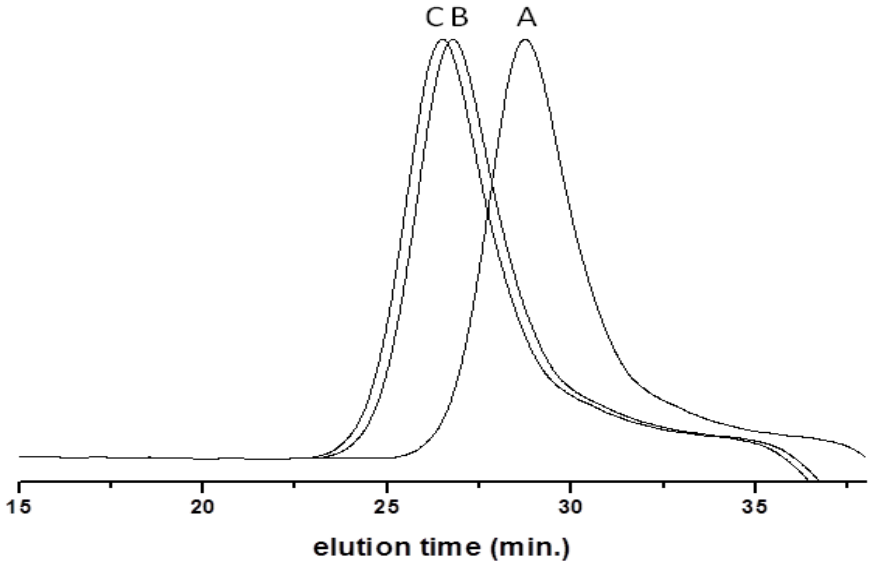

Figure 5.7: SEC traces of star poly(styrene)-NH_2 (A), star PS-b-$PBLG_{30}$ (B) and star PS-b-$PZLL_{30}$ (C).

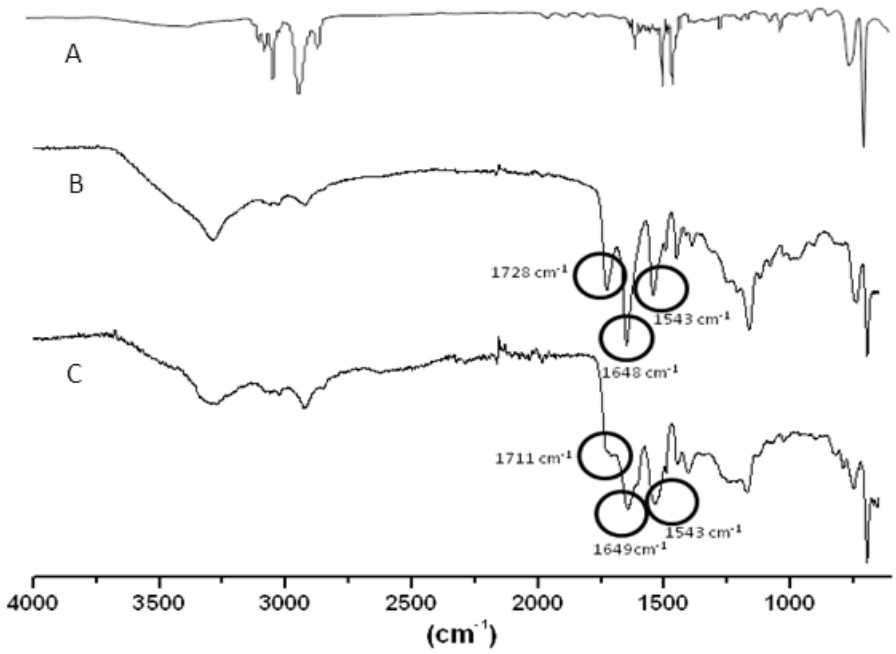

Figure 5.8: FTIR spectra of S-PS-NH_2 (A), S-PS-b-$PBLG_{30}$ (B) and S-PS-b-PGA_{30} (C).

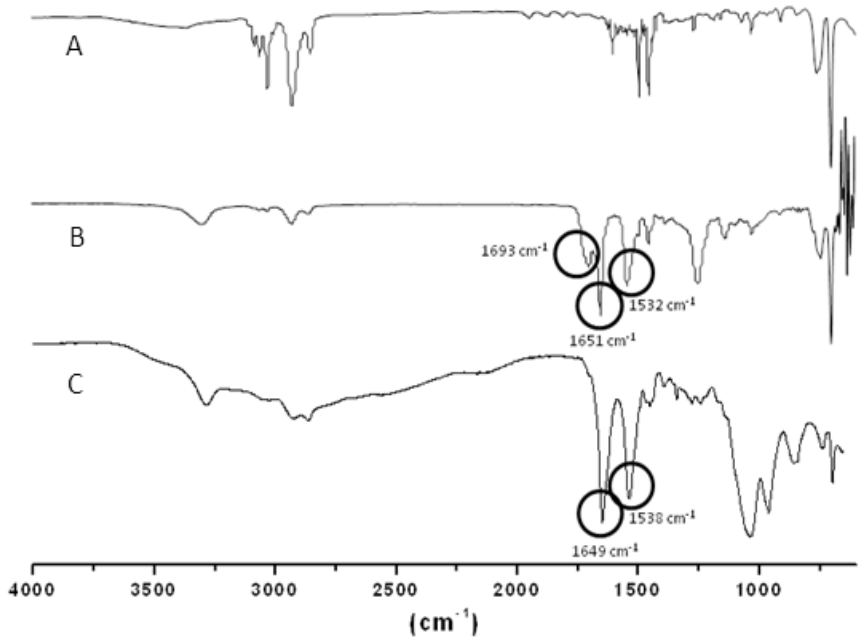

Figure 5.9: FTIR spectra of S-PS-NH_2 (A), S-PS-b-$PZLL_{30}$ (B) and S-PS-b-PLL_{30} (C).

Deprotection of the amino acid side chain protecting groups was performed using standard HBr/AcOH conditions to afford nanogel star polymers with carboxylic acid and amine functionalized polypeptide peripheries. Deprotection of the polypeptide functionalised nanogel star polymers was confirmed by solid state FTIR sprectroscopy by the disappearance of the carbonyl peak of the benzyl ester protecting group at 1728 cm^{-1} **(Figure 5.8)**. An α-helical conformation was retained by the deprotected poly(glutamic acid) (PGA). Similarly S-PS-b-PZLL was successfully deprotected using the aforementioned acid hydrolysis method with FTIR sprectroscopy confirming the successful deprotection and the retention of an α-helical secondary structure **(Figure 5.9)**. Quantitative deprotection and analysis of the deprotected star polymers by ^1H NMR spectroscopy was unsuccessful due to solubility issues associated with these star polymers. Although polypeptides of both an anionic and cationic character were successfully anchored to the polystyrene star polymer platform sufficient solubilization in ideally water was not achievable. Furthermore the use of a range of polar and non-polar solvents such as DMSO, DMF, THF, $CHCl_3$, DCM, acids, bases and solvent mixtures were not successful in solubilising the material. A possible explanation for this could be due to the amphiphilic nature (large hydrophobic polystyrene core and dense hydrophilic polypeptide shell) of such a material in addition to its complex architecture and large molecular weight. By anchoring more polypeptide to the polystyrene core it may be possible to induce more hydrophilicity to the overall molecule and therefore enable better water solubilzation in particular. However as described above the complex architecture of the polystyrene star

polymers limits the capacity of polypeptide conjugation. By utilising the functional amino acid side chains it may be possible to introduce water soluble moieties to these star polymers therefore improving their overall water solubility. Suitable candidates may include coupling polyethylene glycol or sugars through suitable traditional coupling chemistry.[77,78] Sugars in particular would also introduce an interesting biorecogniton property to the star polymers. The interaction of sugars with lectins and particularly their interaction with glycoconjugated polymers is an intensively researched field with significant implications for drug delivery research.[79,80]

Overall the expansion of the polystyrene nanoparticle platform developed by Sly et al. to include alternative compositions was realised. To impart enhanced biocompatibility and degradability, polypeptides were chosen as a suitable alternative owing to their natural composition and versatile functionalities. Post modification of hydroxyl terminated polystyrene star polymers towards primary amines was achieved thus permitting their potential utilisation as multifunctional initiators towards the controlled synthesis of polypeptides by ROP of NCAs. The conjugation of polypeptides to the star polymer periphery to form core/shell type architectures boasting a hydrophobic core and polypeptide shell was successfully performed. Although polypeptide conjugation capacity was limited, it was possible to create protected poly(glutamic aid) and poly(lysine) decorated nanogel star polymers as confirmed by ^{1}H NMR, SEC and FTIR spectrsocopy. In this branched form the polypeptides adopted strong α-helical conformations. Protecting group removal yielded carboxylic acid and amine decorated nanogel star polymers hybrids as confirmed by FTIR spectroscopy. However solubilzation of the described hybrid materials was difficult potentially owing to the complex architecture and amphiphilic nature of such materials. The targeting of these materials towards biomedical applications such as drug delivery and imaging requires sufficient water solubility meaning they are not currently suitable for the described applications. Further modification to impart water solubility may improve the prospects of these materials for biomedical applications. The initial steps taken here towards the creation of hybrid nanogel star polymers may lead to the future development of more diverse compositions and architectures with increased complexity and “intelligence”.

5.2.2 Polyester Core (Degradable) / Polymethacrylate Periphery (Nondegradable)

Nanogel star polymers of biodegradable or biocompatible compositions are an attractive class of new materials owing to their inherent applicability towards the biomedical field. The polystyrene based nanogel platforms developed by Sly et al. although synthetically and structurally versatile, their nondegradable nature and lack of biocompatibility restricts their potential towards biomedical applications.[29] Despite efforts to impart biocompatible features such as polypeptide conjugation the nanogel star polymer composition is still dominated by the large hydrophobic polystyrene core (see above). To overcome this, Sly et al. have developed a facile route towards polyester based nanogel star polymers which should exhibit improved biodegradability due to the inherent properties of polyesters **(Figure 5.10)**.[59,81] Expansion of this degradable platform through the introduction of new functionalities and polymers with biomedical relevance will extend the potential scope and implications of these materials.

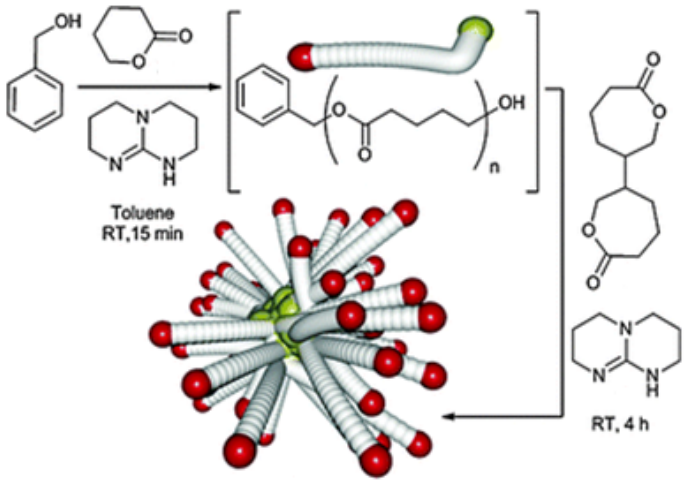

Figure 5.10: Synthesis of poly(ester) based nanogel star polymers via organocatalytic ring opening polymerization (OROP).[59]

Layer by layer (LBL) technology towards controlled drug release and wound care is one such application in which these materials may play a significant role. LBL technology involves the deposition of multiple layers of organic and inorganic compounds onto a surface or substrate typically through electrostatic interactions **(Figure 5.11)**. The beauty of this system is the control and versatility offered by such a technique in which the surface properties such as functionality, wettability, charge, hydrophobicity, adhesion, morphology and loading capacity may be configured by employing different polymer types and controlling the layer thickness.[82] This technology has been applied to a range of applications including advanced drug delivery

technology.[83,84] Concerning the polyester based nanogel star polymers described here, employment of the hydrophobic polyester core for drug entrapment and the subsequent formation of multiple layers it may be plausible to exhibit the controlled release of drugs in addition to providing a biocompatible wound dressing. The hydrolytic susceptibility of polyesters imparts degradability upon this system and by controlling the layer thickness it may be possible to control the drug dose and the drug release time frame i.e. thicker layer means higher overall drug dose and prolonged release time. Furthermore it may be possible to introduce more than one drug or more than one type of cargo into this system which could be released at different stages of the wound healing process by controlling the positioning of cargoes within the different layers. Consequently such a technology provides numerous advantages: physical protection of the wound, initial controlled drug release over a designated time frame, the subsequent controlled release of other functional cargoes such as an additive to reduce scarring therefore resulting in more efficient patient treatment and less stress on hospital resources.

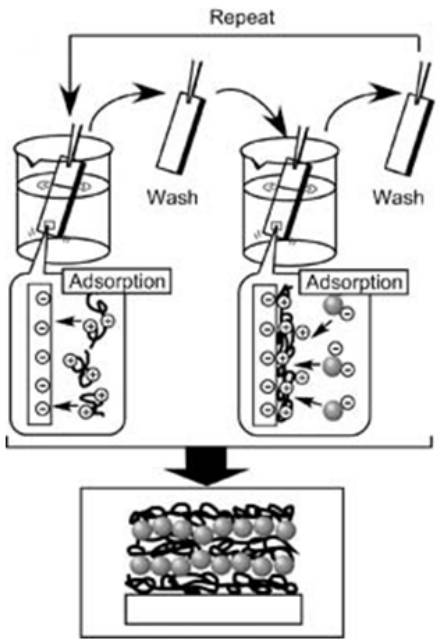

Figure 5.11: Electrostatic interactions for the construction of layer by layer assemblies.[82]

To realise such an objective, the current polyester based material requires further modification to enable layer by layer deposition through electrostatic interactions. To overcome this challenge the introduction of anionic and cationic based polymers to this system is essential. To achieve this, the controlled polymerization technique of RAFT was employed. RAFT was

chosen as is has demonstrated its ability to generate a range of well defined polymers whilst in comparison to techniques such as ATRP it does not require the use of metal catalysts which can prove difficult to remove and therefore impact on the biocompatibility of such polymers.[85-87] In order to combine both OROP of cyclic esters for star formation and RAFT polymerization for functional polymeric arms synthesis, the two typical approaches to nanogel star polymer synthesis were considered: "arm first" and "core first". The "arm first" methodology was employed due to the greater synthetic control offered. Consequently the design of a new dual purpose RAFT chain transfer agent was required to permit synthesis of the desired polymers whilst also possessing a hydroxyl end group functionality to enable OROP of a cyclic ester crosslinker to generate nanogel star polymers.

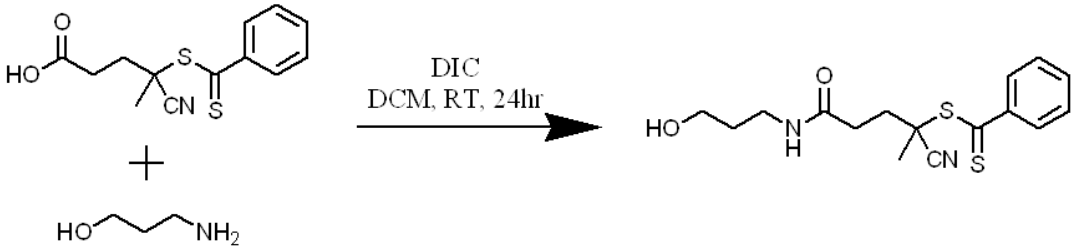

Figure 5.12: Synthesis of hydroxyl functionalized RAFT agent: 2-cyano-5-(3-hydroxypropyl amino)-5-oxopentanoic-2-yl benzodithioate.

The RAFT agent 2-cyano-5-(3-hydroxypropyl amino)-5-oxopentanoic-2-yl benzodithioate was synthesized for the first time by employing diisopropylcarbodiimide (DIC) mediated coupling chemistry of the commercially available 4-Cyano-4-(phenylcarbonothioylthio)pentanoic acid and 3-amino-1-propanol **(Figure 5.12)**. The carboxylic acid functionality of 4-cyano-4-(phenylcarbonothioylthio)pentanoic acid provided a very useful reactive handle for simple hydroxyl group modification using the dual functional 3-amino-1-propanol whilst this dithiobenzoate type RAFT agent is known to be compatible towards a wide range of monomers including methacrylates.[86] The ability of primary amines to cleave the ω-end group of RAFT agents through aminolysis has been well documented so the potential of 3-amino-1-propanol to cleave the ω-end group is a strong possibility.[88] To minimize this, the reaction was carried out initially at 0^{o}C with the slow addition of a very small excess of amino alcohol to the activated carboxylic acid RAFT agent solution. Although some aminolysis may be unavoidable, the targeted RAFT agent was obtained in reasonable yield i.e. 50% using column chromatography with ^{1}H and ^{13}C NMR spectroscopy confirming its successful synthesis **(Figures 5.13 and 5.14)**.

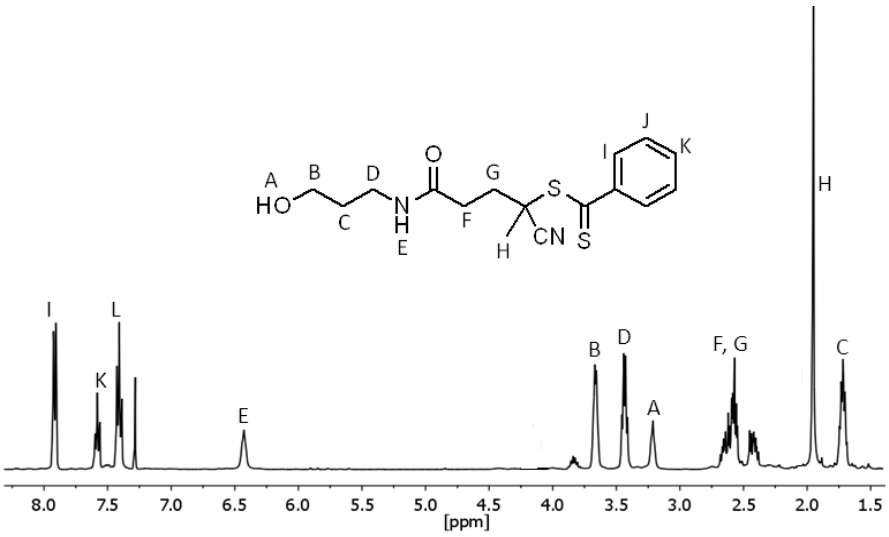

Figure 5.13: ^{1}H NMR spectrum of 2-cyano-5-(3-hydroxypropyl amino)-5-oxopentanoic-2-yl benzodithioate ($CDCl_3$).

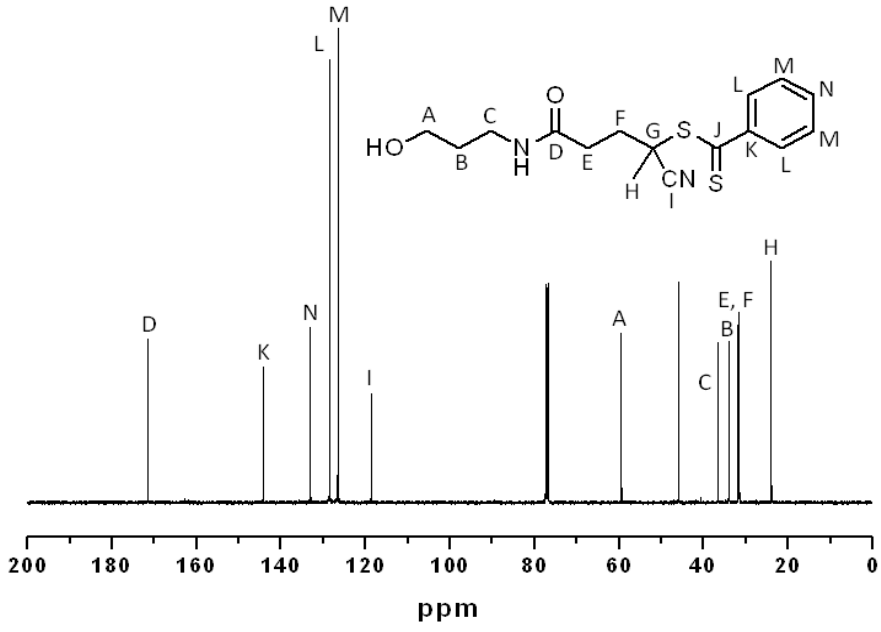

Figure 5.14: ^{13}C NMR spectrum of 2-cyano-5-(3-hydroxypropyl amino)-5-oxopentanoic-2-yl benzodithioate ($CDCl_3$) (J - >200 ppm).

The identification of suitable anionic and cationic type monomers capable of polymerization with the synthesized RAFT agent was very important. This dithiobenzoate type RAFT agent is known to be very compatible towards methacrylate monomers and given the wide range of methacrylate based monomers available the pursuit of anionic and cationic methacrylate based polymers was the logical choice. The monomers 2-(trimethylsilyl)ethyl methacrylate

(TMSEM) and dimethylaminoethyl methacrylate (DMAEMA) were chosen to introduce anionic and cationic properties respectively. Homopolymers of DMAEMA have been shown to exhibit low toxicity whilst TMSEM provides a latent carboxylic acid functionality which can be revealed upon post polymerization and subsequent star formation.[89] The polymerization of DMAEMA towards the generation of cationic nanogel star polymers is depicted in **Figure 5.15** with results summarized in **Table 5.3.**

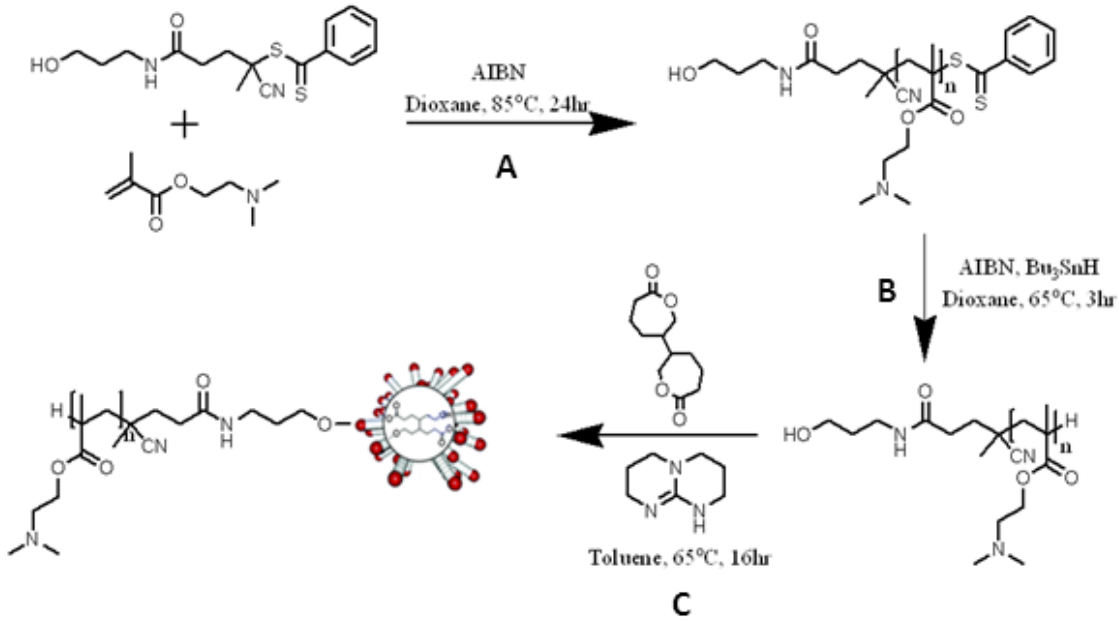

Figure 5.15: Synthesis of linear poly(DMAEMA) via RAFT polymerization (A), removal of ω-RAFT end group to form the corresponding hydrocarbon (B) and the subsequent formation of poly(DMAEMA) functionalized nanogel star polymers via organocatalytic ring opening polymerization of cyclic esters (C).

Table 5.3: Linear (L) and star (S) DMAEMA nanogel star polymers with polyester core.

Polymer	M_n (kDa)[(a)]	PDI	M_n (kDa)[(b)]	Target M_n (kDa)	Size R_h (nm)[(c)]	DMAEMA:BOP[(d)]
L-DMAEMA-RAFT	4.5	1.1	5.2	5.0	N/a	N/a
L-DMAEMA-H	4.5	1.1	5.9	5.0	N/a	N/a
L-DMAEMA-b-PVL	9.0	1.2	9.5	10.2	N/a	N/a
S-DMAEMA-H	144.3	1.2	N/a	N/a	40	11.25[(e)]
S-DMAEMA-H	74.3	1.2	N/a	N/a	22	8.1[(f)]
S-DMAEMA-H	37.6	1.2	N/a	N/a	11	4.6[(g)]

(a) determined by SEC (THF) using RI detector and calibrated against linear PMMA standards (b) determined by ^{1}H NMR spectroscopy using the integral ratios of poly(DMAEMA) and RAFT CTA moieties (c) determined by DLS in THF (d) Molar ratio of DMAEMA to 5-5'-Bis(oxepanyl-2-one) BOP crosslinker (e) Reaction time of 24 h (f) Reaction time of 16 h (g) Reaction time of 4 h.

Initially the polymerization of DMAEMA was carried out in dioxane using AIBN as a radical source. Excellent molecular weight control was observed generating a DMAEMA homopolymer with narrow PDI **(Table 5.3 – L-DMAEMA-RAFT)**. ^{1}H NMR spectroscopy was further used to elucidate molecular weight but also confirmed the presence of both the hydroxyl (peaks A and C) and dithiobenzoate (peaks L, M and N) end groups at α and ω positions of the polymer respectively **(Figure 5.16)**. To avoid possible interference from the dithiobenzoate ω end group in later synthetic steps, the dithiobenzoate group was cleaved to form the corresponding hydrocarbon. End group removal and modification of RAFT derived polymers has been extensively investigated but for the purpose of this work the identification of a simple cleavage method for generation of the corresponding hydrocarbon was of vital importance. The use of tributyltin hydride in conjunction with AIBN is a well known method to remove the RAFT ω-end group and form the corresponding hydrocarbon.[90] This method was successfully employed to

generate hydrogen at the ω end group position with no notable changes in molecular weight properties in addition to retention of the hydroxyl end group **(Table 5.3 – L-DMAEMA-H)**. Removal of the dithiobenzoate was confirmed by ^{1}H NMR spectroscopy due to the disappearance of the aromatic signals at 7.4 – 8 ppm (L, M and N) and retention of peaks A and C at 3.6 and 3.4 ppm respectively **(Figure 5.17)**.

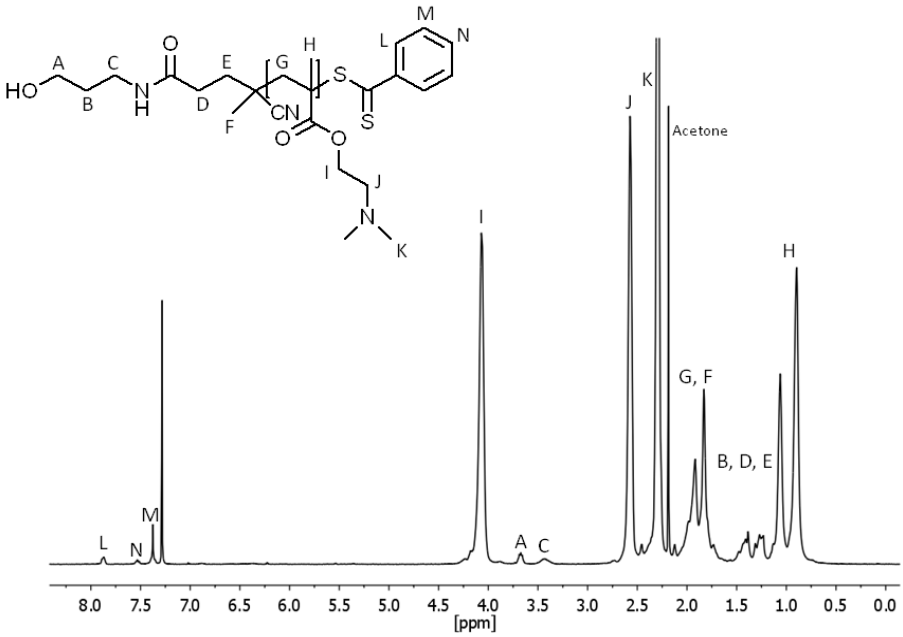

Figure 5.16: ^{1}H NMR spectrum of L-DMAEMA-RAFT ($CDCl_3$).

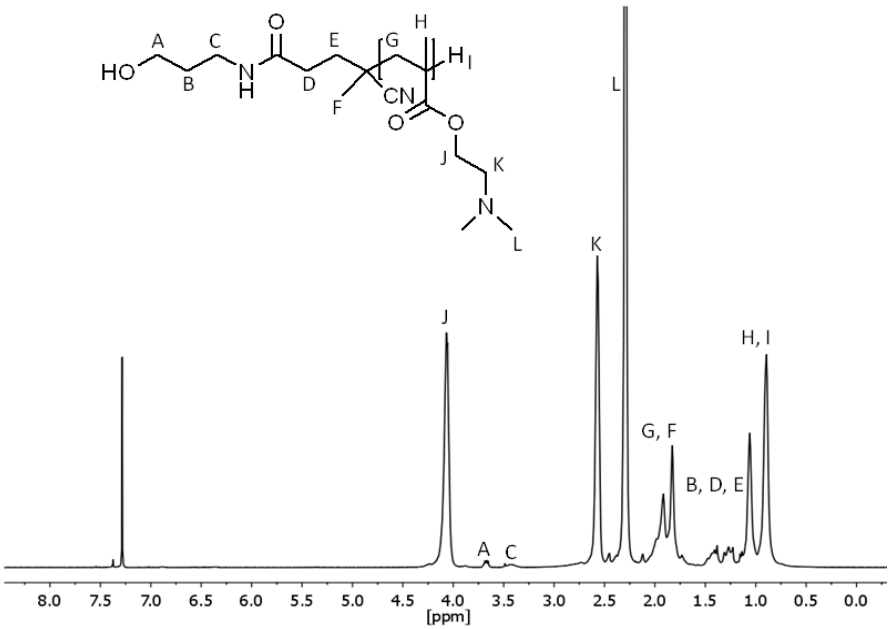

Figure 5.17: ^{1}H NMR spectrum of L-DMAEMA-H ($CDCl_3$).

To test the initial feasibility of the hydroxyl terminated DMAEMA polymer for OROP of cyclic esters, L-DMAEMA-H was employed in the OROP of δ-Valerolactone to form a linear block copolymer using the catalyst 1,5,7-Triazabicyclo[4.4.0]dec-5-ene TBD **(Figure 5.18)**. Employing a similar methodology to the original developed by Sly et al, resulted in the sluggish chain extension of L-DMAEMA-H with poly(valerolactone) (PVL).[59] Although the hydroxyl initiator should readily participate in the reaction, the fact that it is in the form of a large macroinitiator means the reaction rate may be very sluggish. Elevating the temperature to 40°C and a 2 h reaction time resulted in a much more efficient reaction rate in which 88% of valerolactone was converted to its polymeric form as determined by ^{1}H NMR spectroscopy **(Figure 5.19)**. ^{1}H NMR spectroscopy confirmed the presence of polyester denoted by the appearance of new characteristic peaks at 4.07, 2.33 and 1.67 ppm. As noted by Sly et al reaction time is a vital parameter of this methodology as a prolonged reaction time may well result in increased conversion rates but this can be offset by the broadening of PDI due to the TBD catalyst.[59] Furthermore SEC analysis showed the clear shift in retention time of L-DMAEMA-H (M_n 4.5kDa) to a shorter retention time and thus higher molecular weight for L-DMAEMA-b-PVL (M_n 9.0kDa) **(Figure 5.20 and Table 5.3)**. Consequently, the feasibility of this hydroxyl terminated DMAEMA homopolymer as an effective initiator in the controlled OROP of cyclic esters was confirmed.

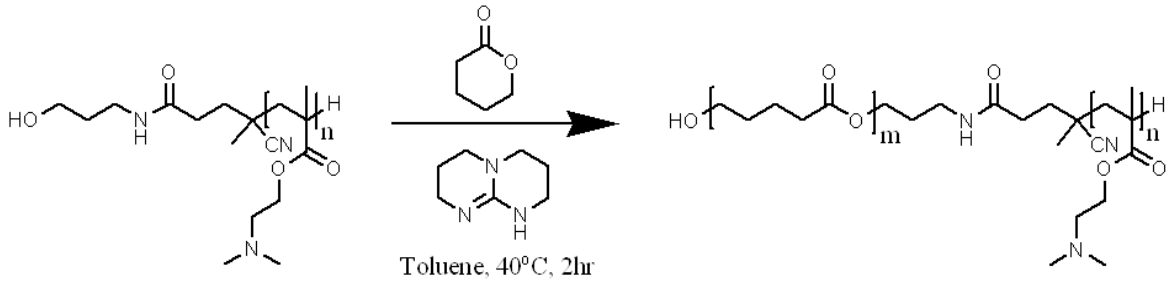

Figure 5.18: OROP of δ-valerolactone with hydroxyl terminated linear poly(DMAEMA).

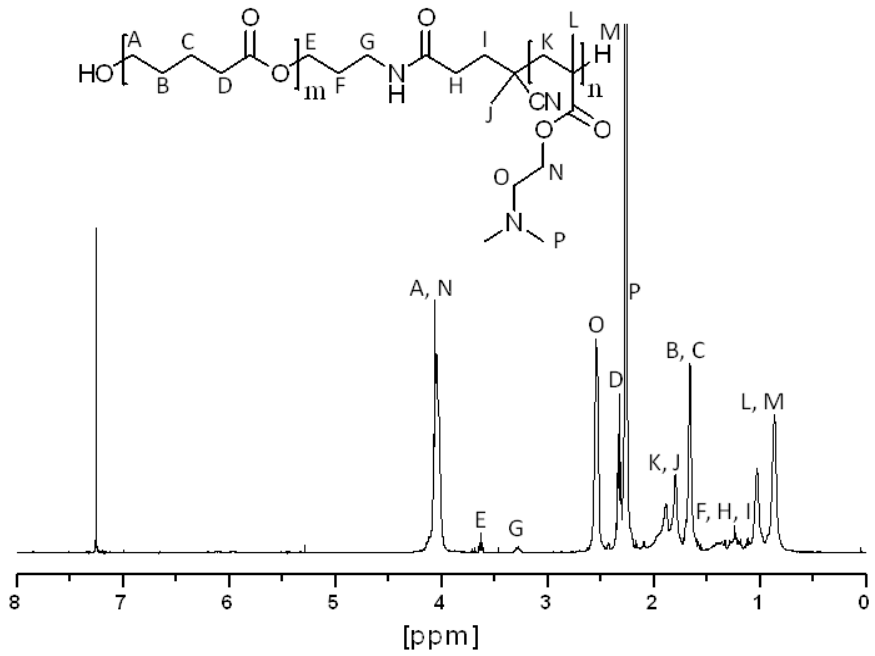

Figure 5.19: ^{1}H NMR spectrum of L-DMAEMA-b-PVL ($CDCl_3$).

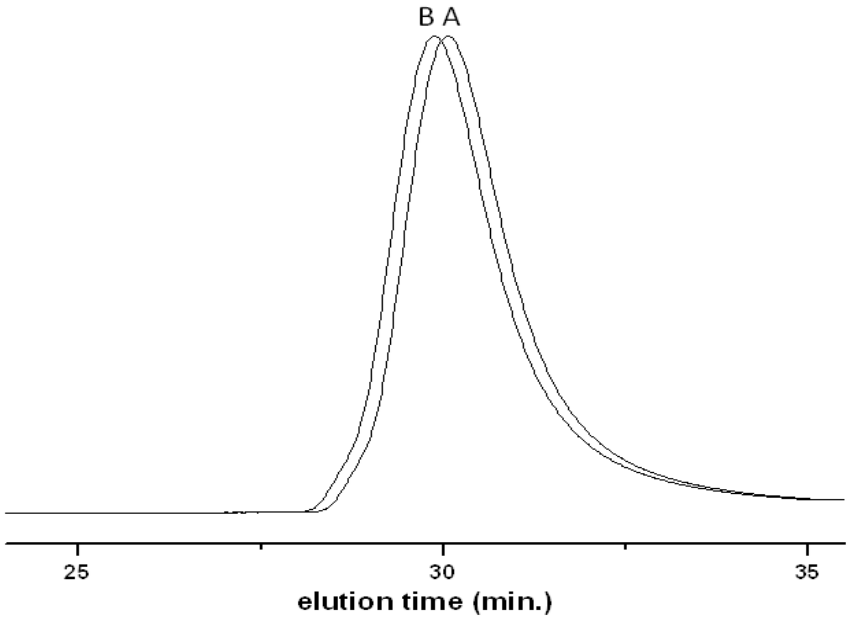

Figure 5.20: SEC Traces of L-DMAEMA-H (A) and L-DMAEMA-b-PVL (B).

Expanding this methodology to include nanogel star polymers with a cationic periphery, L-DMAEMA-H was once again employed for OROP of the cyclic ester crosslinker 5,5'-Bis(oxepanyl-2-one) (BOP). Employing a similar methodology to the above linear analogue resulted in the unsuccessful synthesis of nanogel star polymers. Again this may be accounted

for by the large macroinitiator present but also the cyclic ester used here may not be quite as reactive as valerolactone due to increased stability of its 7-membered ring structure and whilst it also suffers from low solubility in toluene. However, subjecting the reaction to a temperature of 70^{o}C resulted in the successful synthesis of these stars. The reaction end time was denoted by the formation of a clear solution due to the complete dissolution and reaction of BOP. ^{1}H NMR spectroscopy analysis identified the L-DMAEMA-H arms but the presence of polyester could not be confirmed due to its low concentration within overall nanogel star polymer. As a result the number of arms or arm density could not be ascertained. Furthermore the polyester composition constituted the core of the star polymer meaning it may be somewhat shielded by the peripheral L-DMAEMA-H arms and therefore harder to detect. In addition, FTIR spectroscopy could not detect the presence of the ester core due to the already strong presence of ester functionality arising from the methacrylate arms. Therefore to confirm the formation of nanogel star polymers, SEC was utilised which showed the clear shift in retention time of L-DMAEMA-H to a shorter time retention for S-DMAEMA-H highlighting the increase in molecular weight due to the formation of nanogel star polymers **(Figure 5.21)**. The presence of residual unreacted arms was observed, a feature commonly observed in nanogel star polymer synthesis. The purification or removal of these arms was performed using fractionation i.e. the slow precipitation of the crude material into hexane until the higher molecular weight star polymer precipitates first whereas the lower molecular weight arms remain in solution. By varying the crosslinker to macroinitiator ratio i.e. BOP : L-DMAEMA-H it was possible to control the M_n and size of the star polymers highlighting the excellent synthetic and structural control afforded here. Furthermore, it was noted that a low BOP concentration resulted in a shorter reaction time. All star polymers exhibited narrow PDIs (<1.2) with sizes ranging from 11 nm to 40 nm as determined by DLS. A SEC comparison of all three S-DMAEMA-H nanogel polymers shows the shift in retention time to a shorter retention time as M_n increases thus providing a very useful tool to monitor the star polymer growth in real time **(Figure 5.22)**.

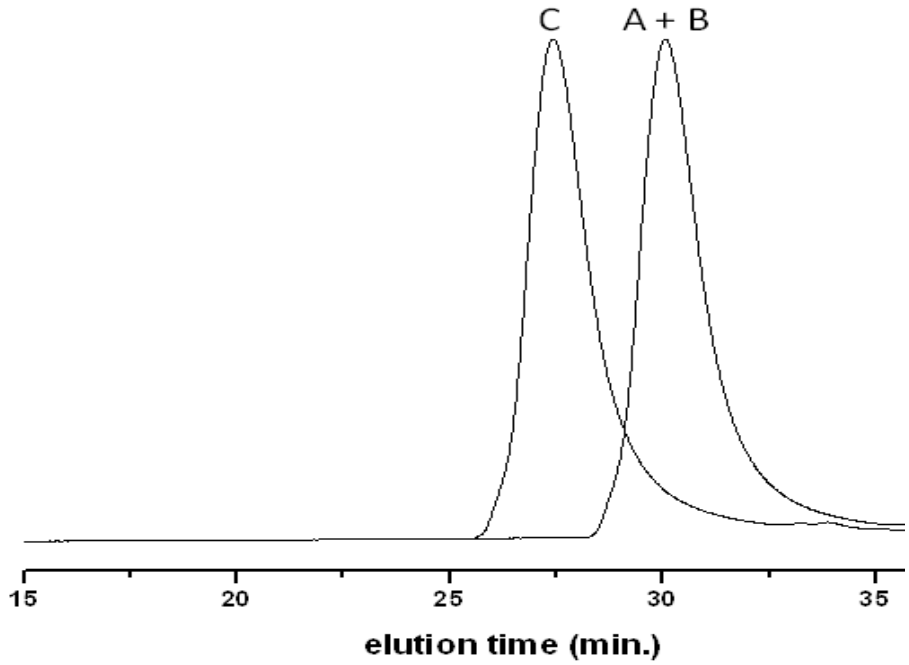

Figure 5.21: SEC Traces of L-DMAEMA-RAFT (A), L-DMAEMA-H (B) and S-DMAEMA-H (C).

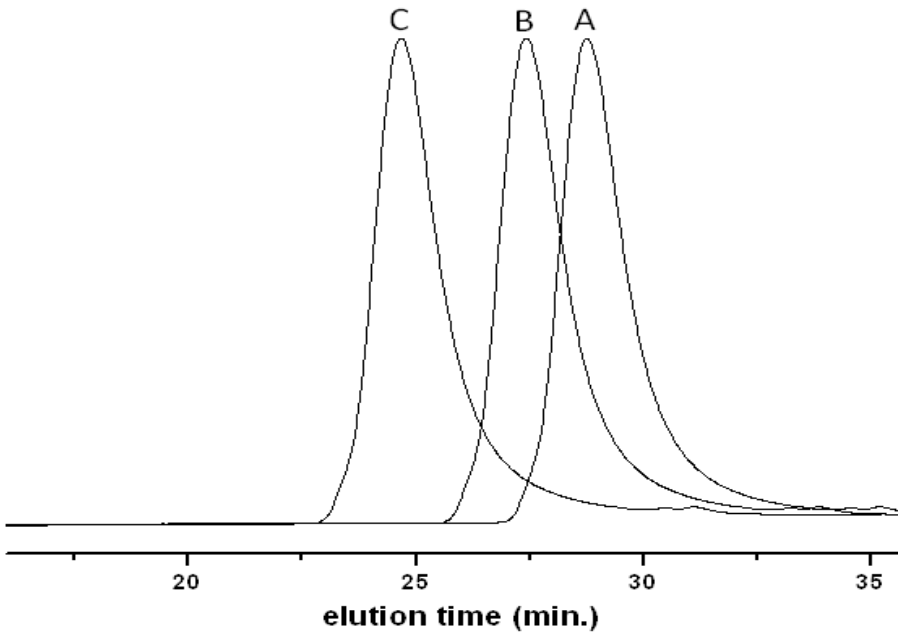

Figure 5.22: SEC Traces of S-DMAEMA-H-11 nm (A), S-DMAEMA-H-22 nm (B) and S-DMAEMA-H-40 nm (C) The size i.e. R_h for each nanogel star polymer was determined by DLS.

The synthesis of an anionic type nanogel star polymer was conducted in a similar fashion to the above cationic nanogel star polymer. The protection of the carboxylic acid functionality was necessary to prevent interference with the RAFT polymerization process and later the star polymer formation process. The choice of protecting group was also important as the use of typical methacrylic acid protecting groups such as tert-butyl and benzyl require deprotection conditions, which are not compatible with the hydrolytically unstable polyester core. Therefore the trimethylsilyl ethyl protecting group was used as it should permit efficient deprotection without the requirement for chemically harsh conditions. A summary of the synthetic steps employed towards the generation anionic nanogel star polymers can be seen in **Figure 5.23.**

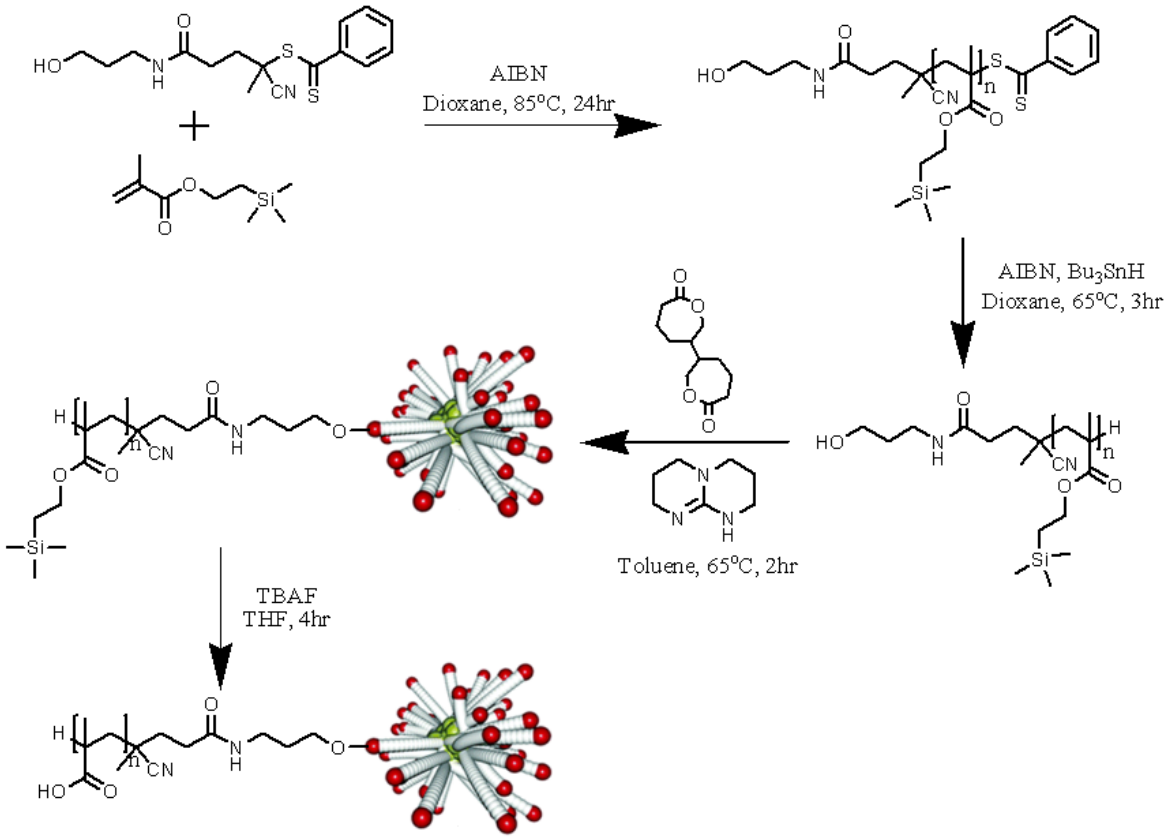

Figure 5.23: Synthesis of linear poly(TMSEM) via RAFT polymerization (A), removal of ω-RAFT end group to form the corresponding hydrocarbon (B) the formation of poly(TMSEM) functionalized nanogel star polymers via organocatalytic ring opening polymerization of cyclic esters (C) and deprotection of trimethylsilyl ethyl protecting group to afford carboxylic acid (anionic) functionalized nanogel star polymers (D).

The hydroxyl functionalised RAFT agent was employed to generate linear poly(TMSEM) (L-TMSEM-RAFT). The polymer generated boasted a M_n in close agreement to the target M_n whilst also exhibiting a narrow PDI **(Table 5.4 – L-TMSEM-RAFT)**. Comparable to DMAEMA derived polymers discussed above, ^{1}H NMR spectroscopy confirmed the M_n of the target polymer and the presence of its protecting groups along with the dithiobenzoate and hydroxyl end groups. The subsequent cleavage of the ω-end group using the reliable AIBN / Bu_3SnH reaction conditions afforded the corresponding hydrocarbon ω-end group with no notable changes in M_n, PDI or modifications to the polymer **(Table 5.4 – L-TMSEM-H)**.

Table 5.4: Linear (L) and star (S) TMSEM nanogel star polymers with polyester core.

Polymer	M_n (kDa)[(a)]	PDI	M_n (kDa)[(b)]	Target M_n	Size R_h (nm)[(c)]	BOP / TMSEM[(d)]
L-TMSEM-RAFT	5.5	1.1	5.6	6.0	N/a	N/a
L- TMSEM-H	5.3	1.1	6.4	6.0	N/a	N/a
S-TMSEM-H	76.0	1.3	N/a	N/a	24	13 [(e)]

(a) determined by SEC (THF) using RI detector and calibrated against linear PMMA standards (b) determined by ^{1}H NMR spectroscopy using the integral ratios of poly(TMSEM) and RAFT CTA moieties (c) determined by DLS in THF (d) Molar ratio of TMSEM to BOP crosslinker (e) Reaction time of 2 h (f)

The synthesis of the star shaped derivatives also required elevated temperatures in order for the reaction to proceed effectively. However in comparison to the DMAEMA stars, it was noted here that not only did the reaction proceeded more quickly but also the presence of unreacted residual L-TMSEM-H arms was not observed by SEC **(Figure 5.25)**. Therefore the reaction proceeded very efficiently and did not require a purification by fractionation step with obvious benefits for time efficiency and yield. ^{1}H NMR spectroscopy and FTIR spectroscopy again provided no evidence for the conjugation of L-TMSEM-H arms to the polyester core due to the absence of any new polyester attributed signals **(Figure 5.24)**. Consequently, the arm number could not be determined. SEC helped confirm nanogel star polymer formation by observing the shift in retention time of the star shaped counterpart to a shorter retention time, an observation indicative of higher molecular weight **(Figure 5.25)**. The star polymer exhibited a narrow PDI of 1.3 and a size, R_h, of 24 nm. In comparison to the DMAEMA stars the

BOP ratio here was greater at a ratio of 13, but for this system a R_h of 24 nm was observed which is surprising given that for DMAEMA a BOP ratio of 11.25 generated a star polymer of 40 nm (R_h). Given the complete consumption of polymeric arms, it can be hypothesized that the TMSEM derived nanogel star polymers have a greater number of arms present and a more compact structure. Furthermore the carboxylic acid TMSEM side chain is protected whereas the DMAEMA tertiary amine side chain is free and so may promote electrostatic repulsion amongst the dense polymeric chains therefore exhibiting a somewhat more enlarged structure. Deprotection of the TMSEM protecting group was attempted using TBAF, a reagent commonly employed to remove this type of protecting group. Upon the attempted deprotection, the polymer precipitated in the DCM solution, a good indication of successful deprotection. However upon filtering and washing the isolated material suffered from solubility issues in both organic and water based solvents rendering ^{1}H NMR spectroscopy analysis unachievable. FTIR spectroscopy (solid state) could also not confirm deprotection of the polymer side chain meaning it therefore cannot be determined if complete deprotection was achieved. What can be confirmed is that after subjection to TBAF the solubility properties of the material were altered drastically. The targeted material was expected to be soluble in water owing to the poly(methacrylic acid) periphery. A possible explanation for these solubility issues could be to the densely branched nature of these materials which may have promoted a crosslinking effect i.e. transesterification of poly(ester) core and interaction with the poly(methacrylic acid) periphery resulting in the formation of a more complex polymeric system. Furthermore, the density i.e. number of poly(methacrylic acid) arms was unknown meaning there may have been insufficient water soluble moieties present to permit overall water solubility. Consequently, this amphiphilic star polymer could not be solubilized in either aqueous or organic solvents. A possible solution to this could be the use of a copolymer such as a low molecular weight PEG acrylate in low concentration to improve the solubility and in particular the water solubility of the final product. Furthermore the presence of PEG may promote greater freedom amongst the polymeric arms and therefore reduce the potential for side chain interactions and crosslinking effects.

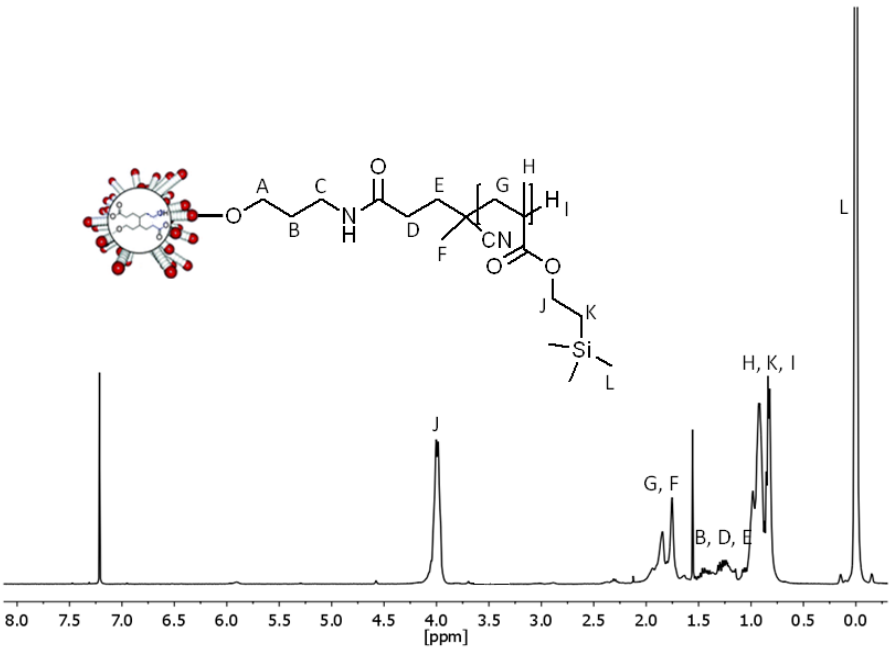

Figure 5.24: ^{1}H NMR spectrum of S-TMSEM-H ($CDCl_3$).

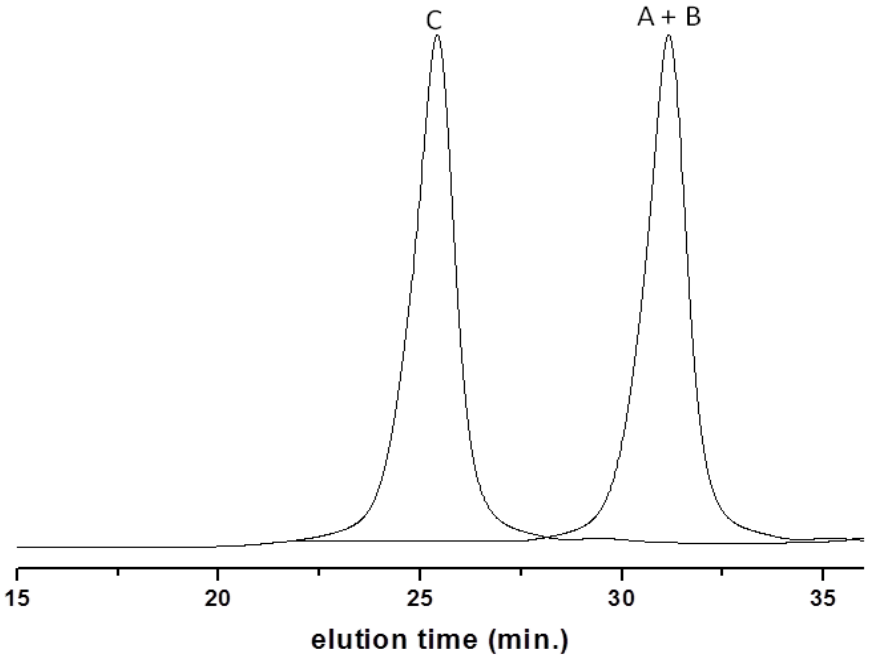

Figure 5.25: SEC Traces of L-TMSEM-RAFT (A), L-TMSEM-H (B) and S-TMSEM-H (C).

The result of this work is the successful expansion of a polyester based nanogel star polymer platform to include new functionalities and the incorporation of biomedically important polymers. The combination of two different polymerization techniques within the one organic nanoparticle platform enabled the highly controlled yet versatile design and production of new nanogel star polymers. This approach boasts great versatility in the types of polymers and functionalities which can be incorporated onto the biodegradable ester core. Furthermore the materials produced display numerous advantages in terms of molecular weight and size control to create a new generation of hybrid nanogel star polymers. Although the targeting of a nanogel star polymer with an anionic periphery requires some minor development work in the future, the potential use of these materials for their targeted goal of layer by layer technology is very achievable. More importantly however is the great potential offered by this early developmental work, to incorporate new polymers of various compositions towards the targeting of numerous biomedical applications such as gene delivery and theranostic applications. The continued development of these novel hybrid materials will be pursued in future work.

5.2.3 Polyester Core (Degradable) / Polyethylene Glycol Periphery (Nondegradable)

As described above **(5.2.2)**, the successful use of hydroxyl terminated polymers towards the generation of hybrid nanogel star polymers presents an opportunity for the development of a new range of nanogel star polymers. The development of novel hydroxyl terminated polymers or the modification of existing polymers may afford a large library of new nanogel star polymers boasting versatility in both composition and functionality. Consequently the potential to readily tailor nanogel star polymers to meet the demands of specific applications is somewhat achievable.

To confirm and demonstrate the versatility of this platform, a hydroxyl terminated form of poly(ethylene glycol) i.e. poly(ethylene glycol) methyl ether (PEG-OH) was proposed to therefore generate nanogel star polymers with PEG arms and a polyester core. PEG-OH is a very cheap commercially available polymer in a range of molecular weights which from a biomedical point of view has some interesting properties. PEG is known to exhibit excellent biocompatibility and stealth like properties in the body and is therefore considered the primary tool for the modification of drug delivery vehicles e.g. liposomes, dendrimers, micelles and star and linear polymers and even drugs themselves to improve their biocompatibility.[91] Furthermore PEG has been utilised to improve or control important drug delivery parameters such as blood circulation time and excretion. The appeal of PEG towards the drug delivery field is further exasperated by its approval from the FDA and demonstrated use in current drug formulations such as Macugen by Pfizer.[92]

In addition to these favourable biomedical properties, PEG also has another interesting property in the form of thermo responsiveness. Linear PEG has a lower critical solution temperature (LCST) which simply means that the polymer undergoes a macroscopic phase separation at a specific temperature.[93] The reason for this is that at below the LCST the polymer is water soluble due to hydrogen bonding with water molecules. However, above the LCST these hydrogen bonds are broken which induces greater hydrophobicity resulting in a coil-to-globule transition and therefore a phase separation. This property is dependent on PEG molecular weight and solvent type.[92] For example 2 kDa PEG has an LCST of approximately 165^{o}C in water. Furthermore, LCSTs have been shown to be affected by a number of other polymer properties such as composition (hydrophobicity / hydrophilicity), polydisperisity and architecture.[94-96] Concerning 2 kDa PEG for example, at present its LCST of 165^{o}C renders it unsuitable for any real world applications. However, by modifying the structural properties of PEG such as the architecture e.g. star shaped it may be possible to induce a lower LCST thus affording a more applicable thermoresponsive PEG derived polymer. Such a phenomena has

been reported for hyperbranched star polymers comprising a poly[3-ethyl-3-(hydroxymethyl)oxetane](HBPO) core and hydrophilic polyethylene oxide (PEG) arms.[97] These hyperbranched polymers exhibited broad PDIs and formed very large macromolecular structures i.e. vesicles in water (> 300 nm – 112 µm) thus inhibiting their potential for biomedical applications. The ability to control the LCST behaviour of these polymeric vesicles through varying the PEO arm length and overall hyperbranched polymer molecular weight was demonstrated. Although LCST was tunable, such a platform lacks the superior structural versatility and control offered by the polyester / PEG based nanoparticle platform. Furthermore, the nanoparticles described here are considerably smaller yet retain the ability to exhibit strong thermoresponsive behaviour, a feature which improves their potential biomedical applicability.

The following work will investigate the feasibility of employing PEG in the OROP of cyclic esters for the generation of nanogel star polymers. The LCST behaviour of these materials will then be investigated as a function of PEG molecular weight and hydrophobic nanogel core density.

As described in **Figure 5.26**, hydroxyl terminated PEG (2 kDa and 5 kDa) was used as an initiator for the OROP of the cyclic ester crosslinker BOP using metal free conditions (TBD catalyst) to form new nanogel star polymers with PEG arms and a polyester core. Similarly, linear block copolymers were synthesised through the use of the cyclic ester δ-valerolactone which could subsequently be used to afford nanogel star polymers of increased hydrophobic character owing to the block copolymer nature of the arms **(Figure 5.27)**.

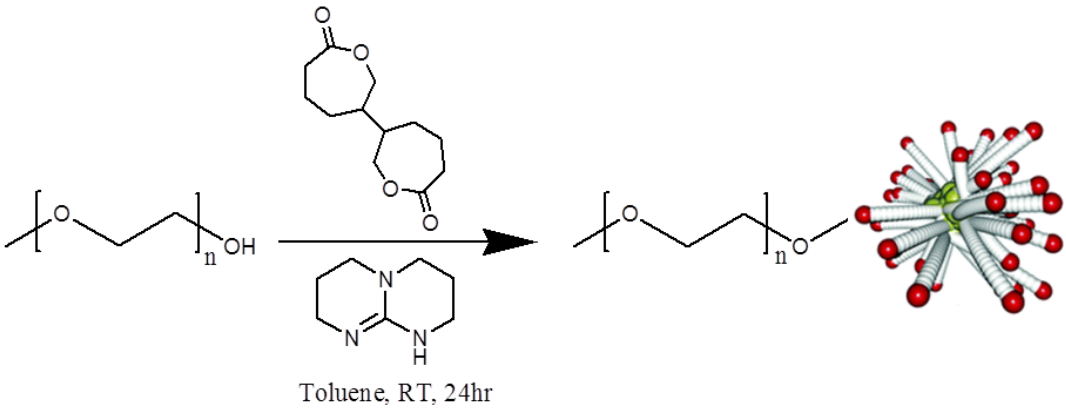

Figure 5.26: Synthesis of nanogel star polymers comprising PEG arms and crosslinked polyester core via OROP of cyclic esters.

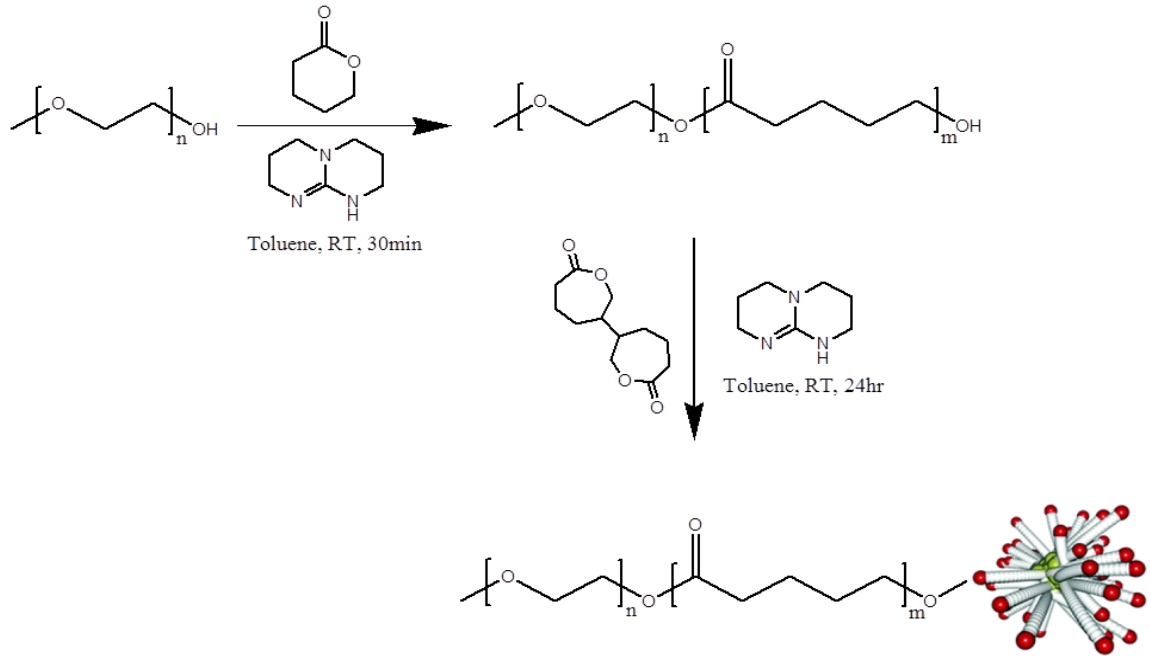

Figure 5.27: Synthesis of nanogel star polymers with PEG-b-PVL arms and crosslinked polyester core via organocatalytic ring opening polymerization of cyclic esters.

A series of nanogel star polymers were synthesized with excellent control observed over arm molecular weight and composition and overall nanogel star polymer molecular weight **(Table 5.5).** Initially PEG-OH (2 kDa) was successfully employed to generate a well defined nanogel star polymer boasting a very low PDI of 1.1, apparent M_n of 28.7 kDa and size (R_h) of 8.6 nm in THF. The reaction required a prolonged reaction time of approximately 20 h compared to the 4 h required by a small initiator such as benzyl alcohol due to 2 kDa PEG being a macroinitiator. The number of arms could not be determined due to the absence of any polyester signals. The reason for this is due to the polyester portion of the molecule being positioned in the core therefore shielding it in ^{1}H NMR spectroscopy analysis. Furthermore, the whole molecule predominantly consists of PEG chains whereas the polyester core only contributes a very small fraction to the overall composition. SEC analysis identified the presence of unreacted linear PEG-OH arm (approx. 30%) but the clear shift in retention time to higher molecular weight confirmed the synthesis of a nanogel star polymer **(Figure 5.28)**. To remove the crude arm, the mixture was purified by a fractionation process to yield the homo star polymer. The fractionation process worked very well in purifying these polymers although yield was sacrificed somewhat. SEC confirmed the absence of any crude PEG-OH arm post fractionation (**Figure 5.28, (C) Inset)**. FTIR spectroscopic analysis indentified the presence of ester

functionality at 1725 cm^{-1} therefore confirming the presence of polyester within the star polymer platform **(Figure 5.29)**.

Table 5.5: PEG functionalized polyester nanogel star polymers and their LCST behavior.

M_n PEG	*Target M_n VL*	M_n VL[(a,b)]	PDI	*M_n Star (kDa)*[(a)]	PDI	No. Arms[(c)]	Size R_h (nm)[(d)]	LCST (^oC)[(e)]
2 kDa	n/a	n/a	1.1	28.7	1.1	n/a	8.6	75
2 kDa	1.5 kDa	1.8 kDa (GPC) 1.1 kDa (NMR)	1.1	48.8	1.5	9	13	70
2 kDa	3 kDa	3.2 kDa (GPC) 2.5 kDa (NMR)	1.1	55.8	1.4	10	14	65
2 kDa	4.5 kDa	5.0 kDa (GPC) 3.2 kDa (NMR)	1.1	61.1	1.5	8	14	60
2 kDa	6.0 kDa	5.9 kDa (GPC) 4.8 kDa (NMR)	1.1	84.5	1.4	8	14.4	40
2 and 5 kDa	n/a	n/a	n/a	51.6	1.1	n/a	10.8	n/a
5 kDa	n/a	n/a	n/a	51.1	1.1	n/a	9.6	n/a
5 kDa	3.0 kDa[(f)]	n/a	n/a	58.2	1.3	n/a	21	n/a

(a) determined by SEC (THF) using RI detector (b) determined by ^{1}H NMR spectroscopy using integral ratio of PEG to polyester moieties (c) determined by ^{1}H NMR spectroscopy using the integral ratio of linear PEG-b-PVL arm and star (d) determined by DLS in THF (e) performed in PBS (f) synthesized using a 1 pot approach.

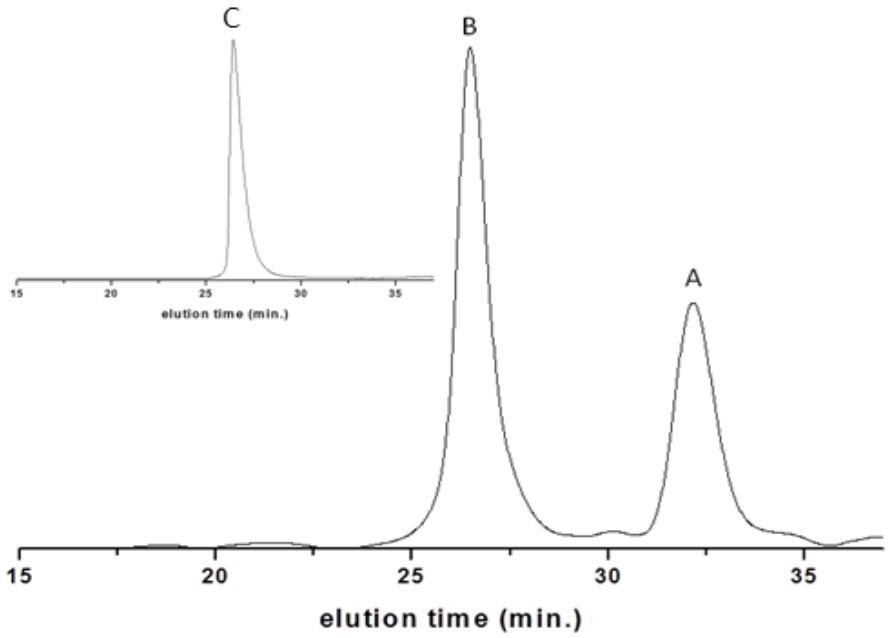

Figure 5.28: SEC trace of L-PEG-2 kDa (A), the corresponding polyester nanogel star polymer, S-PEG-2 kDa (B) and S-PEG-2 kDa after fractionation (C).

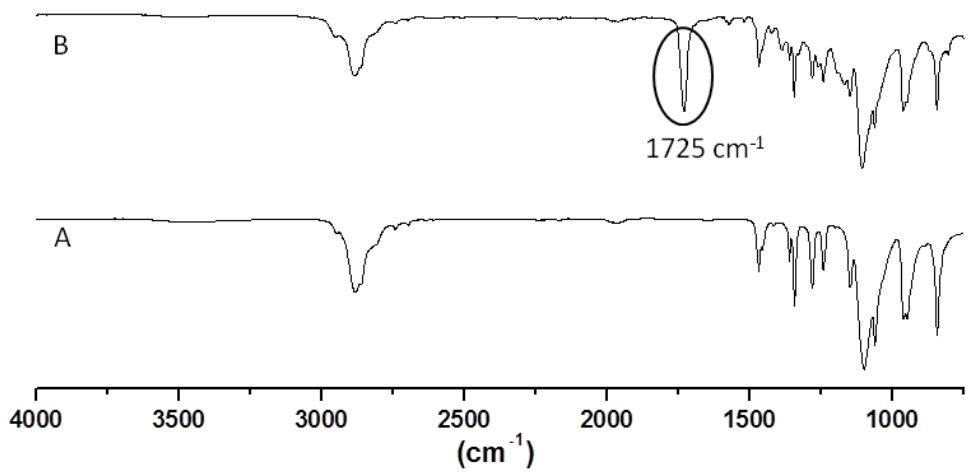

Figure 5.29: FTIR spectra of L-PEG-2 kDa (A) and S-PEG-2 kDa (B).

Expanding on this, the monomer δ-valerolactone was used in conjunction with the same PEG initiator to generate a series of linear block copolymers in which polyester molecular weight was readily controlled by varying the δ-valerolactone to PEG-OH molar ratio **(Table 5.5)**. ^{1}H NMR spectroscopy was used to determine the polyester molecular weight and thus monomer conversion due to the clear distinction of PEG and ester signals **(Figure 5.30)**. Typically 70 – 80% conversion of δ-valerolactone monomer was observed and molecular weights were in

close agreement with the target molecular weight. SEC analysis showed a low PDI of 1.1 highlighting the excellent control observed in such a reaction with apparent M_n in good agreement with the target M_n. To synthesize the nanogel stars, the reaction was performed in two steps i.e. generation of the linear arm, in situ sampling and subsequent addition of BOP crosslinker. This approach provides an excellent level of control over each step. The resultant stars showed the presence of weak ester signals which permitted elucidation of the average arm number (AAN) by comparing the integral values of the ester peaks before and after star formation **(Figure 5.30)**. The weak nature of the ester peaks confirms the synthesis of a molecule with increased PEG composition i.e. several PEG arms and peripheral positioning of these PEG arms i.e. shielding of polyester core. It was noted that all of these block copolymer derived stars produced nanogel stars with 8 – 10 arms and all approximately 13 – 14 nm in size (R_h) **(Table 5.5)**. Therefore the only apparent effect of increasing polyester arm M_n was the increase in overall nanogel star polymer M_n. Although the star polymer with a 4.8 kDa polyester arm M_n (largest) did show a small increase in size (R_h) no significant increase in size was observed amongst the block copolymer stars which may have been expected given the differing star molecular weights. Such an observation may be accounted for by the similar average arm number (AAN) or degree of branching for each star resulting in a similar hydrodynamic volume and therefore size. The degree of branching of star polymers is known to have a large impact on their hydrodynamic volume.[98-100] The clear shift in SEC retention times of both arms and their respective stars could be readily followed highlighting the excellent synthetic control afforded here **(Figure 5.31)**. The increase in M_n of both arms and stars was reflected in a retention time shift to lower retention time thus confirming M_n increase. The PDIs of the generated stars increased to 1.4 – 1.5 which was interesting when compared to the low PDI (1.1) observed for the homo PEG derived star. The block copolymer arm introduces further complexity to the system and greater transesterification possibilities which may account for the observed PDI difference. FTIR sprectroscopy confirmed the presence of ester functionality within both the block copolymer arms and the resultant star owing to the characteristic ester peak observed at 1725 cm^{-1} **(Figure 5.32)**.

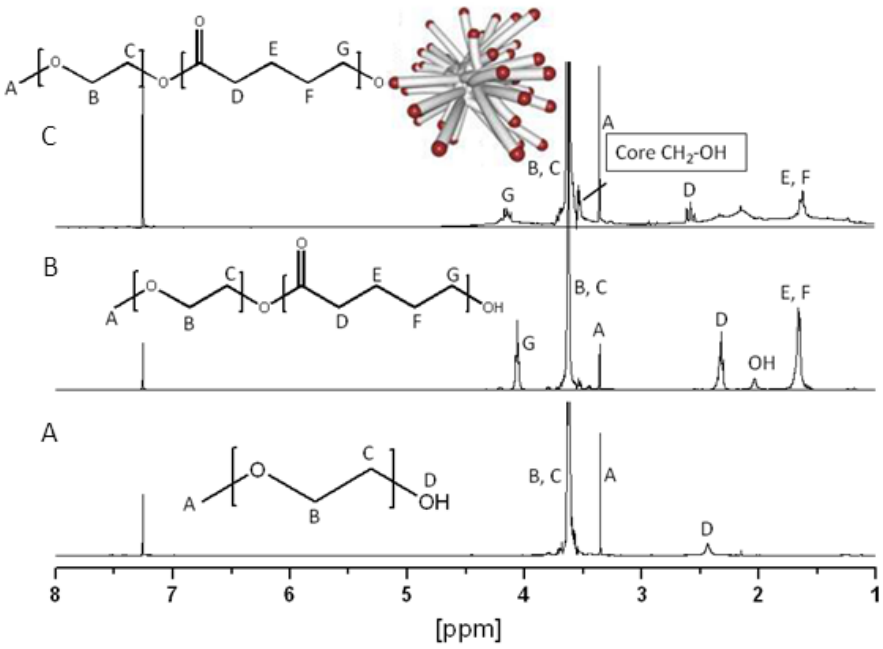

Figure 5.30: ^{1}H NMR spectrum of L-PEG-2k Da (A), L-PEG-2 kDa-b-PVL-1.5 kDa (B) and S-PEG-2 kDa-b-PVL-1.5 kDa (C) ($CDCl_3$).

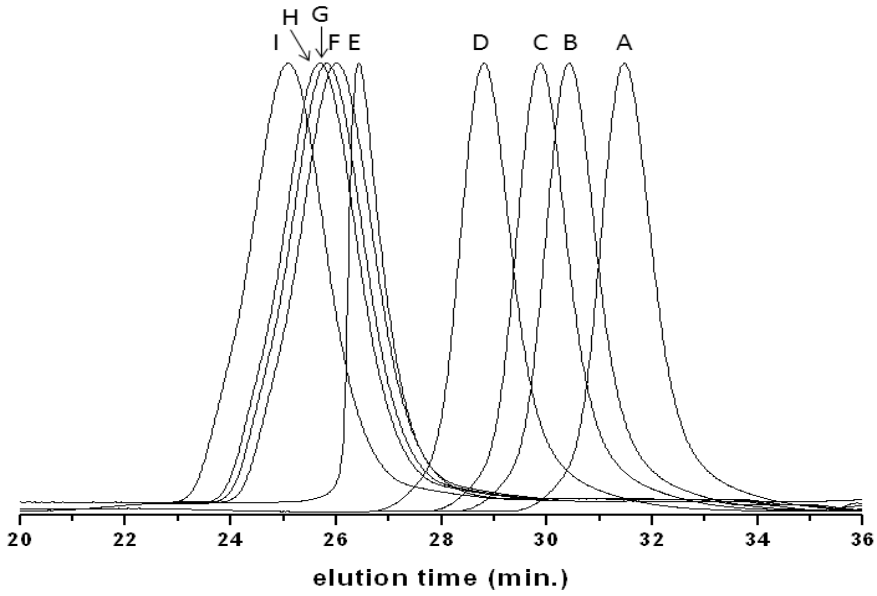

Figure 5.31: SEC Traces of linear PEG-b-PVL block copolymers and their corresponding nanogel star polymers: (A) L-PEG-2 kDa-b-PVL-1.5 kDa, (B) L-PEG-2 kDa-b-PVL-3 kDa, (C) L-PEG-2 kDa-b-PVL-4.5 kDa, (D) L-PEG-2 kDa-b-PVL-6 kDa, (E) S-PEG-2 kDa, (F) S-PEG-2 kDa-b-PVL-1.5 kDa, (G) S-PEG-2 kDa-b-PVL-3 kDa, (H) S-PEG-2 kDa-b-PVL-4.5 kDa, (I) S-PEG-2 kDa-b-PVL-6 kDa.

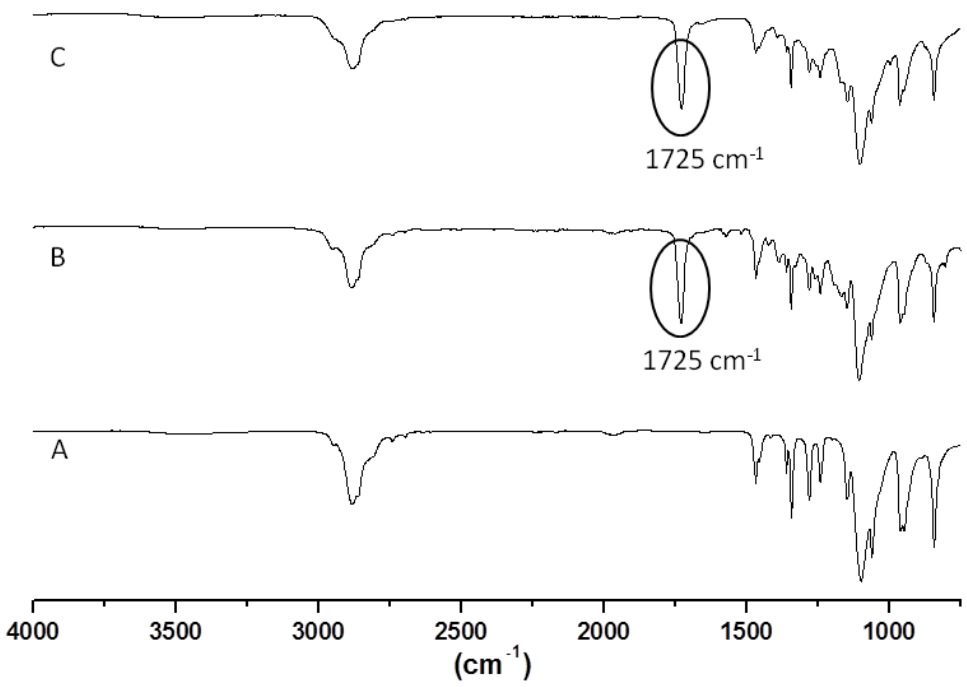

Figure 5.32: FTIR spectra of L-PEG-2 kDa (A), L-PEG-2 kDa-b-PVL-1.5 kDa (B) and S-PEG-2 kDa-b-PVL-1.5 kDa (C).

A different PEG derivative i.e. PEG 5 kDa also permitted the successful synthesis of nanogel star polymers **(Table 5.5)**. As with PEG-2 kDa, the PEG-5 kDa initiator produced a small (R_h = 9.6 nm), well defined, monodisperse (PDI = 1.1) nanogel star polymer. The simultaneous combination of both PEG-2 kDa and PEG-5 kDa in equal molar ratio generated a mixed PEG star polymer very similar in apparent M_n and PDI to the homo PEG-5 kDa star. The size of this star polymer was slightly larger with an R_h of 10.8 nm. As described above, ^{1}H NMR spectroscopy analysis of the homo PEG star polymers could not determine the AAN due to the absence of any ester peaks. FTIR sprectroscopy did however confirm the presence of ester functionality **(Figure 5.33)**. The use of PEG-5 kDa within a block a copolymer arrangement was attempted. The OROP of δ-valerolactone was performed using a 1 pot reaction approach containing both monomer and BOP crosslinker. The rapid polymerization of δ-valerolactone and slow polymerization and solubility of BOP permits the use of such an approach therefore negating the two step approach employed for PEG-2 kDa block copolymers. However the use of such an approach reduces the ability to monitor and control each structural component i.e. M_n and PDI of arm and star. The determination of AAN by ^{1}H NMR spectroscopy proved impossible due to the lack of visible signals attributable to polyester star and lack of a comparative ^{1}H NMR spectroscopy analysis of the linear block copolymer arm. FTIR sprectroscopy did confirm the presence of ester functionality at 1725 cm^{-1} **(Figure 5.33)**. The

star generated via this 1 pot reaction approach yielded an apparent M_n of 58 kDa, R_h of 21 nm and PDI of 1.3 which was lower than the comparative 2 step approach for the PEG-2 kDa block copolymer stars highlighting the effectiveness of a 1 pot approach. The large size of this star compared to the others was due to the large PEG-OH initiator (5 kDa) employed in conjunction with the presence of extra ester functionality in the form of δ-valerolactone with a target M_n of 3 kDa. SEC analysis of the described 5 kDa nanogel star polymer derivatives showed the shift in retention time after star polymer formation owing to an increase in molecular weight **(Figure 5.34)**. Purification was again performed using fractionation to remove any unreacted residual arms resulting in the unimodal distribution of nanogel star polymer molecular weights. The SEC trace of PEG-5 kDa block copolymer star **(C - Figure 5.34)** highlights the broadening of PDI compared to the equivalent homo PEG-5 kDa stars **(A and B - Figure 5.34)**.

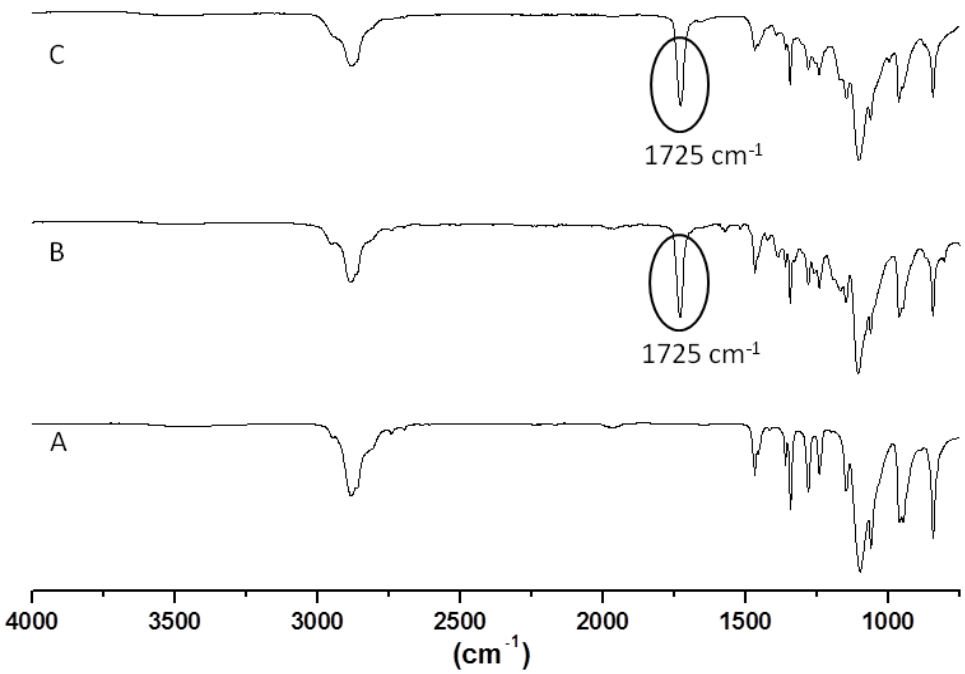

Figure 5.33: FTIR spectra of L-PEG-5 kDa (A), S-PEG-5 kDa (B) and S-PEG-5 kDa-b-PVL-3 kDa (C).

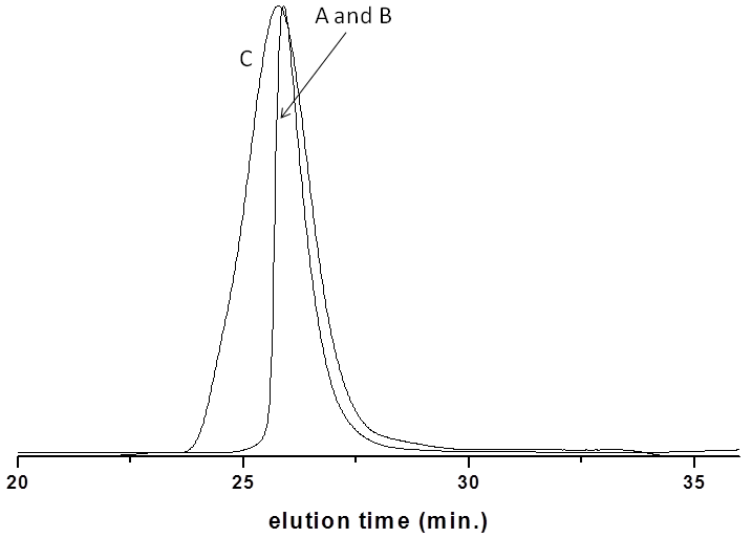

Figure 5.34: SEC traces of L-PEG-5 kDa (A), S-PEG-2/5 kDa (B) and S-PEG-5 kDa-b-PVL-3 kDa (C).

As mentioned, linear PEGs have LCSTs but which are too high to be applicable to any real biomedical application. The incorporation of numerous PEG arms into a star conformation results in a high local density of PEG arms within a size confined structural space. Such a feature may promote increased interaction amongst PEG arms therefore permitting a coil to globule transition at a lower temperature or LCST. Furthermore, the presence of a small hydrophobic polyester core which can be tuned by the incorporation of block copolymers will help to promote greater hydrophobic interactions resulting in a lower LCST. The combination of these tunable density and hydrophobic properties may be enough to reduce the LCST of PEG to a more applicable temperature whilst also potentially enabling the tailoring of LCSTs to meet the demands of a variety of applications.

The LCST behaviour of the described nanogel star polymers was investigated on a temperature controlled spectrometer. The identification of a LCST was denoted by a strong increase in absorbance due to the phase separation induced by the thermoresponsiveness of the polymer. The results are summarized in **Table 5.5**. It is known that PEG-2 kDa has an LCST of 165^{o}C in water (using a sealed system) whereas the S-PEG-2 kDa synthesised here had an LCST of 70^{o}C.[92] The LCST of the nanogel stars was performed in PBS to crudely mimic the human body environment. By simply incorporating numerous PEG arms into a star conformation containing a small hydrophobic core the LCST of PEG-2 kDa was reduced by a substantial 90^{o}C. The effects of sample concentration were negligible as a 20 mg/ml sample concentration resulted in a LCST of 68^{o}C whereas 5 mg/ml and 10 mg/ml sample concentrations both generated a LCST of 75^{o}C **(Figure 5.35)**.

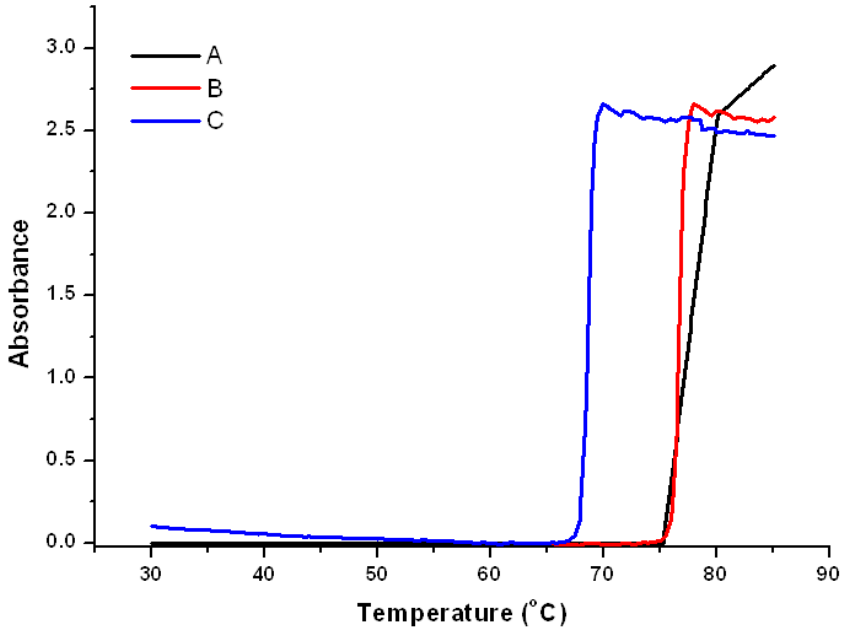

Figure 5.35: LCST behavior of PEG derived polyester nanogel star polymers: (A) S-PEG-2kDa 5 mg/ml, (B) S-PEG-2kDa 10 mg/ml and (C) S-PEG-2kDa 20 mg/ml.

The potential to reduce the LCST further by increasing the hydrophobic content on the star polymers was investigated. A simple way to do this was through the formation of block copolymer arms with PEG-OH and δ-valerolactone. The PEG-2 kDa block copolymer stars each with controlled increments of increased arm hydrophobicity demonstrated the ability to control the LCST behaviour. This facile modulation of the arm hydrophilic / hydrophobic ratio resulted in the incremental decrease in LCST to 70°C, 65°C, 60°C and 40°C for S-PEG-2 kDa-b-PVL-1.5 kDa, S-PEG-2 kDa-b-PVL-3 kDa, S-PEG-2 kDa-b-PVL-4.5 kDa and S-PEG-2 kDa-b-PVL-6 kDa, respectively **(Figure 5.36)**. All of these star polymers exhibited a similar AAN (8 - 10) and size (R_h = 13 - 14 nm) ruling out the possibility of arm density and star size contributing significantly to these LCST differences. The subsequent hydrophobicity increases amongst the block copolymer stars did contribute to a decreased LCST. Such a feature highlights the significant contribution made by the hydrophilic / hydrophobic ratio towards the LCST behaviour of a polymer. A major problem with increasing the hydrophobic content is the inherent water solubility issues associated with such hydrophobic entities. The star polymers initially required 10% THF in PBS for solubility which could later be removed by rotary evaporation. However, S-PEG-2 kDa-b-PVL-4.5 kDa and S-PEG-2 kDa-b-PVL-6 kDa were not soluble in neat PBS due to their large hydrophobic character. The hydrophilic PEG periphery could not permit enough solubility in just PBS and so the final solution for LCST analysis required a little THF (5%) to aid solubility. The presence of THF could potentially influence the

final LCST value but as there is only a small volume of THF present the deviation from the real LCST value was expected to be minimal. Consequently, the modulation of the hydrophobic character for lowering of LCSTs, although very effective, is limited with regards to inhibiting water solubility of the final star polymer. Upon cooling, the LCST behaviour for all star polymers was shown to be reversible. Cooling resulted in the transition from a turbid solution at >LCST to a transparent solution <LCST. To confirm this, the samples were analysed using a heating cycle and an immediate cooling cycle which resulted in an identical LCST trace for the cooling cycle.

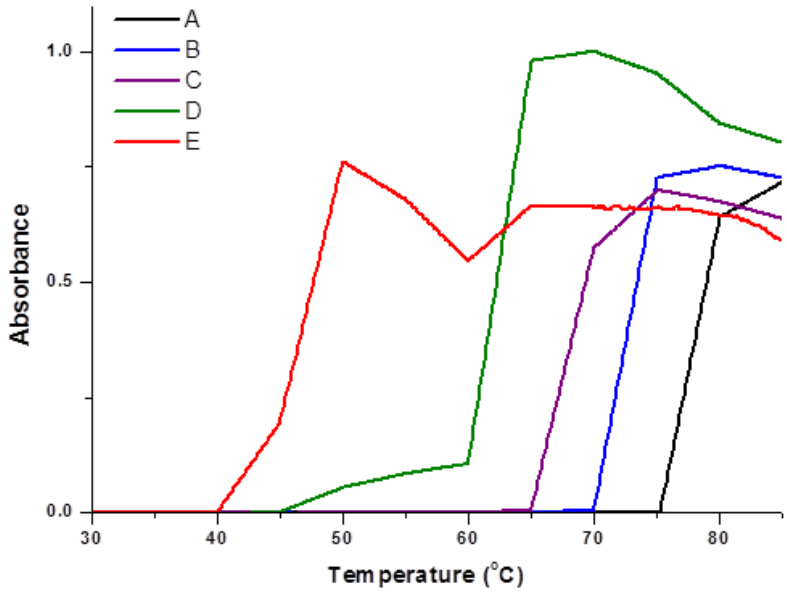

Figure 5.36: LCST behavior of PEG derived polyester nanogel star polymers: (A) S-PEG-2 kDa 5mg/ml, (B) S-PEG-2 kDa-b-PVL-1.5 kDa, (C) S-PEG-2 kDa-b-PVL-3 kDa, (D) S-PEG-2 kDa-b-PVL-4.5 kDa, (E) S-PEG-2 kDa-b-PVL-6 kDa.

The LCST behaviour of PEG is known to be strongly dependent on molecular weight.[92] By increasing PEG molecular weight or length of the PEG chains used it should in theory be possible to further lower the LCST of the above nanogel star polymers. Linear PEG-5 kDa has an LCST of 145°C which upon incorporation into a star shaped architecture should result in an even lower LCST. However, S-PEG-5 kDa did not result in an LCST at <85°C. Such an observation was unexpected given the large shift observed for S-PEG-2 kDa. Similarly, the incorporation of a mixture of PEG-2 kDa and PEG-5 kDa as arms did not result in a measurable LCST i.e. <85°C. By mixing two different arm lengths the amount of disorder within the system should increase and as S-PEG-2 kDa was shown to elicit a lower LCST, the resultant material was expected to exhibit a lower LCST at <85°C. Finally an increase in hydrophobic character through block

copolymer arms was attempted to achieve desirable LCST behaviour for S-PEG-5 kDa. As described previously the synthetic approach involved a 1 pot procedure which should not impact on the hydrophobic properties of the final star polymer. A molecular weight of 3 kDa was targeted for the block copolymer arm which should impact on the LCST behaviour of the nanogel star. However, no LCST at <85^{o}C was observed in spite of its comparatively large size (R_h) of 21 nm. One possible explanation for these PEG-5 kDa observations is related to the arm density of these stars. As this PEG macroinitiator is larger than the corresponding PEG-2 kDa it is likely to have a significant impact on the arm density. For example a larger arm means it is very likely that it is not possible to incorporate as many arms into the same star structure due to steric issues associated with a larger arm. The consequence of this is reduced arm density resulting in fewer favourable interactions amongst PEG arms which are a key feature required to drive the reduction in LCST for this particular nanoparticle platform. Ideally, the determination of AAN for all star polymers would help to confirm this hypothesis. The apparent M_w of these S-PEG-5 kDa polymers was approximately 50 kDa even for the block copolymer star (S-PEG-5 kDa-b-PVL-3 kDa) indicating that overall star molecular weight was restricted due to AAN limitations as a result of the large size of the PEG-5 kDa macroinitiator. In theory a larger PEG arm should have a greater effect on LCST but in reality this was not the case due to structural restrictions of the nanoparticle platform.

The successful employment of hydroxyl terminated PEG as an initiator in the OROP of cyclic esters for nanogel star polymer synthesis further demonstrated the versatility of this polyester based platform. Nanogel star polymers comprising PEG arms and a hydrophobic polyester core were thus generated boasting narrow PDIs. The incorporation of two different molecular weight PEGs and development of block copolymer arms further demonstrated the ability to readily control both arm and core properties. Investigation of the LCST behaviour of the described materials highlighted the significant impact of architecture on the LCST behaviour of linear PEG. Furthermore, the ability to modulate hydrophobic density of arms and subsequent stars offered a nanoparticle platform with LCST tunable capabilities. Initial studies hypothesise that arm density also plays a vital role in regulating LCSTs due to the absence of any LCST for PEG-5 kDa star polymers. Through future development it may be possible to create a PEG functionalised nanogel star polymer with a body temperature LCST rendering it potentially useful for biomedical applications such as drug delivery and theranostics. In addition the incorporation of other thermoresponsive polymers such as PNIPAM or polymers with previously high LCSTs may afford a new range of thermoresponsive nanogel star polymers.

5.3 Conclusion

Nanogel star polymers have emerged as an interesting class of organic nanoparticle platform due to the superior structural and synthetic features afforded. Herein, an array of well defined hybrid nanogel star polymer systems was designed and synthesised using a combination of various polymerization methodologies. Anionic polymerization and ROP of NCAs were employed to generate a series of well defined polystyrene nanogel stars polymers with biocompatible polypeptide peripheries. The resultant materials exhibited narrow PDIs but suffered from limited water solubility owing to the presence of a large hydrophobic polystyrene core. Expansion of this platform to include a degradable polyester core with functional methacrylate peripheries was realised. The OROP of cyclic esters via hydroxyl terminated methacrylate polymers derived by RAFT polymerization afforded a series of nanogel star polymers exhibiting excellent control over constituent arms and star properties. Well defined linear cationic and protected carboxylic acid methacrylate polymers were incorporated into a polyester nanogel star conformation in which the size of these stars was readily tuned. Removal of the carboxylic acid protecting group led to undesirable solubility issues requiring the future development of an alternative polymer. The versatility of this degradable platform was further demonstrated through the use of hydroxyl terminated PEG of two different molecular weights to afford PEG functionalised nanogel star polymers. Structural parameters such as arm molecular weight, composition and overall hydrophobic content of stars were facilely controlled. The modulation of these parameters permitted the tuning of PEG LCST behaviour to afford the drastic decrease in PEG LCST to a temperature more applicable to biomedical applications. Overall the consolidation of several different synthetic approaches within the one organic nanoparticle platform afforded a series of hybrid materials boasting well-defined, multifunctional and structurally versatile properties. This synthetic and structural versatility presents many new opportunities for the development of a new generation of “smart” hybrid nanomaterials which can be easily tailored to meet the demands of specific biomedical applications such as drug delivery (anionic / cationic star polymers for layer-by-layer technology), theranostics (core / shell type star polymers)and antimicrobials (cationic star polymers).

5.4 Experimental

Polystyrene Core (Nondegradable) / Polypeptide Periphery (Degradable) Nanogel Star Polymers Materials

General Methods

Infrared (IR) spectra were obtained from chloroform solutions using a Thermo Nicolet Nexus 670 FTIR spectrophotometer in transmission mode with samples prepared as thin films on 2 mm thick NaCl plates. Similarly, Attenuated Total Reflection (ATR) FTIR spectroscopy measurements were performed on a Perkin-Elmer Spectrum 100 in the spectral region of 650 - 4000 cm-1 and were obtained from 4 scans with a resolution of 2 cm^{-1}. A background measurement was taken before the sample was loaded onto the ATR for measurement. ^{1}H NMR spectroscopy spectra were obtained on a Bruker Avance 2000 spectrometer (1H, 400 MHz) using 5 mm o.d. tubes and were referenced to internal solvent residue ($CDCl_3$: ^{1}H = 7.26 ppm). The following abbreviations for multiplicity are used: s, singlet; m, multiplet; br, broad. Analytical Gel Permeation Chromatography (GPC) using Waters high resolution columns HR1, HR2, HR4E and HR5E (flow rate 1 mL / min, THF) in conjunction with a Waters 996 photodiode array and / or a Waters 411 differential refractometer was used to determine molecular weight distributions, M_w/M_n of polymer samples with respect to linear polystyrene or PMMA standards depending on the type of polymer being analysed.. GPC using DMF as solvent was performed using a similar set up with a Waters differential refractometer and linear PMMA standards. SEC with a light scattering detection (QELS quasi elastic light scattering detector) in conjunction with a Optilab intraferometric refractometer were used to determine M_w, M_w/M_n, and average hydrodynamic radii, R_h. A dn/dc value of 0.187 was used. For all other sizing measurements, analysis was performed by DLS using a Malvern Zetasizer Nano ZS (Malvern Instruments, Ltd., United Kingdom). The appropriate concentration was determined by starting at a 1 mg/ml sample concentration and then performing a series of dilutions to obtain suitable sizing characteristics. Samples were filtered using a 0.4 µm Acrodisc filter prior to measurement. LCST behavior was recorded on a Cary-100 spectrophotometer equipped with a Peltier heated multi-cell holder with a Cary temperature controller and probe. Samples were heated at a rate of $5^{o}C$ per min and held at that temperature for a further 1 minute. A repeat cycle of cooling was performed to check the reversibility of the polymer solutions. Sample preparation involved dissolution of the polymer in 10% THF in PBS solution and then removal of the THF under reduced pressure. Samples were diluted accordingly to the desired sample concentration and measurements were recorded in a 1ml sample cuvette.

Materials

All air and moisture sensitive compounds were handled under a nitrogen atmosphere using general Schlenk-line techniques. α-pinene (98%) bis(trichloromethyl) carbonate (triphosgene) 99% and benzylamine were purchased from Sigma Aldrich. γ-Benzyl-L-glutamate and H-Lys(Z)-OH were supplied by Bachem. Chloroform and ethyl acetate were used directly from the bottle and stored under an inert, dry atmosphere. ε-carbobenzyloxy-L-lysine NCA and γ-benzyl-L-glutamate NCA were synthesised following a literature procedure.[101] 3-(tert-Butyldimethylsilyloxy)-1-propyl lithium (20 wt% solution in cyclohexane) was purchased from FMC Lithium Division and used as received. Styrene, para-benezenedicarboxaldehyde and para-divinylbenzene (p-DVB) were purchased from Sigma Aldrich and either used as received or purified by standard literature procedures. Additional p-DVB was synthesized according to standard literature procedures from p-benzenedicarboxaldehyde. Solvents were either used as obtained from a Pure Solv solvent dispenser purchased from Innovative Technology, Inc., or purchased from Sigma Aldrich and purified by standard literature procedures. All other chemicals were used as obtained from commercial sources and used as received

Synthesis of "protected" 3-(tert-Butyldimethylsilyloxy)-1-propyl-functionalized polystyrene star-polymers

Star polymers were synthesised according to the procedure by Sly et al.[59] Briefly, 3-(tert-Butyldimethylsilyloxy)-1-propyl lithium (8.8 mL, 20 wt % solution in cyclohexane) was added to a stirred solution of styrene (16.0 mL), cyclohexane (250 mL) and THF (16.0 mL) under an argon. After 20 min a sample (4 mL) was taken, quenched in degassed MeOH (approx. 150 mL) and a representative sample of the "free" polystyrene arm collected by filtration as a white amorphous powder (data for free arm: ^{1}H NMR spectroscopy (400 MHz, $CDCl_3$, δ) = 7.12 (br s, 90 H), 6.50-6.70 (br m, 60 H), 3.45 (br s, 2 H), 1.90 (br s, 30 H), 1.46 (br s, 60 H), 1.03 (br s, 4 H), 0.87 (br s, 9H), 0.00 (br s, 6H). Analytical GPC: M_n = 3000, M_w/M_n = 1.07. This data implied an average degree of polymerization = 30). A solution of p-divinylbenzene (0.17. mL) in cyclohexane (1.0 mL) was added to the remaining solution which was then stirred for a further 40 min. The reaction solution was then quenched by its slow addition to a rapidly stirred solution of degassed MeOH and EtOH (1.5 L, 1:1). The precipitate was isolated by filtration and dried under vacuum (16.1 g). The crude polymer was purified by fractionation. Briefly, the star polymer was dissolved in DCM (100 ml) before the slow addition of acetone (150 ml) and then isopropyl alcohol (30 ml). The solution was allowed to stand until the product formed a substantial oily layer on the bottom of the container. The mixture was decanted allowing

isolation of the oil which was then dissolved in DCM (50 mL) and the solution added to MeOH (1 L). The precipitate thus formed was isolated by filtration and dried under vacuum to afford the nanogel star-polymer (12.1 g) as a white amorphous powder. ^{1}H NMR spectroscopy (400 MHz, $CDCl_3$, δ) = 7.12 (br s, 90H), 6.50-6.70 (br m, 60H), 3.45 (br s, 2H), 1.90 (br s, 30H), 1.46 (br s, 60H), 1.03 (br s, 4H) 0.87 (br s, 9H), 0.00 (br s, 6H). DLS (THF): M_w = 111, 000 g/mol, M_w/M_n = 1.2, R_h = 6.4 nm.

Synthesis of "deprotected" hydroxyl functionalised polystyrene star polymer: S-PS-OH

Butyldimethylsilyloxy)-1-propyl- terminated polystyrene nanogel star-polymer (10.0 g) was dissolved in THF (15.0 mL) and tetrabutylammonium fluoride (1.0 M solution in THF, 15.0 mL) was added. The reaction solution was stirred for 24 h at room temperature before being warmed to 50 ^{o}C for 1 h. The solution was allowed to cool to room temperature before it was slowly added to MeOH (1 L) with rapid stirring. The precipitate was isolated by filtration and dried under vacuum to afford the "deprotected" nanogel star-polymer (9.8 g) as a white amorphous powder. ^{1}H NMR spectroscopy (400 MHz, $CDCl_3$, δ) = 7.12 (br s, 90H), 6.50-6.70 (br m, 60H), 3.45 (br s, 2H), 1.90 (br s, 30H), 1.46 (br s, 60H), 1.03 (br s, 4H). DLS (THF): M_w = 110,000 g/mol, M_w/M_n = 1.2, R_h = 6.4 nm.

Synthesis of azide functionalized polystyrene nanogel star polymer: S-PS-N_3

S-PS-OH (0.4 g) in 30ml benzene was distilled using Dean-Stark apparatus. Under N_2 and ice, Dry THF (8 ml) was added to the reaction vessel followed by triphenylphosphine (0.7 g – 2eq.) and DIAD (diisopropyl azodicarboxylate) (0.054 g – 2eq.). Diphenylphosphoryl azide (0.073 g – 2eq.) in approx. 1 ml THF was added and stirred at room temperature for 14 h and 70^{o}C for 2 h. Reaction was cooled and precipitated into methanol. Product was reprecipitated twice from DCM into methanol to obtain the product as a white amorphous powder. ^{1}H NMR spectroscopy (400 MHz, $CDCl_3$, δ) = 7.12 (br s, 90H), 6.50-6.70 (br m, 60H), 3.11 (br s, 2H), 1.90 (br s, 30H), 1.46 (br s, 64H), 1.03 (br s, 4H). DLS (THF): M_w = 109,000 g/mol, M_w/M_n = 1.3, R_h = 6.5 nm.

Synthesis of amino functionalized polystyrene nanogel star polymer: S-PS-NH_2

S-PS-N3 (0.2 g) and 0.035 g of triphenylphosphine (1.5eq.) in 4 ml of dry THF was stirred at 70^{o}C for 4 h. 4 drops of NH_4OH were added and stirred at 50^{o}C for 4 h. The solution was precipitated into hexane and purified by reprecipitation into methanol. The product was freeze dried from benzene as a white solid. ^{1}H NMR spectroscopy (400 MHz, $CDCl_3$, δ) = 7.12 (br s,

90H), 6.50-6.70 (br m, 60H), 2.5 (br s, 2H), 1.90 (br s, 30H), 1.46 (br s, 60H), 1.03 (br s, 4H). DLS (THF): M_w = 44,200 g/mol, M_w/M_n = 1.5, R_h = 4.7 nm.

Synthesis of star shaped PBLG: S-PS-b-PBLG

As a reference procedure, the NCA of γ-benzyl-L-glutamate (BLG) (0.52 g, 2 mmol) was dissolved in 5 mL DMF in a Schlenk tube under a nitrogen atmosphere. S-PS-NH_2 (0.2 g, M_W: approx. 109kDa, no. arms: 36) in dry DMF (1 ml) was added to the reaction solution. The solution was stirred for 72 h at room temperature. The polymer was precipitated into an excess of cold diethyl ether and dried under vacuum (Yield: 90%). ^{1}H NMR spectroscopy (400 MHz, $CDCl_3$, δ) = 7.35 (br s, 85H), 7.12 (br s, 90H), 6.50-6.70 (br m, 60H), 5.18 (br m, 34H), 4.70 (br s, 17H) 2.50 (br s, 2H), 2.50 (br s, 34H), 1.85-2.25 (br s, 34H), 1.85-2.25 (br s, 30H), 1.55 (br s, 60H), 1.46 (br s, 60H), 1.03 (br s, 4H). DLS (THF): M_w = 44,200 g/mol, M_w/M_n = 1.5, R_h = 4.7 nm.

Synthesis of star shaped PZLL: S-PS-b-PZLL

As a reference procedure, the NCA of γ ε-carbobenzyloxy-L-lysine (ZLL) (0.61 g, 2 mmol) was dissolved in 6 mL DMF in a Schlenk tube under a nitrogen atmosphere. S-PS-NH_2 (0.2 g, M_W: approx. 109kDa, no. arms: 36) in dry DMF (1 ml) was added to the reaction solution. The solution was stirred for 72 h at room temperature. The polymer was precipitated into an excess of cold diethyl ether and dried under vacuum (Yield: 90%). ^{1}H NMR spectroscopy (400 MHz, $CDCl_3$, δ) = 7.35 (br s, 68H), 7.12 (br s, 90H), 6.50-6.70 (br m, 60H), 5.18 (br s, 27H), 4.50 (br s, 13H) 3.15 (br s, 27H), 1.25-2.25 (br m, 237H) DLS (THF): M_w = 44,200 g/mol, M_w/M_n = 1.5, R_h = 4.7 nm.

Synthesis of star shaped PGA: S-PS-b-PGA

S-PS-b-PBLG (0.5 g) was dissolved in 5 mL of trifluoroacetic acid (TFA). A 6-fold excess with respect to γ-benzyl-L-glutamate of a 33% solution of HBr in acetic acid was added slowly to the reaction. After 16 h, the solution was precipitated into diethyl ether. The precipitate was washed with ethanol and diethyl ether. The polymer was dissolved in deionised water and dialyzed (molar mass cut-off 8,000 g/mol) for 3 days. The polymer was lyophilized (Yield: 90%). Deprotection was confirmed by ^{1}H NMR spectroscopy due to the absence of signals at 7.2 ppm (benzyl group) and 5.0 ppm and (CH_2-Bz). ^{1}H NMR spectroscopy (400 MHz, D_2O, δ) = 8.15 (br s, 90H), 7.20 (br m, 60H), 5.75 (br m, 17H), 3.55 (br s, 34H) 2.75-3.25 (br m, 66H), 2.50 (br s, 64H) DLS (THF): M_w = 44,200 g/mol, M_w/M_n = 1.5, R_h = 4.7 nm.

Synthesis of star shaped PLL: S-PS-b-PLL

S-PS-b-PBLG (0.5 g) was dissolved in 5 ml of trifluoroacetic acid (TFA). A 6-fold excess with respect to ε-carbobenzyloxy-L-lysine of a 33% solution of HBr in acetic acid was added slowly to the reaction. After 16 h, the solution was precipitated into diethyl ether. The precipitate was washed with ethanol and diethyl ether (Yield: 85%). Deprotection was confirmed by FTIR sprectroscopy due to the absence of the carbonyl functionality of the Z protecting group at 1693 cm^{-1}.

Polyester Core (Degradable) / Polymethacrylate Periphery (Nondegradable)

Materials

1,5,7-triaza-bicyclo[4.4.0]dec-5-ene (TBD) was purchased from the Sigma Aldrich and purified by sublimation. Solvents were either used as obtained from a Pure Solv solvent dispenser supplied by Innovative Technology, Inc., or purchased from Sigma Aldrich and purified by standard literature procedures. 2-(trimethylsilyl)ethyl methacrylate was synthesized following a literature procedure.[102] All other chemicals were used as obtained from commercial sources and used as received.

Synthesis of 5,5'-Bis(oxepanyl-2-one) (BOP)

4,4'-Bicyclohexanone (20.0 g, 102.8 mmol) was added slowly over approx. 30 minutes to a solution of urea-hydrogen peroxide ($CO(NH_2)2.H_2O_2$) (40.0 g, 424.0 mmol) in formic acid (99%, 200 mL) and stirred at room temperature for 4hr. The solution was diluted with water (200 mL) and extracted with chloroform (3 x 200 mL). The organic fractions were combined, washed with an aqueous solution of Na_2CO_3 (3 x 100 mL, 10 wt%), dried over anhydrous $MgSO_4$ and the solvent removed under reduced pressure. The residue was recrystallized (ethyl acetate/acetone) to afford the title compound as a white crystalline solid (10.0 g, 43%), m.p = 167-169 ^oC, lit.[103]= 174 ^oC. ^1H NMR spectroscopy (400MHz, $CDCl_3$): δ (ppm) 4.39-4.34 and 4.21-4.15 (m, 4H, -CH_2OCO- (R,R) and (R,S)), 2.78-2.72 and 2.65-2.58 (m, 4H, -CH_2COO-(R,R) and (R,S)), 1.94-1.84 (m, 4H, - CH_2CH_2OCO-), 1.71-1.61 (m, 4H, - CH_2CH_2COO-), 1.55-1.46 (q, 2H, J = 12 Hz, -CH-).

Synthesis of RAFT agent: 2-cyano-5-(3-hydroxypropyl amino)-5-oxopentanoic-2-yl benzodithioate

4-Cyano-4-(phenylcarbonothioylthio)pentanoic acid (1 g, 3.6 mmol) and DIC (diisopropyl carbodiimide) (0.55 g, 4 mmol) were dissolved in 15 ml dry DCM under nitrogen atmosphere. 3-amino-1-propanol (0.3 g – 4 eq.) in 1 ml dry DCM was added dropwise via syringe at 0^{o}C. The solution was stirred at room temperature for 24 h. The solvent was removed under reduced pressure and purified using column chromatography (8:2 ethyl acetate:ethanol) (Yield: 50%).^{1}H NMR spectroscopy (400MHz, $CDCl_3$): δ (ppm) 7.93 (d, 2H), 7.58 (t, 1H), 7.41 (t, 2H) 6.43 (br s, NH), 3.66 (br t, 2H), 3.43 (q, 2H), 3.21 (br s, OH), 2.45-2.57 (m, 4H), 1.95 (s, 3H), 1.72 (m, 2H). ^{13}C NMR spectroscopy (400MHz, $CDCl_3$): δ (ppm) 171.52 (C=O), 144.39 (C-C=S), 133.10 (-CH), 128.56(2C,-CH), 126.68(2C,-CH), 118.68 (C=N), 59.58 (-CH_2-OH), 45.94 (-C-S), 36.69 (-CH_2-NH), 34.18 (-CH_2), 31.67 (-CH_2-C=O), 31.66 (-CH_2-C), 23.99 (-CH_3-C).

Synthesis of linear poly(DMAEMA): L-DMAEMA-RAFT

RAFT-OH (0.4 g, 1.2 mmol), DMAEMA (6 g, 38.2 mmol) and AIBN (58 mg, 0.035 mmol) were dissolved in 22 ml of dry 1,4 dioxane in a Schlenk flask. The reaction was degassed by 3 cycles of freeze, pump, thaw. The solution was stirred at 85^{o}C for 22 h. The solution was allowed to cool to room temperature and precipitated into hexane. The product was reprecipitated once more to obtain the product as a red coloured solid (Yield: 90%). ^{1}H NMR spectroscopy (400MHz, $CDCl_3$): δ (ppm) 7.85 (d, 2H), 7.49 (t, 1H), 7.34 (t, 2H), 4.02 (br s, 64H), 3.66 (t, 2H), 3.37 (br s, 2H), 2.53 (br s, 64H), 2.25 (br s, 192H), 1.79-1.88 (br m, 67H), 1.1-1.5 (br m, 6H), 0.9-1.06 (br d, 96H).

Removal of ω-RAFT end group: L-DMAEMA-H

L-DMAEMA-RAFT (3.5 g, 0.69 mmol) Bu_3SnH (5 g, 17.1 mmol) and AIBN (525 mg, 3 mmol) were dissolved in 22 ml dry 1,4 dioxane. The solution was degassed by 3 freeze, pump, thaw cycles. The solution was stirred at 60^{o}c for 1 h or until the solution became colourless. The solution was allowed to cool to room temperature and precipitated into cold hexane. The product was reprecipitated twice more from acetone into hexane. The polymer was redissolved in acetone and dialyzed against 15% acetone/H_2O for 18 h and then against acetone for 24 h. The solvent was removed under reduced pressure. The product was freeze dried from benzene to obtain the product as a colorless solid (Yield: 70%).^{1}H NMR spectroscopy (400MHz, $CDCl_3$): δ (ppm) 4.02 (br s, 64H), 3.66 (t, 2H), 3.37 (br s, 2H), 2.53 (br s, 64H), 2.25 (br s, 192H), 1.79-1.88 (br m, 67H), 1.1-1.5 (br m, 6H), 0.9-1.06 (br d, 97H).

Synthesis of linear poly(DMAEMA) / polyester block copolymer: L-DMAEMA-b-PVL

L-DMAEMA-H (0.15 g, 0.03 mmol) was dissolved in 2 g of dry toluene. TBD (2.8 mg, 0.2 mmol) in 0.5 ml of dry toluene and δ-Valerolactone (0.15 g, 1.5 mmol) were added and stirred at 40^{o}C for 2 h under a nitrogen atmosphere. The reaction was quenched with benzoic acid and the product was precipitated into cold diethyl ether. The product was filtered and dried under vacuum (Yield: 90%).^{1}H NMR spectroscopy (400MHz, $CDCl_3$): δ (ppm) 4.02 (br s, 152H), 3.66 (t, 2H), 3.37 (br m, 2H), 2.53 (br s, 64H), 2.33 (br m, 88H), 2.25 (br s, 192H), 1.79-1.88 (br m, 67H), 1.67 (br m, 172H), 1.1-1.5 (br m, 6H), 0.9-1.06 (br d, 97H).

Synthesis of poly(DMAEMA) nanogel star polymers: S-DMAEMA-H

L-DMAEMA-H (0.8 g, 0.16 mmol) was dissolved in 8.5 g of dry toluene. TBD (13 mg, 0.094 mmol) in 0.2 ml dry toluene and BOP (0.3 g, 1.3 mmol) were added and the reaction was stirred for 16 h at 70^{o}c under N_2. The solution was allowed to cool to room temperature and quenched with benzoic acid. The product was precipitated into cold hexane. The product was purified by fractionation to remove residual L-DMAEMA arms. Briefly, 200 mg of polymer was dissolved in 2 ml of acetone and hexane (2 ml) was added slowly to form a cloudy suspension which was allowed to settle over time. The remaining solution was decanted off and the product precipitated from minimal acetone into hexane. The product was dried under reduced pressure to afford a white solid (Yield: 48%). ^{1}H NMR spectroscopy (400MHz, $CDCl_3$): δ (ppm) 4.02 (br s, 64H), 3.66 (t, 2H), 2.53 (br s, 64H), 2.25 (br s, 192H), 1.79-1.88 (br m, 67H), 1.1-1.5 (br m, 6H), 0.9-1.06 (br d, 97H).

Synthesis of linear poly(TMSEM): L-TMSEM-RAFT

RAFT-OH (0.15 g, 0.45 mmol), TMSEM (2.7 g, 14.5 mmol) and AIBN (22 mg, 0.3 mmol) were dissolved in 8 ml of dry 1,4 dioxane in a Schlenk flask. The reaction was degassed by 3 cycles of freeze, pump, thaw. The solution was stirred at 85^{o}C for 22 h. The solution was allowed to cool to room temperature and precipitated into hexane. The product was reprecipitated once more to obtain the product as a red coloured solid (Yield: 86%). ^{1}H NMR spectroscopy (400MHz, $CDCl_3$): δ (ppm) 7.85 (d, 2H), 7.49 (t, 1H), 7.34 (t, 2H), 4.02 (br s, 60H), 3.66 (t, 2H), 3.37 (br s, 2H), 1.75-1.85 (br m, 63H), 1.10-1.35 (br m, 6H), 0.83-0.93 (br d, 150H), 0.01 (br s, 270H).

Removal of ω-RAFT end group: L-TMSEM-H

L-TMSEM-RAFT (2.2 g, 0.39 mmol) Bu_3SnH (2.8 g, 9.6 mmol) and AIBN (262 mg, 1.6 mmol) were dissolved in 7 ml dry 1,4 dioxane. The solution was degassed by 3 freeze, pump, thaw cycles. The solution was stirred at 60^{o}c for 1 h or until the solution became colourless. The

solution was allowed to cool to room temperature and precipitated into cold hexane. The product was reprecipitated twice more from acetone into hexane. The polymer was redissolved in acetone and dialyzed against 15% acetone/H_2O for 18 h and then against acetone for 24 h. The solvent was removed under reduced pressure. The product was freeze dried from benzene to obtain the product as a colorless solid (Yield: 67%).^{1}H NMR spectroscopy (400MHz, $CDCl_3$): δ (ppm) 4.02 (br s, 60H), 3.66 (t, 2H), 3.37 (br s, 2H), 1.75-1.85 (br m, 63H), 1.10-1.35 (br m, 6H), 0.83-0.93 (br d, 151H), 0.01 (br s, 270H).

Synthesis of poly(TMSEM) nanogel star polymers: S-TMSEM-H

L-TMSEM-H (0.4 g, 0.067 mmol) was dissolved in 4.5 g of dry toluene. TBD (10 mg, 0.072 mmol) in 0.2 ml dry toluene and BOP (0.2 g, 0.88 mmol) were added and the reaction was stirred for 2 h at 70^{o}c under N_2. The solution was allowed to cool to room temperature quenched with benzoic acid. The product was precipitated into cold hexane. The product was dried under reduced pressure to afford a white solid (Yield: 87%). ^{1}H NMR spectroscopy (400MHz, $CDCl_3$): δ (ppm) 4.02 (br s, 60H), 3.66 (t, 2H), 3.37 (br s, 2H), 1.75-1.85 (br m, 63H), 1.10-1.35 (br m, 6H), 0.83-0.93 (br d, 151H), 0.01 (br s, 270H).

Removal of ethyl (trimethylsilyl) protecting group: S-MA-H

S-TMSEM-H (0.2 g) was dissolved in 2 ml of dry THF. TBAF solution (1M in THF, 0.1 ml) was added and the reaction was stirred under N_2 overnight. The turbid solution was precipitated into hexane. The filtered product was dried under reduced pressure to yield the product was as an off white solid. The solubility of the product was problematic post deprotection (Yield: 80%).

Polyester Core (Degradable) / Polyethylene Glycol Periphery (Nondegradable)

Materials

1,5,7-triaza-bicyclo[4.4.0]dec-5-ene was purchased from the Sigma Aldrich and purified by sublimation. Solvents were either used as obtained from a Pure Solv solvent dispenser supplied by Innovative Technology, Inc., or purchased from Sigma Aldrich and purified by standard literature procedures. All poly(ethylene) glycol was dried by lyophilization. All other chemicals were used as obtained from commercial sources and used as received.

Synthesis of 5,5'-Bis(oxepanyl-2-one) (BOP)

4,4'-Bicyclohexanone (20.0 g, 102.8 mmol) was added slowly over approx. 30 minutes to a solution of urea-hydrogen peroxide ($CO(NH_2)2.H_2O_2$) (40.0 g, 424.0 mmol) in formic acid (99%, 200 mL) and stirred at room temperature for 4 h. The solution was diluted with water (200 mL) and extracted with chloroform (3 x 200 mL). The organic fractions were combined, washed with an aqueous solution of Na_2CO_3 (3 x 100 mL, 10 wt%), dried over anhydrous Na_2SO_4 and the solvent removed under reduced pressure. The residue was recrystallized (ethyl acetate/acetone) to afford the title compound as a white crystalline solid (10.0 g, 43%), m.p = 167-169 ^oC, lit.[105] = 174 ^oC. ^1H NMR spectroscopy (400MHz, $CDCl_3$): δ (ppm) 4.39-4.34 and 4.21-4.15 (m, 4H, -CH_2OCO- (R,R) and (R,S)), 2.78-2.72 and 2.65-2.58 (m, 4H, -CH_2COO- (R,R) and (R,S)), 1.94-1.84 (m, 4H, - CH_2CH_2OCO-), 1.71-1.61 (m, 4H, - CH_2CH_2COO-), 1.55-1.46 (q, 2H, J = 12 Hz, -CH-).

Synthesis of linear PEG-b-PVL (Representative Procedure)

Poly(ethylene) glycol-2 kDa (0.4 g, 0.2 mmol) was dissolved in 4 g of dry toluene. TBD (5 mg, 0.036 mmol) in 0.5 ml of dry toluene and δ-Valerolactone (0.3 g, 3 mmol) were added and stirred at room temperature for 30 min under a nitrogen atmosphere. The reaction was quenched with benzoic acid and the product was precipitated into cold diethyl ether. The product was filtered and dried under vacuum (Yield: 90%).^1H NMR spectroscopy (400MHz, $CDCl_3$): δ (ppm) 4.02 (br t, 20H), 3.62 (br s, 193H), 3.35 (s, 3H), 2.33 (br s, 20H), 2.11 (br s, OH), 1.67 (br m, 40H).

Synthesis of PEG nanogel star polymers: S-PEG (Representative Procedure)

Poly(ethylene) glycol-2 kDa (0.25 g, 0.125 mmol) was dissolved in 6 g of dry toluene. TBD (5 mg, 0.036 mmol) in 0.5 ml of dry toluene and BOP (0.19 g, 0.84 mmol) were added and stirred at room temperature for 20 h under a nitrogen atmosphere. The reaction was quenched with benzoic acid and the product was precipitated into cold diethyl ether. Briefly, 200 mg of polymer was dissolved in 2 ml of acetone and diethyl ether (3.5 ml) was added slowly to form a cloudy suspension which was allowed to settle over time. The remaining solution was decanted off and the product precipitated from minimal acetone into cold diethyl ether. The product was filtered and dried under vacuum (Yield: 75%).^1H NMR spectroscopy (400MHz, $CDCl_3$): δ (ppm) 4.12 (br t, 4H), 3.62 (br s, 150H), 3.53 (t, 2H from core) 3.35 (s, 3H), 2.51 (br t, 4H), 2.11 (br s, OH), 1.63 (br m, 8H).

Synthesis of PEG-b-PVL nanogel star polymers: S-PEG-b-PVL (Representative Procedure)

Poly(ethylene) glycol-2 kDa (0.4 g, 0.2 mmol) was dissolved in 4 g of dry toluene. TBD (5 mg, 0.036 mmol) in 0.5 ml of dry toluene and δ-Valerolactone (0.3 g, 3 mmol) were added and stirred at room temperature for 30 min under a nitrogen atmosphere. A sample was taken for SEC and ^{1}H NMR spectroscopy analysis. To the reaction solution was added 1.5 g of dry toluene, TBD (3 mg, 0.021 mmol) in 0.5 ml of dry toluene and BOP (0.15 g, 0.66 mmol). The solution was stirred at room temperature overnight. The reaction was quenched with benzoic acid and the product was precipitated into cold diethyl ether. 200 mg of polymer was dissolved in 2 ml of acetone and diethyl ether (3.5 ml) was added slowly to form a cloudy suspension which was allowed to settle over time. The remaining solution was decanted off and the product precipitated from minimal acetone into cold diethyl ether. The product was filtered and dried under vacuum (Yield: 65%).^{1}H NMR spectroscopy (400MHz, $CDCl_3$): δ (ppm) 4.12 (br t, 4H), 3.62 (br s, 150H), 3.53 (t, 2H from core) 3.35 (s, 3H), 2.51 (br t, 4H), 2.11 (br s, OH), 1.63 (br m, 8H).

1 pot synthesis of PEG-b-PVL nanogel star polymers: S-PEG-5kDa-b-PVL-3kDa

Poly(ethylene) glycol-5 kDa (0.5 g, 0.1 mmol) was dissolved in 7 g of dry toluene. TBD (5 mg, 0.036 mmol) in 0.5 ml of dry toluene, δ-valerolactone (0.3 g, 3 mmol) and BOP (0.2 g, 0.88 mmol) were added and stirred at room temperature overnight under a nitrogen atmosphere. The reaction was quenched with benzoic acid and the product was precipitated into cold diethyl ether. 200 mg of polymer was dissolved in 2 ml of acetone and diethyl ether (3.5 ml) was added slowly to form a cloudy suspension which was allowed to settle over time. The remaining solution was decanted off and the product precipitated from minimal acetone into cold diethyl ether. The product was filtered and dried under vacuum (Yield: 70%).^{1}H NMR spectroscopy (400MHz, $CDCl_3$): δ (ppm) 4.12 (br t, 4H), 3.62 (br s, 198H), 3.53 (t, 2H from core) 3.35 (s, 3H), 2.51 (br t, 4H), 2.11 (br s, OH), 1.63 (br m, 8H).

5.5 References

1. E.-K. Lim, Y.-M. H. J. Yang, K. Lee, J.-S. Suh, S. Haam, *Adv. Mater*., **2011**, 23, 2426.
2. S. M. Janib, A. S. Moses, J. A. Mackay, *Adv. Drug Delivery Rev*., **2010**, 62, 1052.
3. R. Hao, R. Xing, Z. Xu, Y. Hou, S. Gao, S. Sun, *Adv. Mater*., **2010**, 22, 2729.
4. H. B. Na, I. C. Song, T. Hyeon, *Adv. Mater*., **2009**, 21, 2133.
5. D. Peer, J. M. Karp, S. Hong, O. C. Farokhzad, R. Margalit, R. Langer, *Nat. Nanotechnol*. **2007**, 2, 751.
6. R. F. Service, *Science*, **2005**, 310, 1132.
7. Jin Xie, Seulki Lee, Xiaoyuan Chen, *Adv. Drug Deliver. Rev*., **2010**, 62, 1064.
8. Y. Liu, H. Miyoshi, M. Nakamura, *Int. J. Cancer*, **2007**, 120, 2527.
9. S. Nie, Y. Xing, G.J. Kim, J.W. Simons, *Annu. Rev. Biomed. Eng*., **2007**, 9, 257.
10. P. Horcajada, T. Chalati, C. Serre, B. Gillet, C. Sebrie, T. Baati, J. F. Eubank, D. Heurtaux, P. Clayette, C. Kreuz, J.-S. Chang, Y. Hwang, V. Marsaud, P.-N. Bories, L. Cynober, S. Gil, G. F´erey, P. Couvreur, R. Grefruxandra, *Nat. Mater*., **2009**, 9, 172.
11. J.-H. Park, G. von Maltzahn, E. Ruoslahti, S. N. Bhatia, M. J. Sailor, *Angew. Chem. Int. Ed*., **2008**, 47, 7284.
12. V. Rodionov, H. Gao, S. Scroggins, D. A. Unruh, A.-J. Avestro, J. M. J. Frechet, *J. Am. Chem. Soc*., **2010**, 132, 2570.
13. Q. Zhao, S.-J. Liu and W. Huang,*Macromol. Chem. Phys*., **2009**, 210, 1580.
14. J. N. H. Reek, S. Arevalo, R. V. Heerbeek, P. C. J. Kamer, P. W. N. M. Van Leeuwen, *Adv. Catal*. **2006**, 49, 71.
15. C. Kojima, C. Regino, Y. Umeda, H. Kobayashi, K. Kono, *Int. J. Pharm*., **2010**, 383, 293.
16. R. Gref, Y. Minamitake, M. T. Peracchia, V. Trubetskoy, V. Torchilin, R. Langer, *Science*, **1994**, 263, 1600.
17. A. S. Hasana, M. Socha, A. Lamprecht, F. El Ghazouani, A. Sapin, M. Hoffman, P. Maincent, N. Ubrich, *Int. J. Pharm*., **2007**, 344, 53.
18. A. Gabizon, *Clin. Cancer Res*., **2001**, 7, 223.
19. T. Wang, G. G. M. D'Souza, D. Bedi, O. A. Fagbohun, L. P. Potturi, B. Papahadjopoulos-Sternberg, V. A. Petrenko, V. P. Torchilin, Nanomedicine, **2010**, 5, 563.

20. K. Matyjaszewski, *Macromolecules*, **2012**, 45, 4015.

21. C. Boyer, M. H. Stenzel, T. P. Davis, *J. Polym. Sci. A: Polym. Chem*, **2011**, 49, 551.

22. H. Gao, *Macromol. Rapid Commun*., **2012**, 33, 722.

23. A. Blencowe, J. F. Tan, T. K. Goh, G. G. Qiao, *Polymer* **2009**, 50, 32.

24. Q. Chen , X. Cao , Y. Xu , Z. An, *Macromol. Rapid Commun*., **2013**, 34, 1507.

25. J. Cheng, T. J. Deming, *Topics in Current Chemistry*, **2012**.

26. J. G. Zilliox, P. Rempp, J. Parrod, *J. Polym. Sci. Polym. Symp*., **1968**, 22, 145.

27. W. Burchard, *Adv. Polym. Sci*., Vol. 143., Berlin, Heidelberg, Springer-Verlag, **1999**., 113.

28. K. Ishizu, F. Taiichi, K. Ochi, Architecture of Star and Hyperbranched Polymers, Caruta BM, *Focus on Polymeric Materials Research*., Nova Science Publishers; **2006**.

29. V. Y. Lee, K. Havenstrite, M. Tjio, M. McNeil, H. M. Blau, R. D. Miller, J. Sly, *J. Adv. Mater*., **2011**, 23, 4464.

30. G. Zheng, C. Pan, *Polymer*, **2005**, 46, 2802.

31. Z. Guan, P. M. Cotts, E. F. McCord, S. J. McLain, *Science*, **1999**, 283, 2059.

32. A. J. Pasquale, T. E. Long, *J. Polym. Sci. Part A Polym. Chem*., **2001**, 39, 216.

33. D. H. Solomon, E. Rizzardo, P. Cacioli, *US Patent,* 4, 581, 429, **1986**.

34. M. K. Georges, R. P. N. Veregin, P. M Kazmaier, G. K Hamer, *Macromolecules,* **1993**, 26, 2987.

35. J. S. Wang, K. Matyjaszewski, *J. Am. Chem. Soc*., **1995**, 117, 5614.

36. M. Kato, M. Kamigaito, M. Sawamoto, T. Higashimura, *Macromolecules*, **1995**, 28, 1721.

37. J. Chiefari, Y. K. Chong, F. Ercole, J. Krstina, J. Jeffery, P .T. L. Tam, R. T. A. Mayadunne, G. F. Meijs, C. L. Moad, G. Moad, E. Rizzardo, S. H. Thang, *Macromolecules*, **1998**, 31, 5559.

38. D. H. Solomon, G. G. Qiao, S. Abrol S., *PCT Int.,* WO99958588, **1999**.

39. C. T. Berge, M. Fryd, J. W. Johnson, G. Moad, E. Rizzardo, C. Scopazzi C, *PCT Int*., WO0002939, **2000**.

40. H. T. Lord, J. F. Quinn, S. D. Angus, M. R. Whittaker, M. H. Stenzel, T. P. Davis., J. *Mater. Chem*., **2003**, 13, 2819.

41. X. Shi, M. Miao, Z. An, *Polym. Chem*., 2013, 4, **1950**.

42. J. Ferreira, J. Syrett, M. Whittaker, D. Haddleton, T. P. Davis, C. Boyer, *Polym. Chem*., **2011**, 2, 1671.

43. K. Y. Baek, M. Kamigaito, M. Sawamoto, *Macromolecules*, **2001**, 34, 215.

44. J. Xia, X. Zhang, K. Matyjaszewski, *Macromolecules*, **1999**, 32, 4482.

45. H. Gao, S. Ohno, K. Matyjaszewski, *J. Am. Chem. Soc*., **2006**, 128, 15111.

46. J. Burdynska, H. Y. Cho, L. Mueller, K. Matyjaszewski, Macromolecules, **2010**, 43, 9229.

47. A. W. Bosman, R. Vestberg, A. Heumann, J. M. J. Frechet, C. J. Hawker, *J. Am. Chem. Soc.,* **2003**, 125, 715.

48. A. Abrol, P. A. Kambouris, M. G. Looney, D. H. Solomon, *Macromol. Rapid Commun*., **1997**, 18, 755.

49. S. Abrol, M. J. Caulfield, G. G. Qiao, D. H. Solomon, *Polymer*, **2001**, 42, 5987.

50. A. W. Bosman, A. Heumann, G. Klaerner, D. Benoit, J. M. J. Frechet, C. J. Hawker, *J. Am. Chem. Soc*., **2001**, 123, 6461.

51. T. Tsoukatos, S. Pispas, N. Hadjichristidis, *J. Polym. Sci. Part A Polym. Chem*., **2001**, 39, 320.

52. J. A. Simms, H. J. Spinelli, *J. Coat. Technol*., **1987**, 57, 125.

53. O. W. Webster, *J. Polym. Sci. Part A Polym. Chem*., **2000**, 38, 2855.

54. G. C. Bazan, R. R. Schrock, *Macromolecules*, **1991**, 24, 817.

55. A. Sulistio, A. Blencowe, A. Widjaya, X. Zhang, G. G. Qiao, *Polym. Chem.*, **2012**, 3, 224.

56. A. Sulistio, J. Lowenthal, A. Blencowe, M. N. Bongiovanni, L. Ong, S. L. Gras, X.Zhang, G. G. Qiao, *Biomacromolecules*, **2011**, 12, 3469.

57. J. T. Wiltshire, G. G. Qiao, *Macromolecules*, **2006**, 39, 4282.

58. J. M. Ren, Q. Fu, A. Blencowe, G. G. Qiao, *ACS Macro Letters*, **2012**, 1, 681.

59. E. A. Appel, V. Y. Lee, T. T. Nguyen, M. McNeil, F. Nederberg, J. L. Hedrick, W. C. Swope, J. E. Rice, R. D. Miller, J. Sly, *Chem. Commun*., **2012**, 48, 6163.

60. J. M. Ren, J. T. Wiltshire, A. Blencowe, G. G. Qiao, *Macromolecules*, **2011**, 44, 3189.

61. S. Kanaoka, M. Sawamoto, T. Higashimura, *Macromolecules*, **1991**, 24, 2309.

62. T. Shibata, S. Kanaoka, S. Aoshima, *J. Am. Chem. Soc*., **2006**, 128, 7497.

63. T. Terashima, M. Kamigaito, K. Y. Baek, T.Ando, M. Sawamoto, *J. Am. Chem. Soc.*, **2003**, 125, 5288.

64. S. A. Bencherif, H. Gao, A. Srinivasan, D. J. Siegwart, J. O. Hollinger, N. R. Washburn, K. Matyjaszewski, *Biomacromolecules*, **2009**, 10, 1795.

65. K.-I. Fukukawa, R. Rossin, A. Hagooly, E. D. Pressly, J. N. Hunt, B. W. Messmore, K. L. Wooley, M. J. Welch and C. J. Hawker, *Biomacromolecules*, **2008**, 9, 1329.

66. T. K. Georgiou, M. Vamvakaki, L. A. Phylactou, C. S. Patrickios, *Biomacromolecules*, **2005**, 6, 2990.

67. J. A.Syrett, D. M. Haddleton, M. R. Whittaker, T. P. Davis, C. Boyer, *Chem. Commun*., **2011**, 47, 1449.

68. R. T. Chacko, J. Ventura, J. Zhuang, S. Thayumanavan, *Adv. Drug Deliv. Rev*., **2012**, 64, 836.

69. J. Huang, A. Heise, *Chem. Soc. Rev*., **2013**, 42, 7373.

70. M. Byrne, P. D. Thornton, S. -A. Cryan, A. Heise, *Polym. Chem.,* **2012**, 3, 2825-2831.

71. M. Byrne, D. Victory, A. Hibbitts, M. Lanigan, A. Heise, S. –A. Cryan, *Biomater. Sci*., **2013**, 1, 1223.

72. H. Lu, J. Wang, Z. Song, L. Yin, Y. Zhang, H. Tang, C. Tu, Y. Lin, J. Cheng, *Chem. Commun*., **2014**, 50, 139.

73. H. R. Kricheldorf, *Angew. Chem., Int. Ed*., **2006**, 45, 5752.

74. N. Hadjichristidis, H. Iatrou, M. Pitsikalis, G. Sakellariou, Chem. Rev., **2009**, 109, 5528.

75. K. C. Kumara Swamy, N. N. Bhuvan Kumar, E. Balaraman, K. V. P. Pavan Kumar, *Chem. Rev*., **2009**, 109, 2551.

76. B. Henkel, E. Bayer, *J. Peptide Sci*., **1998**, 4, 461.

77. R.Mildner, H. Menzel, *J. Polym. Sci. Part A Polym. Chem*., **2013**, 51, 3925.

78. A. Joshi, A. Saraph, V. Poon, J. Mogridge, R. S. Kane, *Bioconugate Chem*., **2006**, 17, 1265.

79. M. Ambrosi, N. R. Cameron, B. G. Davis, *Org. Biomol. Chem*., **2005**, 3 , 1593.

80. J. R. Kramer, T. J. Deming, DOI: 10.1039/c3py01081c.

81. C. M. Thomas, *Chem. Soc. Rev.,* **2010**, 39, 165.

82. K. Ariga, J. P. Hill, Q. Ji, Macromol. Biosci., **2008**, 8, 981.

83. B. G. De Geest, N. N. Sanders, G. B. Sukhorukov, J. Demeestera, S. C. De Smedt, *Chem. Soc. Rev*., **2007**, 36, 636.

84. J. Zhang, L. S. Chua, D. M. Lynn, *Langmuir*, **2004**, 20, 8015.

85. G. Moad, E. Rizzardo, S. H. Thang, *Aust. J. Chem*., **2012**, 65, 985.

86. G. Moad, C. Barner-Kowollik, Edited by C. Barner-Kowollik, From Handbook of RAFT Polymerization, **2008**, 51.

87. G. Moad, E. Rizzardo, S. H. Thang, *Accounts Chem. Res*., **2008**, 41, 1133.

88. H. Willcocka, R. K. O'Reilly, *Polym. Chem*., **2010**, 1, 149.

89. J. Cai, Y. Yue, D. Rui, Y. Zhang, S. Liu, C. Wu, *Macromolecules*, **2011**, 44, 2050.

90. G. Moad, Y.K. Chong, A. Postma, E. Rizzardo, S. H. Thang, *Polymer*, **2005**, 46, 8458.

91. K. Knop, R. Hoogenboom, F. D. Schubert, *Angew. Chem. Int. Ed.,* **2010**, 49, 6288.

92. D. T. Shima, P. Calias, E. T. Cunningham, D. R. Guyer, A. P. Adamis, *Nat. Rev. Drug Discov*., **2006**, 5, 123.

93. S. Saeki, N. Kuwahara, M. Nakata, M. Kaneko, *Polymer*, **1976**, 17, 685.

94. S. Carter,B. Hunt, S. Rimmer, *Macromolecules*, **2005**, 38, 4595.

95. S. Rimmer, S. Carter, R. Rutkaite, J. W. Haycock, L. Swanson, *Soft Matter*, **2007**, 3, 971.

96. M. A. Ward, T. K. Georgiou, *J. Polym. Sci. Part A Polym. Chem*, **2010**, 48, 775.

97. Y. Zhou, D. Yan, W. Dong, Y. Tian, *J. Phys. Chem. B,* **2007**, 111, 1262.

98. J. Ueda, M. Kamigaito, M. Sawamoto, *Macromolecules*, **1998**, 31, 6762.

99. S. Angot, K. S. Murthy, D. Taton, Y. Gnanou, *Macromolecules*, **1998**, 31, 7218.

100. E. S. Kim, B. C. Kim, S. H. Kim, *J. Polym. Sci., Part B: Polym. Phys*., **2004**, 42, 939.

101. G. J. M. Habraken, C. E. Koning, A. Heise, *J. Polym. Sci., Part A: Polym. Chem*., **2009**, 47, 6883.

102. I. Zharov, J. Michl, M. H. Sherwood, R. Sooriyakamaran, C. E. Larson, R. A. DiPietro,

G. Breyta, G. M. Wallraff, *Chem. Mater*., **2002**, 14, 656.

103. A. J. Nijenhuis, D. W. Grijpma, A. J. Pennings, *Polymer*, **1996**, 37, 2783.

Chapter 6

Conclusion and Outlook

Star shaped polymers, in particular star shaped polypeptides are of great interest owing to the unique structural features and inherent biocompatibility associated with such materials. Consequently, the next generation of nanoparticle platforms may stem from this area to afford materials which offer great potential towards biomedical applications such as drug delivery, medical diagnostics and therapeutics. The aim of this thesis was the development of novel star shaped polymers and to investigate their potential towards the biomedical field. ROP of NCAs was the predominant synthetic tool employed in conjunction with amide coupling chemistries for post modification of star shaped polypeptides. Furthermore, the synthetic expertise of IBM was engaged to further the development of advanced star shaped polymeric architectures. To summarize, **platform one** saw the development of a range well-defined star shaped poly(glutamic acid) capable of tunable loading capacities and enzyme triggered controlled release. Although the cargo encapsulated was a simple dye, notable features of this platform towards the delivery of real therapeutics may be considered for the design of more complex delivery platforms. The introduction of sugars (targeting function), pegylation (modulate pharmokinetics) and a fluorescent moiety (imaging / diagnostics) may impart further intelligence to this platform enabling the simultaneous site specific controlled release of therapeutics and diagnostic imaging. **Platform two** involved the employment of a lysine NCA derivative to generate cationic star shaped poly(lysine) which exhibited superior complexation, "polyplex" sizing, cargo protection and transfection efficiencies compared to the analogous linear poly(lysine). More advanced cellular studies are currently being undertaken and preliminary results show superior transfections efficiencies compared commercially gene transfection products. As with platform 1, the ability to readily use the functional amino acid side chain to conjugate functional moieties may help to promote the biomedical applicability of these materials. The formation of advanced glycopolypeptide architectures was performed **(platform 3)** to achieve materials boasting well-defined star shaped architectures and potential to strategically position sugar moieties within a polypeptide chain. These materials

demonstrated their bioactivity through a lectin specific binding interaction and may find great use in biorecogniton applications and the study of more advanced carbohydrate – protein interactions. More advanced studies may be undertaken to ascertain the effects of architecture / sugar positioning on these interactions. Finally, **platform 4** saw collaborative research efforts with IBM devise a series of novel hybrid nanogel star polymers through a combination of various controlled polymerization techniques. These materials were of mixed compositions but boasted well-defined, multifunctional and structurally versatile properties permitting their facile tailoring towards specific biomedical applications. The continued development of these materials towards targeted applications is currently being undertaken and the array of platforms developed provides a solid base from which alterations may be made.

The outlook for this field is very positive given the immense array of synthetic tools available. The ability to readily introduce novelty and "smart" features to these materials should hopefully lead to the development of more advanced and applicable nanoparticle platforms. Advanced biological studies are the next major hurdle in taking these materials from the benchtop to the eventual goal of commercialization.